University of Alberta

Exploring Notch signaling pathways for breast cancer treatment

by

Jianxun Han

A thesis submitted to the Faculty of Graduate Studies and Research
in partial fulfillment of the requirements for the degree of

Doctor of Philosophy

in

Experimental Oncology

Department of Oncology

Fall 2010

Edmonton, Alberta

Examining Committee

Joan Turner, Oncology

Michael Hendzel, Oncology

David Murrary, Oncology

Gordon Chan, Oncology

Judith Hugh, Laboratory Medicine & Pathology

Aly Karsan, Pathology and Laboratory Medicine, University of British Columbia

To my family

Abstract

Breast cancer is the most common cancer and the leading cause of cancer-related death among Canadian women. Despite improvements in treatment and early detection, there is still a need to develop novel therapies for breast cancer management. Aberrant Notch signalling is tumorigenic and is associated with poor clinical outcomes in breast cancer, as well as in several other types of cancer. Activation of Notch signalling requires γ-secretase-mediated Notch receptor cleavage. Thus, strategies to inhibit Notch signalling, including γ-secretase inhibition, are being evaluated for potential anti-tumor effects. The strongest justification for targeting Notch in breast cancer, and more specifically for using γ-secretase inhibitors, came from two studies that reported that the γ-secretase inhibitor (GSI) Z-LLNle-CHO inhibited the growth of breast cancer cells both *in vitro* and *in vivo* without causing significant side effects. In Chapter 2, we compared the enzymatic activities and cytotoxicity of Z-LLNle-CHO to those of two other specific GSIs and three proteasome inhibitors and demonstrated that the cytotoxicity of Z-LLNle-CHO in breast cancer cells is mediated by proteasome inhibition, not by γ-secretase inhibition. In Chapter 3, we characterized the protein complexes formed in breast cancer cells by the intracellular domains (NICD) of the four Notch paralogs. We found that the assembly of NICD protein complexes is dose-dependent and availability of MAML proteins becomes the limiting factor for continuous formation of NICD/RBPjκ/MAML transactivation complex. This suggests that the formation of some non-canonical NICD complex might occur preferentially at high levels of NICD, conditions under which aberrant Notch signalling induces tumorigenesis in breast cancer. Consequently, these non-canonical interactions might be good

targets to specifically block oncogenic, but not physiological, Notch signalling. In addition, we found that the relative affinities of individual NICD paralogs to several known NICD-interacting proteins were different. This may account for the paralog-specific activities of Notch that have been previously reported. Together, these results may be of value for the development of new reagents to block Notch signalling for therapeutic benefit in breast cancer treatment.

Acknowledgement

I have been extremely fortunate during these six and half years to be surrounded by so many kind-hearted persons, to whom I am deeply indebted for their helps. Due to the space limitation, I can only acknowledge few of them here and apologize to those whom I do not name.

First and foremost, I would like to thank my co-supervisors, Dr. Joan Turner and Dr. Michael Hendzel. They gave me complete freedom to pursue what interests me most and, at the same time, provided all the guidance and support that I need throughout my PhD study. At the end, they transformed me from a naïve science-lover to someone who believes that he knows best of his field. It is simply beyond the capacity of language to express my appreciation for their great mentoring.

I would also like to thank Dr. David Murray and Dr. Gordon Chan for sitting on my supervisor committee and providing all those critical and invaluable comments and suggestions along the way when my research project was developed. Gordon has also been advising me on every step of career development over the years just like a big brother. I could not ask for better supervisor committee members. In addition, I would also express my heart-felt appreciation to Dr. Judith Hugh and Dr. Aly Karsan for sitting on my examining committee and providing insightful comments on my thesis.

I am extremely grateful to all the people in Turner's lab whom I have been lucky to work with for offering me a friendly environment that I have enjoyed during these six and half years, with special thanks to Ivy Ma who did many tedious lab works for me. In addition, I am also thankful to the Hendzel's lab, especially Darin McDonald for being my primary technical support all these years. It is hard to imagine how my exprements would be without Darin's helps.

I am greatly obliged to Cell Imaging Facility, Flow Cytometry Facility, and Dr. Xuejun Sun for their enormous technical supports. I am also indebted to Dr. Gordon Chan's lab, Dr. Mary Hitt's lab, Dr. Roseline Godbout's lab, and Dr. Andrew Shaw's lab for generously sharing their equipments and reagents with me.

I have benefited tremendously from the support and help that my old and new friends offered to me. I would like to say a big Thank-you to all of them, with special thanks to Dr. Qiang Shen and Ming Ye. Not only their precious friendship helped me through the difficult times, but also their suggestions inspired me on my research.

I owe my deepest gratitude to my family. I would like to thank my parents, my brother, my sister, and my in-laws. Without their helps and encouragements, I could not have started my doctoral study, let alone finish it. I would also like to thank my little Yishi (Angela) and Sishi (Andy), who were born during my study. Certainly, they are too young to provide any research suggestions, but their smile and happiness keep me away from frustration and depression, and make my life full of hopes. Finally, I would like to thank my wife, Wei Zheng. You are the amazing One. No word can express my gratefulness to you and I just want to say: I LOVE YOU!

Table of contents

List of Tables

List of Figures

List of Abbreviations

3-D: three-dimensional

APP: amyloid precursor protein

CDK: cyclin-dependent kinase

CKO: conditional knockout

CSC: cancer stem cell

CSL: CBF-1/Su(H)/Lag-1

DCIS: ductal carcinomas in situ

DMBA: 7,12-bimethylbenz(a)anthracene

dnMAML1: dominant negative MAML1

DOS: Delta and OSM-11-like proteins

DSB: DNA double-stranded break

DSL: Delta/Serrate/LAG-2

D/V: dorsal/ventral

ED: embryonic day

EGF: epidermal growth factor

EGFR: EGF receptor

ER: estrogen receptor

FDA: U.S. Food and Drug Administration

GFP: green fluorescence protein

GI: gastrointestinal

GSI: γ-secretase inhibitor

HAT: histone acetyltransferase

HD: hterodimerization domain

HDAC: histone deacetylase complex

HSC: hematopoietic stem cell

HUT: hyperplasias of usual type

IB: immunoblotting

IC_{50}: half maximal inhibitory concentration

ICD: intracellular domain

IDC: infiltrating ductal carcinoma

IHC: immunohistochemistry

ILC: infiltrating lobular carcinomas

IP: immunoprecipitation

ISC: intestinal stem cell

JIP1: JNK-interacting protein 1

JNK: c-Jun N-terminal kinase

Lfng: Lunatic fringe

LNR: Lin12-Notch repeats

LTR: long-terminal repeats

MFE: mammosphere forming efficiency

Mfng: Manic fringe

MMTV: mammary tumor virus

Mr: molecular weight

N1EXT: Notch1 extracellular truncation

NICD: Notch intracellular domain

NLS: nuclear localization sequence

NRR: negative regulatory region

PARP: Poly(ADP-ribose) polymerase

PEST: proline/glutamic acid/serine/threonine-rich motif

PR: progesterone receptor

RAM: RBPjκ association module

Rfng: Radical fringe

RNAi: RNA interference

SPP: signal peptide peptidase

SSB: DNA single-stranded break

T-ALL: T cell acute lymphoblastic leukemia

TA: transit-amplifying

TACE: TNF-α converted enzyme

TAD: transactivation domain

TCA: trichloroacetic acid

TMD: transmembrane domain

TNFα: tumor necrosis factor α

TNFR: TNF receptor

TPA: 12-O-tetradecanoylphorbol-13-acetate

VEGF: vascular endothelial growth factor

VEGFR: VEGF receptor

WAP: whey acidic protein

Chapter 1
Introduction

Over the past two decades, cancer research has shifted the paradigm of drug development from cell-based screening to targeted discovery and development, which relies on better understanding and rational targeting of molecular mechanisms underlying particular types of cancer. The success of Imatinib, which is highly effective against chronic myeloid leukemia, has demonstrated the power and advantages of this approach. Many oncogenic signaling pathways are now being explored as potential therapeutic targets, among which is the Notch signaling pathway. In breast cancer, the most common malignant tumour and one of the leading causes of cancer-related death among women worldwide, Notch signaling has been implicated in tumorigenesis and disease progression. In the present study, we used a breast cancer model system to explore the best approach for targeting the Notch signaling pathway for therapeutic benefit. The findings of this study will help us to design better strategies to block oncogenic Notch signaling not only in breast cancer, but also in other types of cancer such as T cell acute lymphoblastic leukemia (T-ALL) in which Notch signaling plays a causative role.

1.1 Breast cancer

1.1.1 Incidence, treatment and mortality

Breast cancer is the most common malignant tumour in women worldwide, with more than 1.2 million new cases every year. The incidence rate is higher in developed countries than in developing countries (1). In Canada, there were an estimated 22,700 new cases in 2009, representing more than a quarter of the newly diagnosed cancers in women. The likelihood of a Canadian woman developing breast cancer during her lifetime is as high as 1 in 9 (2). In the past two decades, the mortality rate of breast cancer in developed countries has started to drop (1). This is largely attributable to improvements in treatment and early detection by annual mammography screening. However, breast cancer is still the leading cause of cancer-related death among women worldwide, with more than 400,000 deaths every year (1). It has been estimated in 2009, one in

28 Canadian women will die from breast cancer (2). Therefore, there is still an urgent need to improve breast cancer management.

Currently, the standard practice for local management of early-stage breast cancer is breast conserving surgery followed by radiotherapy. Radiotherapy can reduce the 20-year local recurrence rate from 39% to 14% (3). Systemic adjuvant therapies, including chemotherapy, hormone therapy, and treatment with a monoclonal antibody (Trastuzumab) against HER2/neu—a receptor tyrosine kinase—are also often included based on the risk of relapse and the genetic nature of the disease and can further improve the rates of disease-free and overall survival (4, 5).

Two major approaches can lead to improved breast cancer treatment: (1) the development of prognostic and predictive markers to identify patients at high risk of recurrence who might benefit from specific therapies, and (2) the development of novel, more effective treatments. The last two decades have witnessed great progress in both of these areas.

1.1.2 Development of novel prognostic and predictive assays

Traditionally, decisions regarding the use of systemic adjuvant therapy in women with invasive breast cancer have been based on clinical and pathological features of the disease. These include patient age, tumor size, tumor grade, nodal status, and the expression of estrogen-receptor (ER), progesterone receptor (PR), and HER-2/neu. However, these factors are not definitive and as a result, some patients may be overtreated while others may receive inadequate treatment.

The rapid advancement of complementary DNA (cDNA) microarray technology makes the development of novel prognostic and predictive assays based on comprehensive gene expression profiles possible. A pioneering study by Perou et al. examined the expression profile of 8012 genes in 65 breast tumor tissue samples from 42 individuals, including 20 of 40 tumors that were sampled twice (6). They performed non-supervised hierarchical clustering analyses based on the similarity of the gene expression profile of a subset of 456 genes whose

expression showed greater variation between different tumors than between paired samples from the same tumors. Samples could be classified into four subtypes: luminal type, basal type, HER-2 type, and normal breast-like. The luminal type was ER+ and expressed at relatively high levels many genes that are expressed by breast luminal cells. Basal type and HER-2 type were both ER- but differed from one another in that the HER-2 type expressed a subset of genes whose expression levels were highly correlated with overexpression of HER-2. A subsequent, more extensive, study from the same group confirmed the presence of distinct subtypes and further divided the luminal type into luminal A and luminal B/C types. Most importantly, the clinical outcome of patients with different subtypes was significantly different, with luminal A subtype associated with the best outcome, and the basal-like and HER-2 positive subtypes associated with the shortest overall survival (7).

Other studies have used different sets of genes to successfully classify breast cancer patients into different subtypes with distinct clinical outcomes (8-10). Interestingly, there were few genes in common among these different molecular profiles. This raises the question as to whether different sets of signature genes can be used to reliably assign individual patients to correct groups. A recent study compared the three platforms (sets of genes) that were used to classify patients into five subtypes as described above (11). Although all three platforms could classify patients into subtypes associated with distinct outcomes, when assigning individual patients from three publicly available datasets to individual subtypes, there was only moderate agreement among the platforms except in the case of patients who were classified as basal subtype. There, the concordance of classifying patients into basal subtype was almost perfect. Together, these findings suggests that stringent standardisation of methodologies will be required before this technology can be used routinely in clinical practice.

Another approach based on cDNA microarray technology used supervised classification instead of non-supervised clustering to search for genes that can separate low-risk from high-risk breast cancer patients (12). Here, researchers compared the gene expression profiles of 44 patients who were disease-free for at least five years after their initial diagnosis with those of 34 patients who

developed distant metastases. They found that an expression profile of as few as 70 genes in combination could reliably separate the good prognosis group from the poor prognosis group with an accuracy of 83%. The prognostic value of this set of 70 genes has since been validated by independent studies, and now this molecular signature has been approved by the U.S. Food and Drug Administration (FDA) for clinical use under the trade name MammaPrint®. In addition to this 70-gene signature, several other platforms, including an activated wound response signature and recurrence-score, have been developed (13, 14).

Fan et al. investigated the concordance among these additional platforms and molecular classification assays. They used a single data set of 295 tumor samples to compare five different sets of signature genes: the 70- and 456-gene signatures, the wound response signature, the recurrence-score platform, and a two-gene-ratio model (15). Generally, these different platforms showed a significant degree of correlation. All the basal-type and 90% of the HER-2 type identified by the 456-gene platform were classified as poor prognosis by the 70-gene platform. In addition, 46 of 55 the luminal B type identified by the 456-gene platform were classified as poor prognosis by the 70-gene platform. Moderate variation occurred only in the samples from good-prognosis patients, with 30% of the luminal A subtype classified as poor prognosis by the 70-gene platform. In such cases, classification by the 70-gene platform might result in overtreatment whereas classification by the 456-gene signature might lead to under treatment.

These cDNA microarray based assays not only provide prognostic information but also may be of value in predicting the response of patients to specific therapies (16). De Ronde et al. compared mRNA molecular subtyping with subtyping of ER, PR, and HER-2 status by immunohistochemistry (IHC), and found that although there was good correlation between ER+ and luminal A/B subtypes, and between triple negative and basal subtypes, HER-2+ tumors were distributed among all molecular subtypes. Most interestingly, only 1 of 12 patients who were HER-2+ by IHC, but luminal A or luminal B by molecular subtyping, responded to the treatment with Trastuzumab and chemotherapy. In contrast, 12 of 21 patients who were molecularly classified as non-luminal types responded to

Trastuzumab and chemotherapy treatment. Thus, molecular subtyping based on cDNA microarray signatures may be of predictive value.

Although cDNA microarray assays have shown great promise, the requirement for fresh or frozen tissue poses a potential barrier for routine clinical use. Therefore, several groups are developing IHC-based classification methods. Makretsov et al. used tissue microarrays constructed from 438 primary breast tumors to examine the expression profile of 31 proteins (17). Using unsupervised hierarchical clustering analysis, they found that 19 of the 31 protein markers could be used to classify tumours into three groups with significantly different disease-specific survival and overall survival outcomes. These 19 proteins included ER, PR, HER-2/neu, cytokeratin 5/6 (CK5/6), and epidermal growth factor receptor (EGFR), all of which have previously been shown to be correlated with breast cancer prognosis. The study further suggested that ER/PR+ tumors might correspond to the luminal subtype classified by cDNA microarray, and that ER/PR/HER-2 triple negative tumors were correlated with the basal-like subtype.

A later study used tissue microarrays to examine the expression profile of 25 well-characterized tumor markers in 1076 breast cancer samples (18). Unsupervised hierarchical clustering analysis was used to divide these tumors into five major groups plus a sixth group that only had four cases. Groups 1 and 2 resembled the luminal A and luminal B subtypes identified by cDNA microarray assays in that these groups were mainly ER+ and were associated with the best prognosis. Group 5 was similar to the basal subtype identified by cDNA microarrays. Tumors in this group were ER- and showed high levels of p53. Interestingly, although samples in both groups 3 and 6 were characterized by overexpression of HER-2/neu, they showed different patterns of mucin 1 (MUC1) and E-cadherin (E-cad) staining. This distinction is physiologically meaningful as difference in the level of cleaved MUC1 isoform has been reported to affect patient's responses to Trastuzumab (19).

While the results of these approaches for classifying breast cancers into clinically distinct subtypes are encouraging, there are several caveats. First of all, the same classifiers (e.g., luminal A) do not always refer to the same groups of

tumors in different studies. Furthermore, different scoring systems were used to define IHC positivity and the range of expression of given protein markers (20). More work will be required to standardize and validate both the cDNA microarray- and IHC-based molecular classification platforms. Nonetheless, substantial progress has been made in the development of better prognostic and predictive assays. As application of these platforms is further refined, it will surely lead to improved clinical management of breast cancer.

1.1.3 Development of novel therapeutic reagents

Trastuzumab and aromatase inhibitors are two examples of the successful development of therapeutic agents that target known oncogenic signaling pathways. Trastuzumab, also called Herceptin, is a humanized monoclonal antibody against HER-2/neu. HER-2/neu is a receptor tyrosine kinase that is overexpressed in 30% of breast cancers due to gene amplification and its overexpression is correlated with worse clinical outcome (21). The FDA approved Trastuzumab in 1998 for treatment of HER-2/neu+ breast cancer. Randomised, controlled clinical trials have since shown that treatment with Trastuzumab for one year after adjuvant chemotherapy significantly benefited HER-2+ breast cancer patients in terms of both disease-free and overall survival (5).

Tamoxifen has been the gold standard of hormonal therapy for ER+ patients since its approval in 1986. It is an ER antagonist, effectively competing with estrogen for the ER, thereby blocking estrogen's mitogenic effect on the growth of breast epithelium. However, long term use of Tamoxifen increases the incidence of endometrial cancer as well as having other side effects (4). An alternative approach to inhibiting estrogen activity is to decrease its plasma level. In contrast to pre-menopausal women in whom estrogen is produced mostly in the ovary, the major source of estrogen in post-menopausal women is conversion of androgen to estrogen by aromatase (22). The effect of aromatase inhibition has been tested in clinical trials for almost 30 years (23). However, the lack of specificity and efficacy limited the use of first and second generation aromatase inhibitors. In contrast, third generation aromatase inhibitors that were developed ~10 years ago are more selective and potent and can suppress plasma estrogen levels by more than 80% (24-26). Several large clinical trials

have shown that third generation aromatase inhibitors are superior to tamoxifen in improving disease-free and overall survival (27, 28). In addition, the side effects of these new aromatase inhibitors are milder than those produced by tamoxifen. As a result, the American Society of Clinical Oncology recommends including an aromatase inhibitor in the treatment regimen of postmenopausal women with ER+ breast cancer (29).

Inspired by the success of Imatinib, a c-Abl-selective tyrosine kinase inhibitor, in treating chronic myeloid leukemia, there has been great interest in developing small molecule kinase inhibitors for other types of cancer. One of the most successful examples in breast cancer is Lapatinib, an EGFR/HER-2 dual kinase inhibitor. Early *in vitro* studies showed that Lapatinib alone could inhibit the growth of breast cancer cell lines and that Lapatinib in combination with tamoxifen could inhibit the growth of breast cancer cells that were resistant to tamoxifen alone (30, 31). In addition, the cellular response to Lapatinib was closely correlated with HER-2 expression levels (30). An early phase I study of Lapatinib in heavily pre-treated patients with metastases reported partial responses in four Trastuzumab-resistant breast cancer patients who overexpressed HER-2 and EGFR (32). A randomized phase III clinical trial comparing Lapatinib plus capecitabine *vs.* capecitabine alone in Trastuzumab-resistant advanced breast cancer patients showed that the addition of Lapatinib significantly delayed disease progression (33). This led to its approval for treatment of some patients (34).

The EGFR-selective kinase inhibitor Gefitinib has also been widely tested in clinical trials. About 20% of breast cancers overexpress EGFR, and its expression is associated with poor clinical outcomes (35). In addition, it has been shown that hormonal treatment could activate the EGFR signaling pathway, and that activated EGFR signaling contributes to the acquired resistance to hormonal treatment (36, 37). Clinical trials have so far reported contradictory results (38-45), a fact that underlies the importance of selecting appropriate patients for inclusion in trials that are directed towards specific molecular targets. However, it has been reported that EGFR expression levels do not predict the response to

Gefitinib (45), suggesting that further studies will be required to identify the relevant predictive factors.

Angiogenesis, the generation of new blood vessels, is required for the growth and metastasis of solid tumors. Vascular endothelial growth factor (VEGF) is an essential angiogenesis factor, and inhibition of the VEGF signaling pathway suppresses tumor growth in xenograft models (46). Two major approaches have been developed to inhibit VEGF-induced angiogenesis: monoclonal antibodies directed against VEGF (Avastin/Bevacizumab), and small molecule inhibitors (Sorafenib, Sunitinib, or Pazopanib) of VEGF receptor (VEGFR) kinase activity (47). Bevacizumab has been approved for the treatment of several types of metastatic solid tumors, including breast. Clinical trials using Sorafenib or Sunitinib alone showed no or very moderate therapeutic benefits in metastatic breast cancer and as a result, both agents are now being tested in combination with standard therapy (48-50). However, it should be noted that a recent study cautioned that short-term treatment with Sunitinib might accelerate metastasis and decrease overall survival (51).

Poly(ADP-ribose) polymerase (PARP) inhibitors are another class of small molecules that are of particular interest in breast cancer. PARP is an essential enzyme for the repair of DNA single-stranded breaks (SSB). Since ~10^4 SSBs occur spontaneously in each cell every day, it has been postulated that when PARP activity is inhibited, SSBs might be converted to double-stranded breaks (DSB) during DNA replication and, subsequently, repaired by homologous recombination. However, if there is a defect in DSB repair, as is the case in cells that lack functional BRCA1 and BRCA2, persistent DSBs could trigger cell cycle arrest and apoptosis. Therefore, PARP inhibition might selectively kill BRCA1/2 defective cells and be useful as a therapy for BRCA1/2 defective breast cancer. Confirmation of this hypothesis in *in vitro* studies spurred great interest in developing and testing PARP inhibitors in clinical settings (52, 53). Currently, eight PARP inhibitors are in clinical trials, and the first phase I trial showed very encouraging results (54). At a dose that is well tolerated, 12 of 19 *BRCA* mutation carriers who had ovarian, breast or prostate cancers benefited from PARP inhibitor treatment whereas this treatment was of no clinical benefit in

patients lacking the *BRCA* mutation (54). These results are very exciting because the *BRCA* mutation is associated with poor clinical outcome and, as yet, there is no effective targeted therapy. In addition, many triple negative breast cancer patients who lack the *BRCA* mutation might nonetheless have BRCA dysfunction as the result of promoter hypermethylation or the overexpression of its negative regulators (55, 56).

In addition, other proteins or signaling pathways, including Cox-2, farnesyl transferase, and G-proteins, are being explored as potential therapeutic targets in breast cancer. The Notch signaling pathway is a new member on the list.

1.2 Notch signaling pathway

1.2.1 Receptors and ligands

Notch receptors are evolutionarily conserved single-pass transmembrane proteins. The first member of this family, *Drosophila Notch*, was cloned in the early 1980s, about 70 years after the phenotype associated with its dysfunction—notches in the wings—was noticed (57, 58). Since then, members of this family from other species, including two Notch receptors in *C. elegans* (Lin-12 and GLP-1), and four Notch paralogs in mammals (Notch 1-4) have been cloned (59-65). They share similar structural domains with 29-36 tandem epidermal growth factor (EGF)-like repeats followed by three Lin12-Notch repeats (LNR) and a heterodimerization domain (HD) in their extracellular domain. Their intracellular domain (ICD) is composed of, sequentially, a RBPjκ association module (RAM) domain, an unstructured linker, seven ankyrin repeats (ANK domain) that are flanked by two nuclear localization sequences (NLS), a poorly defined transactivation domain (TAD), and the very C-terminal proline/glutamic acid/serine/threonine-rich (PEST) motif. *Drosophila* Notch also has a glutamine-rich OPA repeat (Figure 1-1) (66).

The ligands of Notch receptors are also a large family with both single-pass transmembrane proteins and diffusible secreted proteins. The first member of this family, *Drosophila Delta,* had been known long before its cloning to interact genetically with Notch (67). There are two ligands for Notch receptor in *Drosophila*—Delta and Serrate—but there are several members of this family in

C. elegans and in mammals. Based on their structural characteristics, they can be divided into four groups: DSL/DOS/EGF ligands, DSL/EGF ligands, DOS co-ligands, and non-canonical ligands (66). DSL/DOS/EGF ligands include *Drosophila* Delta, Serrate and mammalian Jagged1, Jagged2 and Delta-like 1 (Dll1). They all contain a DSL (Delta/Serrate/LAG-2) domain, a DOS (Delta and OSM-11-like proteins) domain, and several EGF-like repeats. Both DSL and DOS domains are involved in interactions with Notch receptors. Mammalian Dll3 and Dll4 and most of the *C. elegans* ligands are DSL/EGF-type ligands. They may act alone or in combination with DOS co-ligands, most members of which also function in *C. elegans*. Non-canonical ligands, including F3/contactin, NB-3, DNER, and MAGP-1/2, have neither DSL nor DOS domains. Activation of Notch signaling by F3/contactin, NB-3, or DNER has only been reported in the central nervous system and is essential for glia maturation (68-70). The physiological conditions under which the interactions between Notch receptors and MAGP-1/2 occur have not been established, but interestingly, MAGP-2 can not only interact with Notch receptors but also with Jagged1 to induce its cleavage (71, 72). More interestingly, while MAGP-2 activates Notch signaling in non-endothelial cells, it inhibits Notch signaling in endothelial cells (73).

1.2.2 Maturation and activation

Notch receptor maturation and activation is characterized by three proteolytic events that release Notch intracellular domain from the plasma membrane, which then translocates into the nucleus to activate target genes (Figure 1-2).

1.2.2.1 Furin-mediated S1 cleavage

The first cleavage, S1 cleavage, occurs in trans-Golgi and is mediated by furin proprotein convertase at a site ~ 70 amino acids N-terminal to the transmembrane domain (TMD). The two fragments produced by S1 cleavage, Notch extracellular (N^{EC}) and Notch transmembrane (N^{TM}), form a non-covalently linked bipartite protein at the cell surface (74, 75). Since a Notch1 mutant protein that is deleted of furin cleavage sites cannot be found at the cell surface, or is present at much reduced levels, S1 cleavage may be required for efficient delivery of mature Notch receptors to the plasma membrane (74, 76, 77).

Whether S1 cleavage is a general prerequisite for all Notch receptors is controversial. A human Notch2 receptor mutant that cannot be processed by furin showed no defects in reaching the cell surface or in its ability to be activated by Jagged-2 or Dll1 when expressed in U2OS cells (77). Moreover, as shown in Figure 1-1, most *Drosophila* Notch receptors are full-length proteins (78). To make things more complicated, a recent *in vivo* study reported that although most *Drosophila* Notch receptors are full-length proteins, S1 cleavage does occur in *Drosophila* and a mutant protein that cannot be processed cannot rescue the neurogenic phenotype associated with zygotic loss of *Notch* function. The S1 cleavage in *Drosophila* was not impaired when furin activity was inhibited, suggesting that an enzyme other than furin performs S1 cleavage in *Drosophila* (76).

1.2.2.2 Metalloprotease-mediated S2 cleavage

Metalloprotease-mediated S2 cleavage is a key regulatory step for Notch activation. The site of S2 cleavage, ~12 amino acids N-terminal to the TMD, lies within the HD domain. The crystal structure of the negative regulatory region (NRR) of the human Notch2 receptor has been resolved and sheds light on how the S2 cleavage is regulated (79). The NRR is composed of three LNR repeats and an HD domain. Extensive inter-domain contacts wrap the three LNR repeats around the HD domain to form a cauliflower-like structure. The S2 site is buried in an inaccessible pocket in the "stem" HD domain. Thus, receptor activation requires a conformational change that either disrupts the inter-domain interactions and/or destabilizes individual LNRs. It is interesting to note that each individual LNR is stabilized by a calcium ion, which can explain why calcium depletion can activate Notch receptors independent of ligand binding (80).

Based on the NRR structure, it was proposed that forces generated from ligand-binding lift the LNR repeats and expose the S2 sites to allow metalloprotease-mediated S2 cleavage (79). This concept is supported by two lines of evidence. The first used atomic force microscopy to directly measure the force required to detach Delta expressing S2 cells (S2-Dl) from Notch-expressing S2 cells (S2-N) (81). This force is ~50-250 times greater than that required to separate streptavidin from biotin, or an antibody from its antigen. The second study

showed that upon interaction with Notch receptors, both ligands and N^{EC} undergo endocytosis into ligand-expressing cells, even when S2 cleavage is inhibited (82). Therefore, it is possible that endocytosis of ligands bound to receptors generates a force that dissociates the N^{EC} from the N^{TM} at the S1 site, thus exposing the S2 site. However, dissociation of N^{EC} from N^{TM} might not be required to expose the S2 site.

The metalloprotease ADAM17, alternatively named TNF-α converted enzyme (TACE), was suggested to be responsible for the S2 cleavage when the S2 cleavage was first discovered (83). However, ADAM17 mutant mice do not show a Notch loss-of-function phenotype whereas ADAM10/Kuzbanian mutant mice and ADAM10/Kuzbanian mutant *Drosophila* do, suggesting that it is ADAM10, not ADAM17, that is required for S2 cleavage (84-88). This apparent conflict has been resolved by a recent study showing that ADAM10 is required for ligand-induced Notch activation and ADAM17 is required for ligand-independent activation, such as calcium depletion-induced Notch receptor activation (89). ADAM10 in the first study was incapable of performing S2 cleavage because N^{TM}, not full-length Notch, was the substrate (83). The different metalloprotease requirements of ligand-binding and calcium depletion-induced Notch receptor activation suggest that they might induce different conformational changes in the NRR that allow selective access to, and recognition by, ADAM10 *vs.* ADAM17.

1.2.2.3 γ-secretase-mediated S3 cleavage

The C-terminal product of S2 cleavage is immediately processed by γ-secretase, a multiprotein complex that is composed of presenilin, nicastrin, Pen2, and Aph1. There are two presenilin genes and two (human) or three (mice) Aph1 genes. Therefore, there can be four (human) or six (mice) different γ-secretase complexes. It has been reported that γ-secretase complexes containing different presenilins or different Aph1s exhibit distinct activities (90-92). Presenilin is the catalytic subunit and is present as a heterodimer of its N-terminal and C-terminal fragments. The function of other components is less well established. Nicastrin was initially thought to function as the substrate receptor (93). However, a recent study showed that the presenilin1/Pen2/Aph1a trimeric complex could cleave Notch and another substrate, amyloid precursor protein (APP), but is itself

unstable (94). Therefore, nicastrin might function to stabilize the complex. Pen2 was originally considered to be responsible for endoproteolytic processing of inactive full-length presenilin into the catalytically active heterodimer (95). However, a recent study suggests that the expression level of Pen2 might influence the equilibrium between PS1-containing and PS2-containing complexes (96). Aph1 was first described to stabilize the full length presenilin protein in the complex, but it has been shown that Aph1 associates with the γ-secretase substrate even when the complex is disassociated, suggesting that Aph1 may be the substrate receptor for γ-secretase (97). In addition, mutation in Aph1 also affects processing of full-length presenilin (98).

Physical interaction between Notch receptors and the γ-secretase complex is not the sole determinant of S3 cleavage. In fact, Notch was found to be associated with presenilin in the secretory pathway, but was protected from processing. This seemingly puzzling observation was later resolved by studies that showed that the efficiency of γ-secretase-mediated cleavage is greatly affected by the length of the extracellular domain and the nature of N-terminus (93, 99). This could explain why S2 cleavage is required for Notch receptor activation even after dissociation of N^{EC} from N^{TM}.

When the mouse Notch1 intracellular domain (N1ICD) produced from S3 cleavage was sequenced, it was found that N1ICD started with V1744 (mouse numbering, corresponding to human V1754) at its N-terminus. In addition, N1ICD levels were reduced when V1744 was mutated, suggesting that γ-secretase cleaved murine Notch1 between G1743 and V1744 (100). However, the V1744 mutant could be efficiently processed in a cell-free assay, suggesting that V1744 might contribute to the stability of N1ICD rather than being required for S3 cleavage (101). This was later confirmed by Tagami et al. (102). Using mass spectrometry and a cell-free cleavage assay, they first examined cleavage of N1EXTΔC, a fragment that lacks most of the extracellular and intracellular domains of mouse Notch1 protein. They found that the fragment could be cleaved between V1744 and L1745 (L+1), between L1745 and L1746 (L+2), and between L1746 and S1747 (S+3), in addition to between G1743 and V1744. More surprisingly, the highest peak corresponded to cleavage at the S+3 site.

They then confirmed the presence of the N1ICD-S fragment both in cells stimulated with Jagged-1 overexpressing cells and in fetal brain tissues. Although N1ICD-S is present in cells, it is less stable than N1ICD-V due to N-terminal rule-mediated degradation. Therefore, the S3 cleavage is imprecise with at least four potential cutting sites.

1.2.3 Notch signal strength regulation

1.2.3.1 Endocytosis.

Endocytosis regulates the function of both Notch receptors and ligands. Its role in Notch signaling was first deduced when the Notch-mediated neurogenesis was blocked in a *Drosophila* dynamin/shibire mutant background in which endocytosis was blocked (103, 104). Subsequently, other proteins involved in endocytosis, such as syntaxin/avalanche, Rab5, NF2/Merlin, Hrs, Lgd, Vps25, and epsin, have also been implicated in Notch signaling (Figure 1-3) (105-114).

1.2.3.1.1 Ligand monoubiquitination and endocytosis

Two models have been proposed by which ligand endocytosis could positively affect Notch signaling: the first by exerting pulling force required to activate Notch receptors and the second, by making ligands more competent. Nichols et al. examined the role of ligand endocytosis in dissociating N^{EC} from N^{TM}. They found that when Dll1-expressing cells were co-cultured with cells expressing Notch1, the dissociation of N^{EC} from N^{TM} and its co-localization with Dll1 in vesicular structures in the ligand-expressing cells accompanied receptor activation. However, when cells expressing a mutant Dll1 that lacks most of the intracellular domain and cannot be internalized were used, N^{EC} trans-endocytosis was inhibited and the receptor could not be activated. In addition, when a mutant dynamin or a mutant Eps 15 that was known to inhibit endocytosis was transiently transfected into ligand-expressing cells, both the N^{EC} transendocytosis and receptor activation were inhibited. Thus, the authors proposed that ligand endocytosis might generate pulling force to dissociate the N^{EC} from N^{TM} and in turn, induce conformational changes in the NRR region of Notch receptor that are required to active Notch receptors (82). However, this does not rule out the possibility that loss of ligand endocytosis failed to produce active ligands to dissociate and activate the receptor.

In the second model, Wang & Struhl used *Drosophila* with mutant Epsin/Lqf, an adaptor protein that recruits mono-ubiquitinated cell surface proteins to endocytic machinery (113). They found that lack of Epsin/Lqf in signal-sending (ligand-expressing) cells, but not in the signal-receiving (receptor expressing) cells, affects Notch activation. In addition, although seemingly normal accumulation of DSL ligands in endocytic compartments could be detected, there was a moderate decrease in the endocytosis of Delta in a sensitized background. This was interpreted as a requirement for Epsin/Lqf in a small subset of endocytic events that modify ligands during endocytosis and eventually recycle active ligands back to the cell surface. To support this interpretation, they showed that both the full-length (~105 kDa) and truncated (~50 kDa) forms of Delta were present in wild-type cells, but the truncated form was absent in the Epsin/Lqf mutant cells. In addition, replacement of the Delta intracellular domain with an internalization signal from a low density lipoprotein receptor that is associated with rapid recycling back to cell surface after entry into endosomes could bypass the need for Epsin in the activation Notch signaling. However, the presence of the truncated form of Delta could be interpreted as the result, rather than the cause, of receptor activation. In fact, murine Dll1 has been shown to be processed by metalloprotease and γ-secretase to generate truncated forms (115, 116). In addition, the authors failed to show that recycling of Delta or Delta/LDLR chimera to the cell surface is required for Notch activation. Thus, it is possible that Epsin/Lqf is only required for the endocytosis of receptor-bound ligand to generate pulling force and that these internalized ligands will then be cleaved to yield the truncated form.

The requirement for endocytosis and recycling to generate competent ligands was challenged recently (117). Consistent with previous studies, it was found that dynamin-null signal-sending cells could not activate Notch, but surprisingly, signal-sending cells that lack clathrin, the essential component for the clathrin-mediated endocytosis, and signal-sending cells that lack Rab5 or functional Rab11, essential regulators of the canonical recycling pathway, could still activate Notch receptor. Therefore, endocytosis may be required to generate pulling force but not to generate competent ligands to activate Notch receptor.

It is interesting that in Epsin/Lqf null cells Delta could be internalized whereas the receptor could not be activated (113). Thus, it is tempting to speculate that endocytosis could be regulating the availability of ligand on the cell surface. This has not been investigated previously, probably because to date, ligand endocytosis has only been found to positively regulate Notch signaling.

Since Epsin/Lqf functions by recruiting monoubiquitinated cell surface proteins to endocytic machinery, it is expected that ligands will be modified by monoubiquitination and that enzymes mediating this modification will also regulate the Notch signaling pathway. This is indeed the case. Neuralized and mind bomb, two ring finger E3 ubiquitin ligases, were found by genetic interaction studies to positively regulate Notch signaling long before being recognized as E3 ligases (118-121). In many systems, neuralized and mind bomb play redundant roles but neuralized might have preference for Delta-type ligand and mind bomb for Serate/Jagged (122, 123). There are two neuralized homologs (Neur-1 and Neur-2) and two mind bomb homologs (Mib-1 and Mib-2) in mammals. Although Neur-1/Neur-2 double mutants and Mib2 knockout mice are viable and grossly normal, conditional Mib-1 knockouts show phenotypes that are similar to loss of Notch function (124-126). To add to the complexity, recent studies showed that members of the Bearded family negatively regulate Notch signaling by competing with Delta for neuralized (127, 128).

1.2.3.1.2 Endocytosis-mediated receptor S3 cleavage

Cell surface Notch receptors are continuously internalized into early endosomes and then sorted to other endocytic compartments, including recycling endosomes, late endosomes, and lysosomes (129). Receptor internalization could affect Notch signaling in two ways: by facilitating S3 cleavage and by regulating availability of the receptor on the cell surface.

Gupta-Rossi et al. found that mouse Notch1 receptor was monoubiquitinated at K1749 during activation (130). Although the E3 ligase responsible for this monoubiquitination was not identified, they found that a K1749R mutant could not be internalized and was cleaved at the S3 site less efficiently, resulting in impaired Notch activation. In addition, S3 cleavage and activation of N1ΔE, a

fragment mimicking the C-terminal S2 cleavage product, was inhibited when cells were co-transfected with dominant negative dynamin (dynK44A) or dominant negative Eps15 (Eps15DN). Thus, they proposed that monoubiquitination at K1749 triggers the internalization of the S2 cleavage C-terminal product into endosomes where it is cleaved by γ-secretase.

A more comprehensive study later examined Notch receptor endocytosis and S3 cleavage in *Drosophila* cells with defects in different stages of endocytosis (Figure 1-4) (129). The mutants used included those involved in regulating cargo entry into early endosomes (e.g., dynamin/shirbie, GTPase Rab5, or endocytic syntaxin/avalanche); maturation of early endosomes to multivesicular bodies (e.g., Hrs); sorting multivesicular bodies (e.g., Tsg 101, Vps25, and Vps20); and in post-sorting but prelysosomal compartments (e.g., Fab1). When cell surface Notch receptors were labelled with an antibody against the extracellular domain, labelled Notch receptors in individual mutants were trapped in compartments that were consistent with the inactivation of function. Most interestingly and importantly, Notch activation was impaired in dynamin, Rab5, and Avalanche (Avl) mutants, unchanged in Hrs and Fab1 mutants, and enhanced in Tsg 101, Vps25, and Vps20 mutants. This impaired activation was correlated with decreased S3 cleavage. Based on these observations, the authors proposed that S3 cleavage occurs in mature endosomes. When the entry of Notch receptors into mature endosomes was blocked in dynamin, Rab5, and Avl mutants, the receptor could not be activated. On the other hand, when Notch receptors were trapped in mature endosomes in Tsg101, Vps25, and Vps20 mutants, they underwent ligand-independent activation. Why Notch activation was not affected in Hrs mutants remains unexplained.

Ligand-independent Notch activation in endosomes was also observed in *lethal (2) giant disc* (lgd) mutant cells (106, 107, 131). Lgd is a C2-domain protein and the C2 domain is required for its targeting to plasma membrane by binding to phospholipid. Overexpression or absence of Lgd induces general endosome trafficking defects and, consequently, ligand-independent Notch activation. Lgd acts downstream of Hrs as mutation of Rab5 or Hrs could suppress abnormal Lgd-induced Notch activation.

Based on these three studies, it was proposed that Notch S3 cleavage occurs in the endosome, not at the cell surface. However, this cannot explain how a non-cell permeable γ-secretase inhibitor (GSI) could inhibit the cleavage of N1ΔE (132). This question was partially resolved by a study that showed that γ-secretase could cleave Notch at different S3 cleavage sites to produce NICDs with distinct stability (102). It was proposed that S3 cleavage at the cell surface produces stable NICD, but cleavage within endosomes results in unstable NICD. However, shift in the S3 cleavage sites could not explain why Notch signaling was inhibited when the endocytosis was blocked by dominant negative dynamin, Rab5 or Avl, situations that should generate more stable NICD-V than unstable NICD forms. A possible explanation is that blocking endocytosis affected the pulling force generated from ligand binding, which would result in less S2 cleavage (66). However, this explanation does not account for all observations as N1ΔE, which does not require S2 cleavage, was used as substrate in some experiments (130).

1.2.3.1.3 Endocytosis-mediated receptor lysosomal degradation

When cell surface Notch receptors were pulse labelled with an antibody against its extracellular domain, the signal disappeared 5 h later, suggesting that surface labelled Notch receptors were internalized and degraded (129). This internalization was ligand-independent as it also occurred in Drosophila S2 cells where there was no detectable Notch ligand (133, 134). As endocytosis followed by lysosome degradation is a regulatory mechanism for many cell surface proteins, it was hypothesized that this would also be the case for Notch receptors.

Drosophila Deltex and Suppressor of Deltex [Su(dX] are a pair of Notch signaling regulators that act antagonistically on endocytosis-mediated activation and/or degradation of Notch receptor. Deltex was first discovered as a positive Notch signaling regulator through genetic interaction studies in *Drosophila* (135-137). This positive regulation is attributed to the ability of Deltex to promote Notch receptor endocytosis and trafficking to late endosomes/lysosomes, where Notch accumulates in the limiting membrane but not the internal compartments of lysosomes. The local environment in the lysosomes might somehow induce the

ligand-independent shedding of Notch extracellular domain and, consequently, γ-secretase-dependent Notch receptor activation (133, 138). Interestingly, when the maturation and fusion of later endosomes/lysosomes was inhibited by inactivation of the *Drosophila* HOPS complex or when protein trafficking to the limiting membrane was blocked by inactivation of AP-3 complex, Deltex-mediated endocytosis resulted in down-regulation rather than up-regulation of Notch signaling (138). This could explain why Deltex negatively regulates Notch signaling in some contexts (139-141). In addition, Kurtz, the *Drosophila* homolog of non-visual β-arrestin whose functions traditionally were attributed to internalization and desensitization of G-protein coupled receptors, was recently discovered to form a trimeric complex with Notch and Deltex to induce Notch polyubiquitination and degradation (141). Whether the formation of this trimeric complex will affect endosomal sorting of Notch receptors within the endosomal machinery has not been investigated. However, it should be noted that complete elimination of Deltex in *Drosophila* only affected a small subset of Notch signaling, suggesting that Deltex is not essential for most Notch signaling (142). There are four Deltex homologs in mammals that might function redundantly (143, 144).

Su(dX) is a HECT-type E3 ubiquitin ligase and an early genetic interaction study showed that it could suppress the phenotypes induced by the Deltex mutation and negatively regulate Notch signaling in some, but not all, tissues (145). Antagonism of Deltex activity is not mediated by promoting Deltex degradation or preventing Deltex-induced internalization of full-length cell surface Notch receptors in the absence of ligand. Rather, it prevents the retention of Notch receptor at the limiting membrane of late endosomes/lysosomes and results in accumulation of Notch receptors in the internal compartment of lysosomes where receptors will be degraded (146). Also, when Notch was coexpressed with a truncated Su(dX) that lacks its HECT E3 ligase domain, full-length Notch colocalized with Rab11, a marker of recycling endosomal compartment (146). This suggests that Su(dX) might also prevent internalized full-length Notch receptor recycling back to the plasma membrane so that Notch receptor would be sorted into lysosomes for degradation. This regulatory mechanism of Su(dX) also applies to its mammalian homologs, Itch in mice and IAP4 in humans (147).

However, in contrast to Su(dX), AIP4 has also been reported to promote the lysosomal degradation of human Deltex1 (148).

Nedd4 is another HECT E3 ligase that belongs to the same family as Itch/Su(dX). It also negatively regulates Notch signaling in *Drosophila* but at a level that is different from Itch/Su(dX) (149). Expression of an E3 ligase defective truncated Nedd4 or knockdown of Nedd4 by RNAi results in accumulation of full-length Notch receptors at the plasma membrane and ligand-independent Notch activation. Therefore, ubiquitination of Notch receptor by Nedd4 promotes its internalization and reduces its availability for ligands. In addition, inactivating Nedd4 could enhance the Deltex protein level in *Drosophila* S2 cells cotransfected with Notch and Deltex, suggesting Nedd4 might also negatively regulate Notch signaling by promoting the degradation of Deltex. This is in contrast to Su(dX), which does not affect Deltex stability (146). Besides Su(dX)/Itch/IAP4 and Nedd4, another E3 ligase—c-Cbl, has also been reported to induce polyubiquitination and lysosomal degradation of membrane-associated Notch1 receptor, although the details of this regulation are not known (150).

Numb is another negative Notch signaling regulator that promotes Notch internalization and degradation. Numb was first shown to antagonize Notch signaling during asymmetric division of sensory organ precursor cells (151, 152). In this developmental context, Numb is asymmetrically distributed, being present in one daughter cell but absent in the other. Notch signaling is only active in the daughter cell that does not have Numb. It was proposed that Numb induces Notch endocytosis and degradation via interactions with Sanpodo (153, 154). Although the details are still lacking, a genetic interaction study in *Drosophila* has shown that Sanpodo positively regulates Notch signaling downstream of, or in parallel to, ligand binding, but upstream of S3 cleavage (153). Sanpodo could physically interact with both Notch receptor and Numb, and Numb physically associates with α-Adaptin, a protein involved in clathrin-mediated endocytosis. Through these physical interactions, Notch might be internalized for lysosomal degradation. Consistent with this model, in the Numb-containing daughter cell Sanpodo is present in both Rab 5 (early endosomes) and Rab 7 (later endosomes) positive intracellular vesicles, but is barely detected at the cell

surface or in Rab 11 positive intracellular vesicles (recycling endosomes). In cells that lack Numb, Sanpodo is mainly present at the cell surface (154). However, cell surface Notch receptor levels are comparable in two daughter cells, suggesting that depleting Sanpodo, rather than cell surface Notch receptor, is required and sufficient to inhibit Notch signaling in Numb-containing daughter cells.

However, this model was recently challenged by a study that showed endocytosis of Sanpodo and down-regulation of Notch signaling could be uncoupled (155). Through biochemical studies, a N-terminal NPAF motif of Sanpodo was found to associate with the phosphotyrosine-binding domain of Numb. In the presence of Numb, deletion or mutation of NPAF motif resulted in accumulation of Sanpodo at the cell surface. However, expression of this mutant *in vivo* could not rescue the inhibition of Notch signaling by Numb, suggesting that Numb could down-regulate Notch signaling independent of Sanpodo. Also, since Sanpodo has only been shown to be required for Notch signaling during asymmetric cell division and a mammalian Sanpodo homolog has yet to be identified (153), the mechanism by which Numb down-regulates Notch signaling via Sanpodo might not apply to mammalian cells.

In mammalian cells, Numb was proposed to down-regulate Notch signaling by modifying the post-endocytic trafficking of Notch receptors (156). When full-length Notch1 was expressed in HEK293T cells, it was continually internalized as evidenced by loss of pre-labelled receptor from the cell surface. However, a fraction of internalized Notch1 receptors was recycled back to the cell surface within 15 minutes. Although Numb overexpression or knockdown did not affect receptor internalization from the cell surface, overexpression of Numb accelerated the loss of both intracellular and total pre-labelled receptors, suggesting that overexpression of Numb promoted receptor degradation. In contrast, Numb knockdown accelerated only the loss of the intracellular pool without affecting the total amount of pre-labelled Notch receptors, suggesting that knockdown of Numb promoted recycling of receptors back to the cell surface. Furthermore, a truncated Numb that lacks the domain involved in interaction with α-Adaptin could not affect the levels of either the total or the intracellular pools of

pre-labelled Notch receptors. In contrast, mutant Numb that cannot interact with Itch/AIP4 caused accumulation of the intracellular pool without affecting the total of pre-labelled molecules, suggesting that interaction with endocytic machinery is required for trafficking of internalized receptor to later endosomes/lysosomes, and that interaction with Itch/IAP4 is required for degradation of receptor in later endosome/lysosomes.

The activity of Numb in down-regulating Notch signaling is also tightly controlled. One such example is the temporal control that couples Numb activity to the progression of cell cycle. During the development of sensory organ in *Drosophila*, Numb expression is restored in Numb-negative cells after asymmetric cell division. However, Numb does not block the Notch signaling involved in lateral inhibition in resting cells. How Numb could down-regulate Notch signaling immediately after mitosis in order to specify the cell fate of two daughter cells, but then quickly lose its activity, has been puzzling. A possible explanation comes unexpectedly from Golgi (157). Through yeast two-hybrid screening, ACBD3, a Golgi protein, was found to physically interact with Numb and regulate Numb activity. ACBD3 is sequestered in Golgi during interphase of the cell cycle and cannot interact with Numb. As a result, Numb cannot down-regulate Notch signaling during interphase. However, Golgi is fragmented during mitosis and releases ACBD3 into cytosol, upon which ACBD3 binds to Numb via an evolutionarily conserved N-terminal domain of Numb. In this manner, ACBD3 down-regulates Notch signaling. When ACBD3 is forced to stay in the cytoplasm by myristoylation, Numb can inhibit Notch signaling throughout the cell cycle.

Numb protein levels are also regulated by several E3 ligases, including MDM2 and LNX (ligand of Numb-protein X) (158, 159). Although the functional significance of MDM2 in regulating Notch signaling has not been reported, LNX has been shown to be a positive regulator of Notch signaling. When LNX was cotransfected with N1ΔE, it could enhance the transactivation of a reporter gene by Notch *in vitro*. The physiological relevance of this regulation is not known.

1.2.3.2 Phosphorylation, polyubiquitination and NICD stability

Exogenously expressed Notch 1 intracellular domain (N1ICD) or ligand-induced

N2ICD have been detected as multiply phosphorylated forms in the cell nucleus (160-162), and subsequent studies revealed that phosphorylation could both positively and negatively regulate NICD stability.

Sel-10, an F-box E3 ligase, was first identified through genetic screening to negatively regulate Notch signaling in *C. elegans* (163). Since it is composed mainly of an F-box domain that is essential for the formation of the E3 ligase complex and a seven-WD40 repeat domain that acts as a substrate receptor for the E3 ligase complex, a truncated form (Sel-10ΔF) that lacks the F-box domain should still be able to interact with its substrate but as a dominant negative protein. When such a truncated form of murine FBW7/Sel10 homolog was cotransfected with different forms of Notch1 protein into HEK293T cells, it was found that SEL-10ΔF physically interacted only with NICD, but not with cell surface Notch receptors, or a truncated NICD that lacks the PEST domain (164). This interaction was dependent on a phosphorylation event that was later found to be mediated by CDK8 (164, 165). Although cotransfection of wild-type FBW7/SEL-10 with N1ICD did not affect the stability of N1ICD, SEL-10ΔF stabilized N1ICD and enhanced its transactivation activity (164, 166). Cotransfection of N1ICD with both wild-type FBW7/SEL-10 and CDK8 resulted in rapid degradation of N1ICD (165). Therefore, phosphorylation of N1ICD by CDK8 could lead to its polyubiquitination and proteasome degradation, which down-regulates Notch signaling.

In contrast, phosphorylation by GSK-3β stabilized N1ICD (167). Although cotransfection of wild-type GSK-3β and N1ICD does not affect N1ICD phosphorylation levels, treatment with a GSK-3β inhibitor or cotransfection with a dominant negative form of GSK-3β reduced N1ICD phosphorylation. In parallel, treatment with a GSK-3β inhibitor or cotransfection with a dominant negative form of GSK-3β enhanced N1ICD turnover, which could be blocked by proteasome inhibitors, suggesting that phosphorylation by GSK-3β could inhibit N1ICD proteosomal degradation and enhance Notch signaling activity. Consistent with this, the induction of a reporter gene by transfection of N1ICD was stronger in wild-type cells compared to GSK-3β null cells. This stabilization

of N1ICD by GSK-3β mediated phosphorylation might partially account for previous observations that *Drosophila* GSK-3β acts downstream of Notch in lateral inhibition during neurogenesis (168).

However, the consequences of phosphorylation of NICD by GSK-3β might be paralog-dependent. GSK-3β was shown to physically interact with N2ICD via its sixth [should be seventh, according to recent the crystal structure (169)] ANK repeat and phosphorylate several amino acid residues C-terminal to the binding site (170). Co-transfection with GSK-3β did not affect N2ICD protein levels, but inhibited its ability to transactivate a reporter gene. Treatment with the GSK-3β inhibitor LiCl reversed this inhibition. In addition, mRNA levels of two Notch target genes were increased in HEK293T cells treated with LiCl, suggesting that inhibition of endogenous GSK-3β downregulated Notch signaling in non-transfected HEK293T cells. It is not known whether N2ICD signaling is more active than N1ICD signaling in HEK293T cells. However, the discrepancy between this study and the previous one suggests that the effect of GSK-3β-mediated phosphorylation on Notch signaling is paralog-dependent and/or context-dependent.

DYRK1A kinase is another serine/threonine protein kinase that can phosphorylate NICD and down-regulate Notch signaling (171). Similar to the effect of GSK-3β on N2ICD, phosphorylation of N1ICD by DYRK1A did not affect its half-life but attenuated the endogenous Notch signaling both in cultured cells and in the developing neural tube of chicken embryos.

Nemo-like kinase (NLK) was reported to modulate Notch signaling by phosphorylating NICD (172). Interestingly, when NLK was co-transfected into mouse neuroblastoma neuro2a cells together with the NICD of four murine Notch paralogs, it inhibited N1ICD-induced, but enhanced N3IC-induced, reporter gene transactivation without affecting N2IC- or N4IC-induced transactivation. This was dependent on the kinase activity of NLK. Further experiments demonstrated that NLK could phosphorylate N1ICD ANK repeats and impair the formation of the N1ICD/RBPjκ/MAML1 transactivation complex. This regulation has physiological

relevance as previous genetic screens identified *nemo*, the *Drosophila* NLK homolog, as a modifier of Notch signaling (173)

Akt has also been reported to phosphorylate N1ICD and attenuate its transactivation activity (174). Uniquely, Akt phosphorylation induced mislocation of N1ICD from a predominantly nuclear protein to accumulation in perinuclear regions. The physiological relevance of this phosphorylation is uncertain.

1.2.3.3 Receptor glycosylation

Notch receptor glycosylation also regulates Notch signaling. About 10 years ago, three studies showed that Fringe, a known Notch signaling modulator, encodes a glycosyltransferase that extends the *O*-linked fucose moieties on EGF repeats in the Notch extracellular domain with N-acetylglucosamine (175-177). The initial modification of Notch EGF repeats with *O*-linked fucose is mediated by OFUT1 in *Drosophila* and POFUT1 in mammals (178, 179).

1.2.3.3.1 Fucosylation

OFUT1 knockdown affects Notch-dependent lateral inhibition and cell lineage decision, and POFUT1 knockout is embryonically lethal in mice (178, 179). A modified form of Notch receptor secreted from OFUT1 knockdown cells showed reduced binding to ligand-expressing cells (180). Thus, it was proposed that receptor fucosylation regulated receptor-ligand binding and that this was the mechanism underlying the essential requirement of OFUT1/POFUT1 in Notch signaling. However, it was later shown that OFUT1/POFUT1 regulated Notch signaling, in part, by acting as a chaperone during Notch receptor delivery to the plasma membrane (181). In wild-type *Drosophila* wing cells, Notch is mainly present at the cell surface, but in OFUT1 knockdown cells, Notch is located throughout the cytoplasm. When cells were double-stained for Notch and markers for endoplasmic reticulum, Golgi, early endosomes, or later endosomes, Notch was found to be colocalized with endoplasmic reticulum markers. OFUT1 was also present in endoplasmic reticulum although at the time, there was no reported GDP-fucose transporter activity in endoplasmic reticulum. [An endoplasmic reticulum-specific GDP-fucose transporter was recently identified in Drosophila (182)]. Thus, OFUT1 might facilitate Notch receptor delivery to the

cell surface independently of its fucosyltransferase activity. Indeed, two enzymatically inactive OFUT1 mutants could restore Notch relocation to the cell surface. Since OFUT1 can physically associate with Notch EGF repeats, OFUT1 may act as a chaperone during Notch receptor trafficking to the plasma membrane. Identification of this non-enzymatic activity of OFUT1 could explain why, in *Drosophila,* loss of OFUT1 results in a more severe phenotype than does of loss of Fringe (179).

The relative contributions of the enzymatic and non-enzymatic activities of OFUT1/POFUT1 to Notch signaling were examined in *Drosophila* (183). Surprisingly, *Drosophila* expressing enzymatically inactive OFUT1 in an OFUT1 null genetic background could complete embryogenesis but died after hatching. This suggested that *O*-fucosylation was not required for most Notch signaling. The defective neurogenesis phenotype that resulted from insufficient Notch signaling in an OFUT1 null background could be completely rescued by an enzymatically inactive form of OFUT1. However, there were defects in the wing imaginal disc and the phenotype was identical to that resulting from loss of Fringe. This was consistent with the fact that Fringe-mediated glycosylation was based on the presence of *O*-fucose. Therefore, OFUT1 enzymatic activity was only needed when Fringe activity was required for Notch signaling that occured in the developmental contexts examined. It is still possible that fucosylation by OFUT1 has a role beyond providing *O*-fucose for Fringe as altering fucosylation status on the EGF repeats affected ligand binding in the absence of Fringe. Regardless, there is debate as to whether chaperone function is the major non-enzymatic activity of OFUT1. Others have found that the non-enzymatic activity of OFUT1 played an important role in regulating Notch signaling, but this was attributed mainly to its essential role in receptor endocytosis and trafficking to lysosomes for degradation (184).

There are also conflicting data concerning the phenotype of loss of mammalian POFUT1. One study reported that in the absence of POFUT1, there was no defect in Notch receptors reaching the cell surface as comparable levels of cell surface proteins of all four Notch paralogs were detected in both $POFUT1^{+/+}$ and $POFUT1^{-/-}$ mouse embryonic stem (ES) cells(185). In addition, although ligand-

dependent Notch signaling was impaired in POFUT1$^{-/-}$ ES cells, calcium depletion-induced ligand-independent Notch signaling was comparable to that in POFUT1$^{+/+}$ ES cells. This indicated that there were comparable levels of cell surface Notch receptors in POFUT1$^{-/-}$ ES cells. However, another study reported no detectable cell surface Notch1 protein in presomitic mesoderm of POFUT1$^{-/-}$ embryos (186). Rather, most Notch1 proteins were co-localized with an endoplasmic reticulum marker while a small fraction co-localized with caveolin, a marker for clathrin-independent endocytic machinery in POFUT1$^{-/-}$ presomitic mesoderm. A simple explanation for the discrepancy regarding the location of Notch1 protein in the absence of POFUT1 is that these studies used cells representing different developmental stages in which the requirement for POFUT1 might differ. Nonetheless, this suggests a complicated role for POFUT1 in Notch signaling.

1.2.3.3.2 Fringe-mediated glycosylation

The regulation of Notch signaling by Fringe-mediated glycosylation is even more complicated than fucosylation, especially in mammals, as there are three Fringe proteins [Lunatic (Lfng), Manic (Mfng), and Radical (Rfng) Fringe] as compared to a single POFUT1. Although in *Drosophila*, Fringe-mediated modification of Notch EGF repeats generally enhances the binding of Delta to the receptor, but inhibits Serrate binding to receptor (180), the effect of Fringe-mediated modification on ligand-receptor interaction in mammals depends on which receptor, which ligand, which Fringe, and the tissues involved.

Both ligand-specific and receptor-specific effects on Notch signaling were demonstrated when Lfng was cotransfected with Notch into either myoblast C2C12 cells or NIH3T3 fibroblasts (187). Dll1-induced Notch1 signaling was enhanced but Jagged-1-induced Notch1 signaling was suppressed, demonstrating the ligand-specific effect of Fringe-mediated glycosylation. This effect seemed to be correlated with the reported effect of *Drosophila* Fringe on ligand binding. However, the binding of Jagged-1 to Notch1 receptor was not affected. Even more puzzling, Lfng co-expression enhanced both Dll1-induced and Jagged-1-induced Notch2 signaling in myoblast C2C12 cells, suggesting that the effect of glycosylation is not only ligand-specific but also receptor-specific.

The effect of glycosylation on Notch signaling is also dependent on which Fringe extends the *O*-fucose glycan as demonstrated by Yang et al. (188). Consistent with the previous study, they also found that Lfng enhanced Dll1-induced, but suppressed Jagged-1-induced, Notch1 signaling. However, although Mfng inhibited Jagged-1 induced Notch1 signaling in a manner comparable to that of Lfng, enhancement of Dll-1 induced Notch1 signaling by Mfng was much weaker than that of Lfng. In sharp contrast, Rfng enhanced both Dll1- and Jagged-1-induced Notch signaling in NIH3T3 cells. The effect of different Fringe family members on Notch signaling was not directly correlated with the effect on the amount of ligands bound to Notch1 receptor. However, it was noted that the differential effects of Lfng on Dll1- and Jagged-1-induced Notch signaling were correlated with their effects on the ligand-induced, but not calcium-depletion-induced ligand-independent, S2 cleavage, and consequently, the generation of active NICD. This suggests that although modification by Fringe does not affect the binding of the ligand to the receptor, it could affect the affinity of their interaction and thus the pulling force that their interaction could exert (66, 188).

Additionally, the effect of Fringe on Notch signaling is also context-dependent. Although Lfng has been shown to enhance Dll1-induced Notch signaling in most cell types (187-189), it has been suggested to inhibit Notch signaling *in vivo* during somite development where Dll1 is the only ligand expressed (190, 191).

In addition to receptor glycosylation, ligands could also be modified by glycosylation (192). However, since glycosylation only affects Notch signaling when expressed in signal-receiving cells, and glycosylation occurs in endoplasmic reticulum and Golgi, the functional significance of ligand glycosylation is not known (181, 188, 193, 194). Furthermore, other types of glycosylation, such as *O*-glucosylation and xylosylation together with the enzymes required for these types of modifications, have also recently been identified (195, 196). Thus, our understanding of the role of glycosylation in Notch signaling will be rapidly evolving.

1.2.3.4 Other regulators

Several other proteins have been suggested to regulate Notch signaling but

could not be classified into the above categories. Big Brain (Bib), Cripto-1, and d-Asb11 are three examples. *Bib*, the *Drosophila* homolog of aquaporin, is one of the earliest identified neurogenic genes in *Drosophila* and is known to genetically interact with Notch. A recent study suggests that Bib might regulate Notch signaling by affecting the release of NICD from endosomes to allow it to translocate into the nucleus (197). Cripto-1 is the co-receptor for Nodal, another essential molecule for embryonic development. Notch3 was identified in a yeast two-hybrid screening as a candidate Cripto-1-interacting protein. In addition, the other three Notch paralogs were also found to be able to interact with Cripto (198). Since these interactions were mainly found in endoplasmic reticulum/Golgi, Cripto-1 might function as a chaperone to facilitate proper folding and S1 cleavage of Notch receptors before they reach cell surface. Zebrafish d-Asb11 is a member of SOCS-box-containing protein family which is involved in ubiquitination and degradation of target proteins (199). d-Asb11 specifically interacts with DeltaA but not DeltaD and induces its ubiquitination and degradation (200). Thus, d-Asb11 could activate Notch signaling when it was overexpressed in signal-receiving cells but inhibit Notch signaling when it was overexpressed in signal-sending cells, consistent with the well-known cell-autonomous inhibitory and non-cell autonomous activating role of the ligands (201).

1.2.4 Canonical signaling pathway

In the canonical Notch signaling pathway, the key feature of Notch signaling induced trans-activation of target genes is the switch from a CSL-based transcription repressor complex to a CSL-based transcription activator complex.

CSL [CBF-1/Su(H)/Lag-1] is a family of evolutionary conserved DNA binding proteins. CBF-1, also referred to as RBPjκ, is the mammalian homolog and Su(H) and Lag-1 are the *Drosophila* and *C. elegans* homologs, respectively. RBPjκ shares about 80% and 55% of sequence identify with Su(H) and Lag-1, respectively. CSL proteins bind to the consensus DNA sequence CGTGGGAA (202). It is generally believed that in the absence of active NICD, CSL acts as a transcription repressor by recruiting several general or unique transcription co-repressor proteins to the promoter region of Notch target genes to block their

expression. This is supported by the observation that loss of Su(H) could induce the expression of some Notch target genes, even when Notch signaling was blocked by depleting γ-secretase activity (203, 204).

In *Drosophila*, Hairless, a well characterized antagonist of Su(H), acts as an adaptor to recruit two general co-repressors, dCtBP and Groucho, that in turn, recruit histone deacetylase (HDAC) complexes to modify local chromatin structure and block transcription (205). A Hairless homolog has yet to be identified in mammals, although SHARP could act as an adaptor to recruit CtIP/CtBP to RBPjκ binding sites to repress gene expression (206). Several other repressor proteins, such as CBF-1 interacting co-repressor (CIR), SMRT/NCoR, and KyoT2/FLH1C, have also been shown to repress the expression of Notch target genes in some circumstances (207-209). Interestingly and surprisingly, a recent study showed that Asf1, a histone H3/4 chaperone, could specifically repress Notch target genes (210). However, in the absence of active NICD, loss of Su(H) induced only a subset of the genes examined, suggesting that Su(H) represses some, but not all, Notch target genes (203). Consistent with this, in the absence of active Notch signaling, Su(H) bound to the promoter of only 2 of 11 Notch target genes examined, and the expression of these two genes was elevated when Su(H) was depleted by RNAi. For most other genes examined, Su(H) did not occupy the CSL-binding sites at the promoter/enhancer region and Notch activation by calcium depletion induced only a transient interaction between Su(H) and their promoter/ enhancer regions. Therefore, gene repression by CSL in the absence of Notch signaling is not a universal phenomenon among Notch target genes. This could partially explain the discrepancy between the phenotypes resulting from loss of CSL function and gain of Notch function (204). However, it remains to be investigated how Notch activation could induce Su(H) binding to the promoter region of Notch target genes.

After activation of Notch signaling, active NICD translocates into the nucleus and binds to CSL, which leads to the replacement of co-repressor proteins on CSL. The RAM domain of NICD is the major contributor to the affinity between NICD and CSL and was the only domain initially found able to interact with CSL when

co-expressed in cells (211). Although the RAM domain was originally poorly defined as the domain between the S3 cleavage site and the ANK domain, recent studies found that only the first ~20 amino acid residues centered around a WFP motif are essential and sufficient for its interaction with CSL (212, 213). These ~20 amino acid residues are highly conserved and there are no differences in the estimated affinities between RBPjκ and the RAM domain of four individual mammalian Notch paralogs (212).

In addition to NICD and CSL, the formation of a transcription activator complex also needs another protein—mastermind in *Drosophila* or its homologs in mammals (MAML 1-3) (214-217). Mastermind and MAMLs are large nuclear proteins, composed of ~1000-1600 amino acid residues. They share relatively high amino acid similarity in the N-terminal basic domains, where the sequence required for formation of NICD/CSL/MAML is located (amino acid residues 13-74 of human MAML1) (218). However, the overall homology among three human MAMLs is only about 20~35%.

Although Mastermind/MAML could form a stable complex with CSL and NICD, it was not able to interact with any of them alone (216). This paradox was resolved by two studies that determined the structures of CSL/NICD/MAML bound to DNA—one using *C. elegans* homologs and the other using human counterparts (213, 219). Both structures showed that CSL protein adopts a three-domain structure with an N-terminal domain (NTD), a β-trefoil domain (BTD), and a C-terminal domain (CTD). The NTD and CTD domains are structurally similar to the RHC-N and RHC-C domains of NF-κB. The trimeric protein complex binds to DNA via the NTD and BTD of CSL protein. The ANK domain of NICD makes extensive contacts with CSL at two discontinuous surfaces, the major one between the N-terminal ANK repeats and CTD of CSL and a minor one between the C-terminal ANK repeats and NTD of CSL. Association of the NICD ANK domain with CSL creates a groove where ~ 50 amino acid residues of the MAML1 basic domain sit to conceal the NICD ANK:CSL interface from the solvent. The NICD fragment used in the study of the *C. elegans* complex structure contains the RAM domain, and the structure showed that the first 25

amino acid residues of RAM domain were associated with the BTD of CSL. The sequence between these 25 residues and the ANK domain was unstructured.

The formation of a stable trimeric complex in the absence of NICD RAM domain raised an interesting question: what is the role of RAM domain in the formation of a transcriptionally active complex *in vivo* as it is the only structural domain of NICD that could associate with CSL in the absence of MAML? Friedmann et al. compared the structure of DNA-bound CSL in the presence and absence of NICD RAM domain and found that association of CSL with the RAM domain induced a conformation change in the hairpin loop in the NTD from a closed state to an open state (220). This conformation change is required for MAML to interact with CSL. Interestingly, although the RAM domain was not included in the N1ICD fragment used in the human trimeric complex structural study, the NTD hairpin loop adopted an open conformation (219, 221).

Since less than 20 amino acid residues within the N-terminal part of the poorly defined RAM domain interacted with CSL and showed an ordered structure upon binding to CSL, and the sequence between these ~20 amino acid residues and ANK domain did not adopt any ordered structure in the crystallography study, this also raised another intriguing question as to whether this linker region has any effect on the formation of a trans-activation complex. Bertagna et al. noticed that although the sequence of this linker region is not conserved, its length is highly conserved and just fits the space between the RAM binding sites and the binding sites of N-terminal ANK domain (222). By computation modelling, they found that although the binding of the RAM domain and the ANK domain to CSL are two thermodynamically independent events, binding of the RAM domain to CSL will increase the effective concentration of the ANK domain that is available to CSL if both are present in the same chain.

Taken together, it was proposed that when active NICD enters nucleus, the RAM domain of NICD binds to the BTD of CSL and increases the local concentration of the NICD ANK domain to facilitate the interaction between the ANK domain and CSL. Interaction between ANK domain and CSL creates a groove for the N-terminus of MAMLs. At the same time, RAM binding induces a conformational

change in the NTD of CSL to facilitate docking of MAMLs to the complex. Binding of MAML conceals the interface between the NICD ANK domain and CSL and stabilizes the trimeric complex. It should be noted that two NICD/CSL/MAML trimeric complexes could further dimerize given that they sit on two CSL binding sites with correct orientation and space (223). The amino acid residues involved in dimerization are conserved among the four human Notch paralogs, raising the possibility that two trimeric complexes containing different NICD paralogs could dimerize to fine tune Notch signaling.

After the formation of the NICD/CSL/MAML core complex, mastermind/MAMLs could recruit other transcription co-activators, including histone acetyltransferases (HATs), to the complex to facilitate transcription. Although two early studies reported that NICD could interact with p300 directly, and with PCAF directly or indirectly, two later studies showed that p300 interacts with MAML1 more strongly than with N1ICD (224-227). In addition, the PCAF-interacting region within N1ICD overlaps with that required for association with mastermind/MAML (225). Therefore, it is most likely that mastermind/MAMLs act as adaptors to recruit HAT to the transactivation complex. MAML1 interacts with p300 via its amino acid residues 75-300, just C-terminal to the region required for association with NICD/CSL (227). Although a truncated fragment containing aa 1-74 could form a stable complex with NICD/CSL, it could not enhance transcription on chromatin and thus acted as a dominant negative form of MAML1. Interestingly, a MAML1 fragment containing aa 1-300, although stimulating transcription on an *in vitro* chromatin structure more strongly than does full-length MAML1, also in a dominant-negative fashion regulates the expression of Notch target genes *in vivo*, implying that the sequence C-terminal to aa 300 of MAML1 has other functions (215, 227). Indeed, a later study showed that the C-terminus of MAML1 was required for recruiting CycC:CDK8 to the core complex at the promoter region of Hes-1, one of the classical Notch target genes. Subsequent phosphorylation of NICD at the PEST sequence by CycC:CDK8 resulted in NICD degradation (165). However, the MAML1/CDK8 interaction resulted in turnover of NICD and transfection of kinase inactive CDK8 could enhance Hes-1 expression. Thus, the interaction between MAML1 and CDK8

might not be responsible for the dominant-negative nature of the MAML1 (1-300) fragment.

SKIP is an important and unique component of the trans-activation and repression complex. It can interact with both NICD and the co-repressor protein SMRT (228). As a result, it could repress the expression of Hes-1 in the absence of Notch signaling and co-operate with MAML1 to active the transcription of Hes-1 in the presence of active Notch signaling (165, 229).

1.2.5 Non-canonical/CSL-independent Notch signaling

CSL-independent Notch function was first described in a study that examined the phenotype arising from complete loss of Su(H) function (230). Su(H) null embryos showed many phenotypes that were similar to loss of Notch function, as expected. Although loss of Notch function resulted in very low expression of *single-minded*, the gene that specifies mesectoderm, and consequently, failure in generation of mesectodermal cells, lack of Su(H) had virtually no effect on the expression of single-minded on the formation of mesectodermal cells. Therefore, it was proposed that Notch possesses both Su(H)-dependent and Su(H)-independent functions. From then on, many CSL-independent Notch activities were reported (231-237).

De-repression of Notch target genes by loss of CSL could explain some of the observed “CSL-independent” Notch function. Morel and Schweisguth examined the requirement of Su(H) for *Single-minded* expression and formation of midline mesectodermal cells (238). They found that Su(H) was required for activation of *single-minded* in the presence of Notch signaling and for its repression in the absence of Notch signaling. However, de-repression does not explain all the observed CSL-independent Notch functions. Association of Notch with several proteins that might be independent of the NICD/CSL/MAML trimeric complex have been reported (as listed in Table 1). It is possible that these protein interactions contribute to the CSL-independent functions of Notch.

One such example is the interaction between NICD with members of NFκB family. The physical interaction between N1ICD and NFκB was first reported as

early as the interaction between NICD and CSL (239). A later study from the same research group showed that N1ICD directly interacts with p50, but not with p65, via its RAM domain, as assayed by EMSA (240). However, p65 could be co-immunoprecipitated with N2ICD in bone marrow-derived macrophages and was recruited to the NFATc1 promoter region with the same kinetics as those of N2ICD following RANKL-stimulated osteoclastogenesis (241). However, this interaction could also have been mediated by p50 as it was recruited to the promoter with the same kinetics. Interestingly, the NFκB binding site overlaps with an RBPjκ binding site, and RBPjκ was present at the promoter region before stimulation but was displaced upon stimulation. The mechanisms that regulate the use of NFκB- *vs.* RBPjκ-mediated activation of NFATc1 upon Notch2 signaling activation are yet to be clarified, but these findings indicate a fine regulation of multiple signaling pathways.

The consequence of NICD/NFκB interaction might be context dependent as some reported that it suppressed NFκB activity while others reported that NFκB activity was enhanced (239-242). One possible explanation for this discrepancy was proposed by Shin et al. who noted that different studies used different NICD fragments, which could interact with different set of proteins in addition to NFκB (242).

In light of the observed NICD/NFκB interactions, it is interesting to note that when the structure of the NICD/CSL/MAML complex was determined, it was found to be similar to the structure of the NFκB/IκB complex (213, 219). The structural similarities include the following: 1) The overall domain arrangement of the NICD/CSL interaction is similar to that of NFκB/IκB; 2) The structures of the NTDs and CTDs of CSL are similar to the RHR:N and RHR:C domains of p65; 3) IκBα has six ANK repeats that are all essential for interaction with the p50/p65 dimer. Similarly, most of the seven ANK repeats of NICD are also involved in interaction with CSL (243, 244). Thus, NICD might be able to adopt a conformation similar to that of IκBα and bind the NFκB dimer in a manner similar to that of IκBα. Two questions might arise regarding to this hypothesis. First, it is the RAM domain rather than the ANK domain of N1ICD that was found to interact

with p50 (240). Second, interaction between the NICD ANK domain and CSL needs MAML to stabilize it, but the ANK domain of IκBα itself can form a stable complex with p50/p65 dimer. However, it should be remembered that it is also the RAM domain but not the ANK domain of NICD that can associate with CSL in the absence of MAML, and IκBα can only form a complex with p50/p65 dimer, not with either p50 or p65 alone (243, 244). Therefore, interaction between NICD RAM domain and p50 might induce some conformation changes in p50 so that the ANK domain of NICD can sit at the interface between p50 and p65. If this is the case, this also raises the possibility that NICD could interact with IKK in a manner similar to that of IκBα. However, the structure of IKK/IκBα complex has not been determined, nor is it known whether it involves the ANK repeats of IκBα. Nonetheless, since N1ICD binds to p50 via its RAM domain, and its ANK repeats are also likely to be involved in the interaction, the NICD/NFκB interaction most likely is independent of CSL.

An alternative mechanism by which NICD could perform its “CSL-independent” activity is to compete with other proteins for shared interaction proteins, consequently affecting the functions of those other proteins. A clear example of this mechanism is provided by the inhibition of myoblast differentiation by Notch signaling. It has been known for some time that expression of truncated N1ICD fragments lacking the RAM domain could block myoblast C2C12 differentiation (237). Since RAM is required for interaction with RBPjκ, this suggested that the truncated form of N1ICD could block C2C12 differentiation independently of RBPjκ. This was later confirmed by using a dominant negative RBPjκ mutant that could not bind to CSL-binding sites (233). A recent study by Shen et al. provided an answer to how this RBPjκ-independent Notch activity might be transduced (245). They showed that MAML1 was required for the transactivation function of MEF2C, a DNA binding protein essential for C2C12 differentiation. MEF2C interacts with MAML1 through the aa 1-74 of MAML1, the region required for NICD/CSL/MAML complex formation. Therefore, high expression levels of NICD would sequester MAML1 from MEF2C and inhibit the function of MEF2C. In addition to MEF2C, MAML1 has also been reported to interact with p53, β-catenin, and NFκB and to regulate their activity (246-248).

Finally, RBPjκ was recently reported to form a trimeric PTF complex with p48/Ptf1a, an organ-specific basic helix-loop-helix (bHLH) transcription factor, and another class A bHLH protein, such as HEB/TCF12 (249). This trimeric complex is required for development of the pancreas and GABAergic neurons (250, 251). Notably, the RBPjκ-containing trimeric PTF complex could only be detected during pancreas development in the embryo, and RBPjκ is replaced by its paralog, RBPL, in adult pancreas, whose expression would be induced by the RBPjκ-containing PTF complex (249, 250). RBPL does not interact with any Notch paralogs (252). Therefore, high levels of NICD might affect the function of the PTF complex during embryonic development but should have no effect in adults.

Taken together, active NICD could exert its RBPjκ-independent/noncanonical function by interacting with other proteins or by competing with other proteins for mastermind/MAMLs or CSL. However, it should be noted that many of the CSL-independent Notch functions were observed under conditions in which constitutively active forms of NICD or gain-of-function Notch alleles were expressed. Therefore, its relevance to physiological situations is questionable. Nonetheless, it might be important in pathological conditions such as cancer where Notch signaling is elevated.

1.2.6 Effectors

Notch is involved in almost every aspect of cell life—including differentiation, proliferation, and apoptosis—in a temporal and spatially well-controlled manner. Only a subset of Notch target genes and effectors have been identified, mostly within very specific contexts. Many Notch target genes are themselves transcription regulators and therefore, it is difficult to distinguish between its direct and indirect effectors. Nonetheless, there are several well established Notch direct target genes that are important for its multiple functions.

Hairy and Enhancer of Split (Hes)/Hes-related with a Y (Hey) family members are the best studied direct Notch target genes that mediate the regulatory control of Notch over cell fate determination, differentiation and proliferation during

embryonic development and organogenesis [reviewed in (253-255)]. There are nine members in *Drosophila* [*Hairy,* seven *Enhancer of split* (m3, m5, m7, m8, mβ, mδ, and mγ), and a less studied *Hey* ortholog], and ten members in mammals (Hes 1-7 and Hey 1, 2, L). They are bHLH proteins and share a basic domain structure that confers DNA-binding capacity, a helix-loop-helix domain that mediates the dimerization and interaction with other proteins, an Orange domain that regulates the selection of binding partners, and an extreme C-terminal WRPW motif that is involved in transcription repression and self-turnover. The three Hey members differ from the Hes members in that they have a YXXW domain in their extreme C-terminus.

Hes/Hey proteins are themselves transcription repressors that function by two major mechanisms: recruiting an HDAC-containing co-repressor complex or by sequestering other transcription activators. They bind to the consensus sequence CANNNG, but there are slight variations in the DNA sequence to which different Hes/Hey proteins bind. Hes/Hey proteins play redundant as well as unique roles in embryonic development and organogenesis. Hes1 is essential for neurogenesis and pancreas development while Hes7 plays an important role in somitogenesis.

Transactivation of Hes/Hey genes by Notch signaling is highly context-dependent. Ong et al. compared the transactivation strength of four murine NICD paralogs on Hes1 and Hes5 promoters in eight cell lines (256). They found that the activation of Hes1 by any NICD was stronger than that of Hes5 in most of the cell lines except in the case of a neuroblastoma cell line in which activation of Hes5 by all four NICD was higher than that of Hes1. This is attributable to the fact that there are two high affinity CSL-binding sites in a head-to-head orientation that are separated by 16 nucleotides within the Hes1 promoter. Disrupting either one of the CSL-binding sites or changing the orientation of the paired CSL-binding sites greatly impairs the activation of Hes1. This is consistent with a structural study that showed two NICD/CSL/MAML complexes could dimerize (223). However, the authors of this study did not address whether the space between the paired CSL-binding sites would affect the transactivation strength, nor did they address why the transactivation of Hes1 was weaker in the

neuroblastoma cell line. Furthermore, N1ICD was the most potent activator and N3ICD was the weakest activator for both the Hes1 and Hes5 promoters with the exception that N3ICD was stronger than N4ICD on Hes5 promoter. This might be due to the presence of a putative zinc finger protein binding site within the Hes5 promoter close to the CSL-binding sites. Thus, transactivation of Hes/Hey proteins by active Notch signaling is dependent on cellular context, the Notch paralog that is activated and the characteristics of the DNA sequence within the promoter region. Combined with the presence of multiple Hes/Hey members, this allows for tight spatial and temporal control of Hes/Hey protein expression to mediate tissue-specific responses to Notch signaling. However, it should be noted Hes1 can also be upregulated by other signaling pathways such as Sonic hedgehog (Shh), TGF-α, NFκB, and c-Jun N-terminal kinase (JNK) (257-260). Therefore, elevated expression of Hes1 is not a reliable surrogate for Notch activation.

C-myc is an essential transcription factor that is estimated to regulate ~ 10-15% of all cellular genes (261). Recent studies identified c-myc as another gene that is a direct target of Notch but, interestingly, whether it is mediated by RBPjκ-dependent or -independent pathways is uncertain (262-267).

Not all Notch activities are mediated by transcription regulation as not all known NICD interacting proteins are transcription factors (Table 1). One such example is the finding that N1ICD inhibited JNK activity by preventing its interaction with JNK interacting protein 1 (JIP1) (268). JIP1 is required for JNK activity following glucose or oxygen deprivation, but is not required for JNK activation by TNF-α stimulation. N1ICD was shown to physically interact with JIP1 and prevent the association of JIP1 with JNK. Consequently, it inhibited glucose deprivation-induced, but not TNF-α-induced JNK activation.

Interestingly, a later study reported that N1ICD could block nutrition deprivation-induced apoptosis by activating the mTOR-Akt signaling pathway (269). Most interestingly, the cytoplasmic, but not the nuclear, pool of N1ICD was required for this activity. However, it has been reported previously that activated JNK could

inhibit Akt activity (270). Therefore, inhibition of JNK activity by N1ICD could contribute to the activation of mTOR/Akt signaling.

In summary, active Notch signaling can be transduced through multiple pathways in parallel. Considering that many of Notch target genes themselves are transcription regulators, and that NICD regulates several signaling pathway independently of its transactivation activity, it is not surprising that Notch signaling controls multiple cellular activities, such as cell cycle progression, apoptosis, cell motility and invasion (235, 271-281).

1.3. Notch in embryonic development and adult tissue homeostasis

1.3.1 Notch in embryonic development

1.3.1.1 Notch in *Drosophila* embryonic development

Many mutant Notch alleles have been identified in *Drosophila* and these can be classified into three groups: null alleles, recessive visible alleles, and Abruptex mutations. While null alleles result in total loss of Notch function and recessive visibles cause a partial loss, Abruptex mutations enhance Notch activity (282). Since Notch activity during embryonic development in *Drosophila* is highly dose-dependent, the phenotypes displayed from the expression of mutant Notch alleles range from very mild defects in wing or eye morphology to embryonic lethality. Complete loss of Notch function from homozygous or hemizygous expression of null alleles is embryonically lethal with the most striking abnormality presenting as a prominent ectoderm at the expense of mesoderm. In addition, there is no clear separation between nerve tissue and the outer ectoderm, which should be epidermal precursors. In fact, all the ectodermal cells become neuroblasts (283). Therefore, the Notch locus was called the "neurogenic" locus. However, the requirement for Notch signaling is not confined to the development of nervous system, it has been claimed that "there is hardly a tissue that is not affected by Notch" in *Drosophila* (284). Nonetheless, the three best studied phenotypes that represent three different mechanisms of Notch function are: lateral inhibition, cell fate determination, and dorsal-ventral boundaries specification.

Lateral inhibition refers to a regulatory mechanism by which adoption of a particular phenotype by a cell prevents its neighbours with the same development potential from adopting the same phenotype. The best example of this is the separation of neuroblasts from epidermal precursor cells in the ectoderm during embryonic development, the failure of which produces the neurogenic phenotype. In the absence of Notch signaling, most of the ectodermal cells adopt a neuroblast phenotype. In contrast, expressing truncated Notch proteins that enhance Notch activity can result in neuroblast reduction but epidermal precursor cell increases (285).

One of the best studied examples of cell fate determination by Notch is asymmetric cell division during the development of the sensory organ. A sensory organ precursor (SOP) cell is singled out via lateral inhibition at ~ 4 h of embryonic development. This SOP cell then divides asymmetrically to produce a IIa cell and a IIb cell, which then undergo another asymmetric division to produce a hair cell and a socket cell, or a neuron and a sheath cell, respectively. When Notch function is disrupted at ~ 5-7 h stage of embryonic development, two or four cells become neurons at the expense of support cells, depending on the stage of Notch inactivation. In contrast, overexpression of constitutively active Notch produces fewer neurons but more support cells (151).

Although the outcomes of lateral inhibition and cell fate decision in neurogenesis are similar—impaired Notch activity producing more neurons and enhanced Notch activity resulting in more support cells or epidermal precursor cells—the control of Notch activity is different (286). For lateral inhibition, it is generally believed that a cluster of cells starts with equal levels of Notch receptor and ligand, and consequently, equal Notch signaling. By random or unknown mechanisms, one cell receives more Notch signaling and down-regulates the expression of ligand at its plasma membrane. As a result, its neighbour cells receive less Notch signaling. Through this feedback, the cell receiving more Notch signaling establishes its identity as a neuron while the cells that receive less Notch signal differentiate to epidermal precursor cells. In contrast, cell fate decision starts with asymmetric cell division. Although Notch receptor and Delta ligand are equally divided between two daughter cells, only one daughter cell

receives Numb, a negative Notch regulator. Consequently, the daughter cell that inherits Numb has less Notch activity and becomes a neuron.

The dorsal-ventral (D/V) border of the wing imaginal disc forms the wing margin in adult *Drosophila* and the formation of D/V boundary is regulated by Notch. Dorsal cells express Serrate ligand and ventral cells express Delta ligand. Fringe, the enzyme mediating glycosylation of Notch receptor, is only expressed in dorsal cells. Since Fringe inhibits Serrate binding to Notch, dorsal cells receive less Notch signaling than ventral cells and this difference generates the D/V boundary formation. Ectopic expression of either Serrate, Delta, or Fringe disrupts the D/V boundary and yields various wing abnormalities in adult (287).

1.3.1.2 Notch in murine embryonic development

Disruption of Notch function in mice can also cause embryonic lethality; however, the phenotypes resulting from loss of individual Notch paralogs are different.

In contrast to *Drosophila*, where Notch shows a clear dose-dependent effect on embryonic development, heterozygous loss of Notch1 in mice has no noticeable effect on development and growth (288, 289). However, homozygous Notch1 knockout mice die at embryonic day (ED) ~10.5. Extensive cell death, most noticeable in, but not confined to, the central and peripheral nerve system, is observed and may be attributable to growth arrest that occurs before cell death. In contrast to the strong neurogenic phenotype in *Drosophila*, loss of Notch function does not affect neuron growth and differentiation before the embryos die. Instead, the most striking abnormality is defective somitogenesis. Homozygous mutant embryos never form more than 16 somites while the wild-type or heterozygous littermates develop 20-25 somites on ED 9.5.

Heterozygous loss of Notch2 also has no effect on the embryonic and postnatal development, but its homozygous loss is embryonically lethal (290). Homozygous mutant Notch2 embryos die at about the same time as homozygous mutant Notch1 embryos, and there is also widespread apoptosis on ED 9.5. Notch2 $^{-/-}$ embryos differ from Notch1 $^{-/-}$ embryos in that there is no apparent defect in early somitogenesis, although significant apoptosis occurs in

the formed somites. Further, growth retardation in Notch2 $^{-/-}$ embryos starts one day later than that in Notch1$^{-/-}$ embryos.

In contrast, Notch3$^{-/-}$ and Notch4 $^{-/-}$ mice are viable and fertile (291-293), and the female mutant mice can raise their pups. Although Notch3 does not show genetic interaction with Notch1, during embryonic development half of Notch1$^{-/-}$Notch4$^{-/-}$ double mutant embryos show a more severe defect than do Notch1$^{-/-}$ single mutants.

Gene knockout mice with heterozygous/homozygous null mutations of other core components of the Notch signaling pathway (e.g., ligands, RBPjκ, and presenilin), have also been generated (294-305). Jagged2, Dll3, Presenilin 1 (PS1), and PS2 single homozygous knockout mice survive embryonic development whereas Dll1, Jagged1, and RBPjκ single homozygous knockouts, PS1/PS2 double homozygous knockout, and Dll4 heterozygous knockout are embryonically lethal with incomplete penetrance.

In addition to its essential role in early somitogenesis, Notch signaling has also been linked to the development of essentially every organ in vertebrates, such as cardiovascular system, lung, liver, pancreas, kidney, muscle, and nerve system [reviewed in (306-312)].

1.3.2 Notch in adult tissue homeostasis

In adults, the hematopoietic system, together with skin and gut, are the tissues with the highest cell turnover rates. To replenish the lost cells, these tissues rely on the function of rare specialized stem cells that can self-renew as well as produce all lineages. Notch signaling has been implicated in maintaining the stem cells of all three systems but this section will only discuss its role in the hematopoietic system and gut. In addition, the functions of Notch signaling during angiogenesis, an active biological process that permits tissue growth and reorganization in adults, will also be discussed in this section.

1.3.2.1 Notch and the hematopoietic system

Early *in vitro* studies using expression of constitutively active NICD or stimulation

with Notch ligands showed that active Notch signaling could maintain or even increase the hematopoietic stem cell (HSC) population (313-316). To investigate whether canonical Notch signaling is required for maintaining HSCs *in vivo*, Duncan et al. first examined the activation status of Notch signaling in HSC using transgenic mice that express green fluorescence protein (GFP) under the control of an RBPjκ response element. They found that a strong GFP signal was present in the HSC niche, suggesting the presence of active Notch signaling in HSC (317). Then they separated bone marrow cells based on combined expression of cell surface markers and GFP and compared the *in vitro* and *in vivo* colony forming capacity of GFP-positive *vs.* GFP-negative cells within the cell population that expressed HSC/progenitor markers. GFP-positive cells produced colonies representing more cell lineages than did GFP-negative cells, suggesting that GFP-positive cells (active Notch signaling cells) represent more primitive HSC/progenitor cells. Further, they showed that inactivation of canonical Notch signaling by expressing a dominant negative RBPjκ in cells that expressed HSC/progenitor cell surface markers accelerated the differentiation of these cells as evidenced by the expression of lineage-specific surface markers as well as a 65-80% reduction in long-term reconstitution capacity. These results suggest that canonical Notch signaling is required for the maintenance of HSC.

However, Maillard et al. reported contradictory results from a study that tested the effect of canonical Notch signaling on the long-term reconstitution capacity of HSC/progenitors in irradiated hosts (318). They inactivated canonical Notch signaling by expressing dominant negative MAML1 or conditional knockout of RBPjκ in HSC/progenitors. Using a competitor assay in which Notch signaling defective or control (GFP alone) HSC/progenitors were mixed with normal HSC/progenitor cells, they found that 20 weeks after transplantation, Notch signaling inactivation did not impair long-term hematopoietic reconstitution. They then performed a secondary competitor assay in which purified HSC/progenitor cells from the hosts of the first competitor assay were transplanted into secondary recipients. No difference between control and Notch-defective HSC/progenitors could be found. Furthermore, they found that the expression of several Notch target genes, including Hes1, c-myc, Runx1, and Dtx1, was very

low in HSC/progenitor cells. Thus, they concluded that canonical Notch signaling is not required for bone marrow HSC maintenance.

Additional studies will be required to reconcile these divergent observations. Nonetheless, if Notch signaling is dispensable for normal HSC maintenance *in vivo*, this could provide a therapeutic advantage in situations in which inhibition of Notch signaling is contemplated (e.g., cancer therapy). However, even if Notch signaling is not essential for HSC maintenance, it still has an important role in the hematopoietic system as it is indispensible for the development of T-cells and marginal zone B-cells [reviewed in (319)]. In addition, Notch signaling might also regulate the production of other hematopoietic lineages and the specification and activation of T-cells in circulating blood [reviewed in (319)].

1.3.2.2 Notch in intestine renewal

The intestine in mammals is a tube-like structure lined with a specialized epithelium that is folded into millions of valley-like structures, termed crypts. The bottom of each crypt contains 4-6 intestinal stem cells (ISC). During tissue renewal, ISCs first produce transit-amplifying (TA) cells that undergo rapid division (twice a day) and migrate towards the upper part of the crypts. When at the upper part of crypts, TA cells start to differentiate into four distinct cell types—enterocytes, goblet cells, enteroendocrine cells, and Paneth cells. Enterocytes absorb nutrients while the other three types of cells are secretory cells. Each crypt produces ~ 300 cells per day and as a result, the whole epithelium renews every 5 days [reviewed in (320, 321)].

The indispensable role of Notch signaling in intestine renewal was demonstrated in two studies published at the same time (322, 323). Using a gain-of-function approach, Fre et al. conditionally expressed constitutively active N1ICD in intestinal epithelium (322). The transgenic mice, although born at the expected ratio, died within 3 days. Analysis of intestinal tissue showed complete loss of secretory goblet cells in N1ICD-expressing epithelium. In addition, the numbers of the other two types of secretory cells—enteroendocrine and Paneth cells, were also reduced. Increased numbers of proliferating cells were observed at the base of the crypts and increased apoptosis along the disorganized crypts. Since ISC-

specific protein markers were not used, the authors could not confirm the identity of the proliferating cells. Nonetheless, the results demonstrate that elevated Notch1 signaling blocked differentiation in the secretory lineage, especially in goblet cells.

In contrast, van Es et al. employed a loss-of-function approach to address the same question and observed the opposite phenotype (323). They first used two inducible systems to inactivate RBPjκ in adult mice—one specifically in the intestinal epithelium and the other more universal. They found rapidly proliferating TA cells were absent, replaced by post-mitotic goblet cells. No changes in enteroendocrine and Paneth cells were observed. Similar results were obtained when a GSI was used to block Notch signaling, leading to the conclusion that Notch signaling is required for maintaining the proliferating cell population and enterocyte differentiation. As blocking Wnt signaling not only results in loss of the crypt progenitor compartment but also preferentially suppresses the differentiation of goblet cells (324), the authors proposed that the balance between Notch and Wnt signaling determines the cell fate of ISC. Further, maintenance of the ISC population requires both signaling pathways with loss of Notch driving ISCs towards goblet cells and loss of Wnt driving ISCs toward enterocytes.

It was later shown that Notch1 and Notch2 function redundantly to maintain the intestine homeostasis (325). Inactivation of either Notch1 or Notch2 alone had no effect on the renewal of intestinal epithelium while inactivation of both receptors produced the same phenotype as inactivation of RBPjκ. Furthermore, inactivation of both Notch1 and Notch2 could lead to derepression of two cyclin-dependent kinase (CDK) inhibitors—p27 and p57, but not p21, via Hes1. Inactivation of p27 alone could not rescue the growth arrest of crypt cells induced by RBPjκ inactivation. Therefore, the authors proposed that both p27 and p57 contributed the cell cycle arrest that results from Notch signaling inactivation.

1.3.2.3 Notch in angiogenesis

Angiogenesis is the formation of new blood vessels from pre-existing vessels in response to the demands of nutrition and oxygen supply. It requires co-ordinated

control of sprouting, branching, lumen formation and stabilization, and Notch signaling can direct these processes.

Angiogenesis starts with the activation of some endothelial cells in response to a VEGF-A stimulus. These cells break from their neighbouring cells and proliferate to form a new sprout towards the VEGF-A stimulus. The endothelial cells at the tip of the new sprout adopt a special lumenless phenotype with long dynamic filopodia and are called tip cells. Following the tip cells are the stalk cells which form the vascular lumen and are highly proliferative in response to VEGF-A. While the proliferation of stalk cells elongates the sprout, the fusion of filopodia from two tip cells mediates the branching of new vessels [reviewed in (326)]. Notch signaling directs the specification of tip cells versus stalk cells. VEGF signaling up-regulates Dll4 expression (327), therefore, endothelial cells closest to a VEGF-A source have higher Dll4 levels, resulting in stronger Notch signaling in their neighbouring cells. Active Notch signaling can autonomously suppress the tip cell phenotype and, thus specify a stalk cell phenotype (326). Consistent with this, more endothelial cells adopted a tip cell phenotype when Dll4/Notch signaling was absent, resulting in a highly branched and hyperfused vasculature (328-330).

Although the details of how active Notch signaling could suppress the tip cell phenotype are not yet well understood, it may involve VEGF-Notch negative feedback in which active Notch signaling upregulates VEGFR1 and down-regulates VEGFR2 and VEGF3 expression (330-334). Since VEGFR1 has a higher affinity compared to the other two receptors, but is a weaker signal transducer, change in the ratio of VEGFR1/VEGFR2/3 would suppress the response of endothelium to a VEGF-A stimulus and thus, suppress the tip cell phenotype.

Dll4 is not the only ligand to regulate the specification of tip versus stalk cells. Benedito et al. found that Jagged1 functions in an opposite manner to that of Dll4 to promote tip cell generation (335). In this study, angiogenesis was inhibited when Jagged1 was specifically inactivated in endothelium. Further, in contrast to Dll4 whose expression is higher in tip cells, Jagged1 was more abundant in stalk

cells. All three types of Fringe were expressed in endothelial cells, and Fringe activity was found to enhance Dll4-induced Notch signaling but to inhibit Jagged1-induced Notch signaling. Thus, high expression of Jagged1 in stalk cells could compete with Dll4 expressed in the stalk cells to lower the Notch signaling in tip cells and, consequently, maintain tip cell identity. Expression of Jagged1 might also help to fine tune Dll4-induced Notch signaling in stalk cells to maintain an optimized VEGFR level so that stalk cells can still respond to VEGF stimulus to proliferate.

New sprouts need to undergo remodelling to form functional vascular structures and this involves the proliferation of stalk cells, establishment of cell-cell connections between stalk cells, deposition of extracellular matrix, and recruitment of mural cells [vascular smooth muscle cells (vSMC)) and pericytes]. Notch has been shown to inhibit endothelial proliferation and, in co-ordination with the stimulatory effect of VEGF signaling, to control the number of endothelial cells and consequently, the diameter of the blood vessels (334, 336, 337). Active Notch signaling can also enhance the deposition of extracellular matrix components and up-regulate the expression of integrin to promote the endothelium attachment to extracellular matrix (332, 338). Enhanced attachment to extracellular matrix in turn could inhibit the proliferation of endothelium in response to VEGF stimulation (339). Notch3 signaling has been reported to be required for maturation of vSMCs without affecting their proliferation (340).

Formation of functional blood vessels also requires specification of arteriovenous identity as arteries and veins have different histological and mechanical properties. Although Notch1 and Notch4 may act redundantly, the Dll4 ligand is irreplaceable and is required to establish the arterial phenotype within endothelial cells (292, 299-301). This Dll4-induced Notch function is mediated by EphrinB2/EphB4 signaling. EphrinB2 and EphB4 is only expressed in arterial and venous endothelium, respectively, and their interaction specifies the AV identity of endothelial cells (341). EphrinB2 is a direct target gene of Notch signaling (342). In $Dll4^{-/-}$ embryos, EphrinB2 was not expressed in the endothelium and EphB4 was ectopically expressed in dorsal aortae as well as in the cardinal veins (300). Loss of EphrinB2 expression in endothelial cells and ectopic expression of

EphB4 in dorsal aortae was also found in RBPjκ$^{-/-}$ and Notch1$^{-/-}$ embryos, although EphrinB2 expression in all other tissues was normal (299, 343).

Once the new blood vessels have formed, Notch signaling is still required for maintaining vessel integrity, probably by preventing excessive sprouting. Consistent with this, extensive spontaneous angiogenesis was observed in adult mice when RBPjκ was inactivated. This was at least partially mediated by upregulating VEGFR2 and down-regulating VEGFR1 (334).

Therefore, since Notch signaling is essential for tissue homeostasis in adults, possible side effects of Notch inhibition should be considered when blocking Notch signaling is exploited for therapeutic benefits.

1.4. Notch in cancer

Given the important functions of Notch signaling in embryonic development and adult tissue homeostasis, it is not surprising that aberrant Notch signaling is associated with several inherited diseases, such as Alagille syndrome and CADASIL (cerebral autosomal dominant arteriopathy with subcortical infarcts and leukoencephalopathy) [reviewed in (344)]. Aberrant Notch signaling also has been implicated in more than a dozen of types of cancer, including T-cell acute lymphoblastic leukemia (T-ALL), colon cancer, breast cancer, lung cancer, and malignant glioma.

1.4.1 Notch as an oncogene (in T-ALL)

T-ALL is the prototypical example of oncogenic Notch signaling, and the establishment of this relationship dates back to the discovery that the DNA sequence involved in T-ALL [the t(7;9) (q34;q34.3) chromosome translocation] is, in fact, the first mammalian Notch homolog (human Notch1) (62). This translocation produces a truncated form of Notch1 that lacks most of the extracellular domain fused downstream of the promoter/enhancer of the beta T-cell receptor (TCRβ). Consequently, N1ICD is expressed at high levels. When bone marrow cells transduced with truncated Notch1 were transplanted into lethally irradiated mice, ~50% of recipients developed immature T-cell leukemia, confirming that active Notch1 signaling was oncogenic (345).

Because the t(7;9) translocation occurs in <1% of T-ALL patients, the importance of Notch signaling in T-ALL was not appreciated until it was later discovered that more than 50% of T-ALLs harbour Notch1 mutations (346). Most mutations occur within the NRR or PEST domain. Mutations within the NRR would result in abnormal activation and mutations within the PEST domain would slow the turnover of N1ICD. Consequently, both types of mutations result in higher Notch signaling activity, to varying extents. Most common mutations alone are insufficient to induce transformation of T-cells although they enhance T-cell production (347). However, the combination of two types of mutation can enhance their oncogenic potential, suggesting that transformation by N1ICD is dose-dependent. In addition, nonleukemogenic mutations can accelerate active Ras-induced transformation, and interestingly, the resulting T-ALL cells rely on Notch signaling for their survival. Collaboration between active Ras signaling and Notch signaling might, at least partially, depend on elevated Notch signaling, as active Ras signaling itself can induce mutations in the PEST domain of N1ICD (347, 348), further supporting the dose-dependent effect of Notch signaling.

The dependence of T-ALL maintenance on Notch signaling was demonstrated by Weng et al. (349) who used GSIs to treat cells derived from T-ALL induced by N1ICD, or by a truncated Notch1 (N1ΔE) that lacks most of its extracellular domain but still requires γ-secretase-mediated S3 cleavage for activation. The growth of N1ΔE T-ALL, but not N1ICD T-ALL, cells was suppressed by γ-secretase inhibition and this growth arrest could be rescued by transfection of N1ICD. Transfection with dnMAML1 inhibited the growth of both N1ΔE T-ALL cells and N1ICD T-ALL cells, thus establishing the dependence of T-ALL survival on active Notch signaling and the potential of Notch signaling inhibition as a T-ALL treatment.

Several mediators of Notch-induced T-ALL have been identified, among which c-myc is the best studied. C-myc is a direct target of active Notch1 signaling, although whether it is RBP-jκ-dependent or -independent remains to be clarified (262-267). Expression of N1ICD or of different Notch1 mutants that produce elevated Notch signaling also induces c-myc expression and, more importantly, the oncogenic potential of different Notch1 mutants is correlated with their ability

to induce c-myc expression (347). In addition, many Notch target genes (direct or indirect) are also regulated by c-myc (264). Furthermore, ectopic expression of c-myc can rescue some, but not all, Notch1-dependent T-ALL cells from Notch signaling inhibition (262, 265). Therefore, c-myc is an essential mediator of Notch-induced oncogenesis of T-ALL. In addition, several cell cycle-related proteins, including cyclin D1, cyclin D3, CDK2, CDK4, CDK6, p21, and p27, have also been identified as Notch effectors in T-ALL (271, 272, 350-352).

p53, NFκB, and Akt/mTOR have been implicated in regulating apoptosis in Notch-induced T-ALL (271, 353-355). Notch signaling can suppress p53-mediated apoptosis by down-regulating the expression of p19 ^{ARF}, and consequently, promoting MDM2-mediated p53 degradation (353). In addition, Notch signaling can enhance NFκB activity through direct interaction with, and subsequent activation of, IKK. Inhibition of NFκB activity induced apoptosis in T-ALL cell lines and delayed the onset of N1ICD-induced T-ALL *in vivo* (354). However, there are conflicting data regarding the regulation of the Akt/mTOR pathway. Chan et al. reported that inhibition of Notch signaling suppressed the mTOR pathway via c-myc instead of Akt (356). Akt phosphorylation and activity was not affected by Notch inhibition, and ectopic c-myc expression could rescue mTOR activity from Notch inhibition. In contrast, Guo et al. showed that Notch1 knockdown inhibited Akt phosphorylation (271). This discrepancy might be the result of using different cell lines as the former study used HPB-ALL and T-ALL-1 cells and the latter used Sup-T1 cells. It should be noted that the canonical PTEN/PI3K/Akt pathway is disregulated in some T-ALL cell lines due to the mutational loss of PTEN, and this could account for the resistance of some T-ALL cells to Notch inhibition (355). However, Medyouf et al. found that only 2 of 13 primary human T-ALL samples (one PTEN positive and one PTEN negative) were resistant to Notch inhibition (357). They therefore concluded that PTEN loss alone does not confer resistance to Notch inhibition, although it could provide a growth advantage over PTEN positive cells.

FBW7 mutations might also underlie T-ALL resistance to Notch inhibition (358). O'Neil et al. observed that several T-ALL cell lines (e.g., Jurkat, DU528) have detectable N1ICD, although they lack mutations in the NRR region or PEST

domain of Notch1. Therefore, they suspected that the elevated N1ICD levels might result from a failure in turnover. Indeed, in seven human T-ALL cell lines and 7 of 81 primary human T-ALL samples, they found a mutation in the substrate-binding domain of FBW7—the E3 ligase responsible for polyubiquitination-mediated proteasome degradation of N1ICD. The mutant FBW7 could not bind to N1ICD nor could it promote the degradation of c-myc, although it could still bind c-myc. Coincidentally, the seven T-ALL cell lines that expressed a mutant FBW7 were also resistant to GSIs. Thus, the authors proposed that FBW7 mutations could contribute to the resistance of T-ALL to Notch inhibition.

1.4.2 Notch as a tumor suppressor gene (in keratinocytes)

Notch acts as a tumor suppressor in some tissues (359-364), among which skin is best studied.

The tumor suppressor function of Notch1 in keratinocytes was first demonstrated in a study showing that 95% of mice with Notch1 inactivation specifically in skin developed basal cell carcinoma-like tumors (365). Loss of Notch1 also accelerated the development of skin tumors induced by 7,12-bimethylbenz(a)anthracene (DMBA)/12-O-tetradecanoylphorbol-13-acetate (TPA) treatment, and aberrantly activated sonic hedgehog (Shh) and Wnt signaling. Combined with their previous observation that Notch1, but not Notch2, up-regulated p21 expression in keratinocytes, the authors proposed that the tumor suppressor role of Notch1 in keratinocytes is mediated by p21, Shh, and Wnt signaling pathways. Similar observations were later made in mice that expressed dnMAML1 in the epidermis (366).

These observations were later extended to a xenograft model (367). When keratinocytes infected with a retrovirus expressing active Ras were injected subcutaneously into mice, no tumors, or only small nodules, were formed. However, when these cells additionally co-expressed dnMAML1 or were treated with a GSI, they produced moderately to poorly differentiated carcinomas. Keratinocytes expressing dnMAML1 did not grow faster *in vitro* than control cells, but were less committed to differentiation as determined by the expression of

differentiation markers, by a reattachment and regrowth assay, and by a clonogenic assay. In addition, three kinases that act downstream of RhoA and CDC42 GTPases—ROCK 1/2 and MRCKα, were identified as mediators of Notch1 tumor suppressor activity. The expression of these three proteins could be suppressed by ectopic N1ICD or Hes1, and their knockdown could suppress tumor formation by the keratinocytes that express active Ras and dnMAML1.

All three studies suggest that Notch1 acts as a tumor suppressor in a cell autonomous manner. However, more recently it was shown that loss of Notch1 promotes keratinocyte transformation in a non-cell autonomous manner by disrupting skin-barrier integrity and by creating a wound-like microenvironment (368). To test whether loss of Notch1 acts in a cell autonomous manner, Demehri et al. took advantage of the *Msx2-Cre* transgene, whose expression is restricted to clusters of ectodermal cells from ED 9.5 to ED 13. When Msx2-Cre transgenic mice were bred with Notch1$^{flox/flox}$ transgenic mice, the Msx2-Notch1 conditional knockout (Msx2-Notch1 CKO) mice showed a chimeric pattern of Notch1 deletion in skin keratinocytes with three different types of epidermal territories: one with complete Notch1 deletion and no hair, one with normal Notch1 expression and normal hair, and the other between the previous two with mixed Notch1 expression. When DMBA/TPA was applied to the skin of Msx2-Notch1 CKO mice to induce carcinogenesis, tumors were formed from Notch1-expressing as well as Notch1-deficient keratinocytes, suggesting that Notch1 expression does not suppress the keratinocyte transformation in a cell-autonomous manner. Further analysis of the stroma revealed a defect in the skin-barrier and in the accumulation of immune cells in the dermis of Msx2-Notch1 CKO mice. In addition, the fibroblasts in the dermis of Msx2-Notch1 CKO mice displayed a myofibroblast phenotype and the dermal blood vessels of these mice showed increased branching and dilation. Furthermore, the levels of two fibroblast-derived epidermal growth factors—keratinocyte growth factor and stromal cell-derived factor 1, were significantly elevated. All these changes in the dermis were consistent with a wound-like microenvironment that is known to promote tumorigenesis. In addition, application of DMBA alone could produce skin tumors in Msx2-Notch1 CKO mice, but application of TPA alone could not, suggesting loss of Notch1 promotes, but does not initiate, the tumor formation.

Consistent with these mouse studies, the expression of Notch1 and its target genes, such as Hes1, is lower in human squamous cell carcinomas compared to normal skin (367, 369). Therefore, there is compelling evidence that loss of Notch1 can promote the transformation of keratinocytes. Whether this is mediated by a direct effect on keratinocytes, as is the case with classical tumor suppressors, by the non-cell autonomous effect of creating a wound-like microenvironment, or by combination of both, requires further clarification.

1.4.3 Notch and cancer stem cells (brain tumor)

A cancer stem cell (CSC) is defined as "a cell within a tumor that possess the capacity to self-renew and to cause the heterogeneous lineages of cancer cells that comprise the tumor" (370). Putative CSCs were first identified in the 1990s in the hematopoietic system [reviewed in (371)], and later in breast cancer, glioma (372, 373), and in an increasing number of solid tumors [reviewed in (374)]. Given the importance of Notch signaling in regulating normal stem cells in adult tissues, and the close similarity between CSCs and normal adult tissue stem cells, it is not surprising that Notch signaling has been implicated in regulating the 'stemness' of many types of CSC (375-382). This section will briefly discuss the role of Notch signaling in the regulation of brain tumor stem cells.

The brain CSC was first identified using a non-adherent serum-free culture system that produces floating spheroid cell masses called neurospheres (372, 383). Neurospheres are enriched for $CD133^+$ cells, and $CD133^+$ cells can form neurospheres whereas $CD133^-$ cells do not. As few as 100 $CD133^+$ cells could form brain tumors that recapitulated the phenotype of the tumors from which they were derived, whereas 100,000 $CD133^-$ cells could not form tumors although some could survive after injection into mouse brain. Therefore, brain CSCs are defined as cells that are capable of forming neurospheres and/or are $CD133^+$. However, the reliability of CD133 status for identifying brain CSCs has been challenged (384).

To examine the importance of Notch signaling in brain CSC, Fan et al. used a GSI—GSI-18, to block Notch signaling in CSCs derived from medulloblastoma, a type of embryonal brain tumor that is the most common malignant brain tumor in

children (385). They found higher expression of Hes1 mRNA in the $CD133^+$ subpopulation, consistent with active Notch signaling in the CSC subpopulation. GSI-18 inhibition of Notch signaling reduced the $CD133^+$ subpopulation three-fold whereas N2ICD overexpression increased the $CD133^+$ subpopulation two-fold. Notch inhibition also reduced the clonogenicity of a medulloblastoma cell line by 90% and as well, suppressed its growth as a xenografted tumor. The same group later reported similar findings with CSCs derived from glioblastoma, the most common brain cancer in adults (386). Consistent with this, Zhang et al. reported that ectopic expression of N1ICD increased the neurosphere forming capacity of SHG44 glioblastoma cells without affecting their differentiation potential (387).

Notch signaling has also been reported to protect brain CSC from radiation (388). Here, it was shown that Notch signaling was activated by radiation and that blocking Notch signaling after radiation treatment inhibited the adherent growth of $CD133^+$ glioma cells as well as their ability to form neurospheres. This effect was mediated by reduced activation of the PI3K/Akt signaling pathway and reduced expression of Mcl-1, an anti-apoptotic protein. Consequently, apoptosis was increased without any significant effect on the activation of DNA damage responses. Ectopic expression of N1ICD or N2ICD attenuated the radiosensitizing effect of GSI, whereas knockdown of Notch1 or Notch2 sensitized $CD133^+$ glioma cells to radiation. The radioprotective effect of Notch was restricted to the CSC subpopulation of glioma cells as GSI treatment did not affect the radioresponse of $CD133^-$ cells. Taken together, these observations suggest that Notch signaling plays a general role in maintaining the stemness of CSC and protects them from environmental insults.

1.5. Notch in mammary gland development and breast cancer

1.5.1 Notch in mammary gland development

Most of the mammary gland in female mice develops postnatally and undergoes cycles of growth, maturation, and regression with each pregnancy as illustrated in Figure 1-5 [reviewed in (389)]. At birth, only an undeveloped ductal structure is formed in the mammary gland. A specialized structure—the terminal end bud (TEB), composed of a layer of cap cells at its tip and several layers of body cells, starts to appear at the tips of the ductal structure at ~ week 3 (Figure 1-6). Cap

cells at the tip of TEB are highly proliferative and this proliferation leads to the growth of the TEB and the ductal structure. With the elongation of the ductal structure, the cap cells at the trailing edge of the TEB differentiate into myoepithelial cells while the body cells differentiate to luminal cells. At week 10-12, the TEB reaches the edge of mammary fat pads and start to regress. With the onset of the estrous cycle, the ductal structure starts to form lateral buds and alveolar buds in response to the cyclic secretion of ovary hormones. However, branching morphogenesis as a result of massive growth of lateral buds only starts with pregnancy and is completed by the middle of pregnancy. At the same time, many alveolar buds form which will develop into secretory alveoli during the second half of pregnancy. At weaning, the gland undergoes a process involving massive apoptosis and remodelling to return to the pre-pregnancy state.

The involvement of Notch signaling in mammary gland development was first demonstrated in a transgenic mice model in which over-expression of active N4ICD under control of mouse mammary tumor virus (MMTV) long terminal repeats (LTR) disrupted normal mammary gland development (390). When a truncated form of Notch4 that is produced by MMTV insertion was expressed in virgin female mice, the ductal structures that normally fill entire mammary fat pads occupied only about 15-20% of the area. In addition, the leading ductal structures lacked the end buds at their tips. This defect in ductal growth was an intrinsic characteristic of mammary epithelium, and was not due to a defect in the supporting stroma. Exposure of the N4ICD transgenic mice to pregnancy-associated hormones resulted in ductal structures that could grow and branch to fill entire fat pads but they could not differentiate into functional secretory lobulo-alveolar structures.

Transgenic mice over-expressing N1ICD or N3ICD under the regulation of MMTV LTR (391) also showed impaired mammary gland development, but the defects were different from those seen in N4ICD transgenic mice. In MMTV-N1ICD virgin mice, the ductal structures were apparently normal, however, branching morphogenesis during pregnancy was perturbed. Compared to normal mice, the tertiary braches in MMTV-N1ICD and transgenic mice were shorter with fewer alveoli extended from them. Furthermore, there was limited lobular-alveolar

development although no functional secretory alveoli were generated. The overall phenotypes of mammary gland development in MMTV-N3ICD transgenic mice were similar to those in MMTV-N1ICD. However, there was a clear difference during late pregnancy as lobular-alveolar development was enhanced in MMTV-N3ICD but impaired in MMTV-N1ICD transgenic mice. The molecular basis for this difference is unclear.

Although these transgenic mice studies clearly demonstrate that aberrant Notch signaling *disturbs* mammary gland development, they do not substantiate a *requirement* for Notch during mammary gland development. In fact, Notch3$^{-/-}$ and Notch4$^{-/-}$ mice can feed their pubs. It is not known whether depletion of Notch1 or Notch2 can affect mammary gland development as homozygous inactivation of Notch1 or Notch2 is embryonically lethal. To address this question, Buono et al. inactivated RBPjκ or POFUT1 specifically in the mammary gland by using Cre-mediated recombination under the regulation of MMTV LTR to avoid the possible compensation among Notch paralogs in mammary gland development (392). However, since the MMTV-Cre was also expressed in several tissues other than mammary gland, including hematopoietic cells, the mice did not survive for more than a few weeks. Therefore, the authors examined the development potential of mammary epithelium from these mice by transplanting the epithelium to the mammary fat pads of wild-type mice whose mammary epithelium was removed before transplantation.

The transplanted epithelium grew into full ductal structures within eight weeks, suggesting Notch signaling is not required for the early development of mammary gland in virgins. However, the lobular development during middle to late pregnancy was severely impaired, although branching morphogenesis during early pregnancy was largely not affected. By immunohistochemical analysis, it was found that the defect in lobular development was the result of an imbalance between the two cell lineages. The “alveoli” were composed of clusters of basal myoepithelial cells with few luminal cells. Furthermore, the authors showed that the absence of luminal cells was not only the result of lack of proliferation of luminal cells, but was also due to trans-differentiation of luminal cells to myoepithelial cells. Therefore, Notch signaling might control the lineage

maintenance in mammary gland as well as promote the growth of luminal cells, but it suppresses the proliferation of basal myoepithelial cells. It should be noted, however, that Notch signaling in mammary gland development might only be essential within a narrow temporal window as inactivation of RBPjκ does not affect ductal growth during early pregnancy. In addition, inactivation of RBPjκ during middle to late pregnancy using WAP-Cre had no apparent effect on mammary gland development (393).

The lineage specification role of Notch signaling in mammary gland development is supported by two in vitro studies (394, 395). Both studies reported that when Notch signaling was blocked in the bipotent progenitor cells using GSIs or dnMAML1, more myoepithelial cells but fewer luminal progenitor cells were produced. However, Raouf et al. suggested that Notch3 signaling is important for luminal differentiation (395), whereas, Bouras implied that it is Notch1 signaling that promotes the differentiation of bipotent cells to the luminal lineage (394).

Taken together, the function of Notch signaling in mammary gland development could be summarized by the following model: Notch signaling is inactive in the mammary gland in the absence of pregnancy. During early pregnancy, hormone changes in the local environment up-regulate the expression of Notch 1-3 and activate Notch signaling. Consequently, active Notch signaling promotes the differentiation of bipotent cells along the luminal lineage. Luminal differentiation, combined with the proliferation of luminal cells stimulated by other signaling pathways, such as hormone receptor signaling pathway, possibly in concert with active Notch signaling, induces the development of secretory lobular-alveolar structures. Among the four Notch paralogs, Notch3 signaling might be the most competent, but it is not the only one capable of inducing luminal differentiation.

When Notch signaling is inactivated by depleting RBPjκ during early pregnancy, luminal differentiation is blocked but cell proliferation might not be affected. As a result, the mammary epithelium will be composed of mainly myoepithelial cells. However, by middle pregnancy luminal differentiation may have already finished. Therefore, inactivation of Notch signaling by depleting RBPjκ would have no effect on mammary gland development. In addition, since Notch4 might not be

required for any aspect of normal mammary gland development, and Notch1 may be able to compensate for the loss of Notch3 or Notch4, mice without Notch3 or Notch4 might have no overt abnormality in mammary gland development.

On the other hand, constitutive activation of Notch3 signaling by expression of active N3ICD might enhance luminal differentiation and, at the same time, might suppress myoepithelial differentiation by depleting bipotent cells. Since myoepithelial cells are required for branching morphogenesis, overexpression of N3ICD in the mammary gland would result in impaired branching morphogenesis but enhanced lobular-alveolar development. Notch1 signaling may have some overlapping, but still distinct, functions with Notch3 signaling or it may be weaker in promoting luminal differentiation. Thus, when active N1ICD is expressed under the regulation of MMTV LRT, it competes with N3ICD, whose level now would be lower than N1ICD, for common components of Notch signaling such as RBPjκ and MAMLs. Therefore, Notch1 signaling could still induce incomplete luminal differentiation but could also suppress myoepithelial differentiation. Consequently, there could be developmental defects in both branching morphogenesis and alveolar development. When N4ICD is over-expressed in mammary gland, it inhibits both N1ICD and N3ICD signaling. Consequently, there would be no luminal differentiation or lobular-alveolar development, but branching morphogenesis would not be affected.

Although the working model proposed here explains most the phenotypes associated with the inactivation or ectopic activation of signaling by individual Notch homologs, it still needs to be confirmed by manipulating the signaling of individual homologs in a temporally and spatially well-controlled manner. Although the conditional knock-in and knock-out mouse models that have been developed provide limited spatial control, they cannot be used to manipulate Notch signaling in a temporally-controlled manner. Therefore, new research approaches need to be developed.

1.5.2 Notch in breast cancer

A possible link between Notch and breast cancer was first noted when Notch4 was found to be a hot spot for MMTV insertional mutagenesis, resulting in high

N4ICD expression levels (396-398). Later, transgenic mice expressing constitutively active N1ICD, N3ICD, or N4ICD specifically in mammary epithelium all developed mammary gland carcinomas, thus confirming that aberrant Notch signaling could induce breast tumorigenesis (391, 399).

1.5.2.1 Activation of Notch signaling in breast cancer

Unlike in T-ALL, a chromosomal translocation involving Notch loci or an activating mutation has yet to be reported in breast cancer. In fact, among 48 breast cancer samples, only one nonsense mutation in the PEST domain of Notch2 that leads to PEST deletion was found when the NRR and PEST domain were sequenced (400). No mutations in the other three Notch receptors were observed. However, as will be discussed later, Notch2 activation might suppress, rather than promote, breast tumorigenesis. This raises the critical question of how oncogenic Notch signaling could be activated in breast cancer. Two possibilities have been proposed: 1) high expression of Notch receptors and/or ligands, and 2) loss of the negative regulator, Numb.

Using immunohistochemical staining, Rizzo et al. examined the expression of Notch1, Notch4, Jagged1, and Dll1 in 4 normal breast tissues, 5 hyperplasias of usual type (HUT), 27 ductal carcinomas in situ (DCIS), 27 infiltrating ductal carcinoma (IDC), and 14 infiltrating lobular carcinomas (ILC) (401). None of the normal breast tissues expressed high levels (defined as 3+) of Notch1 or Notch4. In contrast, 80% of HUT, 67% of DCIS, 89% of IDC, and 57% of IFC expressed high Notch1 levels. High Notch4 levels were not detected in any HUT or DCIS samples, but were present in 81% of IDC and 93% of IFC. The expression of Jagged1 and Dll1 was not examined in normal tissues, HUT, or DCIS, but 78% of IDC and 64% of IFC expressed high Jagged1 levels. Interestingly, the proportions of samples with high levels of DLL1 expression were exactly reverse of those of Jagged1. However, the authors did not note whether Jagged1 and Dll1 were expressed in a complementary manner. Nonetheless, the co-upregulation of Notch receptors and ligands could possibly lead to elevated Notch signaling.

Another intriguing possibility is that loss of Numb activates Notch signaling. Numb was found to be absent or at low levels in ~50% of breast cancer samples due to enhanced polyubiquitination-mediated proteasomal degradation (402). Since Numb is a negative regulator of Notch signaling, Pece et al. examined Notch1 protein levels and its subcellular distribution in primary cell cultures of breast cancer tissues. They found that although no clear nuclear Notch1 signal could be identified under normal conditions, treatment with a proteasome inhibitor, MG132, resulted in strong accumulation of Notch1 signal in the nuclei of cells without Numb, but not in cells with normal Numb expression. This suggested that Notch1 was activated in the absence of Numb, but that N1ICD was rapidly degraded. This is consistent with the rapid turnover of NICD. Furthermore, they showed that in cells without Numb, endogenous Hes1 mRNA levels and the expression of a reporter gene driven by an RBPjκ-response element were higher than in cells with normal Numb protein levels. Finally, they showed that treatment with a GSI, DFP-AA (also known as Compound E), or ectopic expression of Numb, suppressed the clonogenic growth of cells without Numb, but not that of cells with normal Numb levels. Therefore, loss of Numb activated Notch1 signaling, which in turn, conferred clonogenic growth capacity to the cells. Consistent with this, Stylianou et al. detected N1ICD in the total protein extracts of breast cancer tissues from which Numb was absent (403). In addition, they showed readily detectable N1ICD levels in seven breast cancer cell lines.

Nicastrin, one of the components of the γ-secretase complex, was found to be elevated in ~50% of breast cancer samples, suggesting that enhanced γ-secretase activity might also contribute to aberrant activation of Notch signaling in breast cancer (404). However, the authors did not investigate whether nicastrin expression levels were correlated with the levels of active Notch signaling.

Multiple mechanisms might contribute to the aberrant activation of Notch signaling in breast cancer. However, given that activating mutant Notch alleles in T-ALL are only weak transformers, it remains to be determined whether high levels of Notch receptors and ligands, high nicastrin expression or loss of Numb can generate enough active Notch signaling for breast oncogenesis. In addition,

it remains to be determined whether active Notch signaling is the major effector of loss-of-Numb-induced tumorigenesis as Numb has recently been reported to regulate p53 and hedgehog activity independent of Notch (405, 406).

1.5.2.2 Notch and breast cancer progression

Nonetheless, the significance of aberrant Notch signaling in human breast cancer has been demonstrated by the association of high Notch receptor and ligand expression levels with poor clinical outcomes. Reedijk et al. used RNA *in situ* hybridization to probe expression of four Notch receptors and five canonical Notch ligands in two cohorts of breast cancer samples obtained from 50 or 192 patients (407). High expression samples were identified as those whose signal intensity was in the highest quartile of the signal intensity range for individual probes. High expression of Jagged1, Notch1, or Notch3 correlated with increased mortality within the 50 patient cohort. Similar results were observed in the 192 patient cohort, with the 5-year survival rates for the high *vs.* low expression groups being 42% *vs.* 65% for Jagged1, 49% *vs.* 64% for Notch1, and 48% *vs.* 61% for Notch3. In addition, statistically significant differences in median survival times were found between the Jagged1 and Notch1 high and low expression groups.

Zang et al. also reported elevated levels of Notch receptor and ligand mRNA in breast cancer samples (408). However, higher mRNA levels could be due to a passenger effect, and do not necessarily translate to higher protein expression. Indeed, Reedijk et al. later found no correlation between Jagged1 mRNA and protein levels in a group of 127 breast cancer samples (409). Interestingly, they found high levels of either Jagged1 mRNA or protein were associated with poor clinical outcomes although they identified distinct subgroups among these patients. Furthermore, in an expanded study that included 887 lymph node-negative breast cancer patients, Jagged1 expression still had predictive value (410). In addition, they found high Jagged1 mRNA, but not protein, levels among basal-like breast cancer samples. Therefore, at least in the case of Jagged1, high transcript levels should not be used as surrogate markers of active Notch signaling.

It should be noted that different Notch paralogs can play different, even opposing, roles in breast cancer, a fact that complicates the design of therapeutic strategies to block Notch signaling. Parr et al. reported that high Notch2 mRNA expression levels were associated with good clinical outcomes whereas a reverse relationship pertained to Notch1 expression, thus suggesting a tumor suppressor role for Notch2 in breast cancer (411). This hypothesis was confirmed by O'Neill et al. who showed that ectopic expression of active N2ICD in breast cancer MDA-MB-231 cells retarded cell growth and induced apoptosis *in vitro* whereas ectopic expression of N4ICD enhanced cellular proliferation (412). Similar to their effects *in vitro*, Notch2 and Notch4 signaling elicited opposite effects on the growth of MDA-MB-231 cells as tumor xenografts. It is interesting to note that while there are no reports of transgenic mice constitutively expressing active N2ICD specifically in mammary epithelium, expression of the other three Notch paralogs in mammary epithelium results in the development of mammary gland carcinoma.

1.5.2.3 Dependence of breast cancer on Notch signaling

Several studies also have demonstrated that breast cancer cells rely on Notch signaling for their survival and proliferation. Yamaguchi et al. examined the effect of Notch1 or Notch3 knockdown on the growth of breast cancer cell lines (413) and found that although Notch1 knockdown had only a slight effect, Notch3 knockdown significantly impaired the growth of HER2/neu negative, but not positive, cells. Knockdown of RBPjκ, Jagged1 or Jagged2 also produced in similar results. They therefore concluded that Notch3 signaling is essential for the growth of HER2/neu negative cells. In contrast, others have shown that knockdown of Notch1 by siRNA inhibits breast cancer cell growth (401, 414, 415). These discrepancies might be due to different knockdown efficiencies, or might suggest that the cell growth inhibition was due to an off-target effect.

γ-secretase inhibition of Notch signaling has also been shown to inhibit cell growth (401, 408, 416). Each of these three studies reported that z-Leu-Leu-Nle-CHO, commonly referred as GSI I, could induce cell cycle arrest and apoptosis in breast cancer cells, with ER- cell lines being more sensitive. Combined with the observation that HER-2/neu- breast cancer cells are more sensitive to Notch

inhibition, the observation that ER- cells are also more sensitive to Notch inhibition is very interesting as currently there are no effective treatments against triple negative breast cancer. More intriguingly, two of three studies showed that GSI I could inhibit the growth of breast cancer xenografts at a dose that showed no significant systemic toxicity, including no sign of goblet hyperplasia in gastrointestinal (GI) tract (401, 416). Since GSI I is derived from a proteasome inhibitor, MG132 (z-Leu-Leu-Leu-CHO), and has been reported to be a broad chymotryptic and aspartyl protease inhibitor (417), Lee et al. also used a second GSI, z-Ile-Leu-CHO, to demonstrate that the cytotoxicity of GSI I in breast cancer cells was due to Notch signaling inhibition (416). On the other hand, Rizzo et al. claimed that no proteasome inhibition was observed at the dose that killed breast cancer cells, although data was not shown (401). Together, these two studies provide the strongest support to date for using GSIs to block Notch signaling in breast cancer.

As described above, Notch inhibition is more effective in inhibiting the growth of breast cancer cells that do no have amplification of HER-2/neu and that are ER negative, suggesting that there might be cross-talk between Notch signaling and HER-2 and ER signaling pathways. Ospio et al. investigated this possibility first by examining the transactivating activity of Notch under conditions in which HER-2 signaling levels differed (414). They found that ectopic expression of HER-2/neu in MCF-7 cells suppressed Notch transactivation activity six-fold, and inhibition of HER-2 signaling with trastuzumab, a humanized mouse monoclonal antibody against HER-2, increased Notch transactivation activity two-fold in SKBR3 cells, and five-fold in BT474 cells, two breast cancer cell lines with amplified HER-2/neu. In addition, a dual EGFR/HER-2 kinase inhibitor, TKI, increased Notch transactivation activity three-fold. This was mediated by increased Notch1 activation as HER-2 inhibition decreased membrane-tethered Notch1 protein but increased N1ICD levels and its nuclear accumulation. The combination of trastuzumab or TKI with a GSI—LY411,575 or MRK-003, showed a stronger effect on the growth of HER-2/neu positive cells than use of either reagent alone, while knockdown of Notch1 sensitized both sensitive and resistant BT474 cells to Trastuzumab. The same group later reported similar cross-talk between the ER and Notch signaling pathways (401).

1.5.2.4 Notch and breast CSC

Putative breast CSCs were first identified by using cell surface markers (ESA^+ $CD44^+$ $CD24^{-/low}$ $lineage^-$) (373). Cells expressing this signature were >50-fold more tumorigenic than cells that did not, and the tumors formed by these cells recapitulated the phenotype of the initial tumor. Later, putative CSCs were isolated from primary breast cancer samples and expanded using a non-adherent serum-free cell culture system, producing a spheroidal cell mass called a mammosphere (418). Tumorigenic cells were enriched in mammospheres more than 100-fold and more than 95% of mammosphere cells were $CD44^+$ $CD24^{-/low}$. Although the usefulness of CD24 status in distinguishing between non-CSCs and CSCs in breast cancer has been questioned (419), breast cancer cells capable of forming mammospheres and/or expressing $CD44^+$ $CD24^{-/low}$ are commonly regarded as breast CSC.

The importance of Notch signaling for the maintenance of breast CSC was first appreciated by Farnie et al., who examined the factors that affect the ability of breast cancer cells to form mammospheres (382). They found that treatment with a GSI—DAPT, reduced primary breast cancer cells' mammosphere forming efficiency (MFE). Furthermore, treatment with a human Notch4 antibody reduced MFE to an extent greater than did treatment with DAPT, suggesting Notch4 signaling was involved in maintaining the stemness of breast CSC. This observation also suggests that either some unidentified γ-secretase substrates antagonized Notch4 activity or that the Notch4 polyclonal antibody had some off-target effect.

Harrison et al. also reported that Notch4, but not Notch1, signaling is important for regulating breast CSC activity (379). They isolated $ESA^+CD44^+CD24^{-/low}$ cells from two breast cancer cell lines, MCF-7 and MDA-MB-231, and compared Notch1 and Notch4 levels in the CSC subpopulation with those in the other subpopulations. They found that Notch1 levels were lower, and Notch4 levels higher, in CSC as compared to the other subpopulations. Furthermore, they showed that Notch1 positive cells were in the luminal cell layer within breast cancer tissues, whereas the Notch4 signal was more dominant in the basal cell layer in which breast cancer stem cells are presumed to be located. In addition,

they found that while Notch1 was expressed in the majority of cells in invasive breast tumors, Notch4 expression was greater in the invasive cancer cells themselves. Finally, in MCF-7 cells, Notch4 knockdown produced a greater reduction in the MFE and tumorigenic potential in xenografts than did Notch1 knockdown. They therefore concluded that Notch4 is more important than Notch1 in maintaining breast CSC. However, the anti-Notch1 and anti-Notch4 antibodies they used do not specifically recognize the active NICD, and treatment with GSIs only reduced the signal of “N1ICD”, but not that of “N4ICD”, in both MCF-7 and MDA-MB-231 cells, raising concerns about the validity of their observations.

While the relative importance of Notch3 was not examined in the studies noted above, others have found it to be very important for regulation of breast CSC activity (420). Sansone et al. studied the effect of p66Shc, a mammalian longevity regulator, on the self-renewal potential and hypoxia tolerance of stem cells from normal breast and breast cancer tissues. They found p66Shc was induced by hypoxia and that high levels of p66Shc protected breast cancer cells from hypoxia and promoted the self-renewal of mammospheres derived from both normal and breast cancer tissues. Notch3 was identified as the mediator of this regulation. Its knockdown reduced the ability of primary mammospheres to form secondary mammospheres, and reduced the survival of mammospheres under hypoxic conditions. Among the four Notch paralogs, only Notch3 was up-regulated by p66Shc.

Notch signaling has also been suggested to be radioprotective (421). Phillips et al. reported that breast CSC are relatively radioresistant, and that fractionated, but not single, doses of γ-radiation increased Jagged1 and N1ICD levels, suggesting that active Notch signaling protects CSC from radiation damage. However, trypsin/EDTA was used to prepare the cell samples and EDTA is known to activate Notch by depleting extracellular calcium (80). Therefore, artefacts could have been introduced during sample preparation.

1.5.2.5 RBPjκ-independent tumorigenesis

Few studies have addressed the relative contributions of RBPjκ-dependent and -independent Notch activities to tumorigenesis and cancer cell survival.

Involvement of RBPjκ-independent Notch activity during transformation was first proposed ten years ago in studies that identified ANK repeats as the minimum domain required for Notch1-induced transformation in E1A (an Epstein-Barr virus protein) immortalized rat kidney cells (RKE) (234, 422). Recently, more compelling evidence in support of RBPjκ-independent tumorigenesis was reported (393) by Raafat et al. who developed transgenic mice (WAP-N4ICD/RBPjκ knockout) that express N4ICD and Cre under the control of the whey acidic protein (WAP) promoter and a floxed RBPjκ (393). RBPjκ will be knocked out when N4ICD expression is activated during middle and later pregnancy. In contrast to the previous report of impaired mammary gland development in WAP-N4ICD mice, WAP-N4ICD/RBPjκ knockout mice showed no mammary gland developmental defects and could nurse their pups. However, WAP-N4ICD/RBPjκ knockout mice still developed mammary gland carcinomas, suggesting that N4ICD's oncogenic activity and its function in mammary gland development could be separated, and that the oncogenic activity is RBPjκ-independent. However, the requirement for RBPjκ cannot be completely ruled out as there might be a narrow temporal window in the mammary epithelium during which elevated N4ICD is present with RBPjκ before the already expressed RBPjκ protein is degraded. In addition, it should be noted that the latency of tumor formation in WAP-N4ICD/RBPjκ knockout mice was longer than that in WAP-N4ICD mice. Therefore, the canonical Notch signaling pathway might still be involved in biological processes relevant to tumorigenesis.

Whether the RBPjκ-independent tumorigenic activity described for Notch4 is a property that applies to other Notch paralogs, and/or in other types of cancers remains to be determined. However, it has been reported that inhibition of NFκB signaling pathway could delay the onset of T-ALL (354). The activation of NFκB signaling in T-ALL was at least partially RBPjκ-independent as there was direct interaction between N1ICD and IKKα. Given that the transformation potential of N1ICD in T-ALL is dose-dependent (347), it is tempting to speculate that there is a threshold NICD level for Notch-induced tumorigenesis, at which NICD could activate several non-canonical Notch signaling pathways by its interaction with several proteins (as listed in Table 1) or some yet-to-be-identified partners. At

very low levels, NICD might only activate canonical RBPjκ-dependent signaling pathways, while at increasing levels, NICD might activate other signaling pathways, and it is this co-operation of several signaling pathways that mediates the tumorigenic activity of Notch signaling. Lack of any one of the participating signaling pathways, such as the RBPjκ-dependent canonical signaling pathway or NFκB signaling pathway, would only delay, but not completely block, Notch-induced tumorigenesis.

Several signaling pathways could participate in this process in addition to NFκB. For example, N4ICD has been shown to interact with Smad 2-4, especially Smad 3, to inhibit TGFβ signaling (423), and TGFβ signaling suppresses the progression of early stage breast cancer due to its anti-proliferative activity [reviewed in (424)]. N1ICD has been shown to associate with YY1 to activate the expression of c-myc, possibly independently of RBPjκ (263, 267), and elevated c-myc has long been associated with breast cancer initiation and progression [reviewed in (425)]. In addition, N1ICD was reported to interact with JIP1 to inhibit the activation of JNK (268). Inhibition of JNK could result in multiple, sometimes opposite, phenotypes in breast cancer cells and mammary epithelium, one of which is the formation of tumor-like disordered assemblies of cells during mammary gland acini formation (426).

Better understanding the contribution of RBPjκ-independent signaling pathways to Notch-induced tumorigenesis would not only help us to appreciate how aberrant Notch signaling promotes the development of cancers, but also help us to develop new strategies to treat these diseases. For example, it is not known whether RBPjκ-independent non-canonical Notch signaling is required for the survival of Notch-dependent tumor cells. If this were the case, blocking RBPjκ-independent non-canonical Notch signaling might avoid, or attenuate, the side effects associated with inhibition of RBPjκ-dependent Notch activity, such as impaired T cell development and goblet hyperplasia associated secretory diarrhea.

1.6. Notch as therapeutic target

Several reagents/approaches have been used to block Notch signaling in cell

culture or in animals, including GSI, dnMAML1, neutralizing antibodies, and RNA interference (RNAi). Among them, GSI is the most widely used, and there are at least three clinical trials registered at ClinicalTrials.gov using GSI alone, or in combinations with other chemotherapy drugs, to treat breast cancer.

1.6.1 GSIs

1.6.1.1 Classification of GSIs

Due to their potential use in battling the neurodegenerative disease, specifically Alzheimer's disease, considerable effort has been made to develop potent and specific GSIs. As a result, more than 100 GSIs have been reported or disclosed in the literature or in patent applications. Most of these can be classified into three types based on their structure – peptide isosteres, azepines, and sulfonamides [reviewed in (427)].

Peptidic isostere inhibitors include difluoroketone, difluoroalcohol, and hydroxyethylene, and their analogs [reviewed in (427)]. They contain classic aspartyl protease transition state-mimicking moieties and bind to the catalytically active site of the complex. Therefore, they are also called transition state analogs, and they have been extremely useful in deciphering the structure and catalytic mechanism of the γ-secretase complex. They have also helped to prove that two aspartates of presenilin 1—D257 and D385, confer the aspartate protease activity to the γ-secretase complex. In addition, the non-competitive binding between these transition state analogs and γ-secretase substrates indicates that the substrate binding sites and catalytic active sites are distinct sites within the γ-secretase complex. However, they are not suitable for in vivo experiments due to their peptidic nature, although they could be used in cell culture. L-685,458 is the best known example of this type of GSI with an in vitro half maximal inhibitory concentration (IC_{50}) = 17 nM (428).

Both azepine GSIs and sulfonamide GSIs are non-transition state analogs, and azepines generally contain an aminolactam coupled to a dipeptide mimetic. Since azepine GSIs and sulfonamide GSIs bind to the γ-secretase complex competitively with each other, but not with transition state analog GSIs, it is believed that they bind to a site other than catalytically active site.

Despite the discovery of more than 100 different GSIs, fewer than ten of them are widely used in cancer research due to the fact that most are not commercially available. Azepines, such as DAPT (IC_{50} = 20 nM) (429), Compound E (IC_{50} = 0.3 nM) (430), and LY-411575 (IC_{50} = 78 pM) (431), have been widely used in cell culture and animal studies, and one azepine GSI, LY-450139, is being tested in phase III clinical trials for Alzheimer's disease [reviewed in (432)]. In contrast, sulfonamide GSIs have not been as widely used, probably because they were developed later than azepines. However, one sulfonamide GSI, MK-0752, is being tested in three clinical trials involving breast cancer patients.

1.6.1.2 Specificity of GSIs

The major problem associated with GSIs use is their lack of specificity at three levels: protease inhibition, substrate specificity, and paralogs targeting.

1.6.1.2.1 Specificity at the protease level

Some well characterized and potent GSIs, including L-685,458 and LY-411575, are known to bind and inhibit signal peptide peptidases (SPPs), a family of closely-related presenilin aspartyl proteases that clear signal peptides after they are removed from new synthesized secretory or membrane proteins (433, 434). Fewer than ten SPP substrates have been identified, including tumor necrosis factor α (TNFα) and Fas ligand, with the biological consequences of SPP-mediated clearance largely unknown [reviewed in (435)]. However, knockdown of SPP and SPPL3 in zebrafish resulted in cell death within the nerve system and knockdown of SPPL2 caused caudal vein enlargement, indicating SPPs do have important biological functions (436).

A recent study by Yan et al. suggests that SPPL2-mediated TNFα signal peptide clearance can modulate the response of breast cancer cells to TNFα signaling (437). Newly synthesized TNFα protein is a homotrimeric transmembrane protein (tmTNFα), and cleavage by TACE releases soluble TNFα (sTNFα). Both tmTNFα and sTNFα can bind to TNF receptors (TNFR) to initiate signaling cascades that activate several downstream targets, including NFκB and JNK [reviewed in (438)]. In addition to the canonical TNFα signaling pathway, reverse

signaling in which tmTNFα acts as a receptor has also been discovered [reviewed in (439)]. One possible mechanism by which reverse signaling can be transduced is the release of the intracellular domain of TNFα (TNF-ICD), which then translocates to the nucleus to regulate gene expression (440, 441). Release of TNF-ICD from the plasma membrane is the result of SPPL2-mediated cleavage of TNFα signal peptide, which can be blocked by a SSP-specific inhibitor, $(Z\text{-}LL)_2$-ketone, or L-685,458 (441, 442).

Yan et al. first observed that MDA-MB-231 breast cancer cells expressed high TNFα levels and were resistant to sTNFα-induced cytotoxicity. On the other hand, MCF-7 cells expressed low level of TNFα and were sensitive to sTNFα. Knockdown of TNFα in MDA-MB-231 cells sensitized them to sTNFα-induced cytotoxicity, suggesting a causal relationship between the expression of TNFα and the sensitivity to sTNFα-induced cytotoxicity. To discriminate whether this effect is mediated by conventional TNFα signaling or reverse signaling, they expressed in MCF-7 cells a truncated TNFα that mimics the membrane-anchored fragment after TACE-mediated release of sTNFα, which they named TNF-LS. Expression of TNF-LS desensitized MCF-7 cells to sTNFα-induced cytotoxicity, and this effect was executed by membrane-anchored TNF-LS, but not TNF-ICD, as inhibition of SPPL2 with $(Z\text{-}LL)_2$-ketone treatment enhanced the accumulation of TNF-LS, and consequently, resistance to sTNFα-induced cytotoxicity. Therefore, inhibition of SPPs by GSIs can have biological consequences, including those directly related to cancer cell growth and survival, and should be avoided. Fortunately, many currently available GSIs are very specific to γ-secretase. For example, DAPT does not affect the activity of SPPs (433). Therefore, the off-target effects at the protease level could be avoided with careful selection.

1.6.1.2.2 Specificity at the substrate level

Even the most specific GSIs still affect the activity of multiple proteins as there are more than 25 γ-secretase substrates in addition to Notch receptors [reviewed in (443)]. Among them, several proteins, including cadherins, CD44, and ErbB4, are known to have important functions in cancer cells.

APP is probably the most intensively studied γ-secretase substrate, and almost all the GSIs have been developed with the primary aim of reducing the processing of APP by γ-secretase [reviewed in (427)]. APP cleavage produces small β-amyloid peptides (38-42 aa in length) as well as the intercellular domain of APP (AICD). While β-amyloid peptides have long been associated with the development of Alzheimer's disease, other functions of AICD are not well understood. A recent study demonstrated that AICD could directly bind to the EGFR promoter and suppress its expression (444). This reverse relationship between γ-secretase activity and EGFR level was also confirmed by others (445), although the moderate increase in the EGFR mRNA levels could not explain the more dramatic increase in EGFR protein observed in γ-secretase deficient cells. Although the γ-secretase complex might cleave EGFR to promote its turnover, this possibility has not been investigated probably because no shorter form of EGFR has been observed. However, as the half-life of NICD is very short, the same might be true for the possible "intracellular domain of EGFR". It should be noted that at least one member of EGFR family, ErbB4, is known to be cleaved by the γ-secretase complex.

Unlike other members of EGFR family, activation of ErbB4 by its ligand, heregulin, inhibits the growth of breast cancer cells and this inhibition can be blocked by Compound E (446). A later study using ectopic expression of ErbB4-ICD confirmed its anti-proliferation activity in breast cancer cells and mammary epithelial cells (447). However, not all ErbB4 activities require γ-secretase-mediated cleavage as a mutant ErbB4 that cannot be cleaved by γ-secretase could still phosphorylate Akt, Erk 1/2, and STAT5 upon heregulin stimulation (448). Nonetheless, γ-secretase-mediated release of ErbB4-ICD can have important biological consequences.

The cell adhesion molecule, E-cadherin, is also a γ-secretase substrate, and cleavage of E-cadherin promotes the disassembly of adherens junctions and increases free cytosolic β-catenin, with the former possibly promoting epithelial-mesenchymal transition and the latter enhancing the Wnt signaling activity (449). Interestingly, a recent study reported that the C-terminal fragment of E-cadherin

(E-cad/CTF), the product of γ-secretase-mediated cleavage, could translocate into the nucleus and enhance β-catenin-mediated transactivation, and this enhanced nuclear expression of E-cad/CTF protected fibroblast cells from staurosporine-induced apoptosis (450). Furthermore, cadmium, a toxic heavy metal, induced γ-secretase-mediated E-cadherin cleavage and enhanced cell motility and migration in T47D breast cancer cells, an effect which could be inhibited by DAPT (451). In addition to E-cadherin, γ-protocadherin and N-cadherin can also be processed by γ-secretase (452, 453), and N-cad/CTF affects the CREB-dependent transcription of c-fos mRNA by recruiting CBP, a histone acetyltransferase, to the cytoplasm and promoting its degradation (453).

CD44 is another cell adhesion molecule that is sequentially cleaved by ADAM10 and γ-secretase (454-456). While ADAM10-mediated cleavage has long been associated with increased cell proliferation and migration (454, 457), a recent study reported that the intracellular domain of CD44 generated by γ-secretase-mediated cleavage could transform rat fibroblast cells (458). In addition, cleavage of low density lipoprotein receptor-related protein 1B (LRP1B) by γ-secretase was shown to suppress the anchorage-independent growth of glioma cells (459), and cleavage of voltage-gated sodium channel β2-subunit by γ-secretase complex was reported to regulate cell adhesion and migration (460).

Together with the as yet unidentified consequences of γ-secretase-mediated cleavage of other substrates, treatment with currently available GSIs might produce phenotypes beyond those associated with Notch signaling. Encouragingly, it is now possible to make Notch-sparing GSIs (461, 462), raising the hope that in the future, it might be possible to synthesize Notch-specific GSIs, although it will be a daunting task.

1.6.1.2.3 Specificity at paralog level

Despite the fact that GSIs can interfere with the activity of multiple proteins, the dose-limiting toxicity that caused premature termination of the phase I clinical trial of GSI in T-ALL was mainly GI toxicity (463). This was most likely induced by goblet metaplasia as chronic treatment of mice with the GSI, LY-411,575,

induced goblet hyperplasia and dramatic changes in the GI tract architecture (431). Notch1 and Notch2 play redundant roles in regulating the goblet differentiation, and inactivation of either one alone does not induce abnormal goblet differentiation (325). Similarly, Notch1-3 play complementary roles in regulating hair follicle stem cells, another adult tissue that undergoes rapid renewal (464). Furthermore, different Notch paralogs might have opposite activities in tumor progression, such as Notch2 *vs.* the other three paralogs in breast cancer. Therefore, it would be desirable to specifically block the signaling of individual Notch paralogs, an effect that cannot be achieved with currently available GSIs.

1.6.2 Dominant negative MAML1 peptide

One way to increase the specificity of targeting is to block Notch signaling downstream of S3 cleavage, thus sparing the effects on other γ-secretase substrates. The dominant negative MAML1 (dnMAML1) fragment is such an example. The C-terminal truncated form of MAML1 functions in a dominant negative manner by preventing the recruitment of p300 and other transcription activators to the NICD/RBPjκ/MAML core complex (215, 227). Weng et al. used this strategy to block Notch signaling and induce cell growth arrest in T-ALL cell lines (349). They found that the minimum MAML1 fragment that could form a trimeric complex with N1ICD and RBPjκ corresponds to aa 13-74 of human MAML1. When this fragment of MAML1 was transfected into Notch-dependent T-ALL cell lines, it inhibited the growth of T-ALL cells. However, this polypeptide is still too large to enter cells and is not stable in vivo. To overcome these problems, Moellering et al. designed a high affinity hydrocarbon-stapled peptide based on the structure of the N1ICD/RBPjκ/ MAML1 trimeric complex (465). Peptide stapling, the cross-linking of a non-natural amino acid that is incorporated into neighbouring positions during synthesis, has been shown to enhance the binding affinity and stability of peptides (466). They first designed six overlapping peptides that cover the entire interface between MAML1 and N1ICD/RBPjκ and chose the one corresponding to aa 21-36 of human MAML1, designated SAHM1, for further study. FITC-labelled SAHM1 could easily be engulfed into cells via an energy-consuming mechanism and was present in both

the cytoplasm and the nucleus. Further, SAHM1 could form a complex with N1ICD/RBPjκ and suppress the expression of Notch target genes in T-ALL cells to a level comparable to that of DAPT. SAHM1 inhibited the proliferation and engraftment of T-ALL cells in vitro, and in vivo, intraperitoneal injection of SAHM1 induced regression of established T-ALL. This demonstrates the high efficacy of this approach for blocking Notch signaling for therapeutic benefit.

1.6.3 Neutralizing antibodies

Although the dnMAML1 peptide spares other γ-secretase substrates, it blocks the signaling of all Notch paralogs, which could be problematic. Neutralizing antibodies or RNAi against individual Notch paralogs may further improve specificity when targeting individual Notch paralogs.

Through unbiased screening, Li et al. identified both inhibitory and activating mouse monoclonal antibodies against the NRR domain of human Notch3 protein (467). The two most potent inhibitory antibodies specifically blocked ligand-induced Notch3 activation without interfering with ligand binding. Epitope mapping revealed that amino acid residues from both the LNR1 and HD domains were recognized by the inhibitory antibodies, and that antibody binding kept the NRR in a closed conformation. As expected, active Notch3 signaling induced by ligand binding enhanced the proliferation, migration, and formation of loosely attached spheres of HEK293T cells. Addition of inhibitory antibody into the culture blocked all of these phenotype changes, demonstrating, in principle, the applicability of this approach for clinical use.

Recently, researchers from Genentech used phage display technology to generate high affinity, fully humanized, inhibitory IgG1 against the NRR domain of human Notch1 or Notch2 (468). After in vitro testing, the specificity and efficacy of these antibodies were evaluated in mice. Consistent with their respective involvement in T cell and marginal zone B cell development, anti-Notch1 antibody, but not anti-Notch2 antibody, specifically impaired the T cell development, whereas anti-Notch2 antibody, but not anti-Notch1 antibody, eliminated marginal zone B cells in the spleen.

Since many of Notch-dependent T-ALLs arise from activating mutations in the NRR of Notch1, the region to which this antibody binds, the authors then confirmed that the anti-Notch1 antibody could inhibit the signaling of the four most clinically common NRR mutants. In addition, they showed that this antibody could inhibit the growth of a T-ALL cell line that bears a common mutation within the NRR. Furthermore, they screened ~ 45 cancer cell lines from different tissues and found this anti-Notch1 antibody inhibited the growth of a human colon cancer cell line, MT-3, which harbors an activating Notch1 NRR mutation. The anti-tumor activity was further confirmed in a tumor xenograft model. Most importantly, the authors showed that treatment with either anti-Notch1 or anti-Notch2 antibodies did not result in overt GI toxicity, although histological examination of the revealed mild goblet cell metaplasia after anti-Notch1 treatment. Also, mice treated with both anti-Notch1 and anti-Notch2 antibodies lost 20% of body weight within 6 days due to severe goblet cell metaplasia as expected.

1.6.4 RNA interference

Knockdown of individual Notch paralogs has been widely used to induce cell growth arrest or cell killing in tumor cultures of breast cancer cells or other types cancer cells, but not in clinical settings, mainly due to the concerns over off-target effects, and the challenge to delivering active siRNA into cancer cells in vivo [reviewed in (469)]. However, a recent report suggests that a nanoparticle delivery system could be used to successfully target siRNA to cancer cells (470). In this case, nanoparticles were used to deliver siRNA against the M2 subunit of ribonucleotide reductase (RRM2). As a targeting strategy, the nanoparticles were coated with transferrin protein because many cancer cells express high levels of the transferrin receptor. The nanoparticles were injected intravenously into three patients with metastatic melanoma at escalating doses. The nanoparticles were found in the tumor tissues at concentrations reflecting the injected doses, but not in the adjacent epidermis. Analysis of biopsies from the patient who received highest dose showed reduction in both RRM2 mRNA and protein levels of after treatment. In addition, the presence of RNAi-mediated cleavage product was confirmed using a modified PCR technique that specifically detected the RNAi product. Although the tumor response to nanoparticle-delivered siRNA was not described, these results demonstrate the practicality of

using nanoparticles to target siRNA to tumors. However, the safety concerns over the use of nanoparticles need to be addressed [reviewed in (471)].

1.6.5 Angiogenesis inhibition

Since Dll4/Notch signaling is essential for angiogenesis, a prerequisite for the growth of solid tumors, inhibition of Dll4/Notch signaling could suppress tumor growth even if the cancer cells themselves do not depend on Notch signaling for survival. This hypothesis was first confirmed by two studies that were published at the same time (472, 473). Ridgway et al. found that blocking Dll4/Notch signaling with a neutralizing Dll4 antibody suppressed the growth of HM7 (human colorectal cancer), Colo205 (human colon adeno-carcinoma), Calu6 (human lung adenocarcinoma), MDA-MB-435 (human breast cancer or melanoma), and EL4 (mouse lymphoma) xenografts (472). This inhibition was due to impaired angiogenesis. In contrast to VEGF signaling inhibition, which resulted in reduced blood vessel formation, blocking Dll4/Notch signaling increased the blood vessel density but the new vessels were not functional due to remodelling defects. Furthermore, Dll4 antibody treatment did not cause GI toxicity, suggesting that DLL4 is not essential for intestinal stem cell renewal. Antitumor effects were observed in C6 (rat glioma) and HT1080 (human sarcoma) xenografts when Dll4/Notch signaling was blocked by soluble Dll4, which can bind to, but cannot activate, Notch receptors due to its inability to generate pulling force (473). Furthermore, it was shown that anti-Notch1 (NRR) antibody could also inhibit the growth of HM7 and Calu6 xenografts (468). Most importantly, blocking Dll4/Notch1 signaling did not affect the growth of HM7, Calu6, and C6 cells *in vitro*, indicating this strategy is also applicable to solid tumors that do not have aberrantly active Notch signaling (468, 473).

However, there are safety concerns over inhibiting Dll4/Notch-mediated angiogenesis in cancer treatment (474). Yan et al. showed that treatment with Dll4 antibody for 3-8 weeks induced significant histopathological changes in mouse liver, a less investigated side effect of Notch inhibition. These changes include drastic atrophy of centrilobular hepatic cords, dilation of centrilobular hepatic sinusoids, and bile ductular proliferation. In addition, similar liver damage was observed in mice treated with soluble Dll4, an anti-Notch1 (NRR) antibody,

or a GSI, as well as in rats and cynomolgus monkeys treated with Dll4 antibody. Further analysis suggested that liver damage resulted from activation of liver endothelium, which is otherwise quiescent, and subsequent disruption of hepatocyte homeostasis due to close spatial relationship between liver endothelium and hepatocytes. Aberrant activation of endothelium also caused subcutaneous vascular neoplasms, albeit less frequently (3 out of 15 mice). It was not reported whether these lesions were reversible. However, this does raise safety concerns over the use not only of the Dll4 antibody itself, but also of other Notch signaling inhibitors as liver damage was also observed in mice treated with Notch1 antibody or a γ-secretase inhibitor.

1.7. Statement of problems to be investigated

The strongest justification for using γ-secretase inhibitors—or more generally Notch inhibition—for breast cancer treatment came from two studies that reported that GSI I, Z-LLNle-CHO, inhibited the growth of breast cancer cells, especially ER negative breast cancer cells, both *in vitro* and *in vivo* without causing significant systemic side effects (401, 416). However, GSI I is derived from, and is structurally similar to, MG132 (Z-LLL-CHO), a widely used non-specific proteasome inhibitor. This raised the concern that the cytotoxicity of GSI I was due to off-target effects. To address this, Lee et al. also used a second GSI, z-Ile-Leu-CHO, to demonstrate that the cytotoxicity of GSI I in breast cancer cells was due to Notch signaling inhibition (416). On the other hand, Rizzo et al. reported that no proteasome inhibition was observed at the dose that killed breast cancer cells, although data was not shown (401). While Notch inhibition in T-ALL cells induces G_0/G_1 cell cycle arrest (264, 265, 272, 346, 349, 351, 352), GSI I treatment in breast cancer cells induced G_2/M arrest (401, 416). In addition, GSI treatment in both mice and human causes GI toxicity, which was not observed in these two studies (401, 416). Therefore, whether the cytotoxicity of GSI I to breast cancer cells is actually mediated by Notch inhibition merits further investigation as mis-assignment may lead to futile efforts in further development of these drugs and waste limited resources.

Furthermore, chronic treatment with even the currently most specific reagent for Notch inhibition, paralog-specific neutralizing antibody, causes liver damage and

vascular neoplasms *in vivo* due to the essential role of Dll4/Notch1 signaling in maintaining blood vessel integrity (474). Therefore, identification of new approaches to block oncogenic Notch signaling is of value. Since non-canonical Notch signaling pathways are sufficient to induce breast cancer tumorigenesis in the absence of RBPjκ (393), it is possible that they are also essential for the survival of breast cancer cells. The non-canonical signaling pathways involved in breast cancer tumorigenesis and survival, and their role in maintaining tissue homeostasis in adults, have yet to be determined. However, some of the NICD interacting proteins listed in Table1 might participate in tumorigenic non-canonical Notch signaling pathways, although it should be noted that most of the interactions listed in Table1 were observed in cells with high levels of endogenous NICD, or with ectopic expression of exogenous NICD. Therefore, it is possible that these interactions only, or preferentially, occur when NICD levels are high, the same conditions under which oncogenic Notch signaling occurs. If this is the case, it is also likely that these interactions would not play an essential role in adult tissue homeostasis during which NICD levels are tightly controlled. Consequently, blocking these "oncogenic interactions" without suppressing the physiological activities of participating proteins, including NICD, might provide a safer approach to inhibit oncogenic Notch signaling. Although this strategy is very attractive, there is currently no information regarding the conditions under which these interactions occur. In addition, most of the interactions listed in Table 1 were observed with N1ICD. Whether it also applies to other NICD paralogs remains to be investigated.

Table 1-1. Proteins reported to interact with NICD possibly independent of RBPjκ

NICD-interacting protein	NICD paralog	NICD domain	Cell lines	NICD level	Reference
NFκB p50	N1ICD	Not determined	Sup-T1 T cells	Detectable N1ICD due to truncation in the Notch1 extracellular domain	(62, 239)
NFκB p50	N1ICD	RAM	*In vitro* EMSA	Unknown	(240)
NFκB p50/C-Rel	N1ICD	Not determined	DO11.10 murine T cells	Transfected with N1ICD plasmid	(242)
NFκB p65	N2ICD	Not determined	Bone marrow-derived macrophages	Not known but needs RANKL stimulation	(241)
IKKα	N3ICD	Not determined	T cells	High, N3ICD transgenic mice	(475)
IKKα/β/γ	N1ICD	Not determined	T cells	High, N1ICD transgenic mice	(354)
IKKα	N1ICD	Not determined	Cervical cancer CaSki cell	Detectable due to spontaneous activation	(476)
Smad3	N4ICD	RAM not required	Mammary carcinoma cells	High, N4ICD transgenic mice	(423)
Smad3	N1ICD	Not determined	THP1, HT29, or dentric cells	Moderate to high due to ligand stimulation or transfection	(477)

YY1	N1ICD	ANK repeats	Jurkat, Sup-T1, and K562 cells	Detectable in two T-ALL cells, K562 cells transfected with N1ICD plasmid	(478)
P53	N1ICD	RAMANK	HCT 116	Not known	(479)
HIF1α	N1ICD	Not determined	*In vitro* assay	High	(480)
FIH	N1/2/3ICD	ANK	*in vitro* assay	High	(481, 482)
XIAP	N1ICD	C-terminal to ANK repeats	Jurkat, HEK293T, and DO11.10	Jurkat and 293T transfected with N1ICD and XIAP, DO11.10 stimulated with Jagged-1	(278)
Tip60	N1ICD	RAM	HEK293	Transfected with individual components	(483)
βII-tubulin	N1ICD	ANK	Jurkat, Sup-T1, and K562 cells	Detectable in two T-ALL cells, K562 cells transfected with N1ICD plasmid	(484)
JNK-interacting protein 1	mN1ICD	aa 1898-2197	HEK293	Transfected with mNICD and JIP1	(268)
β-catenin	N1ICD	Not determined	HEK293	Transfected with N1ICD	(485)
LEF-1	N1ICD	C-terminal to ANK repeats	HEK293T	Transfected with N1ICD and LEF-1	(486)
Runx3	N1ICD	Not determined	SMMC7721 & *In vitro*	Co-transfected with Runx3 and N1ICD	(487)
Disabled-1	dNICD	RAM	Drosophila tissues	Unknown	(488, 489)
Wdr12	N1ICD	Not determined	*In vitro*	Unknown	(490)
Myocilin	N2ICD?	Not determined	Yeast two-hybrid	Unknown	(491)

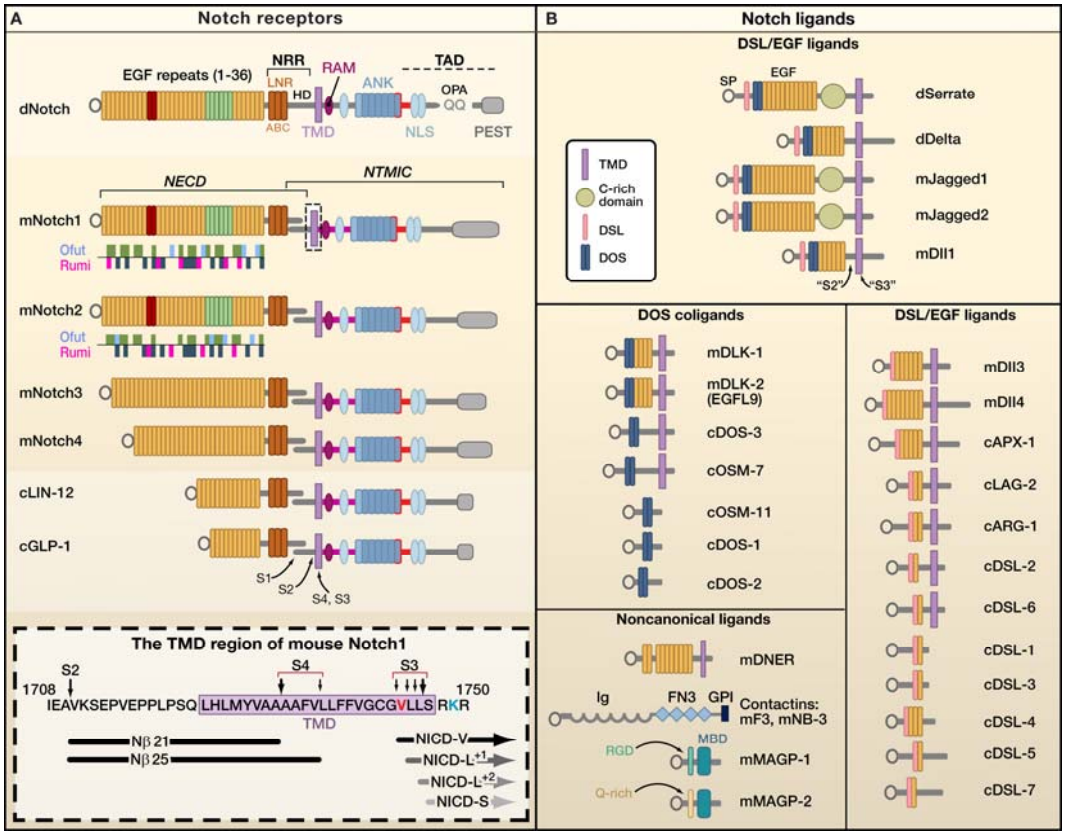

Figure 1-1. Domain organization of the Notch pathway receptors, ligands and co-ligands from fly, worm and mammals. A) Notch receptors are large single-pass transmembrane proteins that contain multiple extracellular EGF-like repeats, three cysteine-rich Lin12-Notch repeats (LNR-A, B and C), and a heterodimerization domain (HD) in their extracellular domain (NECD). Repeats 11–12 (orange) and 24–29 (green) mediate interactions with ligands. Shown under the NECD of mNotch1 and mNotch2 are the putative distribution of shared (green) and unique fucosylation (Cyan) and glycosylation (magenta) sites, which might affect the receptor-ligand interaction. The three LNR repeats and HD domain constitute a Negative Regulatory Region (NRR), which prevents receptor activation (cleavage) in the absence of ligand binding. Close to the transmembrane domain (TMD) in the intracellular domain (NICD) is an RBPjκ-associated module (RAM) domain, followed by seven ankrin repeats (ANK) that are flanked by two nuclear localizing sequence (NLS). The extreme C-terminus contains a proline/glutamic acid/serine/threonine-rich motifs (PEST) that regulates the stability of NICD. Between the ANK repeats and PEST is a loosely

defined and evolutionarily divergent transactivation domain (TAD) as well as a *Drosophila* specific glutamine-rich OPA repeat. B) Ligands and potential ligands of Notch receptors can be classified into several groups based on their domain composition. Classical DSL ligands that contain DSL, DOS and EGF motifs are not found in *C. elegans*. *C. elegans* and mammalian DSL-only ligands lacking the DOS motif (DSL/EGF ligands) are a subtype of DSL ligands that may act alone or in combination with DOS co-ligands. Some DSL/EGF ligands and DOS co-ligands are diffusible ligands. Non-canonical ligands lack DSL and DOS domains. C) Details of the mouse Notch1 TMD (boxed) and flanking residues showing the cleavage sites and corresponding products. Upon ligand binding, Notch is sequentially cleaved by ADAM and γ-secretase at S2 site and S3 sites respectively. S3 cleavage can produce several different products dependent on the scissile bonds, but only NICD-V1744 is stable. The V1744G and K1749R amino acid substitutions (colorized) shift the S3 cleavage site and affect the stability and signalling strength of NICD. γ-secretase further cleaves the TMD (S4 cleavage) until the short Nβ peptides can escape the lipid bilayer; most Nβ peptides are 21 amino acids long. Reproduced with permission from Raphael Kopan & Ma. Xenia G. Ilagan, Cell. 2009; 137(2): 216–233.

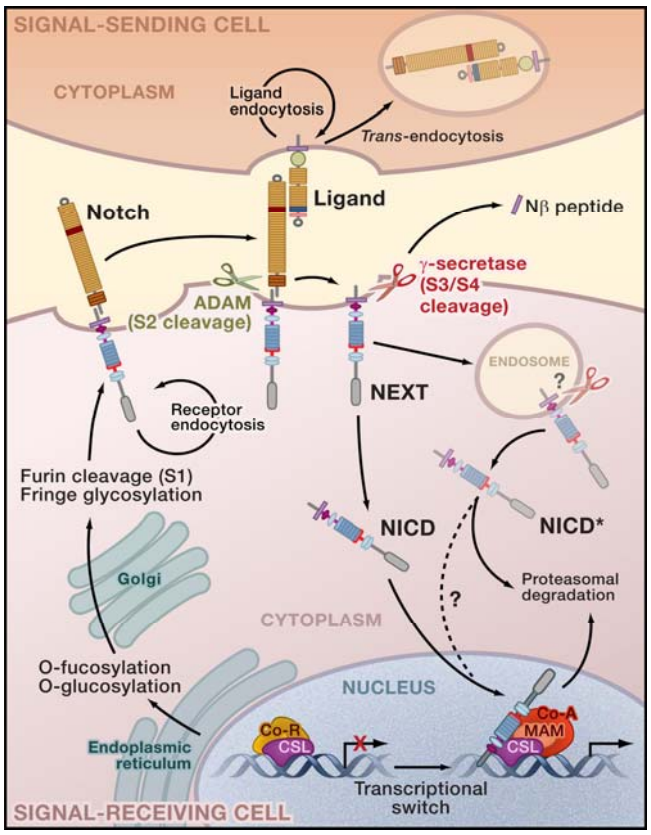

Figure 1-2. The Core Notch Signaling Pathway is mediated by regulated proteolysis. The newly synthesized receptor is cleaved by Furin at Site 1 (S1) within Golgi, and as a result, the receptor at the cell surface is a heterodimer held together by non-covalent interactions. Ligand endocytosis, after binding to receptor, is thought to pull the extracellular domain of receptor to induce a conformational change in the NRR so that the Notch S2 site will be exposed to ADAM metalloproteases. The C-terminal product of S2 cleavage, Notch extracellular truncation fragment (NEXT), will then be processed by the γ-secretase complex, which can occur at the cell surface or in endosomal compartments. However, NICD produced by the cell surface cleavage might be more stable. In the absence of NICD, the sequence-specific DNA-binding protein CSL associates with ubiquitous corepressor (Co-R) proteins and histone deacetylases (HDACs) to repress transcription of target genes. When NICD enters the nucleus, its binding to CSL may trigger an allosteric change that facilitates displacement of transcriptional repressors. Mastermind (MAM) then recognizes the NICD/CSL interface, and this trimeric complex further recruits coactivators (Co-A) to activate transcription. Reproduced with permission from Raphael Kopan & Ma. Xenia G. Ilagan, Cell. 2009; 137(2): 216–233.

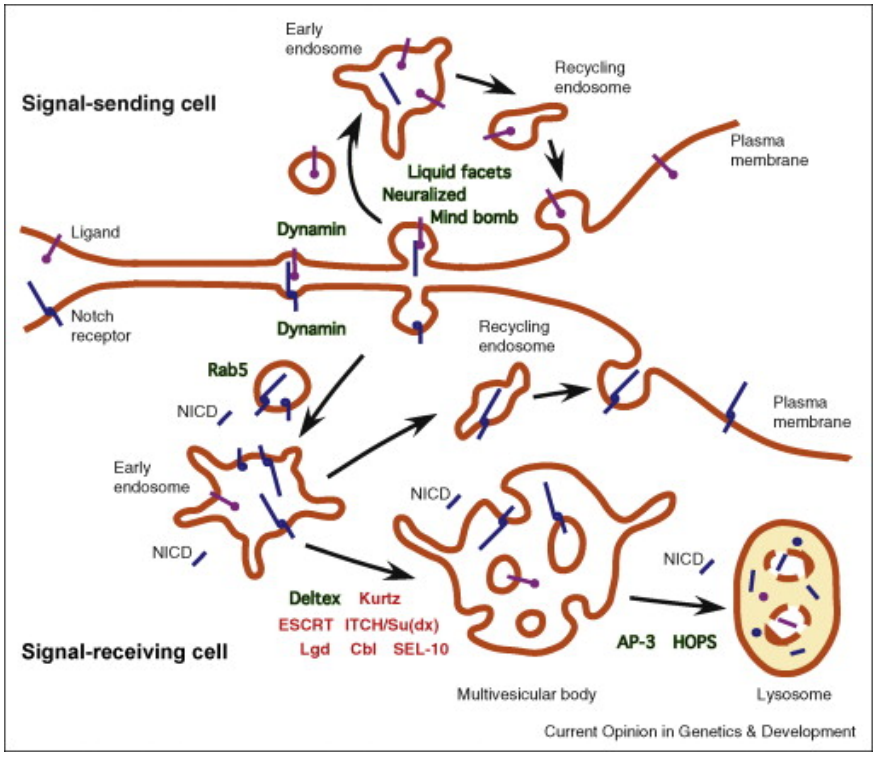

Figure 1-3. Overview of ligand and receptor endocytosis in the Notch signaling pathway. In the signal-sending cell (top), endocytosis of Notch ligands (violet) is proposed to positively regulate Notch activation via two mechanisms: generating pulling force and/or producing more competent ligands through yet-to-be-identified post-translational modification in the recycling compartment. In the signal-receiving cell (bottom), internalization of Notch receptors (blue) is generally thought to negatively regulate its availability at cell surface through lysosome-mediated degradation. However, it might also induce ligand-independent receptor activation. The identities of various endocytic factors involved in these trafficking steps are shown near their approximate sites of activity; those that promote signaling are indicated in green whereas those involved in signaling downregulation are indicated in red. Reproduced with permission from Mark E. Fortini & David Bilder, Curr Opin Genet Dev. 2009; 19(4):323-328.

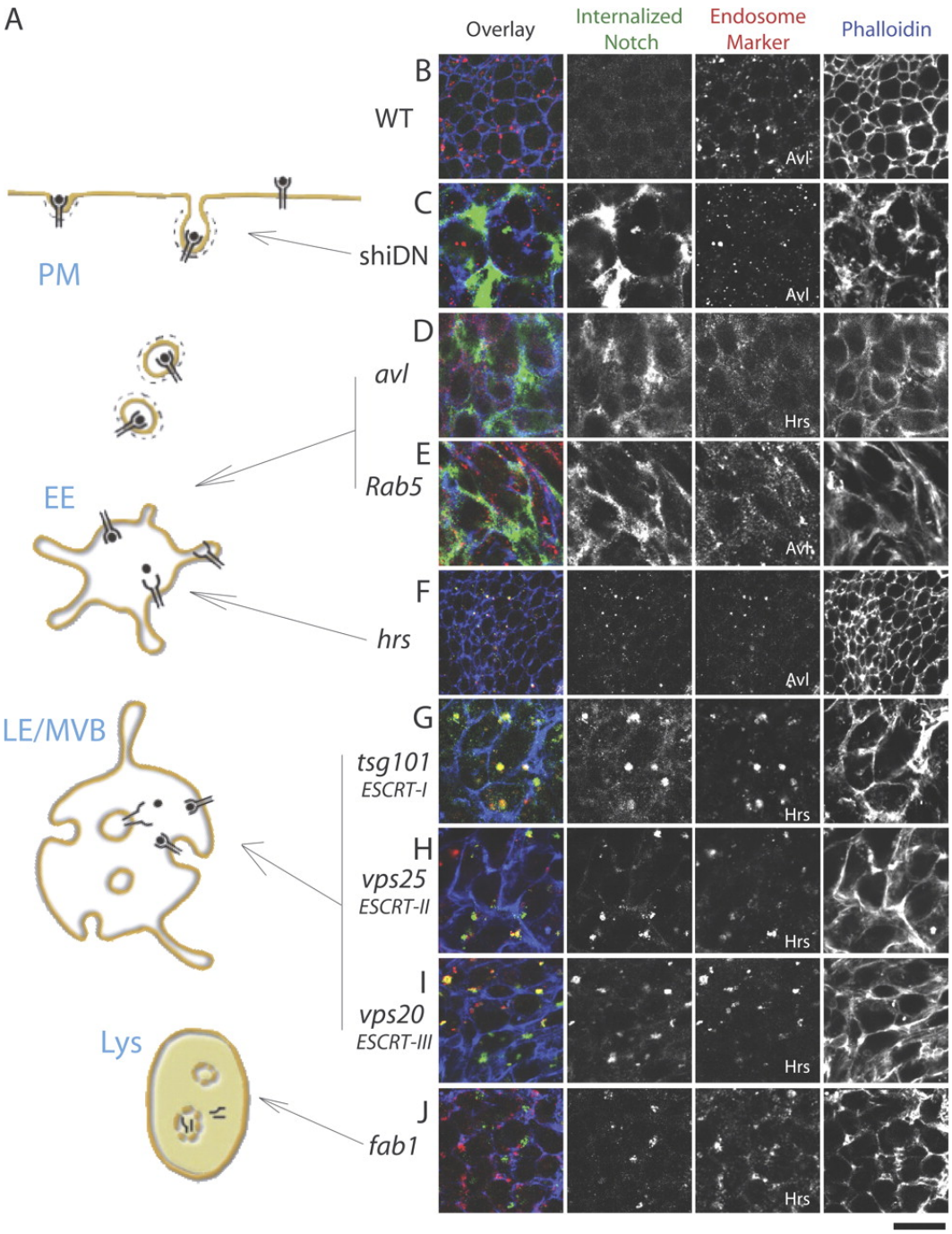

Figure 1-4. Trafficking defects in endocytic mutant tissue lead to Notch accumulation in different compartments. (A) Schematic of endocytic trafficking. Arrows indicate the approximate site of action of each gene product. PM: plasma membrane. EE: early endosomes. LE/MVB: late endosomes/multivesicular bodies. Lys: lysosomes. (B–J) Live trafficking assay for Notch in cultured eye or wing (C) imaginal discs. Avl and Hrs mark endosomal compartments and phalloidin reveals cell outlines. In WT tissue, surface-bound

Notch is internalized and then degraded after 5 h (B). In mutant tissue, Notch is internalized but is not degraded, persisting 5 h after labeling (C–J). In shiDN, avl, and Rab5 mutants, Notch is localized to the cell surface (C–E); in hrs mutants, Notch is bound to Avl-positive organelles (F); in ESCRT mutants, Notch is bound to Hrs-positive organelles (G and I); and in fab1 mutants, Notch is bound in organelles that are neither Avl- nor Hrs-positive. Bar, 10 μm. Reproduced from Thomas Vaccari et al., J Cell Biol. 2008; 180(4): 755-762. No specific permission is required for non-commercial third-party reuse.

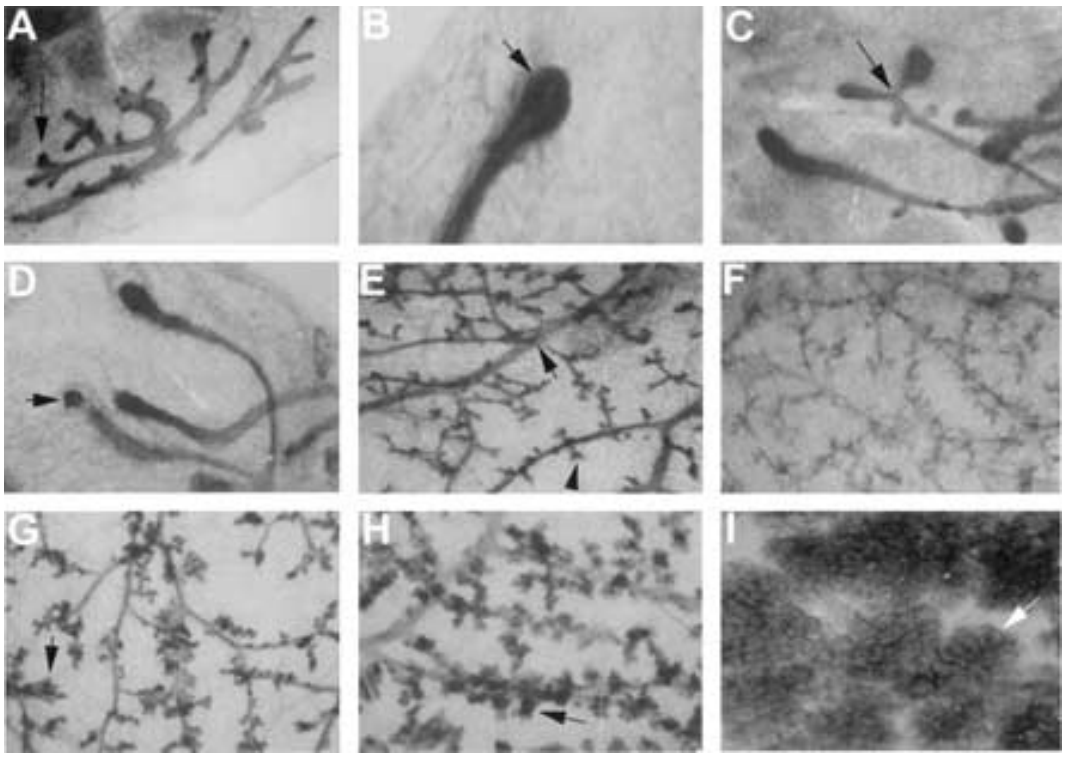

Figure 1-5. Whole-mount analysis of mammary gland structures from FVB mice. The fourth inguinal mammary glands were dissected from female mice at the indicated stages, fixed, and stained with hematoxylin. (A) Epithelial structures from a 3-week virgin. Terminal end buds (TEBs) are indicated by the arrow. (B) A TEB (arrow) from a 5-week virgin. (C) Epithelial structures from a 5-week virgin. Bifurcation of the growing duct is indicated by the arrow. (D) Epithelial structures from a 10-week virgin showing a regressing end bud (arrow). (E) Ducts from a 10-week virgin showing both lateral branches (arrow) and alveolar buds (arrowheads). (F) Epithelial structures from a mammary gland at day 21 of involution. (G) Alveolar structures from a mammary gland at day 8 of pregnancy. The alveolar lobules are beginning to develop (arrow). (H) Alveolar structures from a mammary gland at day 12 of pregnancy. The alveoli are continuing to develop (arrow). (I) Alveolar structures from a mammary gland at day 18 of pregnancy. The arrow indicates the alveoli that have filled the majority of the fat pad. All panels were photographed at 45 × magnification. Panels A–D have been cropped and enlarged to show the structures of interest, so magnification is not exact. Reproduced with permission from Monica M. Richert et al., J Mammary Gland Biol Neoplasia. 2000; 5(2):227-241.

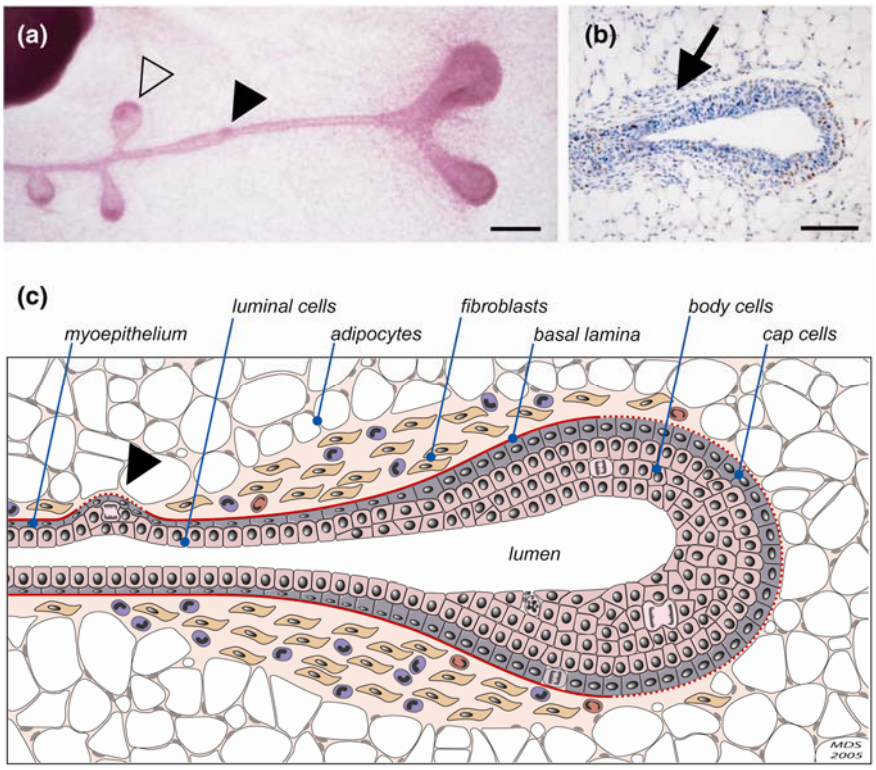

Figure 1-6. Mammary gland terminal end bud (TEB) and duct morphology. (a) High-magnification carmine alum-stained wholemount of a primary duct that has recently passed the central lymph node (upper left corner). The bifurcating TEB is in the final stages of forming two new primary ducts with independent TEBs. Three newly formed lateral (secondary) side-branches are also present along the trailing duct (open arrowhead), as is an area of increased cellularity that may represent a nascent lateral bud (filled arrowhead). Increased stromal cellularity is also apparent surrounding the bifurcating TEB. Scale bar, 200 μm. (b) Immunophotomicrograph of a TEB illustrating its considerable proliferative activity, as indicated by the large number of cells that have undergone DNA replication and have thus incorporated bromodeoxyuridine (brown diaminobenzidine-stained nuclei) during a 2-hour chase period. Hematoxylin counterstaining also reveals the stromal collar, rich in fibroblasts and collagen, that characteristically surrounds the TEB neck (arrow) and its conspicuous absence beyond the invading distal cap. Scale bar, 100 μm. (c) Schematic diagram depicting the salient architectural features of TEBs and their subtending ducts, including their fibroblast-rich stromal collar and high mitotic index. Dotted line illustrates the thinning of the basement membrane at the tips of invading ducts as a result of their partial enzymatic degradation and/or incomplete de

novo synthesis. Reproduced from Mark D. Sternlicht, Breast Cancer Res. 2006; 8(1):201. Reproduction of figures is permitted without formal written permission from the publisher or the copyright holder.

References

1. Hortobagyi GN, de la Garza Salazar J, Pritchard K, Amadori D, Haidinger R, Hudis CA, et al. The global breast cancer burden: variations in epidemiology and survival. Clin Breast Cancer. 2005;6:391-401.
2. Canadian Cancer Society's Steering Committee: Canadian Cancer Statistics 2009. Toronto: Canadian Cancer Society; 2009.
3. Fisher B, Anderson S, Bryant J, Margolese RG, Deutsch M, Fisher ER, et al. Twenty-year follow-up of a randomized trial comparing total mastectomy, lumpectomy, and lumpectomy plus irradiation for the treatment of invasive breast cancer. N Engl J Med. 2002;347:1233-41.
4. Early Breast Cancer Trialists' Collaborative Group (EBCTCG). Effects of chemotherapy and hormonal therapy for early breast cancer on recurrence and 15-year survival: an overview of the randomised trials. Lancet. 2005;365:1687-717.
5. Smith I, Procter M, Gelber RD, Guillaume S, Feyereislova A, Dowsett M, et al. 2-year follow-up of trastuzumab after adjuvant chemotherapy in HER2-positive breast cancer: a randomised controlled trial. Lancet. 2007;369:29-36.
6. Perou CM, Sorlie T, Eisen MB, van de Rijn M, Jeffrey SS, Rees CA, et al. Molecular portraits of human breast tumours. Nature. 2000;406:747-52.
7. Sorlie T, Perou CM, Tibshirani R, Aas T, Geisler S, Johnsen H, et al. Gene expression patterns of breast carcinomas distinguish tumor subclasses with clinical implications. Proc Natl Acad Sci U S A. 2001;98:10869-74.
8. Hu Z, Fan C, Oh DS, Marron JS, He X, Qaqish BF, et al. The molecular portraits of breast tumors are conserved across microarray platforms. BMC Genomics. 2006;7:96.
9. Parker JS, Mullins M, Cheang MC, Leung S, Voduc D, Vickery T, et al. Supervised risk predictor of breast cancer based on intrinsic subtypes. J Clin Oncol. 2009;27:1160-7.
10. Wang Y, Klijn JG, Zhang Y, Sieuwerts AM, Look MP, Yang F, et al. Gene-expression profiles to predict distant metastasis of lymph-node-negative primary breast cancer. Lancet. 2005;365:671-9.
11. Weigelt B, Mackay A, A'Hern R, Natrajan R, Tan DS, Dowsett M, et al. Breast cancer molecular profiling with single sample predictors: a retrospective analysis. Lancet Oncol.
12. van 't Veer LJ, Dai H, van de Vijver MJ, He YD, Hart AA, Mao M, et al. Gene expression profiling predicts clinical outcome of breast cancer. Nature. 2002;415:530-6.
13. Chang HY, Nuyten DS, Sneddon JB, Hastie T, Tibshirani R, Sorlie T, et al. Robustness, scalability, and integration of a wound-response gene expression signature in predicting breast cancer survival. Proc Natl Acad Sci U S A. 2005;102:3738-43.
14. Paik S, Shak S, Tang G, Kim C, Baker J, Cronin M, et al. A multigene assay to predict recurrence of tamoxifen-treated, node-negative breast cancer. N Engl J Med. 2004;351:2817-26.
15. Fan C, Oh DS, Wessels L, Weigelt B, Nuyten DS, Nobel AB, et al. Concordance among gene-expression-based predictors for breast cancer. N Engl J Med. 2006;355:560-9.
16. de Ronde JJ, Hannemann J, Halfwerk H, Mulder L, Straver ME, Vrancken Peeters MJ, et al. Concordance of clinical and molecular breast cancer subtyping

in the context of preoperative chemotherapy response. Breast Cancer Res Treat.119:119-26.
17. Makretsov NA, Huntsman DG, Nielsen TO, Yorida E, Peacock M, Cheang MC, et al. Hierarchical clustering analysis of tissue microarray immunostaining data identifies prognostically significant groups of breast carcinoma. Clin Cancer Res. 2004;10:6143-51.
18. Abd El-Rehim DM, Ball G, Pinder SE, Rakha E, Paish C, Robertson JF, et al. High-throughput protein expression analysis using tissue microarray technology of a large well-characterised series identifies biologically distinct classes of breast cancer confirming recent cDNA expression analyses. Int J Cancer. 2005;116:340-50.
19. Fessler SP, Wotkowicz MT, Mahanta SK, Bamdad C. MUC1* is a determinant of trastuzumab (Herceptin) resistance in breast cancer cells. Breast Cancer Res Treat. 2009;118:113-24.
20. Tang P, Skinner KA, Hicks DG. Molecular classification of breast carcinomas by immunohistochemical analysis: are we ready? Diagn Mol Pathol. 2009;18:125-32.
21. Slamon DJ, Clark GM, Wong SG, Levin WJ, Ullrich A, McGuire WL. Human breast cancer: correlation of relapse and survival with amplification of the HER-2/neu oncogene. Science. 1987;235:177-82.
22. Reed MJ. The role of aromatase in breast tumors. Breast Cancer Res Treat. 1994;30:7-17.
23. Griffiths CT, Hall TC, Saba Z, Barlow JJ, Nevinny HB. Preliminary trial of aminoglutethimide in breast cancer. Cancer. 1973;32:31-7.
24. Dowsett M, Jones A, Johnston SR, Jacobs S, Trunet P, Smith IE. In vivo measurement of aromatase inhibition by letrozole (CGS 20267) in postmenopausal patients with breast cancer. Clin Cancer Res. 1995;1:1511-5.
25. Geisler J, King N, Anker G, Ornati G, Di Salle E, Lonning PE, et al. In vivo inhibition of aromatization by exemestane, a novel irreversible aromatase inhibitor, in postmenopausal breast cancer patients. Clin Cancer Res. 1998;4:2089-93.
26. Geisler J, King N, Dowsett M, Ottestad L, Lundgren S, Walton P, et al. Influence of anastrozole (Arimidex), a selective, non-steroidal aromatase inhibitor, on in vivo aromatisation and plasma oestrogen levels in postmenopausal women with breast cancer. Br J Cancer. 1996;74:1286-91.
27. Boccardo F, Rubagotti A, Aldrighetti D, Buzzi F, Cruciani G, Farris A, et al. Switching to an aromatase inhibitor provides mortality benefit in early breast carcinoma: pooled analysis of 2 consecutive trials. Cancer. 2007;109:1060-7.
28. Thurlimann B, Keshaviah A, Coates AS, Mouridsen H, Mauriac L, Forbes JF, et al. A comparison of letrozole and tamoxifen in postmenopausal women with early breast cancer. N Engl J Med. 2005;353:2747-57.
29. Winer EP, Hudis C, Burstein HJ, Wolff AC, Pritchard KI, Ingle JN, et al. American Society of Clinical Oncology technology assessment on the use of aromatase inhibitors as adjuvant therapy for postmenopausal women with hormone receptor-positive breast cancer: status report 2004. J Clin Oncol. 2005;23:619-29.
30. Konecny GE, Pegram MD, Venkatesan N, Finn R, Yang G, Rahmeh M, et al. Activity of the dual kinase inhibitor lapatinib (GW572016) against HER-2-overexpressing and trastuzumab-treated breast cancer cells. Cancer Res. 2006;66:1630-9.

31. Chu I, Blackwell K, Chen S, Slingerland J. The dual ErbB1/ErbB2 inhibitor, lapatinib (GW572016), cooperates with tamoxifen to inhibit both cell proliferation- and estrogen-dependent gene expression in antiestrogen-resistant breast cancer. Cancer Res. 2005;65:18-25.
32. Burris HA, 3rd, Hurwitz HI, Dees EC, Dowlati A, Blackwell KL, O'Neil B, et al. Phase I safety, pharmacokinetics, and clinical activity study of lapatinib (GW572016), a reversible dual inhibitor of epidermal growth factor receptor tyrosine kinases, in heavily pretreated patients with metastatic carcinomas. J Clin Oncol. 2005;23:5305-13.
33. Cameron D, Casey M, Press M, Lindquist D, Pienkowski T, Romieu CG, et al. A phase III randomized comparison of lapatinib plus capecitabine versus capecitabine alone in women with advanced breast cancer that has progressed on trastuzumab: updated efficacy and biomarker analyses. Breast Cancer Res Treat. 2008;112:533-43.
34. Ryan Q, Ibrahim A, Cohen MH, Johnson J, Ko CW, Sridhara R, et al. FDA drug approval summary: lapatinib in combination with capecitabine for previously treated metastatic breast cancer that overexpresses HER-2. Oncologist. 2008;13:1114-9.
35. Rimawi MF, Shetty PB, Weiss HL, Schiff R, Osborne CK, Chamness GC, et al. Epidermal growth factor receptor expression in breast cancer association with biologic phenotype and clinical outcomes. Cancer. 2010;116:1234-42.
36. Gee JM, Harper ME, Hutcheson IR, Madden TA, Barrow D, Knowlden JM, et al. The antiepidermal growth factor receptor agent gefitinib (ZD1839/Iressa) improves antihormone response and prevents development of resistance in breast cancer in vitro. Endocrinology. 2003;144:5105-17.
37. Sabnis GJ, Jelovac D, Long B, Brodie A. The role of growth factor receptor pathways in human breast cancer cells adapted to long-term estrogen deprivation. Cancer Res. 2005;65:3903-10.
38. Cristofanilli M, Valero V, Mangalik A, Royce M, Rabinowitz I, Arena FP, et al. Phase II, Randomized Trial to Compare Anastrozole Combined with Gefitinib or Placebo in Postmenopausal Women with Hormone Receptor-Positive Metastatic Breast Cancer. Clin Cancer Res.16:1904-14.
39. Green MD, Francis PA, Gebski V, Harvey V, Karapetis C, Chan A, et al. Gefitinib treatment in hormone-resistant and hormone receptor-negative advanced breast cancer. Ann Oncol. 2009;20:1813-7.
40. Arteaga CL, O'Neill A, Moulder SL, Pins M, Sparano JA, Sledge GW, et al. A phase I-II study of combined blockade of the ErbB receptor network with trastuzumab and gefitinib in patients with HER2 (ErbB2)-overexpressing metastatic breast cancer. Clin Cancer Res. 2008;14:6277-83.
41. Guarneri V, Frassoldati A, Ficarra G, Puglisi F, Andreetta C, Michelotti A, et al. Phase II, randomized trial of preoperative epirubicin-paclitaxel +/- gefitinib with biomarker evaluation in operable breast cancer. Breast Cancer Res Treat. 2008;110:127-34.
42. Smith IE, Walsh G, Skene A, Llombart A, Mayordomo JI, Detre S, et al. A phase II placebo-controlled trial of neoadjuvant anastrozole alone or with gefitinib in early breast cancer. J Clin Oncol. 2007;25:3816-22.
43. Baselga J, Albanell J, Ruiz A, Lluch A, Gascon P, Guillem V, et al. Phase II and tumor pharmacodynamic study of gefitinib in patients with advanced breast cancer. J Clin Oncol. 2005;23:5323-33.
44. Polychronis A, Sinnett HD, Hadjiminas D, Singhal H, Mansi JL, Shivapatham D, et al. Preoperative gefitinib versus gefitinib and anastrozole in

postmenopausal patients with oestrogen-receptor positive and epidermal-growth-factor-receptor-positive primary breast cancer: a double-blind placebo-controlled phase II randomised trial. Lancet Oncol. 2005;6:383-91.
45. von Minckwitz G, Jonat W, Fasching P, du Bois A, Kleeberg U, Luck HJ, et al. A multicentre phase II study on gefitinib in taxane- and anthracycline-pretreated metastatic breast cancer. Breast Cancer Res Treat. 2005;89:165-72.
46. Kim KJ, Li B, Winer J, Armanini M, Gillett N, Phillips HS, et al. Inhibition of vascular endothelial growth factor-induced angiogenesis suppresses tumour growth in vivo. Nature. 1993;362:841-4.
47. Bossung V, Harbeck N. Angiogenesis inhibitors in the management of breast cancer. Curr Opin Obstet Gynecol.22:79-86.
48. Burstein HJ, Elias AD, Rugo HS, Cobleigh MA, Wolff AC, Eisenberg PD, et al. Phase II study of sunitinib malate, an oral multitargeted tyrosine kinase inhibitor, in patients with metastatic breast cancer previously treated with an anthracycline and a taxane. J Clin Oncol. 2008;26:1810-6.
49. Moreno-Aspitia A, Morton RF, Hillman DW, Lingle WL, Rowland KM, Jr., Wiesenfeld M, et al. Phase II trial of sorafenib in patients with metastatic breast cancer previously exposed to anthracyclines or taxanes: North Central Cancer Treatment Group and Mayo Clinic Trial N0336. J Clin Oncol. 2009;27:11-5.
50. Kozloff M, Chuang E, Starr A, Gowland PA, Cataruozolo PE, Collier M, et al. An exploratory study of sunitinib plus paclitaxel as first-line treatment for patients with advanced breast cancer. Ann Oncol. 2009.
51. Ebos JM, Lee CR, Cruz-Munoz W, Bjarnason GA, Christensen JG, Kerbel RS. Accelerated metastasis after short-term treatment with a potent inhibitor of tumor angiogenesis. Cancer Cell. 2009;15:232-9.
52. Bryant HE, Schultz N, Thomas HD, Parker KM, Flower D, Lopez E, et al. Specific killing of BRCA2-deficient tumours with inhibitors of poly(ADP-ribose) polymerase. Nature. 2005;434:913-7.
53. Farmer H, McCabe N, Lord CJ, Tutt AN, Johnson DA, Richardson TB, et al. Targeting the DNA repair defect in BRCA mutant cells as a therapeutic strategy. Nature. 2005;434:917-21.
54. Fong PC, Boss DS, Yap TA, Tutt A, Wu P, Mergui-Roelvink M, et al. Inhibition of poly(ADP-ribose) polymerase in tumors from BRCA mutation carriers. N Engl J Med. 2009;361:123-34.
55. Turner NC, Reis-Filho JS, Russell AM, Springall RJ, Ryder K, Steele D, et al. BRCA1 dysfunction in sporadic basal-like breast cancer. Oncogene. 2007;26:2126-32.
56. Esteller M, Silva JM, Dominguez G, Bonilla F, Matias-Guiu X, Lerma E, et al. Promoter hypermethylation and BRCA1 inactivation in sporadic breast and ovarian tumors. J Natl Cancer Inst. 2000;92:564-9.
57. Wharton KA, Johansen KM, Xu T, Artavanis-Tsakonas S. Nucleotide sequence from the neurogenic locus notch implies a gene product that shares homology with proteins containing EGF-like repeats. Cell. 1985;43:567-81.
58. Artavanis-Tsakonas S, Muskavitch MA, Yedvobnick B. Molecular cloning of Notch, a locus affecting neurogenesis in Drosophila melanogaster. Proc Natl Acad Sci U S A. 1983;80:1977-81.
59. Yochem J, Greenwald I. glp-1 and lin-12, genes implicated in distinct cell-cell interactions in C. elegans, encode similar transmembrane proteins. Cell. 1989;58:553-63.

60. Yochem J, Weston K, Greenwald I. The Caenorhabditis elegans lin-12 gene encodes a transmembrane protein with overall similarity to Drosophila Notch. Nature. 1988;335:547-50.
61. Austin J, Kimble J. Transcript analysis of glp-1 and lin-12, homologous genes required for cell interactions during development of C. elegans. Cell. 1989;58:565-71.
62. Ellisen LW, Bird J, West DC, Soreng AL, Reynolds TC, Smith SD, et al. TAN-1, the human homolog of the Drosophila notch gene, is broken by chromosomal translocations in T lymphoblastic neoplasms. Cell. 1991;66:649-61.
63. Weinmaster G, Roberts VJ, Lemke G. Notch2: a second mammalian Notch gene. Development. 1992;116:931-41.
64. Sugaya K, Fukagawa T, Matsumoto K, Mita K, Takahashi E, Ando A, et al. Three genes in the human MHC class III region near the junction with the class II: gene for receptor of advanced glycosylation end products, PBX2 homeobox gene and a notch homolog, human counterpart of mouse mammary tumor gene int-3. Genomics. 1994;23:408-19.
65. Uyttendaele H, Marazzi G, Wu G, Yan Q, Sassoon D, Kitajewski J. Notch4/int-3, a mammary proto-oncogene, is an endothelial cell-specific mammalian Notch gene. Development. 1996;122:2251-9.
66. Kopan R, Ilagan MX. The canonical Notch signaling pathway: unfolding the activation mechanism. Cell. 2009;137:216-33.
67. Vassin H, Bremer KA, Knust E, Campos-Ortega JA. The neurogenic gene Delta of Drosophila melanogaster is expressed in neurogenic territories and encodes a putative transmembrane protein with EGF-like repeats. Embo J. 1987;6:3431-40.
68. Cui XY, Hu QD, Tekaya M, Shimoda Y, Ang BT, Nie DY, et al. NB-3/Notch1 pathway via Deltex1 promotes neural progenitor cell differentiation into oligodendrocytes. J Biol Chem. 2004;279:25858-65.
69. Hu QD, Ang BT, Karsak M, Hu WP, Cui XY, Duka T, et al. F3/contactin acts as a functional ligand for Notch during oligodendrocyte maturation. Cell. 2003;115:163-75.
70. Eiraku M, Tohgo A, Ono K, Kaneko M, Fujishima K, Hirano T, et al. DNER acts as a neuron-specific Notch ligand during Bergmann glial development. Nat Neurosci. 2005;8:873-80.
71. Miyamoto A, Lau R, Hein PW, Shipley JM, Weinmaster G. Microfibrillar proteins MAGP-1 and MAGP-2 induce Notch1 extracellular domain dissociation and receptor activation. J Biol Chem. 2006;281:10089-97.
72. Nehring LC, Miyamoto A, Hein PW, Weinmaster G, Shipley JM. The extracellular matrix protein MAGP-2 interacts with Jagged1 and induces its shedding from the cell surface. J Biol Chem. 2005;280:20349-55.
73. Albig AR, Becenti DJ, Roy TG, Schiemann WP. Microfibril-associate glycoprotein-2 (MAGP-2) promotes angiogenic cell sprouting by blocking notch signaling in endothelial cells. Microvasc Res. 2008;76:7-14.
74. Logeat F, Bessia C, Brou C, LeBail O, Jarriault S, Seidah NG, et al. The Notch1 receptor is cleaved constitutively by a furin-like convertase. Proc Natl Acad Sci U S A. 1998;95:8108-12.
75. Blaumueller CM, Qi H, Zagouras P, Artavanis-Tsakonas S. Intracellular cleavage of Notch leads to a heterodimeric receptor on the plasma membrane. Cell. 1997;90:281-91.
76. Lake RJ, Grimm LM, Veraksa A, Banos A, Artavanis-Tsakonas S. In vivo analysis of the Notch receptor S1 cleavage. PLoS One. 2009;4:e6728.

77. Gordon WR, Vardar-Ulu D, L'Heureux S, Ashworth T, Malecki MJ, Sanchez-Irizarry C, et al. Effects of S1 cleavage on the structure, surface export, and signaling activity of human Notch1 and Notch2. PLoS One. 2009;4:e6613.
78. Kidd S, Lieber T. Furin cleavage is not a requirement for Drosophila Notch function. Mech Dev. 2002;115:41-51.
79. Gordon WR, Vardar-Ulu D, Histen G, Sanchez-Irizarry C, Aster JC, Blacklow SC. Structural basis for autoinhibition of Notch. Nat Struct Mol Biol. 2007;14:295-300.
80. Rand MD, Grimm LM, Artavanis-Tsakonas S, Patriub V, Blacklow SC, Sklar J, et al. Calcium depletion dissociates and activates heterodimeric notch receptors. Mol Cell Biol. 2000;20:1825-35.
81. Ahimou F, Mok LP, Bardot B, Wesley C. The adhesion force of Notch with Delta and the rate of Notch signaling. J Cell Biol. 2004;167:1217-29.
82. Nichols JT, Miyamoto A, Olsen SL, D'Souza B, Yao C, Weinmaster G. DSL ligand endocytosis physically dissociates Notch1 heterodimers before activating proteolysis can occur. J Cell Biol. 2007;176:445-58.
83. Brou C, Logeat F, Gupta N, Bessia C, LeBail O, Doedens JR, et al. A novel proteolytic cleavage involved in Notch signaling: the role of the disintegrin-metalloprotease TACE. Mol Cell. 2000;5:207-16.
84. Peschon JJ, Slack JL, Reddy P, Stocking KL, Sunnarborg SW, Lee DC, et al. An essential role for ectodomain shedding in mammalian development. Science. 1998;282:1281-4.
85. Sotillos S, Roch F, Campuzano S. The metalloprotease-disintegrin Kuzbanian participates in Notch activation during growth and patterning of Drosophila imaginal discs. Development. 1997;124:4769-79.
86. Lieber T, Kidd S, Young MW. kuzbanian-mediated cleavage of Drosophila Notch. Genes Dev. 2002;16:209-21.
87. Pan D, Rubin GM. Kuzbanian controls proteolytic processing of Notch and mediates lateral inhibition during Drosophila and vertebrate neurogenesis. Cell. 1997;90:271-80.
88. Hartmann D, de Strooper B, Serneels L, Craessaerts K, Herreman A, Annaert W, et al. The disintegrin/metalloprotease ADAM 10 is essential for Notch signalling but not for alpha-secretase activity in fibroblasts. Hum Mol Genet. 2002;11:2615-24.
89. Bozkulak EC, Weinmaster G. Selective use of ADAM10 and ADAM17 in activation of Notch1 signaling. Mol Cell Biol. 2009;29:5679-95.
90. Lai MT, Chen E, Crouthamel MC, DiMuzio-Mower J, Xu M, Huang Q, et al. Presenilin-1 and presenilin-2 exhibit distinct yet overlapping gamma-secretase activities. J Biol Chem. 2003;278:22475-81.
91. Serneels L, Dejaegere T, Craessaerts K, Horre K, Jorissen E, Tousseyn T, et al. Differential contribution of the three Aph1 genes to gamma-secretase activity in vivo. Proc Natl Acad Sci U S A. 2005;102:1719-24.
92. Serneels L, Van Biervliet J, Craessaerts K, Dejaegere T, Horre K, Van Houtvin T, et al. gamma-Secretase heterogeneity in the Aph1 subunit: relevance for Alzheimer's disease. Science. 2009;324:639-42.
93. Shah S, Lee SF, Tabuchi K, Hao YH, Yu C, LaPlant Q, et al. Nicastrin functions as a gamma-secretase-substrate receptor. Cell. 2005;122:435-47.
94. Zhao G, Liu Z, Ilagan MX, Kopan R. Gamma-secretase composed of PS1/Pen2/Aph1a can cleave notch and amyloid precursor protein in the absence of nicastrin. J Neurosci. 2010;30:1648-56.

95. Takasugi N, Tomita T, Hayashi I, Tsuruoka M, Niimura M, Takahashi Y, et al. The role of presenilin cofactors in the gamma-secretase complex. Nature. 2003;422:438-41.
96. Placanica L, Tarassishin L, Yang G, Peethumnongsin E, Kim SH, Zheng H, et al. Pen2 and presenilin-1 modulate the dynamic equilibrium of presenilin-1 and presenilin-2 gamma-secretase complexes. J Biol Chem. 2009;284:2967-77.
97. Chen AC, Guo LY, Ostaszewski BL, Selkoe DJ, LaVoie MJ. Aph-1 associates directly with full-length and C-terminal fragments of gamma-secretase substrates. J Biol Chem.285:11378-91.
98. Pardossi-Piquard R, Yang SP, Kanemoto S, Gu Y, Chen F, Bohm C, et al. APH1 polar transmembrane residues regulate the assembly and activity of presenilin complexes. J Biol Chem. 2009;284:16298-307.
99. Struhl G, Adachi A. Requirements for presenilin-dependent cleavage of notch and other transmembrane proteins. Mol Cell. 2000;6:625-36.
100. Schroeter EH, Kisslinger JA, Kopan R. Notch-1 signalling requires ligand-induced proteolytic release of intracellular domain. Nature. 1998;393:382-6.
101. Blat Y, Meredith JE, Wang Q, Bradley JD, Thompson LA, Olson RE, et al. Mutations at the P1' position of Notch1 decrease intracellular domain stability rather than cleavage by gamma-secretase. Biochem Biophys Res Commun. 2002;299:569-73.
102. Tagami S, Okochi M, Yanagida K, Ikuta A, Fukumori A, Matsumoto N, et al. Regulation of Notch signaling by dynamic changes in the precision of S3 cleavage of Notch-1. Mol Cell Biol. 2008;28:165-76.
103. Seugnet L, Simpson P, Haenlin M. Requirement for dynamin during Notch signaling in Drosophila neurogenesis. Dev Biol. 1997;192:585-98.
104. Reddy GV, Gupta B, Ray K, Rodrigues V. Development of the Drosophila olfactory sense organs utilizes cell-cell interactions as well as lineage. Development. 1997;124:703-12.
105. Maitra S, Kulikauskas RM, Gavilan H, Fehon RG. The tumor suppressors Merlin and Expanded function cooperatively to modulate receptor endocytosis and signaling. Curr Biol. 2006;16:702-9.
106. Jaekel R, Klein T. The Drosophila Notch inhibitor and tumor suppressor gene lethal (2) giant discs encodes a conserved regulator of endosomal trafficking. Dev Cell. 2006;11:655-69.
107. Gallagher CM, Knoblich JA. The conserved c2 domain protein lethal (2) giant discs regulates protein trafficking in Drosophila. Dev Cell. 2006;11:641-53.
108. Lu H, Bilder D. Endocytic control of epithelial polarity and proliferation in Drosophila. Nat Cell Biol. 2005;7:1232-9.
109. Jekely G, Rorth P. Hrs mediates downregulation of multiple signalling receptors in Drosophila. EMBO Rep. 2003;4:1163-8.
110. Vaccari T, Bilder D. The Drosophila tumor suppressor vps25 prevents nonautonomous overproliferation by regulating notch trafficking. Dev Cell. 2005;9:687-98.
111. Thompson BJ, Mathieu J, Sung HH, Loeser E, Rorth P, Cohen SM. Tumor suppressor properties of the ESCRT-II complex component Vps25 in Drosophila. Dev Cell. 2005;9:711-20.
112. Tian X, Hansen D, Schedl T, Skeath JB. Epsin potentiates Notch pathway activity in Drosophila and C. elegans. Development. 2004;131:5807-15.
113. Wang W, Struhl G. Drosophila Epsin mediates a select endocytic pathway that DSL ligands must enter to activate Notch. Development. 2004;131:5367-80.

114. Overstreet E, Fitch E, Fischer JA. Fat facets and Liquid facets promote Delta endocytosis and Delta signaling in the signaling cells. Development. 2004;131:5355-66.
115. Sapir A, Assa-Kunik E, Tsruya R, Schejter E, Shilo BZ. Unidirectional Notch signaling depends on continuous cleavage of Delta. Development. 2005;132:123-32.
116. Six E, Ndiaye D, Laabi Y, Brou C, Gupta-Rossi N, Israel A, et al. The Notch ligand Delta1 is sequentially cleaved by an ADAM protease and gamma-secretase. Proc Natl Acad Sci U S A. 2003;100:7638-43.
117. Windler SL, Bilder D. Endocytic Internalization Routes Required for Delta/Notch Signaling. Curr Biol.20:538-43.
118. Pavlopoulos E, Pitsouli C, Klueg KM, Muskavitch MA, Moschonas NK, Delidakis C. neuralized Encodes a peripheral membrane protein involved in delta signaling and endocytosis. Dev Cell. 2001;1:807-16.
119. Lai EC, Deblandre GA, Kintner C, Rubin GM. Drosophila neuralized is a ubiquitin ligase that promotes the internalization and degradation of delta. Dev Cell. 2001;1:783-94.
120. Deblandre GA, Lai EC, Kintner C. Xenopus neuralized is a ubiquitin ligase that interacts with XDelta1 and regulates Notch signaling. Dev Cell. 2001;1:795-806.
121. Itoh M, Kim CH, Palardy G, Oda T, Jiang YJ, Maust D, et al. Mind bomb is a ubiquitin ligase that is essential for efficient activation of Notch signaling by Delta. Dev Cell. 2003;4:67-82.
122. Le Borgne R, Remaud S, Hamel S, Schweisguth F. Two distinct E3 ubiquitin ligases have complementary functions in the regulation of delta and serrate signaling in Drosophila. PLoS Biol. 2005;3:e96.
123. Pitsouli C, Delidakis C. The interplay between DSL proteins and ubiquitin ligases in Notch signaling. Development. 2005;132:4041-50.
124. Koo BK, Yoon MJ, Yoon KJ, Im SK, Kim YY, Kim CH, et al. An obligatory role of mind bomb-1 in notch signaling of mammalian development. PLoS One. 2007;2:e1221.
125. Koo BK, Lim HS, Song R, Yoon MJ, Yoon KJ, Moon JS, et al. Mind bomb 1 is essential for generating functional Notch ligands to activate Notch. Development. 2005;132:3459-70.
126. Barsi JC, Rajendra R, Wu JI, Artzt K. Mind bomb1 is a ubiquitin ligase essential for mouse embryonic development and Notch signaling. Mech Dev. 2005;122:1106-17.
127. De Renzis S, Yu J, Zinzen R, Wieschaus E. Dorsal-ventral pattern of Delta trafficking is established by a Snail-Tom-Neuralized pathway. Dev Cell. 2006;10:257-64.
128. Bardin AJ, Schweisguth F. Bearded family members inhibit Neuralized-mediated endocytosis and signaling activity of Delta in Drosophila. Dev Cell. 2006;10:245-55.
129. Vaccari T, Lu H, Kanwar R, Fortini ME, Bilder D. Endosomal entry regulates Notch receptor activation in Drosophila melanogaster. J Cell Biol. 2008;180:755-62.
130. Gupta-Rossi N, Six E, LeBail O, Logeat F, Chastagner P, Olry A, et al. Monoubiquitination and endocytosis direct gamma-secretase cleavage of activated Notch receptor. J Cell Biol. 2004;166:73-83.

131. Childress JL, Acar M, Tao C, Halder G. Lethal giant discs, a novel C2-domain protein, restricts notch activation during endocytosis. Curr Biol. 2006;16:2228-33.
132. Tarassishin L, Yin YI, Bassit B, Li YM. Processing of Notch and amyloid precursor protein by gamma-secretase is spatially distinct. Proc Natl Acad Sci U S A. 2004;101:17050-5.
133. Hori K, Fostier M, Ito M, Fuwa TJ, Go MJ, Okano H, et al. Drosophila deltex mediates suppressor of Hairless-independent and late-endosomal activation of Notch signaling. Development. 2004;131:5527-37.
134. Fehon RG, Kooh PJ, Rebay I, Regan CL, Xu T, Muskavitch MA, et al. Molecular interactions between the protein products of the neurogenic loci Notch and Delta, two EGF-homologous genes in Drosophila. Cell. 1990;61:523-34.
135. Matsuno K, Diederich RJ, Go MJ, Blaumueller CM, Artavanis-Tsakonas S. Deltex acts as a positive regulator of Notch signaling through interactions with the Notch ankyrin repeats. Development. 1995;121:2633-44.
136. Gorman MJ, Girton JR. A genetic analysis of deltex and its interaction with the Notch locus in Drosophila melanogaster. Genetics. 1992;131:99-112.
137. Xu T, Artavanis-Tsakonas S. deltex, a locus interacting with the neurogenic genes, Notch, Delta and mastermind in Drosophila melanogaster. Genetics. 1990;126:665-77.
138. Wilkin M, Tongngok P, Gensch N, Clemence S, Motoki M, Yamada K, et al. Drosophila HOPS and AP-3 complex genes are required for a Deltex-regulated activation of notch in the endosomal trafficking pathway. Dev Cell. 2008;15:762-72.
139. Lehar SM, Bevan MJ. T cells develop normally in the absence of both Deltex1 and Deltex2. Mol Cell Biol. 2006;26:7358-71.
140. Izon DJ, Aster JC, He Y, Weng A, Karnell FG, Patriub V, et al. Deltex1 redirects lymphoid progenitors to the B cell lineage by antagonizing Notch1. Immunity. 2002;16:231-43.
141. Mukherjee A, Veraksa A, Bauer A, Rosse C, Camonis J, Artavanis-Tsakonas S. Regulation of Notch signalling by non-visual beta-arrestin. Nat Cell Biol. 2005;7:1191-201.
142. Fuwa TJ, Hori K, Sasamura T, Higgs J, Baron M, Matsuno K. The first deltex null mutant indicates tissue-specific deltex-dependent Notch signaling in Drosophila. Mol Genet Genomics. 2006;275:251-63.
143. Kishi N, Tang Z, Maeda Y, Hirai A, Mo R, Ito M, et al. Murine homologs of deltex define a novel gene family involved in vertebrate Notch signaling and neurogenesis. Int J Dev Neurosci. 2001;19:21-35.
144. Storck S, Delbos F, Stadler N, Thirion-Delalande C, Bernex F, Verthuy C, et al. Normal immune system development in mice lacking the Deltex-1 RING finger domain. Mol Cell Biol. 2005;25:1437-45.
145. Fostier M, Evans DA, Artavanis-Tsakonas S, Baron M. Genetic characterization of the Drosophila melanogaster Suppressor of deltex gene: A regulator of notch signaling. Genetics. 1998;150:1477-85.
146. Wilkin MB, Carbery AM, Fostier M, Aslam H, Mazaleyrat SL, Higgs J, et al. Regulation of notch endosomal sorting and signaling by Drosophila Nedd4 family proteins. Curr Biol. 2004;14:2237-44.
147. Chastagner P, Israel A, Brou C. AIP4/Itch regulates Notch receptor degradation in the absence of ligand. PLoS One. 2008;3:e2735.

148. Chastagner P, Israel A, Brou C. Itch/AIP4 mediates Deltex degradation through the formation of K29-linked polyubiquitin chains. EMBO Rep. 2006;7:1147-53.
149. Sakata T, Sakaguchi H, Tsuda L, Higashitani A, Aigaki T, Matsuno K, et al. Drosophila Nedd4 regulates endocytosis of notch and suppresses its ligand-independent activation. Curr Biol. 2004;14:2228-36.
150. Jehn BM, Dittert I, Beyer S, von der Mark K, Bielke W. c-Cbl binding and ubiquitin-dependent lysosomal degradation of membrane-associated Notch1. J Biol Chem. 2002;277:8033-40.
151. Guo M, Jan LY, Jan YN. Control of daughter cell fates during asymmetric division: interaction of Numb and Notch. Neuron. 1996;17:27-41.
152. Spana EP, Doe CQ. Numb antagonizes Notch signaling to specify sibling neuron cell fates. Neuron. 1996;17:21-6.
153. O'Connor-Giles KM, Skeath JB. Numb inhibits membrane localization of Sanpodo, a four-pass transmembrane protein, to promote asymmetric divisions in Drosophila. Dev Cell. 2003;5:231-43.
154. Hutterer A, Knoblich JA. Numb and alpha-Adaptin regulate Sanpodo endocytosis to specify cell fate in Drosophila external sensory organs. EMBO Rep. 2005;6:836-42.
155. Tong X, Zitserman D, Serebriiskii I, Andrake M, Dunbrack R, Roegiers F. Numb independently antagonizes Sanpodo membrane targeting and Notch signaling in Drosophila sensory organ precursor cells. Mol Biol Cell. 2010;21:802-10.
156. McGill MA, Dho SE, Weinmaster G, McGlade CJ. Numb regulates post-endocytic trafficking and degradation of Notch1. J Biol Chem. 2009;284:26427-38.
157. Zhou Y, Atkins JB, Rompani SB, Bancescu DL, Petersen PH, Tang H, et al. The mammalian Golgi regulates numb signaling in asymmetric cell division by releasing ACBD3 during mitosis. Cell. 2007;129:163-78.
158. Yogosawa S, Miyauchi Y, Honda R, Tanaka H, Yasuda H. Mammalian Numb is a target protein of Mdm2, ubiquitin ligase. Biochem Biophys Res Commun. 2003;302:869-72.
159. Nie J, McGill MA, Dermer M, Dho SE, Wolting CD, McGlade CJ. LNX functions as a RING type E3 ubiquitin ligase that targets the cell fate determinant Numb for ubiquitin-dependent degradation. Embo J. 2002;21:93-102.
160. Shimizu K, Chiba S, Hosoya N, Kumano K, Saito T, Kurokawa M, et al. Binding of Delta1, Jagged1, and Jagged2 to Notch2 rapidly induces cleavage, nuclear translocation, and hyperphosphorylation of Notch2. Mol Cell Biol. 2000;20:6913-22.
161. Ronchini C, Capobianco AJ. Notch(ic)-ER chimeras display hormone-dependent transformation, nuclear accumulation, phosphorylation and CBF1 activation. Oncogene. 2000;19:3914-24.
162. Redmond L, Oh SR, Hicks C, Weinmaster G, Ghosh A. Nuclear Notch1 signaling and the regulation of dendritic development. Nat Neurosci. 2000;3:30-40.
163. Hubbard EJ, Wu G, Kitajewski J, Greenwald I. sel-10, a negative regulator of lin-12 activity in Caenorhabditis elegans, encodes a member of the CDC4 family of proteins. Genes Dev. 1997;11:3182-93.
164. Gupta-Rossi N, Le Bail O, Gonen H, Brou C, Logeat F, Six E, et al. Functional interaction between SEL-10, an F-box protein, and the nuclear form of activated Notch1 receptor. J Biol Chem. 2001;276:34371-8.

165. Fryer CJ, White JB, Jones KA. Mastermind recruits CycC:CDK8 to phosphorylate the Notch ICD and coordinate activation with turnover. Mol Cell. 2004;16:509-20.
166. Wu G, Lyapina S, Das I, Li J, Gurney M, Pauley A, et al. SEL-10 is an inhibitor of notch signaling that targets notch for ubiquitin-mediated protein degradation. Mol Cell Biol. 2001;21:7403-15.
167. Foltz DR, Santiago MC, Berechid BE, Nye JS. Glycogen synthase kinase-3beta modulates notch signaling and stability. Curr Biol. 2002;12:1006-11.
168. Ruel L, Bourouis M, Heitzler P, Pantesco V, Simpson P. Drosophila shaggy kinase and rat glycogen synthase kinase-3 have conserved activities and act downstream of Notch. Nature. 1993;362:557-60.
169. Lubman OY, Kopan R, Waksman G, Korolev S. The crystal structure of a partial mouse Notch-1 ankyrin domain: repeats 4 through 7 preserve an ankyrin fold. Protein Sci. 2005;14:1274-81.
170. Espinosa L, Ingles-Esteve J, Aguilera C, Bigas A. Phosphorylation by glycogen synthase kinase-3 beta down-regulates Notch activity, a link for Notch and Wnt pathways. J Biol Chem. 2003;278:32227-35.
171. Fernandez-Martinez J, Vela EM, Tora-Ponsioen M, Ocana OH, Nieto MA, Galceran J. Attenuation of Notch signalling by the Down-syndrome-associated kinase DYRK1A. J Cell Sci. 2009;122:1574-83.
172. Ishitani T, Hirao T, Suzuki M, Isoda M, Ishitani S, Harigaya K, et al. Nemo-like kinase suppresses Notch signalling by interfering with formation of the Notch active transcriptional complex. Nat Cell Biol. 2010;12:278-85.
173. Kankel MW, Hurlbut GD, Upadhyay G, Yajnik V, Yedvobnick B, Artavanis-Tsakonas S. Investigating the genetic circuitry of mastermind in Drosophila, a notch signal effector. Genetics. 2007;177:2493-505.
174. Song J, Park S, Kim M, Shin I. Down-regulation of Notch-dependent transcription by Akt in vitro. FEBS Lett. 2008;582:1693-9.
175. Moloney DJ, Panin VM, Johnston SH, Chen J, Shao L, Wilson R, et al. Fringe is a glycosyltransferase that modifies Notch. Nature. 2000;406:369-75.
176. Bruckner K, Perez L, Clausen H, Cohen S. Glycosyltransferase activity of Fringe modulates Notch-Delta interactions. Nature. 2000;406:411-5.
177. Munro S, Freeman M. The notch signalling regulator fringe acts in the Golgi apparatus and requires the glycosyltransferase signature motif DXD. Curr Biol. 2000;10:813-20.
178. Shi S, Stanley P. Protein O-fucosyltransferase 1 is an essential component of Notch signaling pathways. Proc Natl Acad Sci U S A. 2003;100:5234-9.
179. Okajima T, Irvine KD. Regulation of notch signaling by o-linked fucose. Cell. 2002;111:893-904.
180. Okajima T, Xu A, Irvine KD. Modulation of notch-ligand binding by protein O-fucosyltransferase 1 and fringe. J Biol Chem. 2003;278:42340-5.
181. Okajima T, Xu A, Lei L, Irvine KD. Chaperone activity of protein O-fucosyltransferase 1 promotes notch receptor folding. Science. 2005;307:1599-603.
182. Ishikawa HO, Ayukawa T, Nakayama M, Higashi S, Kamiyama S, Nishihara S, et al. Two pathways for importing GDP-fucose into the endoplasmic reticulum lumen function redundantly in the O-fucosylation of Notch in Drosophila. J Biol Chem.285:4122-9.

183. Okajima T, Reddy B, Matsuda T, Irvine KD. Contributions of chaperone and glycosyltransferase activities of O-fucosyltransferase 1 to Notch signaling. BMC Biol. 2008;6:1.
184. Sasamura T, Ishikawa HO, Sasaki N, Higashi S, Kanai M, Nakao S, et al. The O-fucosyltransferase O-fut1 is an extracellular component that is essential for the constitutive endocytic trafficking of Notch in Drosophila. Development. 2007;134:1347-56.
185. Stahl M, Uemura K, Ge C, Shi S, Tashima Y, Stanley P. Roles of Pofut1 and O-fucose in mammalian Notch signaling. J Biol Chem. 2008;283:13638-51.
186. Okamura Y, Saga Y. Pofut1 is required for the proper localization of the Notch receptor during mouse development. Mech Dev. 2008;125:663-73.
187. Hicks C, Johnston SH, diSibio G, Collazo A, Vogt TF, Weinmaster G. Fringe differentially modulates Jagged1 and Delta1 signalling through Notch1 and Notch2. Nat Cell Biol. 2000;2:515-20.
188. Yang LT, Nichols JT, Yao C, Manilay JO, Robey EA, Weinmaster G. Fringe glycosyltransferases differentially modulate Notch1 proteolysis induced by Delta1 and Jagged1. Mol Biol Cell. 2005;16:927-42.
189. Tsukumo S, Hirose K, Maekawa Y, Kishihara K, Yasutomo K. Lunatic fringe controls T cell differentiation through modulating notch signaling. J Immunol. 2006;177:8365-71.
190. Morimoto M, Takahashi Y, Endo M, Saga Y. The Mesp2 transcription factor establishes segmental borders by suppressing Notch activity. Nature. 2005;435:354-9.
191. Dale JK, Maroto M, Dequeant ML, Malapert P, McGrew M, Pourquie O. Periodic notch inhibition by lunatic fringe underlies the chick segmentation clock. Nature. 2003;421:275-8.
192. Panin VM, Shao L, Lei L, Moloney DJ, Irvine KD, Haltiwanger RS. Notch ligands are substrates for protein O-fucosyltransferase-1 and Fringe. J Biol Chem. 2002;277:29945-52.
193. Luo Y, Haltiwanger RS. O-fucosylation of notch occurs in the endoplasmic reticulum. J Biol Chem. 2005;280:11289-94.
194. Haines N, Irvine KD. Glycosylation regulates Notch signalling. Nat Rev Mol Cell Biol. 2003;4:786-97.
195. Sethi MK, Buettner FF, Krylov VB, Takeuchi H, Nifantiev NE, Haltiwanger RS, et al. Identification of glycosyltransferase 8 family members as xylosyltransferases acting on O-glucosylated notch epidermal growth factor repeats. J Biol Chem.285:1582-6.
196. Acar M, Jafar-Nejad H, Takeuchi H, Rajan A, Ibrani D, Rana NA, et al. Rumi is a CAP10 domain glycosyltransferase that modifies Notch and is required for Notch signaling. Cell. 2008;132:247-58.
197. Kanwar R, Fortini ME. The big brain aquaporin is required for endosome maturation and notch receptor trafficking. Cell. 2008;133:852-63.
198. Watanabe K, Nagaoka T, Lee JM, Bianco C, Gonzales M, Castro NP, et al. Enhancement of Notch receptor maturation and signaling sensitivity by Cripto-1. J Cell Biol. 2009;187:343-53.
199. Kile BT, Schulman BA, Alexander WS, Nicola NA, Martin HM, Hilton DJ. The SOCS box: a tale of destruction and degradation. Trends Biochem Sci. 2002;27:235-41.
200. Diks SH, Sartori da Silva MA, Hillebrands JL, Bink RJ, Versteeg HH, van Rooijen C, et al. d-Asb11 is an essential mediator of canonical Delta-Notch signalling. Nat Cell Biol. 2008;10:1190-8.

201. Miller AC, Lyons EL, Herman TG. cis-Inhibition of Notch by endogenous Delta biases the outcome of lateral inhibition. Curr Biol. 2009;19:1378-83.
202. Tun T, Hamaguchi Y, Matsunami N, Furukawa T, Honjo T, Kawaichi M. Recognition sequence of a highly conserved DNA binding protein RBP-J kappa. Nucleic Acids Res. 1994;22:965-71.
203. Krejci A, Bray S. Notch activation stimulates transient and selective binding of Su(H)/CSL to target enhancers. Genes Dev. 2007;21:1322-7.
204. Koelzer S, Klein T. Regulation of expression of Vg and establishment of the dorsoventral compartment boundary in the wing imaginal disc by Suppressor of Hairless. Dev Biol. 2006;289:77-90.
205. Nagel AC, Krejci A, Tenin G, Bravo-Patino A, Bray S, Maier D, et al. Hairless-mediated repression of notch target genes requires the combined activity of Groucho and CtBP corepressors. Mol Cell Biol. 2005;25:10433-41.
206. Oswald F, Winkler M, Cao Y, Astrahantseff K, Bourteele S, Knochel W, et al. RBP-Jkappa/SHARP recruits CtIP/CtBP corepressors to silence Notch target genes. Mol Cell Biol. 2005;25:10379-90.
207. Hsieh JJ, Zhou S, Chen L, Young DB, Hayward SD. CIR, a corepressor linking the DNA binding factor CBF1 to the histone deacetylase complex. Proc Natl Acad Sci U S A. 1999;96:23-8.
208. Kao HY, Ordentlich P, Koyano-Nakagawa N, Tang Z, Downes M, Kintner CR, et al. A histone deacetylase corepressor complex regulates the Notch signal transduction pathway. Genes Dev. 1998;12:2269-77.
209. Taniguchi Y, Furukawa T, Tun T, Han H, Honjo T. LIM protein KyoT2 negatively regulates transcription by association with the RBP-J DNA-binding protein. Mol Cell Biol. 1998;18:644-54.
210. Goodfellow H, Krejci A, Moshkin Y, Verrijzer CP, Karch F, Bray SJ. Gene-specific targeting of the histone chaperone asf1 to mediate silencing. Dev Cell. 2007;13:593-600.
211. Hsieh JJ, Henkel T, Salmon P, Robey E, Peterson MG, Hayward SD. Truncated mammalian Notch1 activates CBF1/RBPJk-repressed genes by a mechanism resembling that of Epstein-Barr virus EBNA2. Mol Cell Biol. 1996;16:952-9.
212. Lubman OY, Ilagan MX, Kopan R, Barrick D. Quantitative dissection of the Notch:CSL interaction: insights into the Notch-mediated transcriptional switch. J Mol Biol. 2007;365:577-89.
213. Wilson JJ, Kovall RA. Crystal structure of the CSL-Notch-Mastermind ternary complex bound to DNA. Cell. 2006;124:985-96.
214. Lin SE, Oyama T, Nagase T, Harigaya K, Kitagawa M. Identification of new human mastermind proteins defines a family that consists of positive regulators for notch signaling. J Biol Chem. 2002;277:50612-20.
215. Wu L, Aster JC, Blacklow SC, Lake R, Artavanis-Tsakonas S, Griffin JD. MAML1, a human homologue of Drosophila mastermind, is a transcriptional co-activator for NOTCH receptors. Nat Genet. 2000;26:484-9.
216. Kitagawa M, Oyama T, Kawashima T, Yedvobnick B, Kumar A, Matsuno K, et al. A human protein with sequence similarity to Drosophila mastermind coordinates the nuclear form of notch and a CSL protein to build a transcriptional activator complex on target promoters. Mol Cell Biol. 2001;21:4337-46.
217. Wu L, Sun T, Kobayashi K, Gao P, Griffin JD. Identification of a family of mastermind-like transcriptional coactivators for mammalian notch receptors. Mol Cell Biol. 2002;22:7688-700.

218. Nam Y, Weng AP, Aster JC, Blacklow SC. Structural requirements for assembly of the CSL.intracellular Notch1.Mastermind-like 1 transcriptional activation complex. J Biol Chem. 2003;278:21232-9.
219. Nam Y, Sliz P, Song L, Aster JC, Blacklow SC. Structural basis for cooperativity in recruitment of MAML coactivators to Notch transcription complexes. Cell. 2006;124:973-83.
220. Friedmann DR, Wilson JJ, Kovall RA. RAM-induced allostery facilitates assembly of a notch pathway active transcription complex. J Biol Chem. 2008;283:14781-91.
221. Kovall RA. More complicated than it looks: assembly of Notch pathway transcription complexes. Oncogene. 2008;27:5099-109.
222. Bertagna A, Toptygin D, Brand L, Barrick D. The effects of conformational heterogeneity on the binding of the Notch intracellular domain to effector proteins: a case of biologically tuned disorder. Biochem Soc Trans. 2008;36:157-66.
223. Nam Y, Sliz P, Pear WS, Aster JC, Blacklow SC. Cooperative assembly of higher-order Notch complexes functions as a switch to induce transcription. Proc Natl Acad Sci U S A. 2007;104:2103-8.
224. Oswald F, Tauber B, Dobner T, Bourteele S, Kostezka U, Adler G, et al. p300 acts as a transcriptional coactivator for mammalian Notch-1. Mol Cell Biol. 2001;21:7761-74.
225. Kurooka H, Honjo T. Functional interaction between the mouse notch1 intracellular region and histone acetyltransferases PCAF and GCN5. J Biol Chem. 2000;275:17211-20.
226. Wallberg AE, Pedersen K, Lendahl U, Roeder RG. p300 and PCAF act cooperatively to mediate transcriptional activation from chromatin templates by notch intracellular domains in vitro. Mol Cell Biol. 2002;22:7812-9.
227. Fryer CJ, Lamar E, Turbachova I, Kintner C, Jones KA. Mastermind mediates chromatin-specific transcription and turnover of the Notch enhancer complex. Genes Dev. 2002;16:1397-411.
228. Zhou S, Fujimuro M, Hsieh JJ, Chen L, Miyamoto A, Weinmaster G, et al. SKIP, a CBF1-associated protein, interacts with the ankyrin repeat domain of NotchIC To facilitate NotchIC function. Mol Cell Biol. 2000;20:2400-10.
229. Oswald F, Kostezka U, Astrahantseff K, Bourteele S, Dillinger K, Zechner U, et al. SHARP is a novel component of the Notch/RBP-Jkappa signalling pathway. Embo J. 2002;21:5417-26.
230. Lecourtois M, Schweisguth F. The neurogenic suppressor of hairless DNA-binding protein mediates the transcriptional activation of the enhancer of split complex genes triggered by Notch signaling. Genes Dev. 1995;9:2598-608.
231. Matsuno K, Go MJ, Sun X, Eastman DS, Artavanis-Tsakonas S. Suppressor of Hairless-independent events in Notch signaling imply novel pathway elements. Development. 1997;124:4265-73.
232. Rusconi JC, Corbin V. A widespread and early requirement for a novel Notch function during Drosophila embryogenesis. Dev Biol. 1999;215:388-98.
233. Nofziger D, Miyamoto A, Lyons KM, Weinmaster G. Notch signaling imposes two distinct blocks in the differentiation of C2C12 myoblasts. Development. 1999;126:1689-702.
234. Dumont E, Fuchs KP, Bommer G, Christoph B, Kremmer E, Kempkes B. Neoplastic transformation by Notch is independent of transcriptional activation by RBP-J signalling. Oncogene. 2000;19:556-61.

235. MacKenzie F, Duriez P, Wong F, Noseda M, Karsan A. Notch4 inhibits endothelial apoptosis via RBP-Jkappa-dependent and -independent pathways. J Biol Chem. 2004;279:11657-63.
236. Levy OA, Lah JJ, Levey AI. Notch signaling inhibits PC12 cell neurite outgrowth via RBP-J-dependent and -independent mechanisms. Dev Neurosci. 2002;24:79-88.
237. Shawber C, Nofziger D, Hsieh JJ, Lindsell C, Bogler O, Hayward D, et al. Notch signaling inhibits muscle cell differentiation through a CBF1-independent pathway. Development. 1996;122:3765-73.
238. Morel V, Schweisguth F. Repression by suppressor of hairless and activation by Notch are required to define a single row of single-minded expressing cells in the Drosophila embryo. Genes Dev. 2000;14:377-88.
239. Guan E, Wang J, Laborda J, Norcross M, Baeuerle PA, Hoffman T. T cell leukemia-associated human Notch/translocation-associated Notch homologue has I kappa B-like activity and physically interacts with nuclear factor-kappa B proteins in T cells. J Exp Med. 1996;183:2025-32.
240. Wang J, Shelly L, Miele L, Boykins R, Norcross MA, Guan E. Human Notch-1 inhibits NF-kappa B activity in the nucleus through a direct interaction involving a novel domain. J Immunol. 2001;167:289-95.
241. Fukushima H, Nakao A, Okamoto F, Shin M, Kajiya H, Sakano S, et al. The association of Notch2 and NF-kappaB accelerates RANKL-induced osteoclastogenesis. Mol Cell Biol. 2008;28:6402-12.
242. Shin HM, Minter LM, Cho OH, Gottipati S, Fauq AH, Golde TE, et al. Notch1 augments NF-kappaB activity by facilitating its nuclear retention. Embo J. 2006;25:129-38.
243. Huxford T, Huang DB, Malek S, Ghosh G. The crystal structure of the IkappaBalpha/NF-kappaB complex reveals mechanisms of NF-kappaB inactivation. Cell. 1998;95:759-70.
244. Jacobs MD, Harrison SC. Structure of an IkappaBalpha/NF-kappaB complex. Cell. 1998;95:749-58.
245. Shen H, McElhinny AS, Cao Y, Gao P, Liu J, Bronson R, et al. The Notch coactivator, MAML1, functions as a novel coactivator for MEF2C-mediated transcription and is required for normal myogenesis. Genes Dev. 2006;20:675-88.
246. Zhao Y, Katzman RB, Delmolino LM, Bhat I, Zhang Y, Gurumurthy CB, et al. The notch regulator MAML1 interacts with p53 and functions as a coactivator. J Biol Chem. 2007;282:11969-81.
247. Alves-Guerra MC, Ronchini C, Capobianco AJ. Mastermind-like 1 Is a specific coactivator of beta-catenin transcription activation and is essential for colon carcinoma cell survival. Cancer Res. 2007;67:8690-8.
248. Jin B, Shen H, Lin S, Li JL, Chen Z, Griffin JD, et al. The maml1 co-activator regulates constitutive NF-{kappa}B signaling and cell survival. J Biol Chem. 2010;285:14356-65.
249. Beres TM, Masui T, Swift GH, Shi L, Henke RM, MacDonald RJ. PTF1 is an organ-specific and Notch-independent basic helix-loop-helix complex containing the mammalian Suppressor of Hairless (RBP-J) or its paralogue, RBP-L. Mol Cell Biol. 2006;26:117-30.
250. Masui T, Long Q, Beres TM, Magnuson MA, MacDonald RJ. Early pancreatic development requires the vertebrate Suppressor of Hairless (RBPJ) in the PTF1 bHLH complex. Genes Dev. 2007;21:2629-43.

251. Hori K, Cholewa-Waclaw J, Nakada Y, Glasgow SM, Masui T, Henke RM, et al. A nonclassical bHLH Rbpj transcription factor complex is required for specification of GABAergic neurons independent of Notch signaling. Genes Dev. 2008;22:166-78.
252. Minoguchi S, Taniguchi Y, Kato H, Okazaki T, Strobl LJ, Zimber-Strobl U, et al. RBP-L, a transcription factor related to RBP-Jkappa. Mol Cell Biol. 1997;17:2679-87.
253. Fischer A, Gessler M. Delta-Notch--and then? Protein interactions and proposed modes of repression by Hes and Hey bHLH factors. Nucleic Acids Res. 2007;35:4583-96.
254. Iso T, Kedes L, Hamamori Y. HES and HERP families: multiple effectors of the Notch signaling pathway. J Cell Physiol. 2003;194:237-55.
255. Kageyama R, Ohtsuka T, Kobayashi T. The Hes gene family: repressors and oscillators that orchestrate embryogenesis. Development. 2007;134:1243-51.
256. Ong CT, Cheng HT, Chang LW, Ohtsuka T, Kageyama R, Stormo GD, et al. Target selectivity of vertebrate notch proteins. Collaboration between discrete domains and CSL-binding site architecture determines activation probability. J Biol Chem. 2006;281:5106-19.
257. Ingram WJ, McCue KI, Tran TH, Hallahan AR, Wainwright BJ. Sonic Hedgehog regulates Hes1 through a novel mechanism that is independent of canonical Notch pathway signalling. Oncogene. 2008;27:1489-500.
258. Zheng Y, Lin L, Zheng Z. TGF-alpha induces upregulation and nuclear translocation of Hes1 in glioma cell. Cell Biochem Funct. 2008;26:692-700.
259. Ottaviani S, Tahiri K, Frazier A, Hassaine ZN, Dumontier MF, Baschong W, et al. HES1, a new target for interleukin-1{beta} in chondrocytes. Ann Rheum Dis. 2009.
260. Curry CL, Reed LL, Nickoloff BJ, Miele L, Foreman KE. Notch-independent regulation of Hes-1 expression by c-Jun N-terminal kinase signaling in human endothelial cells. Lab Invest. 2006;86:842-52.
261. Knoepfler PS. Myc goes global: new tricks for an old oncogene. Cancer Res. 2007;67:5061-3.
262. Weng AP, Millholland JM, Yashiro-Ohtani Y, Arcangeli ML, Lau A, Wai C, et al. c-Myc is an important direct target of Notch1 in T-cell acute lymphoblastic leukemia/lymphoma. Genes Dev. 2006;20:2096-109.
263. Liao WR, Hsieh RH, Hsu KW, Wu MZ, Tseng MJ, Mai RT, et al. The CBF1-independent Notch1 signal pathway activates human c-myc expression partially via transcription factor YY1. Carcinogenesis. 2007;28:1867-76.
264. Palomero T, Lim WK, Odom DT, Sulis ML, Real PJ, Margolin A, et al. NOTCH1 directly regulates c-MYC and activates a feed-forward-loop transcriptional network promoting leukemic cell growth. Proc Natl Acad Sci U S A. 2006;103:18261-6.
265. Sharma VM, Calvo JA, Draheim KM, Cunningham LA, Hermance N, Beverly L, et al. Notch1 contributes to mouse T-cell leukemia by directly inducing the expression of c-myc. Mol Cell Biol. 2006;26:8022-31.
266. Klinakis A, Szabolcs M, Politi K, Kiaris H, Artavanis-Tsakonas S, Efstratiadis A. Myc is a Notch1 transcriptional target and a requisite for Notch1-induced mammary tumorigenesis in mice. Proc Natl Acad Sci U S A. 2006;103:9262-7.

267. Hsu KW, Hsieh RH, Lee YH, Chao CH, Wu KJ, Tseng MJ, et al. The activated Notch1 receptor cooperates with alpha-enolase and MBP-1 in modulating c-myc activity. Mol Cell Biol. 2008;28:4829-42.
268. Kim JW, Kim MJ, Kim KJ, Yun HJ, Chae JS, Hwang SG, et al. Notch interferes with the scaffold function of JNK-interacting protein 1 to inhibit the JNK signaling pathway. Proc Natl Acad Sci U S A. 2005;102:14308-13.
269. Perumalsamy LR, Nagala M, Banerjee P, Sarin A. A hierarchical cascade activated by non-canonical Notch signaling and the mTOR-Rictor complex regulates neglect-induced death in mammalian cells. Cell Death Differ. 2009;16:879-89.
270. Sunters A, Madureira PA, Pomeranz KM, Aubert M, Brosens JJ, Cook SJ, et al. Paclitaxel-induced nuclear translocation of FOXO3a in breast cancer cells is mediated by c-Jun NH2-terminal kinase and Akt. Cancer Res. 2006;66:212-20.
271. Guo D, Ye J, Dai J, Li L, Chen F, Ma D, et al. Notch-1 regulates Akt signaling pathway and the expression of cell cycle regulatory proteins cyclin D1, CDK2 and p21 in T-ALL cell lines. Leuk Res. 2009;33:678-85.
272. Joshi I, Minter LM, Telfer J, Demarest RM, Capobianco AJ, Aster JC, et al. Notch signaling mediates G1/S cell-cycle progression in T cells via cyclin D3 and its dependent kinases. Blood. 2009;113:1689-98.
273. Campa VM, Gutierrez-Lanza R, Cerignoli F, Diaz-Trelles R, Nelson B, Tsuji T, et al. Notch activates cell cycle reentry and progression in quiescent cardiomyocytes. J Cell Biol. 2008;183:129-41.
274. Noseda M, Niessen K, McLean G, Chang L, Karsan A. Notch-dependent cell cycle arrest is associated with downregulation of minichromosome maintenance proteins. Circ Res. 2005;97:102-4.
275. Ronchini C, Capobianco AJ. Induction of cyclin D1 transcription and CDK2 activity by Notch(ic): implication for cell cycle disruption in transformation by Notch(ic). Mol Cell Biol. 2001;21:5925-34.
276. Curry CL, Reed LL, Golde TE, Miele L, Nickoloff BJ, Foreman KE. Gamma secretase inhibitor blocks Notch activation and induces apoptosis in Kaposi's sarcoma tumor cells. Oncogene. 2005;24:6333-44.
277. Jang MS, Miao H, Carlesso N, Shelly L, Zlobin A, Darack N, et al. Notch-1 regulates cell death independently of differentiation in murine erythroleukemia cells through multiple apoptosis and cell cycle pathways. J Cell Physiol. 2004;199:418-33.
278. Liu WH, Hsiao HW, Tsou WI, Lai MZ. Notch inhibits apoptosis by direct interference with XIAP ubiquitination and degradation. Embo J. 2007;26:1660-9.
279. Wang Z, Li Y, Banerjee S, Kong D, Ahmad A, Nogueira V, et al. Down-regulation of Notch-1 and Jagged-1 inhibits prostate cancer cell growth, migration and invasion, and induces apoptosis via inactivation of Akt, mTOR, and NF-kappaB signaling pathways. J Cell Biochem.109:726-36.
280. Chen J, Imanaka N, Chen J, Griffin JD. Hypoxia potentiates Notch signaling in breast cancer leading to decreased E-cadherin expression and increased cell migration and invasion. Br J Cancer.102:351-60.
281. Wang X, Adam JC, Montell D. Spatially localized Kuzbanian required for specific activation of Notch during border cell migration. Dev Biol. 2007;301:532-40.
282. Bastien D. Gomperts IMK, Peter E.R. Tatham. Notch. Signal transduction. 2nd ed. Amsterdam; Boston; London: Elsevier/Academic Press; 2009.

283. Poulson P. Chromosomal deficiencies and the embryonic development of *Drosophila melanogaster*. Proc Natl Acad Sci U S A. 1937;23:133-7.
284. Artavanis-Tsakonas S, Rand MD, Lake RJ. Notch signaling: cell fate control and signal integration in development. Science. 1999;284:770-6.
285. Lieber T, Kidd S, Alcamo E, Corbin V, Young MW. Antineurogenic phenotypes induced by truncated Notch proteins indicate a role in signal transduction and may point to a novel function for Notch in nuclei. Genes Dev. 1993;7:1949-65.
286. Greenwald I. LIN-12/Notch signaling: lessons from worms and flies. Genes Dev. 1998;12:1751-62.
287. Panin VM, Papayannopoulos V, Wilson R, Irvine KD. Fringe modulates Notch-ligand interactions. Nature. 1997;387:908-12.
288. Swiatek PJ, Lindsell CE, del Amo FF, Weinmaster G, Gridley T. Notch1 is essential for postimplantation development in mice. Genes Dev. 1994;8:707-19.
289. Conlon RA, Reaume AG, Rossant J. Notch1 is required for the coordinate segmentation of somites. Development. 1995;121:1533-45.
290. Hamada Y, Kadokawa Y, Okabe M, Ikawa M, Coleman JR, Tsujimoto Y. Mutation in ankyrin repeats of the mouse Notch2 gene induces early embryonic lethality. Development. 1999;126:3415-24.
291. Krebs LT, Xue Y, Norton CR, Sundberg JP, Beatus P, Lendahl U, et al. Characterization of Notch3-deficient mice: normal embryonic development and absence of genetic interactions with a Notch1 mutation. Genesis. 2003;37:139-43.
292. Krebs LT, Xue Y, Norton CR, Shutter JR, Maguire M, Sundberg JP, et al. Notch signaling is essential for vascular morphogenesis in mice. Genes Dev. 2000;14:1343-52.
293. Kitamoto T, Takahashi K, Takimoto H, Tomizuka K, Hayasaka M, Tabira T, et al. Functional redundancy of the Notch gene family during mouse embryogenesis: analysis of Notch gene expression in Notch3-deficient mice. Biochem Biophys Res Commun. 2005;331:1154-62.
294. Kusumi K, Sun ES, Kerrebrock AW, Bronson RT, Chi DC, Bulotsky MS, et al. The mouse pudgy mutation disrupts Delta homologue Dll3 and initiation of early somite boundaries. Nat Genet. 1998;19:274-8.
295. Xue Y, Gao X, Lindsell CE, Norton CR, Chang B, Hicks C, et al. Embryonic lethality and vascular defects in mice lacking the Notch ligand Jagged1. Hum Mol Genet. 1999;8:723-30.
296. Jiang R, Lan Y, Chapman HD, Shawber C, Norton CR, Serreze DV, et al. Defects in limb, craniofacial, and thymic development in Jagged2 mutant mice. Genes Dev. 1998;12:1046-57.
297. Hrabe de Angelis M, McIntyre J, 2nd, Gossler A. Maintenance of somite borders in mice requires the Delta homologue DII1. Nature. 1997;386:717-21.
298. Sidow A, Bulotsky MS, Kerrebrock AW, Bronson RT, Daly MJ, Reeve MP, et al. Serrate2 is disrupted in the mouse limb-development mutant syndactylism. Nature. 1997;389:722-5.
299. Krebs LT, Shutter JR, Tanigaki K, Honjo T, Stark KL, Gridley T. Haploinsufficient lethality and formation of arteriovenous malformations in Notch pathway mutants. Genes Dev. 2004;18:2469-73.
300. Duarte A, Hirashima M, Benedito R, Trindade A, Diniz P, Bekman E, et al. Dosage-sensitive requirement for mouse Dll4 in artery development. Genes Dev. 2004;18:2474-8.

301. Gale NW, Dominguez MG, Noguera I, Pan L, Hughes V, Valenzuela DM, et al. Haploinsufficiency of delta-like 4 ligand results in embryonic lethality due to major defects in arterial and vascular development. Proc Natl Acad Sci U S A. 2004;101:15949-54.
302. Shen J, Bronson RT, Chen DF, Xia W, Selkoe DJ, Tonegawa S. Skeletal and CNS defects in Presenilin-1-deficient mice. Cell. 1997;89:629-39.
303. Herreman A, Hartmann D, Annaert W, Saftig P, Craessaerts K, Serneels L, et al. Presenilin 2 deficiency causes a mild pulmonary phenotype and no changes in amyloid precursor protein processing but enhances the embryonic lethal phenotype of presenilin 1 deficiency. Proc Natl Acad Sci U S A. 1999;96:11872-7.
304. Donoviel DB, Hadjantonakis AK, Ikeda M, Zheng H, Hyslop PS, Bernstein A. Mice lacking both presenilin genes exhibit early embryonic patterning defects. Genes Dev. 1999;13:2801-10.
305. Oka C, Nakano T, Wakeham A, de la Pompa JL, Mori C, Sakai T, et al. Disruption of the mouse RBP-J kappa gene results in early embryonic death. Development. 1995;121:3291-301.
306. Luo D, Renault VM, Rando TA. The regulation of Notch signaling in muscle stem cell activation and postnatal myogenesis. Semin Cell Dev Biol. 2005;16:612-22.
307. Collins BJ, Kleeberger W, Ball DW. Notch in lung development and lung cancer. Semin Cancer Biol. 2004;14:357-64.
308. Lemaigre F, Zaret KS. Liver development update: new embryo models, cell lineage control, and morphogenesis. Curr Opin Genet Dev. 2004;14:582-90.
309. McCright B. Notch signaling in kidney development. Curr Opin Nephrol Hypertens. 2003;12:5-10.
310. Kim W, Shin YK, Kim BJ, Egan JM. Notch signaling in pancreatic endocrine cell and diabetes. Biochem Biophys Res Commun.392:247-51.
311. Lasky JL, Wu H. Notch signaling, brain development, and human disease. Pediatr Res. 2005;57:104R-9R.
312. High FA, Epstein JA. The multifaceted role of Notch in cardiac development and disease. Nat Rev Genet. 2008;9:49-61.
313. Vercauteren SM, Sutherland HJ. Constitutively active Notch4 promotes early human hematopoietic progenitor cell maintenance while inhibiting differentiation and causes lymphoid abnormalities in vivo. Blood. 2004;104:2315-22.
314. Lauret E, Catelain C, Titeux M, Poirault S, Dando JS, Dorsch M, et al. Membrane-bound delta-4 notch ligand reduces the proliferative activity of primitive human hematopoietic CD34+CD38low cells while maintaining their LTC-IC potential. Leukemia. 2004;18:788-97.
315. Stier S, Cheng T, Dombkowski D, Carlesso N, Scadden DT. Notch1 activation increases hematopoietic stem cell self-renewal in vivo and favors lymphoid over myeloid lineage outcome. Blood. 2002;99:2369-78.
316. Karanu FN, Murdoch B, Gallacher L, Wu DM, Koremoto M, Sakano S, et al. The notch ligand jagged-1 represents a novel growth factor of human hematopoietic stem cells. J Exp Med. 2000;192:1365-72.
317. Duncan AW, Rattis FM, DiMascio LN, Congdon KL, Pazianos G, Zhao C, et al. Integration of Notch and Wnt signaling in hematopoietic stem cell maintenance. Nat Immunol. 2005;6:314-22.

318. Maillard I, Koch U, Dumortier A, Shestova O, Xu L, Sai H, et al. Canonical notch signaling is dispensable for the maintenance of adult hematopoietic stem cells. Cell Stem Cell. 2008;2:356-66.
319. Radtke F, Fasnacht N, Macdonald HR. Notch signaling in the immune system. Immunity.32:14-27.
320. Wang P, Hou SX. Regulation of intestinal stem cells in mammals and Drosophila. J Cell Physiol.222:33-7.
321. Casali A, Batlle E. Intestinal stem cells in mammals and Drosophila. Cell Stem Cell. 2009;4:124-7.
322. Fre S, Huyghe M, Mourikis P, Robine S, Louvard D, Artavanis-Tsakonas S. Notch signals control the fate of immature progenitor cells in the intestine. Nature. 2005;435:964-8.
323. van Es JH, van Gijn ME, Riccio O, van den Born M, Vooijs M, Begthel H, et al. Notch/gamma-secretase inhibition turns proliferative cells in intestinal crypts and adenomas into goblet cells. Nature. 2005;435:959-63.
324. Ireland H, Kemp R, Houghton C, Howard L, Clarke AR, Sansom OJ, et al. Inducible Cre-mediated control of gene expression in the murine gastrointestinal tract: effect of loss of beta-catenin. Gastroenterology. 2004;126:1236-46.
325. Riccio O, van Gijn ME, Bezdek AC, Pellegrinet L, van Es JH, Zimber-Strobl U, et al. Loss of intestinal crypt progenitor cells owing to inactivation of both Notch1 and Notch2 is accompanied by derepression of CDK inhibitors p27Kip1 and p57Kip2. EMBO Rep. 2008;9:377-83.
326. Phng LK, Gerhardt H. Angiogenesis: a team effort coordinated by notch. Dev Cell. 2009;16:196-208.
327. Hayashi H, Kume T. Foxc transcription factors directly regulate Dll4 and Hey2 expression by interacting with the VEGF-Notch signaling pathways in endothelial cells. PLoS One. 2008;3:e2401.
328. Suchting S, Freitas C, le Noble F, Benedito R, Breant C, Duarte A, et al. The Notch ligand Delta-like 4 negatively regulates endothelial tip cell formation and vessel branching. Proc Natl Acad Sci U S A. 2007;104:3225-30.
329. Hellstrom M, Phng LK, Hofmann JJ, Wallgard E, Coultas L, Lindblom P, et al. Dll4 signalling through Notch1 regulates formation of tip cells during angiogenesis. Nature. 2007;445:776-80.
330. Siekmann AF, Lawson ND. Notch signalling limits angiogenic cell behaviour in developing zebrafish arteries. Nature. 2007;445:781-4.
331. Funahashi Y, Shawber CJ, Vorontchikhina M, Sharma A, Outtz HH, Kitajewski J. Notch regulates the angiogenic response via induction of VEGFR-1. J Angiogenes Res. 2010;2:3.
332. Harrington LS, Sainson RC, Williams CK, Taylor JM, Shi W, Li JL, et al. Regulation of multiple angiogenic pathways by Dll4 and Notch in human umbilical vein endothelial cells. Microvasc Res. 2008;75:144-54.
333. Holderfield MT, Henderson Anderson AM, Kokubo H, Chin MT, Johnson RL, Hughes CC. HESR1/CHF2 suppresses VEGFR2 transcription independent of binding to E-boxes. Biochem Biophys Res Commun. 2006;346:637-48.
334. Dou GR, Wang YC, Hu XB, Hou LH, Wang CM, Xu JF, et al. RBP-J, the transcription factor downstream of Notch receptors, is essential for the maintenance of vascular homeostasis in adult mice. Faseb J. 2008;22:1606-17.
335. Benedito R, Roca C, Sorensen I, Adams S, Gossler A, Fruttiger M, et al. The notch ligands Dll4 and Jagged1 have opposing effects on angiogenesis. Cell. 2009;137:1124-35.

336. Noseda M, Chang L, McLean G, Grim JE, Clurman BE, Smith LL, et al. Notch activation induces endothelial cell cycle arrest and participates in contact inhibition: role of p21Cip1 repression. Mol Cell Biol. 2004;24:8813-22.
337. Liu ZJ, Xiao M, Balint K, Soma A, Pinnix CC, Capobianco AJ, et al. Inhibition of endothelial cell proliferation by Notch1 signaling is mediated by repressing MAPK and PI3K/Akt pathways and requires MAML1. Faseb J. 2006;20:1009-11.
338. Trindade A, Kumar SR, Scehnet JS, Lopes-da-Costa L, Becker J, Jiang W, et al. Overexpression of delta-like 4 induces arterialization and attenuates vessel formation in developing mouse embryos. Blood. 2008;112:1720-9.
339. Leong KG, Hu X, Li L, Noseda M, Larrivee B, Hull C, et al. Activated Notch4 inhibits angiogenesis: role of beta 1-integrin activation. Mol Cell Biol. 2002;22:2830-41.
340. Domenga V, Fardoux P, Lacombe P, Monet M, Maciazek J, Krebs LT, et al. Notch3 is required for arterial identity and maturation of vascular smooth muscle cells. Genes Dev. 2004;18:2730-5.
341. Wang HU, Chen ZF, Anderson DJ. Molecular distinction and angiogenic interaction between embryonic arteries and veins revealed by ephrin-B2 and its receptor Eph-B4. Cell. 1998;93:741-53.
342. Grego-Bessa J, Luna-Zurita L, del Monte G, Bolos V, Melgar P, Arandilla A, et al. Notch signaling is essential for ventricular chamber development. Dev Cell. 2007;12:415-29.
343. Kim YH, Hu H, Guevara-Gallardo S, Lam MT, Fong SY, Wang RA. Artery and vein size is balanced by Notch and ephrin B2/EphB4 during angiogenesis. Development. 2008;135:3755-64.
344. Gridley T. Notch signaling and inherited disease syndromes. Hum Mol Genet. 2003;12 Spec No 1:R9-13.
345. Pear WS, Aster JC, Scott ML, Hasserjian RP, Soffer B, Sklar J, et al. Exclusive development of T cell neoplasms in mice transplanted with bone marrow expressing activated Notch alleles. J Exp Med. 1996;183:2283-91.
346. Weng AP, Ferrando AA, Lee W, Morris JPt, Silverman LB, Sanchez-Irizarry C, et al. Activating mutations of NOTCH1 in human T cell acute lymphoblastic leukemia. Science. 2004;306:269-71.
347. Chiang MY, Xu L, Shestova O, Histen G, L'Heureux S, Romany C, et al. Leukemia-associated NOTCH1 alleles are weak tumor initiators but accelerate K-ras-initiated leukemia. J Clin Invest. 2008;118:3181-94.
348. Kindler T, Cornejo MG, Scholl C, Liu J, Leeman DS, Haydu JE, et al. K-RasG12D-induced T-cell lymphoblastic lymphoma/leukemias harbor Notch1 mutations and are sensitive to gamma-secretase inhibitors. Blood. 2008;112:3373-82.
349. Weng AP, Nam Y, Wolfe MS, Pear WS, Griffin JD, Blacklow SC, et al. Growth suppression of pre-T acute lymphoblastic leukemia cells by inhibition of notch signaling. Mol Cell Biol. 2003;23:655-64.
350. Sicinska E, Aifantis I, Le Cam L, Swat W, Borowski C, Yu Q, et al. Requirement for cyclin D3 in lymphocyte development and T cell leukemias. Cancer Cell. 2003;4:451-61.
351. Dohda T, Maljukova A, Liu L, Heyman M, Grander D, Brodin D, et al. Notch signaling induces SKP2 expression and promotes reduction of p27Kip1 in T-cell acute lymphoblastic leukemia cell lines. Exp Cell Res. 2007;313:3141-52.
352. Rao SS, O'Neil J, Liberator CD, Hardwick JS, Dai X, Zhang T, et al. Inhibition of NOTCH signaling by gamma secretase inhibitor engages the RB

pathway and elicits cell cycle exit in T-cell acute lymphoblastic leukemia cells. Cancer Res. 2009;69:3060-8.
353. Beverly LJ, Felsher DW, Capobianco AJ. Suppression of p53 by Notch in lymphomagenesis: implications for initiation and regression. Cancer Res. 2005;65:7159-68.
354. Vilimas T, Mascarenhas J, Palomero T, Mandal M, Buonamici S, Meng F, et al. Targeting the NF-kappaB signaling pathway in Notch1-induced T-cell leukemia. Nat Med. 2007;13:70-7.
355. Palomero T, Sulis ML, Cortina M, Real PJ, Barnes K, Ciofani M, et al. Mutational loss of PTEN induces resistance to NOTCH1 inhibition in T-cell leukemia. Nat Med. 2007;13:1203-10.
356. Chan SM, Weng AP, Tibshirani R, Aster JC, Utz PJ. Notch signals positively regulate activity of the mTOR pathway in T-cell acute lymphoblastic leukemia. Blood. 2007;110:278-86.
357. Medyouf H, Gao X, Armstrong F, Gusscott S, Liu Q, Gedman AL, et al. Acute T-cell leukemias remain dependent on Notch signaling despite PTEN and INK4A/ARF loss. Blood.115:1175-84.
358. O'Neil J, Grim J, Strack P, Rao S, Tibbitts D, Winter C, et al. FBW7 mutations in leukemic cells mediate NOTCH pathway activation and resistance to gamma-secretase inhibitors. J Exp Med. 2007;204:1813-24.
359. Sriuranpong V, Borges MW, Ravi RK, Arnold DR, Nelkin BD, Baylin SB, et al. Notch signaling induces cell cycle arrest in small cell lung cancer cells. Cancer Res. 2001;61:3200-5.
360. Kunnimalaiyaan M, Vaccaro AM, Ndiaye MA, Chen H. Overexpression of the NOTCH1 intracellular domain inhibits cell proliferation and alters the neuroendocrine phenotype of medullary thyroid cancer cells. J Biol Chem. 2006;281:39819-30.
361. Nakakura EK, Sriuranpong VR, Kunnimalaiyaan M, Hsiao EC, Schuebel KE, Borges MW, et al. Regulation of neuroendocrine differentiation in gastrointestinal carcinoid tumor cells by notch signaling. J Clin Endocrinol Metab. 2005;90:4350-6.
362. Kunnimalaiyaan M, Chen H. Tumor suppressor role of Notch-1 signaling in neuroendocrine tumors. Oncologist. 2007;12:535-42.
363. Talora C, Cialfi S, Segatto O, Morrone S, Kim Choi J, Frati L, et al. Constitutively active Notch1 induces growth arrest of HPV-positive cervical cancer cells via separate signaling pathways. Exp Cell Res. 2005;305:343-54.
364. Qi R, An H, Yu Y, Zhang M, Liu S, Xu H, et al. Notch1 signaling inhibits growth of human hepatocellular carcinoma through induction of cell cycle arrest and apoptosis. Cancer Res. 2003;63:8323-9.
365. Nicolas M, Wolfer A, Raj K, Kummer JA, Mill P, van Noort M, et al. Notch1 functions as a tumor suppressor in mouse skin. Nat Genet. 2003;33:416-21.
366. Proweller A, Tu L, Lepore JJ, Cheng L, Lu MM, Seykora J, et al. Impaired notch signaling promotes de novo squamous cell carcinoma formation. Cancer Res. 2006;66:7438-44.
367. Lefort K, Mandinova A, Ostano P, Kolev V, Calpini V, Kolfschoten I, et al. Notch1 is a p53 target gene involved in human keratinocyte tumor suppression through negative regulation of ROCK1/2 and MRCKalpha kinases. Genes Dev. 2007;21:562-77.

368. Demehri S, Turkoz A, Kopan R. Epidermal Notch1 loss promotes skin tumorigenesis by impacting the stromal microenvironment. Cancer Cell. 2009;16:55-66.
369. Thelu J, Rossio P, Favier B. Notch signalling is linked to epidermal cell differentiation level in basal cell carcinoma, psoriasis and wound healing. BMC Dermatol. 2002;2:7.
370. Clarke MF, Dick JE, Dirks PB, Eaves CJ, Jamieson CH, Jones DL, et al. Cancer stem cells--perspectives on current status and future directions: AACR Workshop on cancer stem cells. Cancer Res. 2006;66:9339-44.
371. Reya T, Morrison SJ, Clarke MF, Weissman IL. Stem cells, cancer, and cancer stem cells. Nature. 2001;414:105-11.
372. Singh SK, Clarke ID, Terasaki M, Bonn VE, Hawkins C, Squire J, et al. Identification of a cancer stem cell in human brain tumors. Cancer Res. 2003;63:5821-8.
373. Al-Hajj M, Wicha MS, Benito-Hernandez A, Morrison SJ, Clarke MF. Prospective identification of tumorigenic breast cancer cells. Proc Natl Acad Sci U S A. 2003;100:3983-8.
374. Visvader JE, Lindeman GJ. Cancer stem cells in solid tumours: accumulating evidence and unresolved questions. Nat Rev Cancer. 2008;8:755-68.
375. Zhang S, Balch C, Chan MW, Lai HC, Matei D, Schilder JM, et al. Identification and characterization of ovarian cancer-initiating cells from primary human tumors. Cancer Res. 2008;68:4311-20.
376. Gal H, Amariglio N, Trakhtenbrot L, Jacob-Hirsh J, Margalit O, Avigdor A, et al. Gene expression profiles of AML derived stem cells; similarity to hematopoietic stem cells. Leukemia. 2006;20:2147-54.
377. Ji Q, Hao X, Meng Y, Zhang M, Desano J, Fan D, et al. Restoration of tumor suppressor miR-34 inhibits human p53-mutant gastric cancer tumorspheres. BMC Cancer. 2008;8:266.
378. Wang Z, Li Y, Kong D, Banerjee S, Ahmad A, Azmi AS, et al. Acquisition of epithelial-mesenchymal transition phenotype of gemcitabine-resistant pancreatic cancer cells is linked with activation of the notch signaling pathway. Cancer Res. 2009;69:2400-7.
379. Harrison H, Farnie G, Howell SJ, Rock RE, Stylianou S, Brennan KR, et al. Regulation of breast cancer stem cell activity by signaling through the Notch4 receptor. Cancer Res.70:709-18.
380. Charles N, Ozawa T, Squatrito M, Bleau AM, Brennan CW, Hambardzumyan D, et al. Perivascular nitric oxide activates notch signaling and promotes stem-like character in PDGF-induced glioma cells. Cell Stem Cell.6:141-52.
381. Sikandar SS, Pate KT, Anderson S, Dizon D, Edwards RA, Waterman ML, et al. NOTCH signaling is required for formation and self-renewal of tumor-initiating cells and for repression of secretory cell differentiation in colon cancer. Cancer Res.70:1469-78.
382. Farnie G, Clarke RB, Spence K, Pinnock N, Brennan K, Anderson NG, et al. Novel cell culture technique for primary ductal carcinoma in situ: role of Notch and epidermal growth factor receptor signaling pathways. J Natl Cancer Inst. 2007;99:616-27.
383. Singh SK, Hawkins C, Clarke ID, Squire JA, Bayani J, Hide T, et al. Identification of human brain tumour initiating cells. Nature. 2004;432:396-401.

384. Clement V, Dutoit V, Marino D, Dietrich PY, Radovanovic I. Limits of CD133 as a marker of glioma self-renewing cells. Int J Cancer. 2009;125:244-8.
385. Fan X, Matsui W, Khaki L, Stearns D, Chun J, Li YM, et al. Notch pathway inhibition depletes stem-like cells and blocks engraftment in embryonal brain tumors. Cancer Res. 2006;66:7445-52.
386. Fan X, Khaki L, Zhu TS, Soules ME, Talsma CE, Gul N, et al. NOTCH pathway blockade depletes CD133-positive glioblastoma cells and inhibits growth of tumor neurospheres and xenografts. Stem Cells.28:5-16.
387. Zhang XP, Zheng G, Zou L, Liu HL, Hou LH, Zhou P, et al. Notch activation promotes cell proliferation and the formation of neural stem cell-like colonies in human glioma cells. Mol Cell Biochem. 2008;307:101-8.
388. Wang J, Wakeman TP, Lathia JD, Hjelmeland AB, Wang XF, White RR, et al. Notch promotes radioresistance of glioma stem cells. Stem Cells.28:17-28.
389. Richert MM, Schwertfeger KL, Ryder JW, Anderson SM. An atlas of mouse mammary gland development. J Mammary Gland Biol Neoplasia. 2000;5:227-41.
390. Smith GH, Gallahan D, Diella F, Jhappan C, Merlino G, Callahan R. Constitutive expression of a truncated INT3 gene in mouse mammary epithelium impairs differentiation and functional development. Cell Growth Differ. 1995;6:563-77.
391. Hu C, Dievart A, Lupien M, Calvo E, Tremblay G, Jolicoeur P. Overexpression of activated murine Notch1 and Notch3 in transgenic mice blocks mammary gland development and induces mammary tumors. Am J Pathol. 2006;168:973-90.
392. Buono KD, Robinson GW, Martin C, Shi S, Stanley P, Tanigaki K, et al. The canonical Notch/RBP-J signaling pathway controls the balance of cell lineages in mammary epithelium during pregnancy. Dev Biol. 2006;293:565-80.
393. Raafat A, Lawson S, Bargo S, Klauzinska M, Strizzi L, Goldhar AS, et al. Rbpj conditional knockout reveals distinct functions of Notch4/Int3 in mammary gland development and tumorigenesis. Oncogene. 2009;28:219-30.
394. Bouras T, Pal B, Vaillant F, Harburg G, Asselin-Labat ML, Oakes SR, et al. Notch signaling regulates mammary stem cell function and luminal cell-fate commitment. Cell Stem Cell. 2008;3:429-41.
395. Raouf A, Zhao Y, To K, Stingl J, Delaney A, Barbara M, et al. Transcriptome analysis of the normal human mammary cell commitment and differentiation process. Cell Stem Cell. 2008;3:109-18.
396. Gallahan D, Callahan R. Mammary tumorigenesis in feral mice: identification of a new int locus in mouse mammary tumor virus (Czech II)-induced mammary tumors. J Virol. 1987;61:66-74.
397. Gallahan D, Kozak C, Callahan R. A new common integration region (int-3) for mouse mammary tumor virus on mouse chromosome 17. J Virol. 1987;61:218-20.
398. Robbins J, Blondel BJ, Gallahan D, Callahan R. Mouse mammary tumor gene int-3: a member of the notch gene family transforms mammary epithelial cells. J Virol. 1992;66:2594-9.
399. Gallahan D, Jhappan C, Robinson G, Hennighausen L, Sharp R, Kordon E, et al. Expression of a truncated Int3 gene in developing secretory mammary epithelium specifically retards lobular differentiation resulting in tumorigenesis. Cancer Res. 1996;56:1775-85.

400. Lee SH, Jeong EG, Yoo NJ, Lee SH. Mutational analysis of NOTCH1, 2, 3 and 4 genes in common solid cancers and acute leukemias. Apmis. 2007;115:1357-63.
401. Rizzo P, Miao H, D'Souza G, Osipo C, Song LL, Yun J, et al. Cross-talk between notch and the estrogen receptor in breast cancer suggests novel therapeutic approaches. Cancer Res. 2008;68:5226-35.
402. Pece S, Serresi M, Santolini E, Capra M, Hulleman E, Galimberti V, et al. Loss of negative regulation by Numb over Notch is relevant to human breast carcinogenesis. J Cell Biol. 2004;167:215-21.
403. Stylianou S, Clarke RB, Brennan K. Aberrant activation of notch signaling in human breast cancer. Cancer Res. 2006;66:1517-25.
404. Filipovic A, Gronau JH, Green AR, Wang J, Vallath S, Shao D, et al. Biological and clinical implications of nicastrin expression in invasive breast cancer. Breast Cancer Res Treat.
405. Colaluca IN, Tosoni D, Nuciforo P, Senic-Matuglia F, Galimberti V, Viale G, et al. NUMB controls p53 tumour suppressor activity. Nature. 2008;451:76-80.
406. Di Marcotullio L, Ferretti E, Greco A, De Smaele E, Po A, Sico MA, et al. Numb is a suppressor of Hedgehog signalling and targets Gli1 for Itch-dependent ubiquitination. Nat Cell Biol. 2006;8:1415-23.
407. Reedijk M, Odorcic S, Chang L, Zhang H, Miller N, McCready DR, et al. High-level coexpression of JAG1 and NOTCH1 is observed in human breast cancer and is associated with poor overall survival. Cancer Res. 2005;65:8530-7.
408. Zang S, Ji C, Qu X, Dong X, Ma D, Ye J, et al. A study on Notch signaling in human breast cancer. Neoplasma. 2007;54:304-10.
409. Dickson BC, Mulligan AM, Zhang H, Lockwood G, O'Malley FP, Egan SE, et al. High-level JAG1 mRNA and protein predict poor outcome in breast cancer. Mod Pathol. 2007;20:685-93.
410. Reedijk M, Pinnaduwage D, Dickson BC, Mulligan AM, Zhang H, Bull SB, et al. JAG1 expression is associated with a basal phenotype and recurrence in lymph node-negative breast cancer. Breast Cancer Res Treat. 2008;111:439-48.
411. Parr C, Watkins G, Jiang WG. The possible correlation of Notch-1 and Notch-2 with clinical outcome and tumour clinicopathological parameters in human breast cancer. Int J Mol Med. 2004;14:779-86.
412. O'Neill CF, Urs S, Cinelli C, Lincoln A, Nadeau RJ, Leon R, et al. Notch2 signaling induces apoptosis and inhibits human MDA-MB-231 xenograft growth. Am J Pathol. 2007;171:1023-36.
413. Yamaguchi N, Oyama T, Ito E, Satoh H, Azuma S, Hayashi M, et al. NOTCH3 signaling pathway plays crucial roles in the proliferation of ErbB2-negative human breast cancer cells. Cancer Res. 2008;68:1881-8.
414. Osipo C, Patel P, Rizzo P, Clementz AG, Hao L, Golde TE, et al. ErbB-2 inhibition activates Notch-1 and sensitizes breast cancer cells to a gamma-secretase inhibitor. Oncogene. 2008;27:5019-32.
415. Zang S, Chen F, Dai J, Guo D, Tse W, Qu X, et al. RNAi-mediated knockdown of Notch-1 leads to cell growth inhibition and enhanced chemosensitivity in human breast cancer. Oncol Rep.23:893-9.
416. Lee CW, Raskett CM, Prudovsky I, Altieri DC. Molecular dependence of estrogen receptor-negative breast cancer on a notch-survivin signaling axis. Cancer Res. 2008;68:5273-81.
417. Weinmaster G, Kopan R. A garden of Notch-ly delights. Development. 2006;133:3277-82.

418. Ponti D, Costa A, Zaffaroni N, Pratesi G, Petrangolini G, Coradini D, et al. Isolation and in vitro propagation of tumorigenic breast cancer cells with stem/progenitor cell properties. Cancer Res. 2005;65:5506-11.
419. Rappa G, Lorico A. Phenotypic characterization of mammosphere-forming cells from the human MA-11 breast carcinoma cell line. Exp Cell Res.
420. Sansone P, Storci G, Giovannini C, Pandolfi S, Pianetti S, Taffurelli M, et al. p66Shc/Notch-3 interplay controls self-renewal and hypoxia survival in human stem/progenitor cells of the mammary gland expanded in vitro as mammospheres. Stem Cells. 2007;25:807-15.
421. Phillips TM, McBride WH, Pajonk F. The response of CD24(-/low)/CD44+ breast cancer-initiating cells to radiation. J Natl Cancer Inst. 2006;98:1777-85.
422. Jeffries S, Capobianco AJ. Neoplastic transformation by Notch requires nuclear localization. Mol Cell Biol. 2000;20:3928-41.
423. Sun Y, Lowther W, Kato K, Bianco C, Kenney N, Strizzi L, et al. Notch4 intracellular domain binding to Smad3 and inhibition of the TGF-beta signaling. Oncogene. 2005;24:5365-74.
424. Kretzschmar M. Transforming growth factor-beta and breast cancer: Transforming growth factor-beta/SMAD signaling defects and cancer. Breast Cancer Res. 2000;2:107-15.
425. Hynes NE, Stoelzle T. Key signalling nodes in mammary gland development and cancer: Myc. Breast Cancer Res. 2009;11:210.
426. Whyte J, Bergin O, Bianchi A, McNally S, Martin F. Key signalling nodes in mammary gland development and cancer. Mitogen-activated protein kinase signalling in experimental models of breast cancer progression and in mammary gland development. Breast Cancer Res. 2009;11:209.
427. Olson RE, Albright CF. Recent progress in the medicinal chemistry of gamma-secretase inhibitors. Curr Top Med Chem. 2008;8:17-33.
428. Shearman MS, Beher D, Clarke EE, Lewis HD, Harrison T, Hunt P, et al. L-685,458, an aspartyl protease transition state mimic, is a potent inhibitor of amyloid beta-protein precursor gamma-secretase activity. Biochemistry. 2000;39:8698-704.
429. Dovey HF, John V, Anderson JP, Chen LZ, de Saint Andrieu P, Fang LY, et al. Functional gamma-secretase inhibitors reduce beta-amyloid peptide levels in brain. J Neurochem. 2001;76:173-81.
430. Seiffert D, Bradley JD, Rominger CM, Rominger DH, Yang F, Meredith JE, Jr., et al. Presenilin-1 and -2 are molecular targets for gamma-secretase inhibitors. J Biol Chem. 2000;275:34086-91.
431. Wong GT, Manfra D, Poulet FM, Zhang Q, Josien H, Bara T, et al. Chronic treatment with the gamma-secretase inhibitor LY-411,575 inhibits beta-amyloid peptide production and alters lymphopoiesis and intestinal cell differentiation. J Biol Chem. 2004;279:12876-82.
432. Henley DB, May PC, Dean RA, Siemers ER. Development of semagacestat (LY450139), a functional gamma-secretase inhibitor, for the treatment of Alzheimer's disease. Expert Opin Pharmacother. 2009;10:1657-64.
433. Weihofen A, Lemberg MK, Friedmann E, Rueeger H, Schmitz A, Paganetti P, et al. Targeting presenilin-type aspartic protease signal peptide peptidase with gamma-secretase inhibitors. J Biol Chem. 2003;278:16528-33.
434. Iben LG, Olson RE, Balanda LA, Jayachandra S, Robertson BJ, Hay V, et al. Signal peptide peptidase and gamma-secretase share equivalent inhibitor binding pharmacology. J Biol Chem. 2007;282:36829-36.

435. Golde TE, Wolfe MS, Greenbaum DC. Signal peptide peptidases: a family of intramembrane-cleaving proteases that cleave type 2 transmembrane proteins. Semin Cell Dev Biol. 2009;20:225-30.
436. Krawitz P, Haffner C, Fluhrer R, Steiner H, Schmid B, Haass C. Differential localization and identification of a critical aspartate suggest non-redundant proteolytic functions of the presenilin homologues SPPL2b and SPPL3. J Biol Chem. 2005;280:39515-23.
437. Yan D, Qin N, Zhang H, Liu T, Yu M, Jiang X, et al. Expression of TNF-alpha leader sequence renders MCF-7 tumor cells resistant to the cytotoxicity of soluble TNF-alpha. Breast Cancer Res Treat. 2009;116:91-102.
438. Wajant H, Pfizenmaier K, Scheurich P. Tumor necrosis factor signaling. Cell Death Differ. 2003;10:45-65.
439. Eissner G, Kolch W, Scheurich P. Ligands working as receptors: reverse signaling by members of the TNF superfamily enhance the plasticity of the immune system. Cytokine Growth Factor Rev. 2004;15:353-66.
440. Domonkos A, Udvardy A, Laszlo L, Nagy T, Duda E. Receptor-like properties of the 26 kDa transmembrane form of TNF. Eur Cytokine Netw. 2001;12:411-9.
441. Friedmann E, Hauben E, Maylandt K, Schleeger S, Vreugde S, Lichtenthaler SF, et al. SPPL2a and SPPL2b promote intramembrane proteolysis of TNFalpha in activated dendritic cells to trigger IL-12 production. Nat Cell Biol. 2006;8:843-8.
442. Fluhrer R, Grammer G, Israel L, Condron MM, Haffner C, Friedmann E, et al. A gamma-secretase-like intramembrane cleavage of TNFalpha by the GxGD aspartyl protease SPPL2b. Nat Cell Biol. 2006;8:894-6.
443. Lleo A. Activity of gamma-secretase on substrates other than APP. Curr Top Med Chem. 2008;8:9-16.
444. Zhang YW, Wang R, Liu Q, Zhang H, Liao FF, Xu H. Presenilin/gamma-secretase-dependent processing of beta-amyloid precursor protein regulates EGF receptor expression. Proc Natl Acad Sci U S A. 2007;104:10613-8.
445. Li T, Wen H, Brayton C, Das P, Smithson LA, Fauq A, et al. Epidermal growth factor receptor and notch pathways participate in the tumor suppressor function of gamma-secretase. J Biol Chem. 2007;282:32264-73.
446. Ni CY, Murphy MP, Golde TE, Carpenter G. gamma -Secretase cleavage and nuclear localization of ErbB-4 receptor tyrosine kinase. Science. 2001;294:2179-81.
447. Feng SM, Sartor CI, Hunter D, Zhou H, Yang X, Caskey LS, et al. The HER4 cytoplasmic domain, but not its C terminus, inhibits mammary cell proliferation. Mol Endocrinol. 2007;21:1861-76.
448. Vidal GA, Naresh A, Marrero L, Jones FE. Presenilin-dependent gamma-secretase processing regulates multiple ERBB4/HER4 activities. J Biol Chem. 2005;280:19777-83.
449. Marambaud P, Shioi J, Serban G, Georgakopoulos A, Sarner S, Nagy V, et al. A presenilin-1/gamma-secretase cleavage releases the E-cadherin intracellular domain and regulates disassembly of adherens junctions. Embo J. 2002;21:1948-56.
450. Ferber EC, Kajita M, Wadlow A, Tobiansky L, Niessen C, Ariga H, et al. A role for the cleaved cytoplasmic domain of E-cadherin in the nucleus. J Biol Chem. 2008;283:12691-700.

451. Park CS, Kim OS, Yun SM, Jo SA, Jo I, Koh YH. Presenilin 1/gamma-secretase is associated with cadmium-induced E-cadherin cleavage and COX-2 gene expression in T47D breast cancer cells. Toxicol Sci. 2008;106:413-22.
452. Haas IG, Frank M, Veron N, Kemler R. Presenilin-dependent processing and nuclear function of gamma-protocadherins. J Biol Chem. 2005;280:9313-9.
453. Marambaud P, Wen PH, Dutt A, Shioi J, Takashima A, Siman R, et al. A CBP binding transcriptional repressor produced by the PS1/epsilon-cleavage of N-cadherin is inhibited by PS1 FAD mutations. Cell. 2003;114:635-45.
454. Murai T, Miyazaki Y, Nishinakamura H, Sugahara KN, Miyauchi T, Sako Y, et al. Engagement of CD44 promotes Rac activation and CD44 cleavage during tumor cell migration. J Biol Chem. 2004;279:4541-50.
455. Murakami D, Okamoto I, Nagano O, Kawano Y, Tomita T, Iwatsubo T, et al. Presenilin-dependent gamma-secretase activity mediates the intramembranous cleavage of CD44. Oncogene. 2003;22:1511-6.
456. Lammich S, Okochi M, Takeda M, Kaether C, Capell A, Zimmer AK, et al. Presenilin-dependent intramembrane proteolysis of CD44 leads to the liberation of its intracellular domain and the secretion of an Abeta-like peptide. J Biol Chem. 2002;277:44754-9.
457. Anderegg U, Eichenberg T, Parthaune T, Haiduk C, Saalbach A, Milkova L, et al. ADAM10 is the constitutive functional sheddase of CD44 in human melanoma cells. J Invest Dermatol. 2009;129:1471-82.
458. Pelletier L, Guillaumot P, Freche B, Luquain C, Christiansen D, Brugiere S, et al. Gamma-secretase-dependent proteolysis of CD44 promotes neoplastic transformation of rat fibroblastic cells. Cancer Res. 2006;66:3681-7.
459. Liu CX, Ranganathan S, Robinson S, Strickland DK. gamma-Secretase-mediated release of the low density lipoprotein receptor-related protein 1B intracellular domain suppresses anchorage-independent growth of neuroglioma cells. J Biol Chem. 2007;282:7504-11.
460. Kim DY, Ingano LA, Carey BW, Pettingell WH, Kovacs DM. Presenilin/gamma-secretase-mediated cleavage of the voltage-gated sodium channel beta2-subunit regulates cell adhesion and migration. J Biol Chem. 2005;280:23251-61.
461. Kreft A, Harrison B, Aschmies S, Atchison K, Casebier D, Cole DC, et al. Discovery of a novel series of Notch-sparing gamma-secretase inhibitors. Bioorg Med Chem Lett. 2008;18:4232-6.
462. Augelli-Szafran CE, Wei HX, Lu D, Zhang J, Gu Y, Yang T, et al. Discovery of notch-sparing gamma-secretase inhibitors. Curr Alzheimer Res.7:207-9.
463. Deangelo DJ, Stone RM, Silverman LB, Stock W, Attar EC, Fearen I, et al. A phase I clinical trial of the notch inhibitor MK-0752 in patients with T-cell acute lymphoblastic leukemia/lymphoma (T-ALL) and other leukemias. Journal of Clinical Oncology, 2006 ASCO Annual Meeting Proceedings. 2006;24:6585.
464. Demehri S, Kopan R. Notch signaling in bulge stem cells is not required for selection of hair follicle fate. Development. 2009;136:891-6.
465. Moellering RE, Cornejo M, Davis TN, Del Bianco C, Aster JC, Blacklow SC, et al. Direct inhibition of the NOTCH transcription factor complex. Nature. 2009;462:182-8.
466. Schafmeister CE PJ, Verdine GL. An All-Hydrocarbon Cross-Linking System for Enhancing the Helicity and Metabolic Stability of Peptides. J Am Chem Soc. 2000;122:5891-2.

467. Li K, Li Y, Wu W, Gordon WR, Chang DW, Lu M, et al. Modulation of Notch signaling by antibodies specific for the extracellular negative regulatory region of NOTCH3. J Biol Chem. 2008;283:8046-54.
468. Wu Y, Cain-Hom C, Choy L, Hagenbeek TJ, de Leon GP, Chen Y, et al. Therapeutic antibody targeting of individual Notch receptors. Nature. 2010;464:1052-7.
469. Castanotto D, Rossi JJ. The promises and pitfalls of RNA-interference-based therapeutics. Nature. 2009;457:426-33.
470. Davis ME, Zuckerman JE, Choi CH, Seligson D, Tolcher A, Alabi CA, et al. Evidence of RNAi in humans from systemically administered siRNA via targeted nanoparticles. Nature.464:1067-70.
471. Singh N, Manshian B, Jenkins GJ, Griffiths SM, Williams PM, Maffeis TG, et al. NanoGenotoxicology: the DNA damaging potential of engineered nanomaterials. Biomaterials. 2009;30:3891-914.
472. Ridgway J, Zhang G, Wu Y, Stawicki S, Liang WC, Chanthery Y, et al. Inhibition of Dll4 signalling inhibits tumour growth by deregulating angiogenesis. Nature. 2006;444:1083-7.
473. Noguera-Troise I, Daly C, Papadopoulos NJ, Coetzee S, Boland P, Gale NW, et al. Blockade of Dll4 inhibits tumour growth by promoting non-productive angiogenesis. Nature. 2006;444:1032-7.
474. Yan M, Callahan CA, Beyer JC, Allamneni KP, Zhang G, Ridgway JB, et al. Chronic DLL4 blockade induces vascular neoplasms. Nature. 2010;463:E6-7.
475. Vacca A, Felli MP, Palermo R, Di Mario G, Calce A, Di Giovine M, et al. Notch3 and pre-TCR interaction unveils distinct NF-kappaB pathways in T-cell development and leukemia. Embo J. 2006;25:1000-8.
476. Song LL, Peng Y, Yun J, Rizzo P, Chaturvedi V, Weijzen S, et al. Notch-1 associates with IKKalpha and regulates IKK activity in cervical cancer cells. Oncogene. 2008;27:5833-44.
477. Asano N, Watanabe T, Kitani A, Fuss IJ, Strober W. Notch1 signaling and regulatory T cell function. J Immunol. 2008;180:2796-804.
478. Yeh TS, Lin YM, Hsieh RH, Tseng MJ. Association of transcription factor YY1 with the high molecular weight Notch complex suppresses the transactivation activity of Notch. J Biol Chem. 2003;278:41963-9.
479. Kim SB, Chae GW, Lee J, Park J, Tak H, Chung JH, et al. Activated Notch1 interacts with p53 to inhibit its phosphorylation and transactivation. Cell Death Differ. 2007;14:982-91.
480. Gustafsson MV, Zheng X, Pereira T, Gradin K, Jin S, Lundkvist J, et al. Hypoxia requires notch signaling to maintain the undifferentiated cell state. Dev Cell. 2005;9:617-28.
481. Zheng X, Linke S, Dias JM, Zheng X, Gradin K, Wallis TP, et al. Interaction with factor inhibiting HIF-1 defines an additional mode of cross-coupling between the Notch and hypoxia signaling pathways. Proc Natl Acad Sci U S A. 2008;105:3368-73.
482. Coleman ML, McDonough MA, Hewitson KS, Coles C, Mecinovic J, Edelmann M, et al. Asparaginyl hydroxylation of the Notch ankyrin repeat domain by factor inhibiting hypoxia-inducible factor. J Biol Chem. 2007;282:24027-38.
483. Kim MY, Ann EJ, Kim JY, Mo JS, Park JH, Kim SY, et al. Tip60 histone acetyltransferase acts as a negative regulator of Notch1 signaling by means of acetylation. Mol Cell Biol. 2007;27:6506-19.

484. Yeh TS, Hsieh RH, Shen SC, Wang SH, Tseng MJ, Shih CM, et al. Nuclear betaII-tubulin associates with the activated notch receptor to modulate notch signaling. Cancer Res. 2004;64:8334-40.
485. Jin YH, Kim H, Ki H, Yang I, Yang N, Lee KY, et al. Beta-catenin modulates the level and transcriptional activity of Notch1/NICD through its direct interaction. Biochim Biophys Acta. 2009;1793:290-9.
486. Ross DA, Kadesch T. The notch intracellular domain can function as a coactivator for LEF-1. Mol Cell Biol. 2001;21:7537-44.
487. Gao J, Chen Y, Wu KC, Liu J, Zhao YQ, Pan YL, et al. RUNX3 directly interacts with intracellular domain of Notch1 and suppresses Notch signaling in hepatocellular carcinoma cells. Exp Cell Res.316:149-57.
488. Le Gall M, De Mattei C, Giniger E. Molecular separation of two signaling pathways for the receptor, Notch. Dev Biol. 2008;313:556-67.
489. Giniger E. A role for Abl in Notch signaling. Neuron. 1998;20:667-81.
490. Nal B, Mohr E, Silva MI, Tagett R, Navarro C, Carroll P, et al. Wdr12, a mouse gene encoding a novel WD-Repeat Protein with a notchless-like amino-terminal domain. Genomics. 2002;79:77-86.
491. Fautsch MP, Vrabel AM, Johnson DH. The identification of myocilin-associated proteins in the human trabecular meshwork. Exp Eye Res. 2006;82:1046-52.

Chapter 2*

The cytotoxicity of γ-secretase inhibitor I to breast cancer cells is mediated by proteasome inhibition, not by γ-secretase inhibition

2.1 Introduction

Notch is a family of single-pass type I transmembrane protein receptors that, in mammals, includes four homologs, Notch 1-4 (1). Ligand-induced Notch receptor activation requires at least two cleavages that release the intracellular domain from the cytomembrane and allow it to translocate into the nucleus where it activates its target genes (1). The final cleavage is performed by γ-secretase, whose substrates include all four Notch receptors and their ligands as well as β-amyloid precursor protein, E-cadherin, CD44, ErbB-4, and ephrin-B1 (2-8).

Aberrant Notch signaling can induce oncogenesis and may promote the progression of breast cancer. Transgenic mice overexpressing active Notch1, Notch3, or Notch4 homologs all developed mammary carcinoma (9, 10). Furthermore, a recent clinical study reported that the expression level of Notch1, Notch3, and JAG-1, one of the Notch ligands, were inversely correlated with the overall clinical outcomes in breast cancer patients (11). These observations have prompted great interest in targeting Notch signaling in breast cancer for therapeutic benefit. However, it should be noted that Notch2 signaling has been reported to function as a tumor suppressor in breast cancer cells (12).

Amongst the several options to block Notch signaling, inhibition of γ-secretase by small molecules offers a promising approach and has been used extensively to study the downstream targets of Notch signaling pathway (13, 14). However, experimental data supporting the concept that γ-secretase inhibitors (GSIs) could

---

* A version of this chapter has been published. Breast Cancer Res. 2009; 11(4): R57

inhibit the growth of, or kill, breast cancer cells have been scarce. Two recent reports have provided the strongest evidence by showing that Z-LLNle-CHO, commonly considered as a GSI, has such an effect both *in vitro* and *in vivo* (15, 16).

Proteasome inhibitors are a class of recently developed anticancer drugs. Z-LLNle-CHO, as a derivative of a widely used proteasome inhibitor MG-132, has been reported to inhibit chymotryptic protease activity, a core function of the proteasome (17). In this study, we compared the activity and cytotoxic effects of Z-LLNle-CHO to those of two other widely used and highly specific GSIs, DAPT and L-685,458, and to those of three structurally unrelated proteasome inhibitors, MG132, lactacystin, and Bortezomib. Our results suggest that the cell killing effect of Z-LLNle-CHO is not mediated by γ-secretase inhibition, but mediated by proteasome inhibition.

2.2 Materials and Methods

2.2.1 Reagents

Z-Leu-Leu-Nle-CHO (Z-LLNle-CHO, also called GSI I), N-[N-(3,5-Difluorophenacetyl-L-alanyl)]-S-phenylglycine *t*-Butyl Ester (commonly called DAPT or GSI IX), {1S-Benzyl-4R-[1-(1S-carbamoyl-2-phenethylcarbamoyl)-1S-3-methylbutylcarbamoyl]-2R-hydroxy-5-phenylpentyl}carbamic acid *tert*-butyl ester (commonly called L-685,458 or GSI X), Z-Leu-Leu-Leu-aldehyde (Z-LLL-CHO, commonly referred as MG132), lactacystin, and edaravone were purchased from Calbiochem and dissolved in DMSO. Bortezomib was purchased from LC Laboratories and dissolved in DMSO. Tiron was from Sigma and dissolved in water.

2.2.2 Cell culture

Three estrogen receptor (ER) positive cell lines, MCF-7, T47D, and BT474, and three ER negative cell lines, SKBR3, MDA-MB-231, and MDA-MB-468 were used in this study. Both SKBR3 and BT474 cells also overexpress HER2/neu. The culture medium was DMEM/F-12 medium (Gibco) supplemented with 10% fetal bovine serum (FBS) (Gibco) and GlutaMAX (Gibco) for all cell lines except

for SKBR3, which was cultured in McCoy's 5A medium (Gibco) supplemented with 10% FBS and GlutaMAX. In addition, MCF-7 culture medium was supplemented with non-essential amino acids (Gibco), sodium pyruvate (Gibco), and 10 μg/ml of insulin (Sigma). T47D culture medium was also supplemented with insulin (10 μg/ml). All cell lines were maintained at 37^{o}C in a humidified atmosphere of 5% CO_2 in air.

2.2.3 Cell viability and proliferation assay

Cell viability and proliferation was measured using the CellTiter 96® AQ_{ueous} One Solution Cell Proliferation Assay (MTS) kit (Promega). Cells (3000 – 8000/well) were seeded into 96-well plates in triplicate and allowed to attach overnight before being treated with increasing concentrations of drugs. All wells, including the control, were exposed to the same concentration of DMSO to eliminate any possible effect of the vehicle on cell viability and proliferation. MTS reagent (20 μl) was added to each well 72 h later and, after 1- 4 h incubation, the absorbance at 490 nm was measured using a microplate reader (FLUOstar OPTIMA from BMG LABTECH). Relative cell viability and proliferation of individual samples was calculated by normalizing their absorbance to that of the corresponding control sample. The mean and standard deviation (SD) of three independent experiments were used to plot dose-response curves. The concentrations that kill and/or inhibit cell growth by 50% (EC_{50}) were calculated from the equations that best fit the linear range of the dose-response curves.

2.2.4 Protein sample preparation

Cells at 80% confluence were treated overnight with drugs at the indicated concentrations and control cultures received DMSO. The next day, cells were incubated with trypsin/EDTA (Gibco) solution for 10 min before collection by centrifugation. Cell pellets were then washed once with ice-cold PBS, lysed in lysis buffer [100 mM Tris-HCl (pH 6.8), 10% glycerol, 2% SDS, 1 mM EDTA, 0.002% bromophenol blue, 2 mM NaF, 1 mM Na_3VO_4, 1 X protease inhibitor cocktail (Roche Applied Science)], boiled for 5 min, and passed through a 21 gauge needle. The positive control samples were prepared in the same way as the GSI-treated samples and the negative control samples were prepared by

adding the lysis buffer directly to the culture plates after washing with PBS without trypsin/EDTA incubation. Protein concentrations were quantified using a BCA protein assay (Pierce).

2.2.5 Western blot analysis

Protein samples (50 μg/lane) were separated in 8% SDS-PAGE gels and transferred to Trans-Blot® pure nitrocellulose membranes (0.2 μm, Bio-Rad). The membranes were blocked with 5% skim milk in TTBS [0.1% Tween-20, 100 mM Tris-HCl (pH 7.4), 150 mM NaCl] at room temperature for 1 h before being probed overnight at 4°C with primary antibody solution. The primary antibodies used were anti-Notch1 (Val1744) (Cell Signaling Technology, 1:1,000), anti-ubiquitin (clone FK2 from Millipore, 1:1,000) and anti-actin (Abcam, 1:5,000). After washing with TTBS for 4 X 10 minutes, the membranes were incubated with HRP-conjugated anti-rabbit or anti-mouse (Jackson ImmunoResearch Laboratories, 1:15,000) secondary antibody solution at 4°C for 3 h. After another round of four washes with TTBS, the membranes were incubated with SuperSignal West Pico Chemiluminescent Substrate (Pierce), exposed to Fuji film, and then developed to visualize the protein signal.

2.2.6 Construction of Flag-tagged Notch1 extracellular truncation (N1EXT) vector

Synthetic DNA oligos corresponding to the cDNA encoding human Notch1 signal peptide flanked by restriction enzyme recognition sequences were integrated into pCMV-Tag4A vector (Stratagene) using Sac II/BamH I sites. Then the cDNA encoding the amino acid residues 1721-2555 (corresponding to the substrate of γ-secretase) was amplified using reverse transcription-coupled PCR of MCF-7 total cellular RNA and integrated into the vector containing the Notch1 signal peptide-encoding sequence using BamH I/EcoR I sites. The sequence of the new construct was verified by sequencing using T3/T7 primers.

2.2.7 Transfection and treatment

N1EXT plasmid DNA was transfected into MCF-7 and SKBR3 cells plated on glass coverslips using Lipofectamine 2000 reagent (Invitrogen). Culture medium

was replaced 6 h after transfection with fresh medium containing 5 μM of DAPT, 2 μM of L-685,458, or Z-LLNle-CHO at the calculated EC_{50} values of individual cell lines. After overnight incubation to allow the expression of exogenous protein, cells were fixed with 4% paraformaldehyde solution for indirect immunofluorescent microscopy.

2.2.8 Indirect immunofluorescent microscopy

Fixed cells were first permeabilized with 0.5% Triton X-100 in PBS at room temperature for 5 min and then probed with anti-Flag monoclonal antibody (clone M2 from Sigma, 1:500) at room temperature for 1 h. After five washes with PBS, cells were incubated with Alexa 488-conjugated goat anti-mouse secondary antibody (Molecular Probes, 1:250) at room temperature for 45 minutes and further counterstained with 0.5 μg/ml of DAPI after five washes with PBS. Images were taken using LSM 510 laser scanning confocal microscope with a Plan-Neofluar 40X/1.3NA oil-immersed objective lane (Carl Zeiss). The optical slice thickness was less than 0.9 μm.

2.2.9 Determination of ubiquitin distribution

MCF-7 and MDA-MB-231 cells plated on glass coverslips were treated with drugs at the indicated concentrations for 4 h before being fixed in 4% paraformaldehyde solution. Fixed cells were immunostained in the same way as above except that anti-ubiquitin monoclonal antibody (clone FK2 from Millipore, 1:1,000) was used as the primary antibody. Images were taken using LSM 710 laser scanning confocal microscope with a Plan-Apochromat 20X/0.8NA objective lens (Carl Zeiss). The optical slice thickness was 1.8 μm.

2.2.10 Proteasome activity assay

Proteasome activity was measured using the Proteasome-Glo™ Chymotrypsin-Like Cell-Based Assay kit (Promega). Briefly, MCF-7 (6000 cells/well) and MDA-MB-231 (10^4 cells/well) cells were plated into white-walled 96-well plates. After overnight incubation to allow cell attachment, cells were treated with drugs at indicated concentrations for 2 h. Equal volumes of Proteasome-Glo™ reagent

were then added and the luminescence signal was measured using a microplate reader (FLUOstar OPTIMA).

2.3 Results

2.3.1 Among the three GSIs, only Z-LLNle-CHO induces cell death

We first compared the cytotoxicity of Z-LLNle-CHO to two other widely used GSIs, DAPT and L-685,458. Treatment with Z-LLNle-CHO resulted in a dose-dependent decrease in cell viability/proliferation of all six breast cancer cell lines tested with ER negative cell lines being more sensitive than ER positive cell lines. The calculated ED_{50} values were 3.25 μM, 2.5 μM, 2.4 μM, 1.8 μM, 1.6 μM and 1.4 μM for MCF-7, BT474, T47D, MDA-MB-231, SKBR3, and MDA-MB-468 respectively. However, DAPT and L-685,458 had no cell killing and/or growth inhibitory effects at concentrations up to 5 μM and 2 μM respectively (Figure 2-1).

2.3.2 All three GSIs inhibit γ-secretase activity

We then examined whether the lack of cell killing/growth inhibition by DAPT and L-685,458 was due to their lower potency in inhibiting γ-secretase activity. To address this question, we first performed immunoblot analysis using an antibody that only recognizes cleaved Notch1 intracellular domain (N1ICD) (18, 19). Since N1ICD is a product of γ-secretase, its abundance is a good indicator of γ-secretase activity. However, the endogenous N1ICD level (the negative control lanes in Figure 2-2a) is too low to be detected confidently. Therefore, we took advantage of the fact that calcium depletion activates Notch1 in the absence of ligand binding (20). As shown in Figure 2-2a, DAPT at 5 μM and L-685,458 at 2 μM could block calcium depletion-induced Notch1 cleavage in all six cell lines. At the same time, Z-LLNle-CHO, at the concentrations that inhibited cell growth/viability by 50%, failed to do so to a comparable level in SKBR3 and MDA-MB-468 cells although similar inhibition was observed in the other four cell lines treated with this drug.

To confirm the potency of DAPT and L-685,458 on inhibiting γ-secretase activity in intact cells, we transfected MCF-7 and SKBR3 cells with a plasmid expressing a Flag-tagged N1EXT fragment that mimics the immediate substrate of γ-

secretase and then treated them with the same concentrations of GSIs as used for the Western blot analysis. Without any intervention, the exogenous protein will be cleaved by γ-secretase as long as it is transported to the plasma membrane in order to produce N1ICD that can be visualized as nuclear signal when transfected cells are immunostained with an anti-Flag antibody (control panels in Figure 2-2b). In contrast, when γ-secretase activity is inhibited, the exogenous protein cannot be cleaved and therefore will accumulate at plasma membrane. As shown in Figure 2-2b, all the DAPT- and L-685,458-treated cells and Z-LLNle-CHO-treated MCF-7 cells showed exclusively membrane signal. However, 24% and 58% of Z-LLNle-CHO-treated SKBR3 displayed mainly nuclear signal or a mixture of nuclear and plasma membrane signal respectively. This is consistent with the immunoblotting data demonstrating that DAPT and L-685,458 could completely inhibit γ-secretase activity at tested concentrations in both cell lines but Z-LLNle-CHO could only do so in MCF-7 cells (Figure 2-2c).

Taken together, since complete inhibition of γ-secretase activity by two structurally unrelated GSIs had no effect on cell viability and proliferation, it is unlikely that the cell killing/growth inhibitory effect of Z-LLNle-CHO on breast cancer cell lines was mediated by γ-secretase inhibition.

2.3.3 Z-LLNle-CHO has proteasome inhibitory activity

Z-LLNle-CHO is derived from a widely used proteasome inhibitor MG132 (Z-LLL-CHO) and has been reported to be a broad chymotryptic and aspartyl protease inhibitor (17). Therefore, we examined whether Z-LLNle-CHO also has proteasome inhibitor activity at the concentrations that showed dose-dependent cytotoxicity. We first used a cell-based proteasome activity kit to measure proteasome activity after cells were treated with MG132, Z-LLNle-CHO, or DAPT. As shown in Figure 2-3a, both Z-LLNle-CHO and MG132 showed a dose-dependent inhibition of the proteasome at concentrations that showed cytotoxic effects while DAPT did not. Next, we examined whether or not inhibition of proteasome activity caused accumulation of polyubiquitinated protein, one of the major causes of proteasome inhibitor-induced cell death (21), by subjecting the protein samples from cells treated with 5 (MCF-7) or 2.5 (MDA-MB-231) μM of Z-LLNle-CHO overnight to immunoblotting with an anti-ubiquitin antibody. We used

Bortezomib, a specific proteasome inhibitor that has been approved to treat multiple myeloma in patients, as positive control. The results showed that treatment with Z-LLNle-CHO indeed resulted in similar accumulation of polyubiquitinated protein that was observed with Bortezomib (lane 2 and 5 of Figure 2-3b). Finally, we took advantage of a recent observation that when proteasome-mediated protein degradation was inhibited, cellular ubiquitin would undergo a nuclear-to-cytoplasmic redistribution that could be detected by anti-ubiquitin FK2 antibody (22). In untreated MCF-7 and MDA-MB-231 cells, FK2 staining showed dominant nuclear signal (Figure 2-3c). After a 4 h treatment with either Bortezomib or Z-LLNle-CHO but not with DAPT, cells displayed a strong cytoplasmic ubiquitin signal, confirming proteasome activity was inhibited by Z-LLNle-CHO.

2.3.4 The cellular sensitivity of six breast cancer cell lines to Z-LLNle-CHO is the same as that to proteasome inhibitors

We next asked whether or not the cell killing effect of Z-LLNle-CHO is mediated by its proteasome inhibition activity. If this is the case, the relative cellular sensitivity of different breast cancer cell lines to Z-LLNle-CHO should reflect that produced by other proteasome inhibitors. Therefore, we treated the same six breast cancer cell lines with increasing doses of three structurally unrelated proteasome inhibitors, MG132, lactacystin, and Bortezomib, and measured the effects on cell viability/proliferation using the MTS assay. Similar to the results shown in Figure 2-1, ER positive cell lines were more resistant to all the three proteasome inhibitors than ER negative cell lines (Figure 2-4). In addition, our results were also consistent with a previous study using Bortezomib alone (23). These data strongly suggest that the cell killing effects of Z-LLNle-CHO in breast cancer cells is mediated by its proteasome inhibitory function.

2.3.5 The cytotoxicity of Z-LLNle-CHO can be reversed by restoration of proteasome activity

Recent studies showed that the proteasome inhibitory activity as well as the cell killing effects of Bortezomib and MG132 could be specifically blocked by tiron and edaravone respectively (24, 25). Since Z-LLNle-CHO is structurally similar to

MG132, we speculated that edaravone might also be able to reverse the cytotoxicity of Z-LLNle-CHO by blocking its proteasome inhibition activity. Therefore, we first treated MCF-7 and MDA-MB-231 cells with different combinations of Bortezomib/Z-LLNle-CHO with tiron/edaravone and measured the cell growth using MTS assay. Consistent with previous studies, tiron but not edaravone rescued cells from Bortezomib-induced cell killing. Most importantly, we found edaravone but not tiron could rescue cells from Z-LLNle-CHO-induced cell killing (Figure 2-5a).

Next, we tested whether or not edaravone could rescue proteasome activity from Z-LLNle-CHO-induced inhibition. We exposed cells to edaravone at the concentration that showed best cell growth rescue in the presence of Z-LLNle-CHO and measured proteasome activity using the three approaches we used above. We used tiron to reverse Bortezomib-induced proteasome inhibition as control. We found that edaravone indeed rescued the proteasome activity from Z-LLNle-CHO-, but not Bortezomib-induced inhibition. Although the proteasome activity of edaravone rescued from Z-LLNle-CHO-induced inhibition was not to the same extent as tiron rescued Bortezomib-induced inhibition in the cell based proteasome assay (Figure 2-5b), the rescued proteasome activity was enough to prevent the accumulation of polyubiquitinated proteins (lane 4 compared to lane 2 in Figure 2-3b) and redistribution of cellular ubiquitin (Figure 2-3c, treatment 4 *vs*. treatment 2). In addition, we found edaravone also partially restored γ-secretase activity from Z-LLNle-CHO-induced inhibition (Figure 2-5c).

2.3.6 γ-secretase inhibition activity of Z-LLNle-CHO does not contribute to its cytotoxicity to breast cancer cells

To investigate whether the cytotoxicity of Z-LLNle-CHO to breast cancer cells is due to the summation or synergy of its dual activities, we tested whether combination of a specific γ-secretase inhibitor with a specific proteasome inhibitor could produce additive or synergetic effect on cell killing. We subjected cells to increasing concentrations of lactacystin with or without 5 μM of DAPT that completely inhibited γ-secretase activity in the cell lines tested. We found the dose-response curves of individual cell lines treated with or without DAPT was

almost identical (Figure 2-6), which suggests there was no additive or synergetic effects of inhibiting both γ-secretase activity and proteasome activity. Therefore, γ-secretase inhibitory activity of Z-LLNle-CHO most likely does not contribute to its cell killing effect in breast cancer cells.

2.4 Discussion

Blocking Notch signaling by inhibiting γ-secretase activity with small molecules has been suggested to be a promising approach to battle breast cancer (13, 14). In fact, there are three ongoing clinical trials registered in ClinicalTrials.gov using GSI in the treatment of breast cancer. However, experimental data supporting the effectiveness of GSIs in the inhibition of cell growth or killing of breast cancer cells have been scarce. Two recent reports, however, have now shown that Z-LLNle-CHO, commonly called GSI I, has such an effect both *in vitro* and *in vivo* (15, 16).

In the present study, we first compared the cytotoxicity and activity of Z-LLNle-CHO to two other popularly used GSIs, DAPT and L-685,458. We found that completely inhibiting γ-secretase activity by DAPT and L-685,458 had no effect on cell viability and proliferation of a panel of six breast cancer cell lines with different genetic backgrounds. In contrast, Z-LLNle-CHO could cause cell death even at concentrations that did not completely inhibit γ-secretase activity. Therefore, we conclude that the cell killing effect of Z-LLNle-CHO on breast cancer cells is not mediated by γ-secretase inhibition.

We next measured the proteasome inhibition potential of Z-LLNle-CHO. In contrast to two previous reports that Z-LLNle-CHO at concentrations that inhibited cell growth did not significantly inhibit proteasome activity (see supplemental materials in (15, 26)), we found that it could inhibit proteasome activity by about 50% in intact cells even at a concentration that did not show significant cytotoxicity in two cell lines tested. Our result is consistent with a recent study that was published during the revision of this manuscript (27). The new study showed that Z-LLNle-CHO at ~ 0.3 μM (calculated by us based on scale) inhibited proteasome activity by 80% and slowed cell growth by 20% in

MCF-7 cells. Since the approach the new study used to measure proteasome activity is different from ours, the extent of proteasome activity inhibition cannot be compared between their data and ours. However, both studies show that Z-LLNle-CHO could significantly inhibit proteasome activity at concentrations that showed dose-dependent cytotoxicity. The previous two studies used the same method to measure proteasome activity as the latest study but differed from ours. Therefore, it is easy to explain the discrepancy between their data and ours but we cannot explain the discrepancy between their data and the latest study.

Furthermore, we found that the relative cellular sensitivity of six breast cancer cell lines to Z-LLNle-CHO was the same as that to three widely used but structurally unrelated proteasome inhibitors and was also consistent with a previous study (23). This consistency strongly suggests that the cell killing effect of Z-LLNle-CHO is due to its proteasome inhibitory function. Most convincingly, we found that the cytotoxic effect of Z-LLNle-CHO could be reversed by a specific chemical—edaravone—that blocked its proteasome inhibitory activity. Finally, we tested but did not find any additive effect of the combination of a specific γ-secretase inhibitor and a specific proteasome inhibitor on breast cancer cell growth. Therefore, we conclude that the cytotoxicity of Z-LLNle-CHO to breast cancer cells is mediated by proteasome inhibition.

We noticed that edaravone treatment also partially rescued γ-secretase activity from Z-LLNle-CHO induced inhibition. However, since inhibition of γ-secretase alone or in combination with proteasome inhibition had no effect on cell survival/proliferation or cellular response to proteasome inhibition, we do not consider partially restored γ-secretase activity as a major contributor to the reversion of the cytotoxicity induced by Z-LLNle-CHO. Likewise, although edaravone has been reported to protect cells from apoptosis through acting as an antioxidant (28, 29), we do not think its free radical scavenging activity to be a major contributor as it had no effect on Bortezomib-induced cytotoxicity. In addition, another antioxidant—tiron—had no effect on on Z-LLNle-CHO-induced cytotoxicity. Therefore, the ability of edaravone to restore proteasome activity through unknown mechanism(s) most likely accounts for the reversion of Z-LLNle-CHO's cytotoxicity upon edaravone treatment.

The MTS assay we employed in this study to measure cell viability and proliferation is based on the reduction of a colorless tetrazolium compound to a formazan product that has a maximal absorbance at 490 nm. Since the level of intracellular reactive oxygen species has been reported to affect the MTS reading (30, 31), inclusion of antioxidants in the culture medium might affect the apparent viability. However, treatment with either tiron or edaravone alone at tested concentrations did not significantly affect cell viability and proliferation as assayed by the MTS reagent (data not shown). In addition, the cytotoxicity of individual treatment regimens as measured by the MTS assay is consistent with the changes in the cell number and morphology as observed by light microscopy before adding the MTS reagent to culture medium. Therefore, the cell viability and proliferation data reflects the real cytotoxicity of individual treatment regimens.

Both previous studies used transient transfection of N1ICD to rescue the cell death induced by Z-LLNle-CHO treatment and argued that the reversion of the phenotype by N1ICD transfection indicated that Z-LLNle-CHO induced cell death through inhibiting Notch signaling pathway (15, 16). However, transient overexpression of N1ICD has been reported to inhibit wild-type p53-induced apoptosis in immortalized epidermal cells (32), to inhibit dexamethasone, etoposide, or Fas-ligand induced apotosis in mature T-cells (33), and to protect H460 (lung cancer), HepG2 (liver cancer), HT1080 (fibrosarcoma) from several chemotherapy drugs (34). Therefore, an alternative interpretation of the data from the two previous studies is that N1ICD over-expression provided pro-survival signals that antagonize Z-LLNle-CHO's pro-apoptotic effects.

It is worth noting that many of the effects of Z-LLNle-CHO reported in previous studies, including G2/M arrest and regulation of apoptosis-related protein, are consistent with the reported effects of other proteasome inhibitors (35-39). In addition, similar to the additive effects of 4-OH-TAM and Z-LLNle on the inhibition of T47D:A18 cells growth (15), additive or even synergistic effects have also been reported between tamoxifen and Bortezomib in some but not all ER+ breast cancer cell lines tested (40, 41). Although the similarities between the biological effects of Z-LLNle-CHO and those of other proteasome inhibitors do not

necessarily mean that they function the same, our finding that Z-LLNle-CHO inhibits breast cancer cell growth as a proteasome inhibitor can explain the data produced with the use of Z-LLNle-CHO in previous studies.

It should be pointed out that although the latest study found that Z-LLNle-CHO has proteasome inhibitory function at concentrations that showed dose-dependent cytotoxicity (27), the authors did not consider its proteasome inhibitory activity as the major contributor to its cell killing effects because the cytotoxicity of Z-LLNle-CHO and MG132 was “markedly different”, although their proteasome inhibition potential was similar. However, by careful analysis of their data, we found that the proteasome inhibition potentials of Z-LLNle-CHO and MG132 differed by more than 2-fold, not less than the difference in cytotoxicity, within the range of concentrations that Z-LLNle-CHO and MG132 showed “markedly different” cytotoxicity (below 0.6 μM). Most importantly, Z-LLNle-CHO at 0.75 μM in their study slowed MCF-7 cell growth by 80%, but only inhibited γ-secretase activity by 25%. Meanwhile, it inhibited proteasome activity by 80%. Therefore, their data is more consistent with our conclusion that the cytotoxicity of Z-LLNle-CHO was not due to γ-secretase inhibition, but due to proteasome inhibition.

The observation that both Z-LLNle-CHO and MG132 at given concentrations inhibited proteasome activities to comparable levels in MCF-7 and MDA-MB-231 cells, but showed different cytotoxicity, is not surprising as this has also been observed for Bortezomib (23). The reduced sensitivity of ER positive MCF-7 cells may be a consequence of pro-survival signal provided by estrogen receptor signaling pathway in these ER+ breast cancer cells. This hypothesis is consistent with the observed additive or even synergistic effect between tamoxifen and Z-LLNle-CHO or Bortezomib. However, this requires further investigation. Regardless of the mechanisms, our results, together with the previous reports, suggest that the future clinical trials testing the effectiveness of proteasome inhibitors in treating breast cancer should take the ER status into consideration when enrolling patients.

The observation that two specific GSIs, DAPT and L-685,458, had no effect on the survival and proliferation of breast cancer cells does not eliminate the

potential use of GSIs or other approaches to block Notch signaling for breast cancer treatment. The results presented here were obtained from *in vitro* cell culture experiments. The effects of GSIs on the tumors grown *in vivo*, where the Notch signaling might be more active due to enhanced ligand-receptor interaction, could be different and need further investigation. Alternatively, these drugs might block the signaling pathway of some as yet unidentified substrate(s) which antagonizes the effect of reduced Notch1 signaling on breast cancer cell survival and proliferation. There are at least a dozen known γ-secretase substrates and most of the available GSIs have no preference for specific substrates. Rather than laboriously testing all potential candidates that antagonize Notch1, it might be better to develop substrate-specific GSIs. To this end, it is encouraging to note that compounds that can preferentially modulate γ-secretase activity against Aβ42 over Notch have recently been reported (42). These compounds target the substrate (Aβ42) rather than γ-secretase active site itself. In principle, it should also be possible to find drugs that target individual Notch homologs. Alternatively, it might be useful to develop neutralizing antibody against individual Notch homologs just as the Trastuzumab targets HER2/neu.

Furthermore, the results of this study do not diminish the potential use of Z-LLNle-CHO for breast cancer treatment. In fact, we believe that clarifying its role as a proteasome and γ-secretase dual inhibitor will help to direct its potential development for clinical use. However, we do caution that results obtained using Z-LLNle-CHO as the sole GSI to study the biological outcomes of blocking Notch signaling (43-45) should be interpreted cautiously or reproduced using more specific GSIs.

2.5 Conclusions

The present study demonstrated that the cytotoxicity of Z-LLNle-CHO toward breast cancer cells was not mediated by γ-secretase inhibition as reported previously, but by proteasome inhibition. This clarification might help its potential development as a chemotherapeutic agent. The results presented also call for careful interpretation of data produced with using Z-LLNle-CHO as the sole γ-secretase inhibitor.

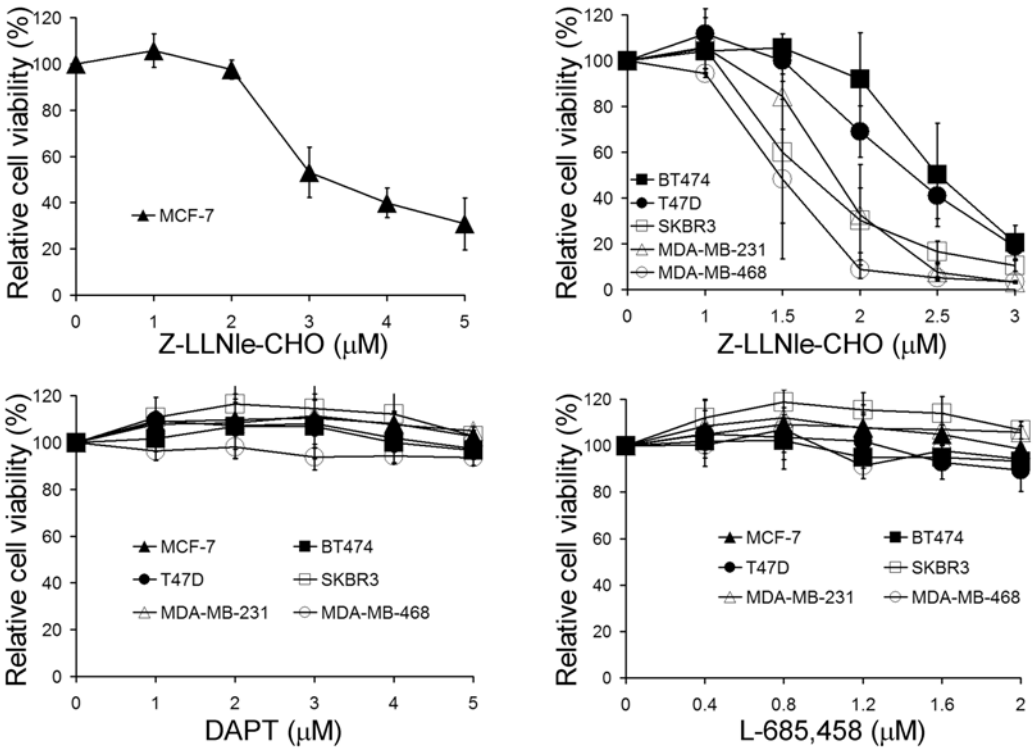

Figure 2-1. Effect of three different GSIs on the viability/proliferation of six breast cancer cell lines. Breast cancer cells were treated with Z-LLNle-CHO, DAPT or L-685,458 for 72 h before relative cell viability/proliferation was measured by MTS assay. Results represent the mean ± SD of three independent experiments.

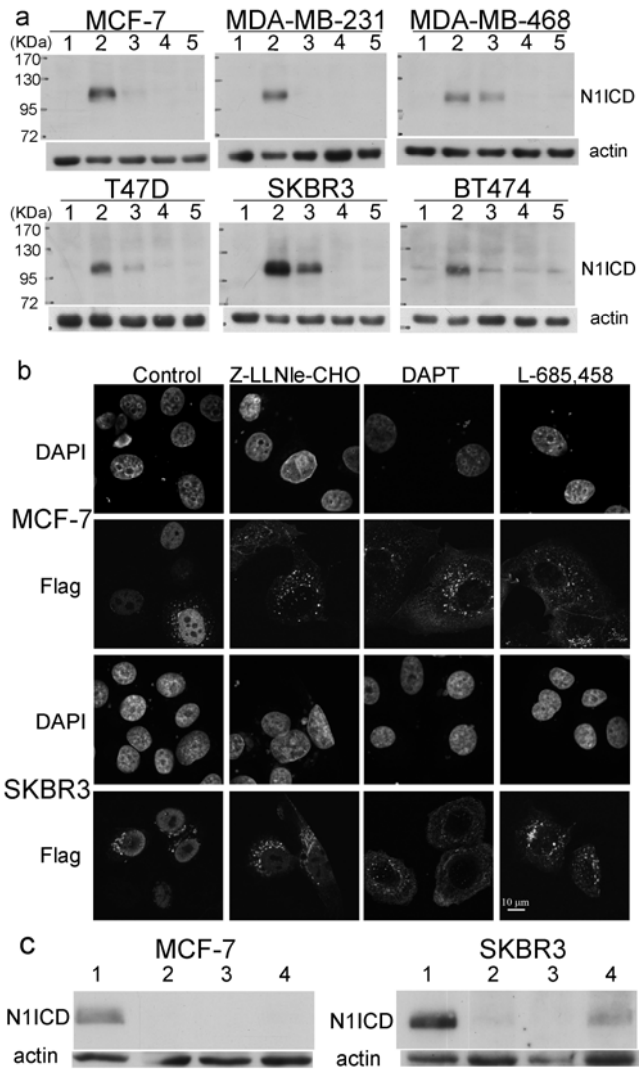

Figure 2-2. DAPT and L-685,458 inhibit γ-secretase activity. (a) Cells were treated overnight with Z-LLNle-CHO at calculated ED_{50} values, 5 μM of DAPT or 2 μM of L-685,458 before protein samples were prepared. Extracellular calcium was depleted by incubation with 0.53 mM of EDTA for 10 min to activate Notch1 before sample preparation for all samples except the negative controls. Protein samples were then subjected to Western blot analysis with an antibody (V1744) that specifically recognizes active Notch1 intracellular domain (product of γ-secretase-mediated cleavage). Stronger V1744 signal intensity indicates greater γ-secretase activity. The treatment conditions were (from lane 1 to lane 5): 1) DMSO vehicle only and without calcium depletion as negative control; 2) DMSO vehicle only and with calcium depletion to activate Notch1 as positive control; 3) Z-LLNle-CHO at concentrations equal to the IC_{50} of individual cell lines; 4) DAPT at 5 μM; 5) L-685,458 at 2 μM. (b) MCF-7 (top panels) and SKBR3 (bottom panels) cells were transfected with plasmid DNA expressing a Flag-tagged protein that mimics the immediate substrate of γ-secretase, treated overnight with Z-LLNle-CHO at calculated ED_{50} values, 5 μM of DAPT or 2 μM of L-685,458, and then immunostained with anti-Flag antibody. The appearance of nuclear Flag signal indicates the presence of active γ-secretase. Please note the

γ-value of Flag signal was enhanced to visualize weak nuclear or cytomembrane signal. (c) Protein samples were prepared without calcium depletion from MCF-7 and SKBR3 cells that were transfected and treated in the same way as the cells in panel b and were subjected to immunoblotting with anti-Notch1 (V1744) antibody. The treatment conditions were (from lane 1 to lane 4): DMSO vehicle only; DAPT; L-685,458; and Z-LLNle-CHO.

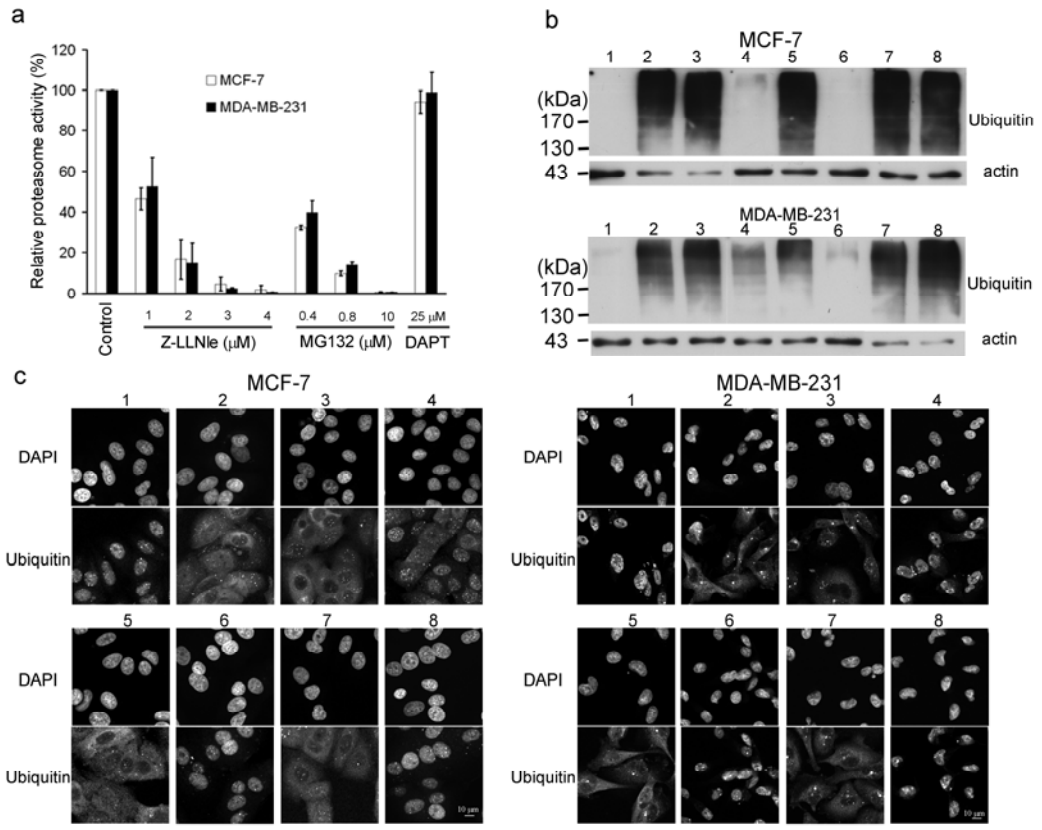

Figure 2-3. Z-LLNle-CHO has a proteasome inhibitory function. (a) Proteasome activity in intact cells was directly measured using a cell-based assay after MCF-7 and MDA-MB-231 cells were treated with indicated drugs for 2 h. Results represent the mean ± SD of three independent experiments. (b) Protein samples were prepared from MCF-7 and MDA-MB-231 cells that were treated with different combinations of drugs overnight and were subject to immunoblotting with anti-ubiquitin antibody (clone FK2 from Millipore, 1:1,000). Actin immunoblotting was used as loading control. The treatment conditions were (from lane 1 to lane 8): 1) DMSO vehicle only; 2) Z-LLNle-CHO alone; 3) Z-LLNle-CHO plus tiron; 4) Z-LLNle-CHO plus edaravone; 5) Bortezomib alone; 6) Bortezomib plus tiron; 7) Bortezomib plus edaravone; 8) lactacystin. The concentrations of Z-LLNle-CHO, tiron, edavarone, Bortezomib, and lactacystin are 5 μM, 2 mM, 100 μM, 100 nM, 20 μM for MCF-7 cells, and 2.5 μM, 0.5 mM, 100 μM, 40 nM, 5 μM for MDA-MB-231 cells respectively. The accumulation of polyubiquitinated proteins is an indicator of proteasome inhibition. (c) MCF-7 and MDA-MB-231 cells were treated with different combinations of drugs for 4 h and then immunostained with anti-ubiquitin FK2 antibody. The treatment conditions

were (from 1 to 8): 1) DMSO vehicle only; 2) Z-LLNle-CHO alone; 3) Z-LLNle-CHO plus tiron; 4) Z-LLNle-CHO plus edaravone; 5) Bortezomib alone; 6) Bortezomib plus tiron; 7) Bortezomib plus edaravone; 8) DAPT. The concentrations of Z-LLNle-CHO, tiron, edaravone, and Bortezomib were the same as that were used for preparation of protein samples in subsection b. 5 μM of DAPT was used for both MCF-7 and MDA-MB-231 cells. The redistribution of nuclear ubiquitin to cytoplasm is a phenomenon that can be induced by proteasome inhibition.

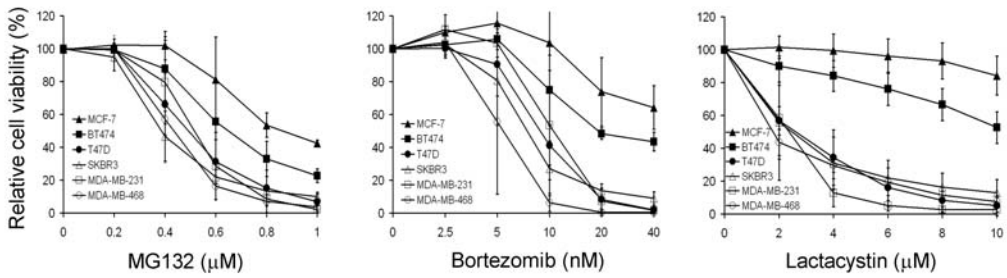

Figure 2-4. The relative sensitivity of six cell lines to three proteasome inhibitors is the same as that to Z-LLNle-CHO. Cells were treated with MG132, Bortezomib, or lactacystin at indicated concentrations for 72 h before cell viability was measured by MTS assay. Results represent the mean ± SD of three independent experiments. Please note the relative cellular sensitivity of the same six breast cancer cell lines to three structurally unrelated proteasome inhibitors was the same as that to Z-LLNle-CHO in Figure 2-1.

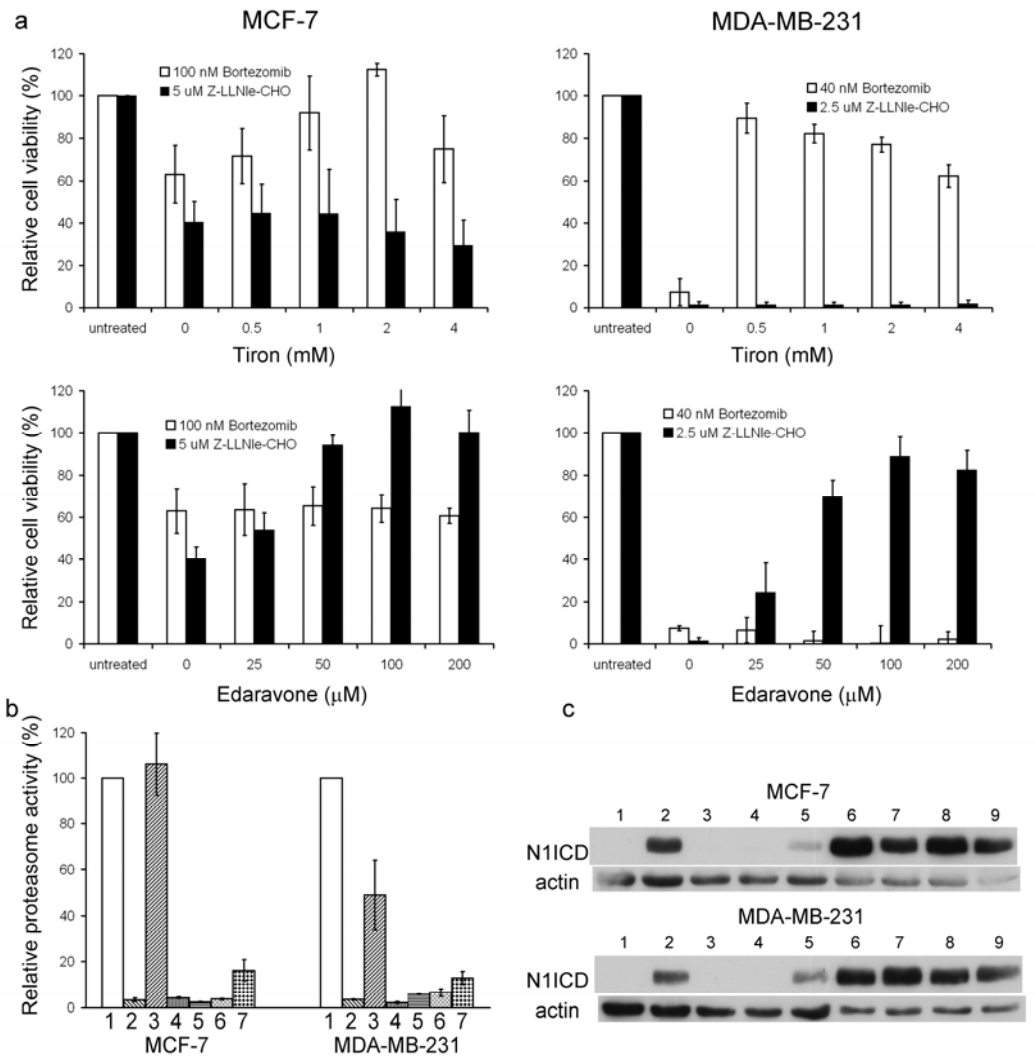

Figure 2-5. The cytotoxicity effect of Z-LLNle-CHO could be reversed by edaravone that blocks its proteasome inhibitory function. (a) Cells were treated with indicated drugs for 72 h before cell growth was measured using MTS assay. Results represent the mean ± SD of three independent experiments. (b) Proteasome activity in intact cells was directly measured using a cell-based assay after cells were treated with different combinations of drugs for 2 h. The treatment conditions were (from left to right): 1) DMSO vehicle only; 2) Bortezomib alone; 3) Bortezomib plus tiron; 4) Bortezomib plus edaravone; 5) Z-LLNle-CHO alone; 6) Z-LLNle-CHO plus tiron; and 7) Z-LLNle-CHO plus edaravone. The concentrations of Bortezomib, tiron, edavarone, and Z-LLNle-CHO are 100 nM, 2 mM, 100 μM, and 5 μM for MCF-7 cells, and 40 nM, 0.5 mM, 100 μM, and 2.5 μM for MDA-MB-231 cells respectively. Results represent the

mean ± SD of three independent experiments. (c) The same protein samples used for immunoblotting in Figure 2-3b plus another negative control sample were subjected to immunoblotting with anti-Notch1 (V1744) antibody that specifically recognizes active Notch1 intracellular domain. The treatment conditions were (from lane 1 to lane 9): 1) Negative control; 2) DMSO vehicle only; 3) Z-LLNle-CHO alone; 4) Z-LLNle-CHO plus tiron; 5) Z-LLNle-CHO plus edaravone; 6) Bortezomib alone; 7) Bortezomib plus tiron; 8) Bortezomib plus edaravone; 9) lactacystin.

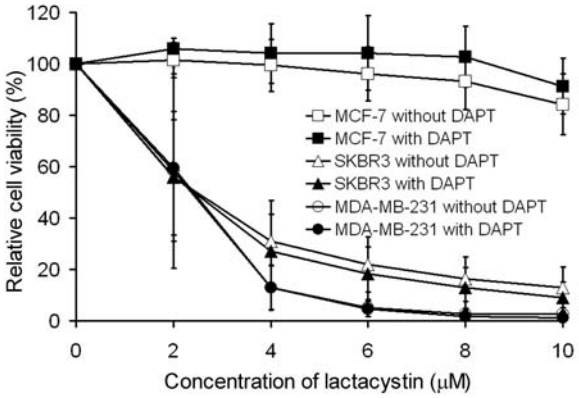

Figure 2-6. No additive effect from the combination of γ-secretase inhibition and proteasome inhibiton. Cells were exposed to increasing concentrations of lactacystin with or without 5 μM of DAPT for 72 h and cell growth was measured by MTS assay. Results represent the mean ± SD of three independent experiments.

References:

1. Callahan, R. and Raafat, A. Notch signaling in mammary gland tumorigenesis. J Mammary Gland Biol Neoplasia, *6:* 23-36, 2001.
2. LaVoie, M. J. and Selkoe, D. J. The Notch ligands, Jagged and Delta, are sequentially processed by alpha-secretase and presenilin/gamma-secretase and release signaling fragments. J Biol Chem, *278:* 34427-34437, 2003.
3. Murakami, D., Okamoto, I., Nagano, O., Kawano, Y., Tomita, T., Iwatsubo, T., De Strooper, B., Yumoto, E., and Saya, H. Presenilin-dependent gamma-secretase activity mediates the intramembranous cleavage of CD44. Oncogene, *22:* 1511-1516, 2003.
4. De Strooper, B., Annaert, W., Cupers, P., Saftig, P., Craessaerts, K., Mumm, J. S., Schroeter, E. H., Schrijvers, V., Wolfe, M. S., Ray, W. J., Goate, A., and Kopan, R. A presenilin-1-dependent gamma-secretase-like protease mediates release of Notch intracellular domain. Nature, *398:* 518-522, 1999.
5. Marambaud, P., Shioi, J., Serban, G., Georgakopoulos, A., Sarner, S., Nagy, V., Baki, L., Wen, P., Efthimiopoulos, S., Shao, Z., Wisniewski, T., and Robakis, N. K. A presenilin-1/gamma-secretase cleavage releases the E-cadherin intracellular domain and regulates disassembly of adherens junctions. Embo J, *21:* 1948-1956, 2002.
6. Park, C. S., Kim, O. S., Yun, S. M., Jo, S. A., Jo, I., and Koh, Y. H. Presenilin 1/gamma-secretase is associated with cadmium-induced E-cadherin cleavage and COX-2 gene expression in T47D breast cancer cells. Toxicol Sci, *106:* 413-422, 2008.
7. Vidal, G. A., Naresh, A., Marrero, L., and Jones, F. E. Presenilin-dependent gamma-secretase processing regulates multiple ERBB4/HER4 activities. J Biol Chem, *280:* 19777-19783, 2005.
8. Tomita, T., Tanaka, S., Morohashi, Y., and Iwatsubo, T. Presenilin-dependent intramembrane cleavage of ephrin-B1. Mol Neurodegener, *1:* 2, 2006.
9. Gallahan, D., Jhappan, C., Robinson, G., Hennighausen, L., Sharp, R., Kordon, E., Callahan, R., Merlino, G., and Smith, G. H. Expression of a truncated Int3 gene in developing secretory mammary epithelium specifically retards lobular differentiation resulting in tumorigenesis. Cancer Res, *56:* 1775-1785, 1996.
10. Hu, C., Dievart, A., Lupien, M., Calvo, E., Tremblay, G., and Jolicoeur, P. Overexpression of activated murine Notch1 and Notch3 in transgenic mice blocks mammary gland development and induces mammary tumors. Am J Pathol, *168:* 973-990, 2006.
11. Reedijk, M., Odorcic, S., Chang, L., Zhang, H., Miller, N., McCready, D. R., Lockwood, G., and Egan, S. E. High-level coexpression of JAG1 and NOTCH1 is observed in human breast cancer and is associated with poor overall survival. Cancer Res, *65:* 8530-8537, 2005.
12. O'Neill, C. F., Urs, S., Cinelli, C., Lincoln, A., Nadeau, R. J., Leon, R., Toher, J., Mouta-Bellum, C., Friesel, R. E., and Liaw, L. Notch2 signaling induces apoptosis and inhibits human MDA-MB-231 xenograft growth. Am J Pathol, *171:* 1023-1036, 2007.
13. Shih Ie, M. and Wang, T. L. Notch signaling, gamma-secretase inhibitors, and cancer therapy. Cancer Res, *67:* 1879-1882, 2007.

14. Shi, W. and Harris, A. L. Notch signaling in breast cancer and tumor angiogenesis: cross-talk and therapeutic potentials. J Mammary Gland Biol Neoplasia, *11:* 41-52, 2006.
15. Rizzo, P., Miao, H., D'Souza, G., Osipo, C., Song, L. L., Yun, J., Zhao, H., Mascarenhas, J., Wyatt, D., Antico, G., Hao, L., Yao, K., Rajan, P., Hicks, C., Siziopikou, K., Selvaggi, S., Bashir, A., Bhandari, D., Marchese, A., Lendahl, U., Qin, J. Z., Tonetti, D. A., Albain, K., Nickoloff, B. J., and Miele, L. Cross-talk between notch and the estrogen receptor in breast cancer suggests novel therapeutic approaches. Cancer Res, *68:* 5226-5235, 2008.
16. Lee, C. W., Raskett, C. M., Prudovsky, I., and Altieri, D. C. Molecular dependence of estrogen receptor-negative breast cancer on a notch-survivin signaling axis. Cancer Res, *68:* 5273-5281, 2008.
17. Weinmaster, G. and Kopan, R. A garden of Notch-ly delights. Development, *133:* 3277-3282, 2006.
18. Nakajima, M., Shimizu, T., and Shirasawa, T. Notch-1 activation by familial Alzheimer's disease (FAD)-linked mutant forms of presenilin-1. J Neurosci Res, *62:* 311-317, 2000.
19. Huppert, S. S., Ilagan, M. X., De Strooper, B., and Kopan, R. Analysis of Notch function in presomitic mesoderm suggests a gamma-secretase-independent role for presenilins in somite differentiation. Dev Cell, *8:* 677-688, 2005.
20. Rand, M. D., Grimm, L. M., Artavanis-Tsakonas, S., Patriub, V., Blacklow, S. C., Sklar, J., and Aster, J. C. Calcium depletion dissociates and activates heterodimeric notch receptors. Mol Cell Biol, *20:* 1825-1835, 2000.
21. McConkey, D. J. and Zhu, K. Mechanisms of proteasome inhibitor action and resistance in cancer. Drug Resist Updat, *11:* 164-179, 2008.
22. Dantuma, N. P., Groothuis, T. A., Salomons, F. A., and Neefjes, J. A dynamic ubiquitin equilibrium couples proteasomal activity to chromatin remodeling. J Cell Biol, *173:* 19-26, 2006.
23. Codony-Servat, J., Tapia, M. A., Bosch, M., Oliva, C., Domingo-Domenech, J., Mellado, B., Rolfe, M., Ross, J. S., Gascon, P., Rovira, A., and Albanell, J. Differential cellular and molecular effects of bortezomib, a proteasome inhibitor, in human breast cancer cells. Mol Cancer Ther, *5:* 665-675, 2006.
24. Llobet, D., Eritja, N., Encinas, M., Sorolla, A., Yeramian, A., Schoenenberger, J. A., Llombart-Cussac, A., Marti, R. M., Matias-Guiu, X., and Dolcet, X. Antioxidants block proteasome inhibitor function in endometrial carcinoma cells. Anticancer Drugs, *19:* 115-124, 2008.
25. Fernandez, Y., Miller, T. P., Denoyelle, C., Esteban, J. A., Tang, W. H., Bengston, A. L., and Soengas, M. S. Chemical blockage of the proteasome inhibitory function of bortezomib: impact on tumor cell death. J Biol Chem, *281:* 1107-1118, 2006.
26. Song, L. L., Peng, Y., Yun, J., Rizzo, P., Chaturvedi, V., Weijzen, S., Kast, W. M., Stone, P. J., Santos, L., Loredo, A., Lendahl, U., Sonenshein, G., Osborne, B., Qin, J. Z., Pannuti, A., Nickoloff, B. J., and Miele, L. Notch-1 associates with IKKalpha and regulates IKK activity in cervical cancer cells. Oncogene, *27:* 5833-5844, 2008.
27. Rasul, S., Balasubramanian, R., Filipovic, A., Slade, M. J., Yague, E., and Coombes, R. C. Inhibition of gamma-secretase induces G2/M arrest and triggers apoptosis in breast cancer cells. Br J Cancer, *100:* 1879-1888, 2009.

28. Watanabe, T., Yuki, S., Egawa, M., and Nishi, H. Protective effects of MCI-186 on cerebral ischemia: possible involvement of free radical scavenging and antioxidant actions. J Pharmacol Exp Ther, *268:* 1597-1604, 1994.
29. Sasano, N., Enomoto, A., Hosoi, Y., Katsumura, Y., Matsumoto, Y., Shiraishi, K., Miyagawa, K., Igaki, H., and Nakagawa, K. Free radical scavenger edaravone suppresses x-ray-induced apoptosis through p53 inhibition in MOLT-4 cells. J Radiat Res (Tokyo), *48:* 495-503, 2007.
30. Cory, A. H., Owen, T. C., Barltrop, J. A., and Cory, J. G. Use of an aqueous soluble tetrazolium/formazan assay for cell growth assays in culture. Cancer Commun, *3:* 207-212, 1991.
31. Collier, A. C. and Pritsos, C. A. The mitochondrial uncoupler dicumarol disrupts the MTT assay. Biochem Pharmacol, *66:* 281-287, 2003.
32. Nair, P., Somasundaram, K., and Krishna, S. Activated Notch1 inhibits p53-induced apoptosis and sustains transformation by human papillomavirus type 16 E6 and E7 oncogenes through a PI3K-PKB/Akt-dependent pathway. J Virol, *77:* 7106-7112, 2003.
33. Sade, H., Krishna, S., and Sarin, A. The anti-apoptotic effect of Notch-1 requires p56lck-dependent, Akt/PKB-mediated signaling in T cells. J Biol Chem, *279:* 2937-2944, 2004.
34. Mungamuri, S. K., Yang, X., Thor, A. D., and Somasundaram, K. Survival signaling by Notch1: mammalian target of rapamycin (mTOR)-dependent inhibition of p53. Cancer Res, *66:* 4715-4724, 2006.
35. Gatto, S., Scappini, B., Pham, L., Onida, F., Milella, M., Ball, G., Ricci, C., Divoky, V., Verstovsek, S., Kantarjian, H. M., Keating, M. J., Cortes-Franco, J. E., and Beran, M. The proteasome inhibitor PS-341 inhibits growth and induces apoptosis in Bcr/Abl-positive cell lines sensitive and resistant to imatinib mesylate. Haematologica, *88:* 853-863, 2003.
36. Denlinger, C. E., Rundall, B. K., Keller, M. D., and Jones, D. R. Proteasome inhibition sensitizes non-small-cell lung cancer to gemcitabine-induced apoptosis. Ann Thorac Surg, *78:* 1207-1214; discussion 1207-1214, 2004.
37. Yin, D., Zhou, H., Kumagai, T., Liu, G., Ong, J. M., Black, K. L., and Koeffler, H. P. Proteasome inhibitor PS-341 causes cell growth arrest and apoptosis in human glioblastoma multiforme (GBM). Oncogene, *24:* 344-354, 2005.
38. Brignole, C., Marimpietri, D., Pastorino, F., Nico, B., Di Paolo, D., Cioni, M., Piccardi, F., Cilli, M., Pezzolo, A., Corrias, M. V., Pistoia, V., Ribatti, D., Pagnan, G., and Ponzoni, M. Effect of bortezomib on human neuroblastoma cell growth, apoptosis, and angiogenesis. J Natl Cancer Inst, *98:* 1142-1157, 2006.
39. Fennell, D. A., Chacko, A., and Mutti, L. BCL-2 family regulation by the 20S proteasome inhibitor bortezomib. Oncogene, *27:* 1189-1197, 2008.
40. Zhou, Y., Yau, C., Gray, J. W., Chew, K., Dairkee, S. H., Moore, D. H., Eppenberger, U., Eppenberger-Castori, S., and Benz, C. C. Enhanced NF kappa B and AP-1 transcriptional activity associated with antiestrogen resistant breast cancer. BMC Cancer, *7:* 59, 2007.
41. Zhou, Y., Eppenberger-Castori, S., Eppenberger, U., and Benz, C. C. The NFkappaB pathway and endocrine-resistant breast cancer. Endocr Relat Cancer, *12 Suppl 1:* S37-46, 2005.
42. Kukar, T. L., Ladd, T. B., Bann, M. A., Fraering, P. C., Narlawar, R., Maharvi, G. M., Healy, B., Chapman, R., Welzel, A. T., Price, R. W., Moore, B., Rangachari, V., Cusack, B., Eriksen, J., Jansen-West, K., Verbeeck, C., Yager,

D., Eckman, C., Ye, W., Sagi, S., Cottrell, B. A., Torpey, J., Rosenberry, T. L., Fauq, A., Wolfe, M. S., Schmidt, B., Walsh, D. M., Koo, E. H., and Golde, T. E. Substrate-targeting gamma-secretase modulators. Nature, *453:* 925-929, 2008.
43. Rosati, E., Sabatini, R., Rampino, G., Tabilio, A., Di Ianni, M., Fettucciari, K., Bartoli, A., Coaccioli, S., Screpanti, I., and Marconi, P. Constitutively activated Notch signaling is involved in survival and apoptosis resistance of B-CLL cells. Blood, *113:* 856-865, 2009.
44. Ban, J., Bennani-Baiti, I. M., Kauer, M., Schaefer, K. L., Poremba, C., Jug, G., Schwentner, R., Smrzka, O., Muehlbacher, K., Aryee, D. N., and Kovar, H. EWS-FLI1 suppresses NOTCH-activated p53 in Ewing's sarcoma. Cancer Res, *68:* 7100-7109, 2008.
45. Qin, J. Z., Stennett, L., Bacon, P., Bodner, B., Hendrix, M. J., Seftor, R. E., Seftor, E. A., Margaryan, N. V., Pollock, P. M., Curtis, A., Trent, J. M., Bennett, F., Miele, L., and Nickoloff, B. J. p53-independent NOXA induction overcomes apoptotic resistance of malignant melanomas. Mol Cancer Ther, *3:* 895-902, 2004.

Chapter 3*

Characterization and comparison of protein complexes initiated by the intracellular domain of individual Notch paralogs

3.1 Introduction

Notch signaling is an evolutionarily conserved signaling pathway that is essential for embryonic development, organogenesis, and tissue homeostasis. Aberrant Notch signaling is associated with several inherited developmental diseases and various types of cancer [reviewed in (1-3)]. Newly synthesized Notch receptor protein is cleaved by Furin-like protease (S1) within the trans-Golgi before being delivered to plasma membrane where it is present as a non-covalently linked heterodimer of the two S1 cleavage products. Upon ligand binding, the bipartite receptor undergoes two additional cleavages, S2 and S3 cleavage, mediated by ADAM10 and the γ-secretase complex, respectively, to release active intracellular domain (NICD). NICD then translocates into the nucleus to form a trimeric core transactivation complex with the sequence-specific DNA binding protein, CSL [CBF-1/Su(H)/Lag-1], and Mastermind or Mastermind-like proteins (MAML), which further recruits other transcription activators to activate the transcription of Notch target genes [reviewed in (4)].

Whereas *Drosophila* only has one Notch receptor, mammals have four Notch paralogs. Inactivation of either Notch1 or Notch2 is embryonically lethal in mice, but Notch3 or Notch4 single knockout mice are viable and fertile, suggesting different mammalian Notch paralogs have redundant as well as unique activities (5-8). Distinct functions of individual Notch paralogs can result from different expression profiles (9), co-expression of different Notch ligands (10, 11), differential response to Fringe-mediated glycosylations (12, 13), differences in the structural domain composition of individual NICD, and/or from possible

* A version of this chapter has been submitted to J Biol Chem. for publication.

interactions with other transcription regulators at given gene promoters (14).

All NICDs contain four highly conserved structural domains, including the RBPjκ-associated module (RAM), seven ankryin repeats (ANK), a nuclear localization sequence (NLS), and proline/glutamic acid/serine/threonine-rich motifs (PEST). In addition, the NICD of mammalian Notch 1-3 have a poorly defined transactivation domain (TAD) between the ANK repeats and PEST domain [reviewed in (4)]. While RAM-ANK is required and sufficient for the formation of the NICD/CSL/MAML core complex, a short sequence within the TAD domain is required for the formation of the high molecular weight N1ICD transactivation complex (15). Experiments using chimeric molecules composed of the RAM-ANK fragment and the fragment C-terminal to RAM-ANK from different NICDs have demonstrated that both the RAM-ANK fragment and the fragment C-terminal to RAM-ANK contribute to the transactivation strength of individual NICD paralogs at given promoters (14). Since all NICD bind to the same DNA-binding protein, CSL (CBF-1 or RBPjκ in mammalian cells), the difference in the transactivation strength must derive from preferential interactions with different MAML proteins (there are three mammalian MAML proteins) and/or other nuclear proteins.

Several nuclear proteins, including NFκB, IKKα, Smad3, YY1, and p53, have been reported to interact with NICD (16-24). Since some of these interactions involve the NICD ANK domain, the domain required for the formation of the NICD/RBPjκ/MAML core trimeric complex, they are most likely RBPjκ-independent. Any differences in these RBPjκ-independent interactions among NICD paralogs would likely contribute to paralog-specific Notch activities. However, most of these interactions were demonstrated by using N1ICD. Whether they also happen with other NICD paralogs and whether individual NICD paralogs have different affinities for these interacting proteins remain to be investigated.

In the present study, we observed that ectopically expressed NICD proteins participated in multiple protein complexes, and the assembly of N1/2/3ICD protein complexes, but not that of N4ICD, was clearly dose-dependent. In addition, under current experimental conditions, the availability of MAML proteins

became the limiting factor for continuous formation of N1ICD/RBPjκ/MAML-based complexes. Furthermore, we confirmed the associations of NICD with NFκB, IKKα, YY1, and Smad3, and found that there were differences in the relative affinities of individual NICD to these proteins. These observations help to explain the dose-dependent and paralog-specific Notch activities as well as provide clues to the development of novel reagents to block Notch signaling for therapeutic benefit in cancer treatment.

3.2 Materials and Methods

3.2.1 Plasmid construction

cDNAs encoding the NICD of human Notch1 [amino acid residues (aa) 1754-2555], Notch2 (aa 1697-2471), and Notch3 (aa 1662-2321) were amplified from reverse transcription-coupled PCR (RT-PCR) of MCF-7 total cellular RNA, and cDNA encoding human N4ICD (aa 1467-2003) was PCR-amplified from human fetal brain marathon-ready cDNA (Clontech, Mountain View, CA). The NICD cDNAs were ligated into the pCMV-Tag4A vector (Stratagene, La Jolla, CA) using BamH1/EcoR1 sites. The sequences of new constructs were verified by sequencing with T3/T7 and gene-specific primers.

3.2.2 Cell culture and transfection

Three human breast cancer cell lines with different genetic background, MCF-7, SKBR3, and MDA-MB-231, were used in this study. MCF-7 cells are positive for estrogen receptor (ER) and progesterone receptor (PR), whereas the other two cell lines are ER negative. SKBR3 cells differ from MDA-MB-231 cells in that they express amplified HER2/neu. Both MCF-7 and MDA-MB-231 cells were cultured in DMEM/F-12 medium (Gibco/Invitrogen, Carlsbad, CA) while SKBR3 cells were propagated in McCoy's 5A medium (Gibco/Invitrogen). All medium was supplemented with 10% fetal bovine serum (FBS) (Gibco/Invitrogen) and GlutaMAX (Gibco/Invitrogen). In addition, MCF-7 culture medium was supplemented with non-essential amino acids (Gibco/Invitrogen), sodium pyruvate (Gibco/Invitrogen), and 10 μg/ml of insulin (Sigma, St. Louis, MO). All cell lines were maintained at 37°C in a humidified atmosphere of 5% CO_2 in air.

Plasmid DNA (5-7.5 μg/plate) was transfected into 10-cm culture plates using Plus reagent and Lipofectamine LTX (Invitrogen) at a ratio of 1:1:3. Culture medium was replaced 6 h after transfection to minimize the cytotoxicity of transfection reagents.

3.2.3 Flow cytometry

Flow cytometry was used to monitor the transfection efficiency of individual transfection experiments. In brief, cold (-20°C) 70% ethanol (1 ml) was added to tubes containing pellets of 5 x 10^5 cells, and the fixed cells were then kept at 4°C for up to a week before analysis. On the day of analysis, fixed cells were rehydrated with phosphate buffered saline (PBS) for 10 minutes before incubation with 200 μl of anti-Flag primary antibody solution (Clone M2, Sigma, 1:500 in PBS) at room temperature for 1 h. After washing once with PBS, the cells were incubated with Alexa 488-conjugated goat anti-mouse secondary antibody solution (Molecular probes/Invitrogen, 1:200 in PBS) at room temperature for 1 h. After a second wash, stained cells were analyzed using a FACScalibur™ flow cytometer (BD Biosciences, San Jose, CA).

3.2.4 Nuclear extract preparation

Nuclear protein extracts were prepared from MCF-7 cells 48 h after transfection, or from SKBR3 cells 24 h after transfection due to higher cytotoxicity of transfection reagents to SKBR3 cells, in a manner similar to that previously described (25). In brief, cells were collected with EDTA-free trypsin to avoid artificial activation of endogenous Notch receptors, and washed once with ice-cold PBS before resuspension in 5 packed cell volumes of ice-cold hypotonic buffer [20 mM HEPES (pH 7.4), 10 mM KCl, and 1.5 mM $MgCl_2$]. After incubation on ice for 20 min, plasma membranes were disrupted by 10-15 strokes of a tight Dounce homogenizer (Wheaton, Millville, NJ) until ~90% of the cells were permeable for Trypan Blue stain (Gibco/Invitrogen). Crude nuclei were pelleted at 3,000 × *g* for 10 min at 4°C, and washed once with ice-cold hypotonic buffer before resuspension in an equal volume of high salt buffer [20 mM HEPES (pH 7.4), 420 mM NaCl, and 1.5 mM $MgCl_2$]. The samples were incubated on ice for 1 h before clearing the nuclear protein extract at 20,817 × *g* for 15 min at 4°C.

Crude nuclei of MDA-MB-231 cells were prepared by differential permeabilization because the cells are too small to be disrupted by Dounce homogenization even after swelling in hypotonic buffer. In brief, after one wash with ice-cold PBS, the cells were resuspended in two packed cell volumes of digitonin-containing isotonic buffer [20 mM HEPES (pH 7.4), 120 mM KCl, 1.5 mM $MgCl_2$, and 0.02% digitonin]. After a 10-min incubation on ice during which ~90% of cells could be stained with Trypan Blue, three packed cell volumes of isotonic buffer without digitonin were added into the sample to prevent the disruption of nuclear membrane during centrifugation. Crude nuclei were pelleted and processed in the same way as described above.

3.2.5 Size exclusion chromatography

Nuclear extract (400-750 μg) from three to six 10-cm plates of cells was loaded onto a Superose 6 10/300 GL column (GE Healthcare, Piscataway, NJ) connected to a Biologic Duoflow system (Bio-Rad, Hercules, CA) via a 250 μl sample loop, and was run in column running buffer [20 mM HEPES (pH 7.4), 150 mM NaCl, and 1.5 mM $MgCl_2$] at 0.4 ml/min. Twenty-seven 0.35 ml-fractions were collected with a collection window from 7.4 ml to 16.85 ml after sample injection. Protein in individual fractions was then precipitated with 20% trichloroacetic acid (TCA, Sigma) solution for subsequent immunoblotting analysis, or pooled for immunoprecipitation (IP). Gel filtration standard (Bio-Rad) supplemented with ferritin (Mr, 440 kDa, Sigma) and bovine serum albumin (Mr, 67 kDa, Sigma) was used to estimate the molecular weight of the protein complexes.

3.2.6 Molecular weight calculation

The molecular weights (*Mr*) of complexes within individual fractions were calculated using the equation derived from molecular weight calibration curve as previously described (26). Since the elution volume of thyroglobulin does not fit the linear molecular weight calibration curve on this column [data not shown, and Fig 5 in (27)], we first used the equation derived from calibration curve excluding the K_{av} of thyroglobulin. However, the calculated *Mr* of several fractions that elute between thyroglobulin and ferritin is much higher than the actual *Mr* of thyroglobulin (670 kDa). To avoid possible confusion, we calculate a second set

of *Mr* values for protein complexes that eluted off volume before ferritin using the equation derived from K_{av} of thyroglobulin and ferritin only. The results are shown in Table 1. We speculate that the first set of values might overestimate, whereas the second set of values might underestimate, the *Mr* of protein complexes that elute before ferritin. In the following sections of this report, we use the first set of values to describe protein complexes eluted off the column after ferritin, but used the second set of values to describe the protein complexes that elute off column before ferritin to avoid possible confusion.

3.2.7 TCA precipitation

TCA (87.5 μl) was added to each fraction and the mixtures were incubated on ice for 1 h before pelleting the protein precipitate by centrifugation at 15,000 × *g* for 10 min at 4°C. Protein precipitates were then washed three times with cold acetone and air dried. To re-solubilize the protein precipitate, 1× lithium dodecyl sulfate (LDS) sample buffer supplemented with reducing reagent (20 μl/tube, Invitrogen) was added into each sample and samples were heated at 70°C for 10 min before loading onto 15-well 4-12% NuPage®Bis-Tris gels (Invitrogen).

3.2.8 Immunoprecipitation

Pooled column fractions or freshly prepared nuclear extracts were incubated with ANTI-FLAG®M2 affinity gel (Sigma) with end-over-end mixing at 4°C for 1 h. The affinity gels were then collected by centrifugation, and washed four times with IP washing buffer [50 mM Tris·Cl (pH 7.4), 300 mM NaCl, 5 mM EDTA, 0.1% (w/v) Triton X-100, and 0.02% (w/v) sodium azide] followed by one wash with PBS solution (28). The NICD complexes were then eluted into 1× LDS sample buffer at 70°C for 5 min. After transferring eluted proteins into new microcentrifuge tubes, reducing reagent was added into the eluted proteins, and samples were heated at 70°C for an additional 5 min before loading onto 4-12% or 10% NuPage®Bis-Tris gels (Invitrogen). Nuclear extract from non-transfected cells was subjected to the same IP procedure to be used as negative control.

3.2.9 Immunoblotting analysis

Separated proteins were transferred to Trans-Blot® pure nitrocellulose membrane

(0.2 μm, Bio-Rad), and the membranes were blocked with Odyssey blocking buffer (LI-COR Biosciences, Lincoln, NE) at room temperature for 1 h before being probed overnight at 4°C with primary antibody solution. The primary antibodies used were anti-Notch1 (C-20, Santa Cruz Biotechnology, Santa Cruz, CA, 1:500), anti-Notch4 (H-225, Santa Cruz Biotechnology, 1:250), anti-Flag (Clone M2, Sigma, 1:1,000), anti-RBPjκ (T6709, Institute of Immunology, Tokyo, Japan, 1:1,000) (29), anti-MAML1 (Bethyl Laboratories, Montgomery, TX, 1:1,000), anti-MAML2 (Cell Signaling Technology, Danvers, MA, 1:200), anti-MAML3 (Bethyl Laboratories, 1:1,000), anti-IKKα (Epitomics, Burlingame, CA, 1:500), anti-p65/NFκB (Santa Cruz Biotechnology, 1:500), anti-YY1 (Santa Cruz Biotechnology, 1:300), and anti-Smad3 (Cell Signaling Technology, 1:250). All primary antibodies were diluted in Odyssey blocking buffer. After washing four times with TTBS for 10 minutes, the membranes were incubated with regular (for TCA precipitated samples), or light chain specific (for IP samples) HRP-conjugated goat anti-mouse/rabbit/rat (Jackson ImmunoResearch Laboratories, West Grove, PA, 1: 4,000 - 1:20,000) secondary antibody solution at room temperature for 1 h. After another round of four washes with TTBS, the membranes were incubated with SuperSignal West Pico Chemiluminescent Substrate (Pierce, Rockland, IL), exposed to Fuji film, and then developed to visualize the protein signal.

3.2.10 Densitometry analysis

The X-ray films were scanned using an Artixscan 1800f scanner (Microtek, Taiwan) with a resolution at 600 dpi, and then the signal intensity of individual bands was measured using ImageJ program. The percentages (%) of total intensity of a protein in individual fractions were calculated by dividing its intensities in individual fractions by the total intensity of this protein from all fractions. The results were then plotted using Excel.

3.3 Results

3.3.1 NICD-interacting proteins undergo redistribution during nuclear extract preparation

Size exclusion chromatography is a technique that can be used to identify and

separate protein complexes that contain a protein of interest based on its elution profile, and has been used previously to characterize a high molecular weight N1ICD complex (15). Therefore, we used it as a primary approach to examine the effect of NICD concentration on the protein complex formation of individual NICD paralogs, and to compare the protein complexes that contain individual NICD paralogs. Since the endogenous N1ICD level in these cell lines is below the detection limit (30), we transiently expressed Flag-tagged NICD in cells so that we could confidently detect NICD-containing protein complexes and identify NICD-interacting proteins using a specific anti-Flag antibody. Due to the transient transfection nature of the experiments, not all cells expressed the exogenous NICD-Flag protein. Thus, it was necessary to first determine whether the NICD-Flag levels within individual transfected cells, as determined by flow cytometry, or the NICD-Flag levels within the nuclear protein extract, as determined by immunoblotting, was the most appropriate measure to correlate with protein complex formation.

We reasoned that if NICD-interacting proteins undergo redistribution, i.e., NICD complexes undergo dissociation and reformation during nuclear extract preparation, only the NICD protein levels in the prepared nuclear protein extracts need be assessed. Otherwise, the NICD levels within individual transfected cells would need to be correlated to the elution profile. Figure 3-1 shows the elution profiles of MAML1 from a non-transfected MCF-7 sample and a transiently transfected MCF-7 sample in which 1 in 7 cells was transfected. Differences in the two profiles are readily apparent while there was no significant increase in MAML1 protein levels in the total cellular protein of the transfected sample. This result shows that the entire MAML1 pool from the extract is redistributed to higher molecular weight complexes in the extract despite the fact that the expression of transfected N1ICD was only present in 13 percent of the cells used to generate the extract. This is most easily explained by the reformation of NICD complexes during nuclear extract preparation. Therefore, the amount of NICD in the nuclear extract, rather than that in the original individual transfected cells, determines the effect of NICD levels on its complex formation. At the same time, it allows NICD levels to be easily modulated by mixing cells from transfected plates with cells from non-transfected plates at different ratios.

3.3.2 N1ICD-Flag preferentially forms an ~ 500 kDa complex(es) upon increasing concentration

We next examined the elution profile of N1ICD-Flag in three samples with different N1ICD-Flag protein levels. These three samples were from three independent transfection experiments, and the sample M was the same sample that was probed with anti-MAML1 antibody in Figure 3-1. Sample L was prepared by mixing one volume of cells from a transfected plate (20% of cells transfected) with nine volumes of cells from non-transfected plates. While total protein staining shown in Figure 3-2a revealed equal protein loading, immunoblotting with anti-Notch1 antibody showed clear differences in the N1ICD-Flag protein levels in the three nuclear protein extracts. From Figure 3-2b, we can see that N1ICD-Flag was present in fractions with *Mr* ranging from ~ 350 kDa to more than 1 MDa with no clear separation, indicating the presence of multiple N1ICD-Flag-containing protein complexes with overlapping molecular weights. However, a major peak could still be identified at all three concentrations tested. At the lowest concentration, it peaked in fractions 16-17 (~600 kDa), but the peak shifted with increasing protein concentration to fractions 18-20, corresponding to complexes of reduced *Mr* of ~500 kDa.

3.3.3 The ~500 kDa complex(es) is not based on the N1IC/RBPjκ/ MAML complex

We initially postulated that the preferentially formed 500 kDa complexes were based on the N1IC/RBPjκ/MAML1 complex because it is the core of the canonical Notch transactivation complex. However, after carefully comparing the elution profile of N1ICD-Flag (Figure 3-2b) with that of MAML1 (Figure 3-1a) from the same sample (sample M), we observed that there was more MAML1 protein in fraction 9 than fraction 19 while the opposite was true for N1ICD-Flag. This suggests that a large fraction of N1ICD-Flag proteins in the 500 kDa complex(es) might not associate with RBPjκ/MAML1.

To confirm this, pooled fractions 10-17 and pooled fractions 18-20 were immunoprecipitated separately using ANTI-FLAG®M2 affinity gel. Immunoblotting analysis of the immunoprecipitates with anti-Flag, anti-RBPjκ, and anti-MAML

antibodies confirmed our hypothesis. There was more N1ICD-Flag protein in the immunoprecipitate from pooled fractions 18-20 than that from pooled fractions 10-17 (Figure 3-3a). In contrast, there was slightly less RBPjκ and almost no detectable MAML proteins in pooled fractions 18-20.

Then we reasoned that if the preferentially formed N1ICD complex with increasing N1ICD-Flag concentration is not based on N1ICD/RBPjκ/MAML core complex, N1ICD-Flag in a unfractionated nuclear extract sample that has high concentration of N1ICD-Flag should pull down proportionally less RBPjκ/MAML than that in a sample that contain less N1ICD-Flag. This is what we observed (Figure 3-3b). Therefore, the preferential increase in 500 kDa complex(es) reflects N1ICD in complexes other than the N1ICD/RBPjκ/MAML core complex.

3.3.4 Availability of MAML proteins becomes the limiting factor for continuous formation of N1IC/RBPjκ/MAML complexes with increasing N1ICD-Flag level

Because the availability of NICD protein is the limiting factor for the formation of NICD transactivation complexes, under physiological conditions, activation of Notch signaling pathway depends on the release of free NICD molecules from the plasma membrane. However, the almost complete absence of MAML proteins in the IP of pooled fractions 18-20 where N1ICD-Flag preferentially accumulates suggests that there was no free MAML available to associate with the increased N1ICD-Flag under these experimental conditions. To test this hypothesis, we probed the non-transfected control sample (Figure 3-1), and samples L and H (Figure 3-2) with antibodies against RBPjκ and three MAML members and compared their elution profiles.

As shown in Figure 3-4, although low level N1ICD-Flag in sample L shifted a fraction of RBPjκ proteins to high molecular weight complexes, there was still a significant amount of RBPjκ protein in fraction 27 that corresponds to free RBPjκ monomers (55 kDa). When N1ICD-Flag increased to a level seen in sample H, the free RBPjκ monomers almost completely disappeared. In contrast, there were no free MAML monomer proteins (120~150 kDa) under any conditions

tested, and in the non-transfected control sample, MAML proteins were relatively equally distributed throughout fractions 12-19 (~ 500-900 kDa). When exogenous N1ICD-Flag was introduced into MCF-7 cells, MAML proteins accumulated in fractions 11-15 (~700-900 kDa). Although more MAML proteins were eluted in fractions 11-15 in sample H compared to those in sample L, the difference in the MAML1 elution profiles of sample L and non-transfected control was greater than that between sample H and sample L. This suggests that MAML proteins, but not RBPjκ proteins, are easily exhausted with the expression of exogenous N1ICD-Flag. While modest expression could impact both proteins, a further increase in N1ICD-Flag level only altered the distribution of RBPjκ among protein complexes. Therefore, under current experimental conditions, the availability of MAML proteins became the limiting factor for continuous N1IC/RBPjκ/MAML complexes formation.

3.3.5 Associations of N1ICD-Flag with several known NICD-interacting proteins are not the major contributors to the 500 kDa complex(es)

To investigate the possible identities of the 500 kDa complex(es), we probed the immunoblot shown in Figure 3-3 with antibodies directed against several known NICD-interacting proteins. We found clear evidence that IKKα is associated with N1ICD-Flag (Figure 3-5). In addition, three NFκB members—p65, p52, and p50, and Smad3, also appear to enrich in the immunoprecipitated material relative to the small amount that non-specifically associates with the beads. However, none of these interactions were stronger in pooled fractions 18-20, where the 500 kDa complex(es) preferentially formed with increasing N1ICD-Flag level, than in pooled fractions 10-17, suggesting that they were not the major contributors to the 500 kDa complexes.

3.3.6 N4ICD-Flag shows a distinct elution profile from the other three NICD paralogs

We then compared the elution profiles of the other three NICD paralogs to that of N1ICD-Flag. As shown in Figure 3-6, the elution profiles of N2ICD-Flag were almost identical to those of N1ICD-Flag, with a the peak in fractions 18-20 at high

expression level and a peak shift to fractions 16-17 at low concentration. N3ICD-Flag showed a slightly different elution profile. Although the samples examined had a 10-fold difference in N3ICD-Flag concentration, N3ICD-Flag in both samples peaked in fractions 20-22, which corresponds to a 440 kDa complex(es). This peak was slightly less pronounced when the protein level was lower, suggesting a dose-dependent assembly of N3ICD-Flag complexes similar to that of N1ICD-Flag and N2ICD-Flag. In contrast, N4ICD-Flag exhibited a unique elution profile. Further, there was almost no difference in the elution profile when N4ICD-Flag concentration changed 10-fold. In addition, N4ICD-Flag was present in fractions that ranged from void volume to those corresponding to its free monomer, with a minor peak in the void volume and a major peak with a *Mr* of 150 kDa. This distinct elution profile was not due to unique interactions with RBPjκ and MAML proteins as the elution profiles for these proteins in the high level N4ICD-Flag sample were very similar to those of N1ICD-Flag samples with a low to moderate concentration of N1ICD-Flag.

3.3.7 The intracellular domains of Notch 2-4 have different affinities to several NICD-interacting proteins

Different elution profiles suggest the presence of paralog-specific protein complexes. Therefore, we tested whether the NICD of Notch 2-4 paralogs also interact with IKKα, p65/NFκB, YY1, and Smad3, and whether there is any difference in their interactions. Unfractionated nuclear protein extracts from N2/3/4ICD-Flag transfected MCF-7 cells were immunoprecipitated with ANTI-FLAG®M2 affinity gel. As shown in Figure 3-7, the expression level of N2ICD-Flag was much lower than that of N3ICD-Flag and N4ICD-Flag, but all could pull down comparable amounts of RBPjκ, implying that at least a fraction of N3ICD-Flag and N4ICD-Flag proteins was not associated with RBPjκ and MAML proteins. In addition, the three NICD paralogs displayed different affinities to IKKα, p65/NFκB, YY1, and Smad3. Although we could not order the affinities of NICD paralogs to these four proteins because of differences in their expression levels, it is evident that N3ICD-Flag has a lower affinity for p65/NFκB compared to the other two NICD paralogs, and N4ICD-Flag has a higher affinity for YY1 compared to N3ICD-Flag.

3.3.8 The elution profiles of individual NICD-Flag paralogs in three breast cancer cell lines are largely conserved

Lastly, we asked whether the interaction profiles of individual NICD-Flag paralogs in different breast cancer cells lines are conserved by comparing their elution profiles. Since MCF-7 cells are positive for both ER and PR, we included ER/PR-negative, but HER2/neu amplified, SKBR3 cells and ER/PR/HER2 triple negative MDA-MB-231 cells. Since we could not achieve a high NICD protein concentration in MDA-MB-231 cells due to poor transfection efficiency in MDA-MB-231 cells (only one fourth of that in MCF-7 and SKBR3 cells), we examined only one MDA-MB-231 sample but two SKBR3 samples with different protein concentrations for each NICD paralog. The concentration differences between two SKBR3 samples were 4-fold for N2ICD-Flag level, and 10-fold for the other three paralogs.

As shown in Figure 3-8, the overall elution profiles of individual NICD paralogs are largely conserved among these three cell lines with those of the MDA-MB-231 samples, similar to those of the low protein concentration MCF-7 and SKBR3 samples. First, similar to those of MCF-7 samples, the peaks of N1ICD-Flag and N2ICD-Flag were in fractions 18-20 (~500 kDa) for high level SKBR3 samples, and those of MDA-MB-231 sample were in fractions 16-17 (~600 kDa). Secondly, the peak of N3ICD-Flag was in fractions 20-22 (~ 350-450 kDa) in both SKBR3 samples and the MDA-MB-231 sample, with more proteins accumulated in these three fractions from samples with higher N3ICD-Flag protein concentration, as was the case in MCF-7 samples. Lastly, in both SKBR3 samples, N4ICD-Flag was present in fractions that ranged from the void volume to the fraction that corresponds to its free monomer. This was similar to the N4ICD-Flag elution profile in MCF-7 samples.

However, there are several noticeable differences in the elution profiles. First, the N1ICD-Flag peak in SKBR3 samples expressing low amounts of N1ICD was in fractions 20-21 (~440 kDa) instead of 16-17 (~600 kDa). Secondly, N3ICD-Flag from the MDA-MB-231 sample showed a minor peak in fractions 12-14 (~800 kDa), which was not observed with low level MCF-7 and SKBR3 samples. Lastly, N4ICD-Flag in the MDA-MB-231 sample was not present in fractions 1-9 (>

1MDa). Although the basis of these differences remain to be investigated, the strong similarities suggest that most of the interaction profiles of individual NICD paralogs are conserved in these breast cancer cell lines.

3.4 Discussions

Size exclusion chromatography has previously been used to characterize N1ICD-containing complexes in a N1ICD-transformed rat kidney cell line—RKE—and in N1ICD transiently transfected HEK293T (15). Although the fractions were numbered differently, we still can find the corresponding fractions by locating the elution volumes of standard protein markers as the same chromatography column and the same fraction size were used in the previous study and our study. Direct comparison of the elution profiles of N1ICD, MAML1, and RBPjκ from the two studies revealed some similarities as well as some differences. In previous work using N1ICD-transformed RKE cells, N1ICD eluted in fractions with *Mr* ranging from ~ 30–1100 kDa (calculated based on our calibration curve) with two major peaks with *Mr* of ~ 1 MDa (1.5 MDa according to their calculation) and ~ 550 kDa respectively, RBPjκ and MAML1 eluted in all fractions with a major peak with a *Mr* of ~ 67 kDa and ~ 1 MDa, respectively [See Figure 3 in (15)]. In addition, similar to our results, immunoprecipitation of pooled fractions of 1 MDa complexes and pooled fractions of 550 kDa complexes from RKE sample with anti-N1ICD antibody pulled down much more N1ICD, but much less MAML1, from 550 kDa complexes than that from 1 MDa complexes. Similar results were observed in transiently transfected HEK293T cells [See Figure 5 in (15)]. Therefore, both studies demonstrated that a large fraction of N1ICD protein is present in ~ 500-550 kDa complex(es), and that the majority of N1ICD proteins in this complex were not associated with RBPjκ and MAML proteins.

However, a major difference between our study and the previous work is that we did not observe a significant N1ICD peak with a *Mr* of ~ 1 MDa, although we both observed that most of MAML1 proteins were present in complexes with such a molecular weight. This is probably because the relative abundance of other N1ICD-interacting proteins compared to MAML proteins were much higher in our cells compared to the cells used in the previous study. As a result, the amount of N1ICD in other protein complexes with *Mr* of ~ 550-900 kDa was more than that

in N1ICD/MAML-containing complexes with a *Mr* of 1 MDa in our study, and consequently, we could not identify a peak with a *Mr* of 1 MDa..

The identification of MAML proteins as the limiting factors for continuous formation of NICD/RBPjκ/MAML transactivation complexes is unexpected but significant. It provides a molecular explanation for the occurrence of competition between NICD and MEF2C for MAML1, which underlies the non-canonical function of Notch signaling in inhibiting myogeneis (31). Since MAML1 can also associate with other transcription factors including NFκB, p53, and β-catenin, and regulates their transactivities (32-34), Notch activation has the potential to compete for MAML and, through sequestration of MAML, to regulate these MAML-dependent signaling pathways.

A dose-dependent assembly of NICD complex, as observed in this study, is suggestive of a plausible molecular mechanism for the reported dose-dependent effect of NICD on cellular phenotype (35). We hypothesize that under conditions where NICD level is stoichiometrically lower than available MAML proteins, there is probably no or very little association of NICD with its other potential interacting proteins due to its high affinity binding to RBPjκ/MAML proteins. As the NICD concentration increases, MAML is limiting and the abundance of NICD exceeds the available MAML. At this point, NICD becomes available for assembly in additional complexes, such as NICD/NFκB and NICD/YY1. Each new NICD complex might introduce a new non-canonical Notch signaling pathway to cells. Therefore, higher NICD levels will activate more non-canonical Notch signalling pathways and result in a dose-dependent effect on cellular phenotype. In this way, active NICD could function through three mechanisms: 1) activating Notch direct target genes through NICD/RBPjκ/MAML transactivation complex, 2) depriving MAML, or even RBPjκ, from its other interacting proteins to affect their activities, and 3) introducing new pathways through the formation of novel NICD complexes. This raises the possibility that inhibiting non-canonical NICD complex formation may be a better choice in the treatment of human cancers than approaches that directly target NICD production as formation of these complexes might be more important for the oncogenic than for the physiological Notch signalling. In this respect, it is noteworthy that at least in some cases,

Notch signalling through the third mechanism alone is sufficient for tumorigenesis (36).

The different elution profiles of individual paralogs suggest the presence of paralog-specific protein complexes, consistent with the observation that the NICD of Notch 2-4 showed different relative affinities to IKKα, p65/NFκB, YY1, and Smad3. These observations are informative as the difference in protein complex assembly among NICD paralogs might at least partially account for the paralog-specific activities reported previously (14, 37, 38). It should be noted these paralog-specific activities were observed with expression of exogenous active NICD, a condition that allows the formation of non-canonical NICD complexes.

In summary, this study identifies MAML proteins as the limiting factor for continuous formation of NICD/RBPjκ/MAML complexes at high protein levels of NICD and reveals dose-dependent and paralog-specific interactions between NICD and their interacting proteins. These results not only help to explain the dose-dependent and paralog-specific activities of NICD, but may also be instructive in the generation of new reagents to block Notch signalling for therapeutic benefit.

Table 3-1. Calculated molecular weights (Mr) of individual fractions

Fraction	Calculated Mr	Fraction	Calculated Mr	Fraction	Calculated Mr
1	182267 (2037)	10	12378 (1014)	19	840 (505)
2	135184 (1885)	11	9180 (938)	20	623 (467)
3	100264 (1744)	12	6809 (868)	21	462 (432)
4	74364 (1614)	13	5050 (804)	22	342
5	55154 (1494)	14	3745 (744)	23	254
6	40907 (1383)	15	2778 (688)	24	188
7	30340 (1279)	16	2060 (637)	25	139
8	22502 (1184)	17	1528 (589)	26	103
9	16689 (1096)	18	1133 (545)	27	76

Note: 1) the unit of calculated molecular weight is kDa; 2) the values outside the bracket were calculated using the equation derived from calibration curve excluding K_{av} of thyroglobulin and the values inside the bracket were from the equation derived from K_{av} of only thyroglobulin and ferritin.

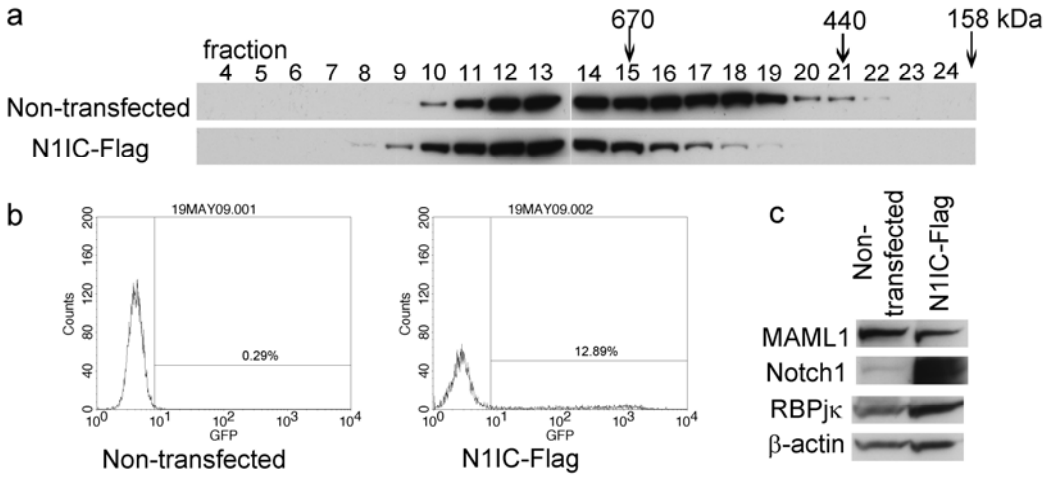

Figure 3-1. NICD interacting proteins undergo redistribution during nuclear extract preparation. (a) Immunoblotting analysis comparing the elution profiles of MAML1 from non-transfected and transiently transfected MCF-7 cells. The elution time point of thyroglobulin (Mr, 670 kDa), ferritin (Mr, 440 kDa), and γ-globulin (Mr, 158 kDa) are labeled. (b) Flow cytometric analysis showing the transfection efficiency of the transfected sample used in (a). (c) Immunoblotting analysis showing the MAML1, Notch1, RBPjκ protein levels in the transfected and non-transfected samples.

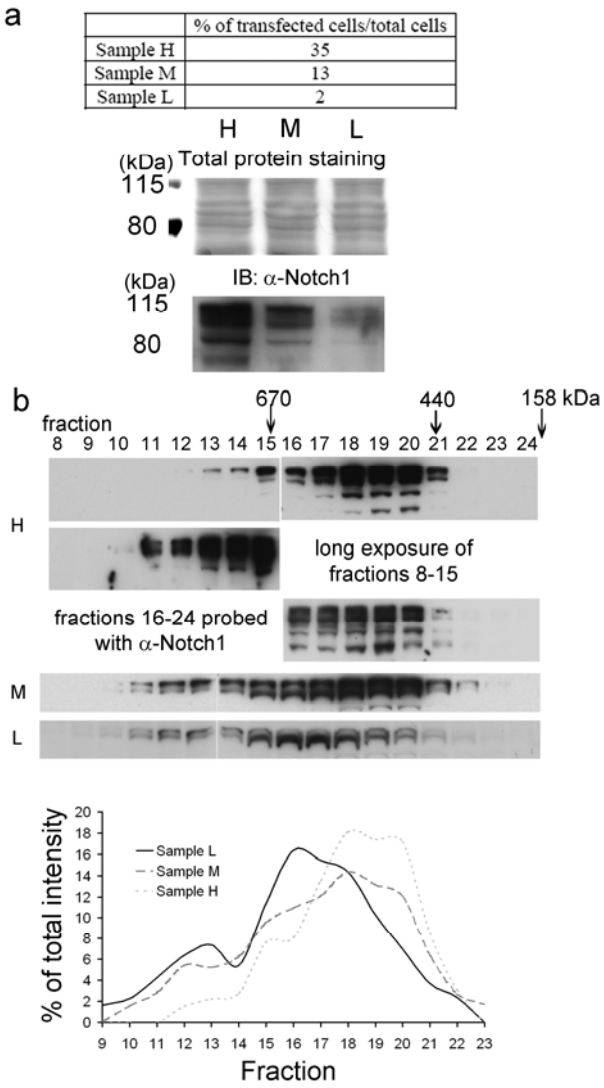

Figure 3-2. N1ICD-Flag preferentially forms a ~ 500 kDa complex(es) with increasing expression level. (a) Immunoblotting analysis to show different N1ICD-Flag protein levels in the three nuclear extract samples examined by size exclusion chromatography. The table at the top describes the percentage of transfected cells within individual samples; the total protein staining by CPTS solution in the middle showing equal loading; the immunoblotting at the bottom to show the difference in the N1ICD-Flag level in these three samples. (b) Comparison of the elution profiles of N1ICD-Flag protein in these three nuclear extracts. The top panels show the immunoblotting analysis and the bottom shows a line graph describing the elution profiles in a graphic manner.

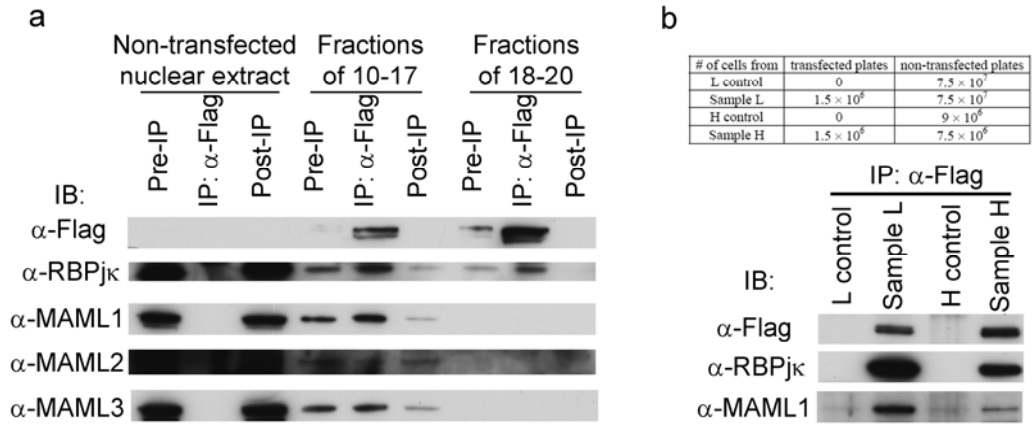

Figure 3-3. The ~500 kDa complex(es) is not based on N1ICD/RBPjκ/MAML complex. (a) Immunoblotting analysis of the immunoprecipitates from pooled fractions 10-17 and pooled fractions 18-20 with antibodies against Flag, RBPjκ, and MAML proteins. Differences in the relative signal intensity of N1ICD-Flag, RBPjκ and MAMLs within the two IPs indicated that a fraction of N1ICD-Flag proteins in pooled fractions 18-20 were not associated with RBPjκ and MAMLs. (b) Immunoblotting analysis of the immunoprecipitates from two nuclear protein samples with 5-fold difference in their N1ICD-Flag concentration. The proportionally less RBPjκ and MAML1 in the immunoprecipitate from the sample with high concentration of N1ICD-Flag is consistent with the notion that the preferentially formed ~500 kDa N1ICD complexes is not based on N1ICD/RBPjκ/MAML core complex.

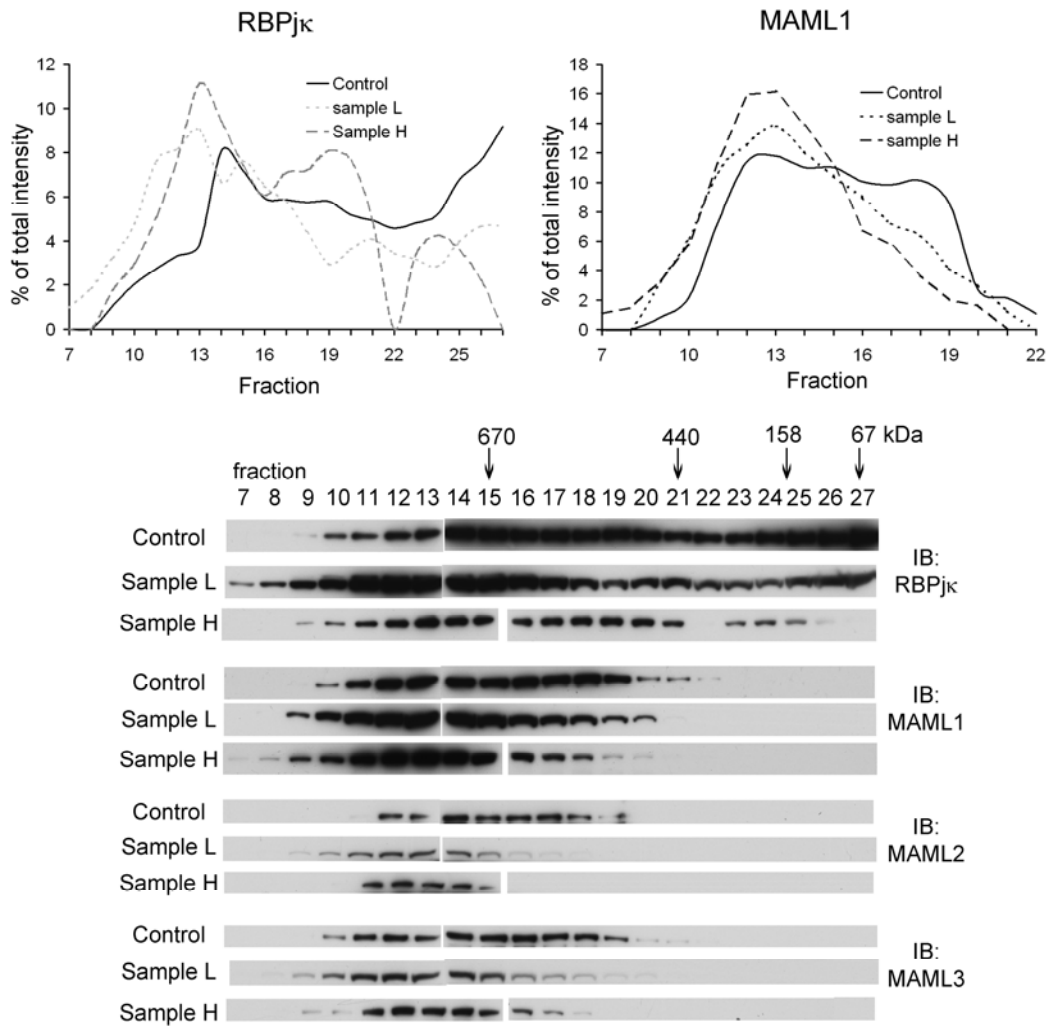

Figure 3-4. Availability of MAMLs is the limiting factor for continuous formation of N1ICD/RBPjκ/MAML complexes. The top panel are the plotted elution profiles of RBPjκ and MAML1 proteins and the bottom panel shows the original immunoblotting data in three samples with different N1ICD-Flag levels. Control sample was the non-transfected control sample shown in Figure 3-1a, and samples L and H were the same samples that were used in Figure 3-2.

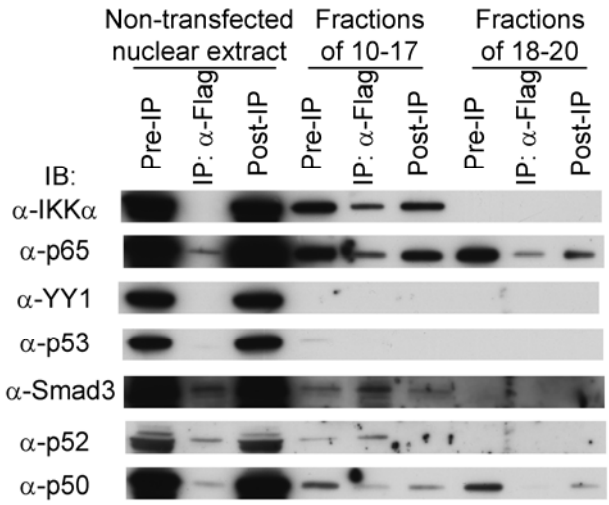

Figure 3-5. Associations of N1ICD-Flag with several proteins are not the major contributor to the 500 kDa complex(es). Immunoblotting analysis showing that the associations of N1ICD-Flag with several known NICD-interacting proteins preferentially occurred in pooled fractions 10-17 instead of pooled fractions 18-20 where the 500 kDa complex(es) was present.

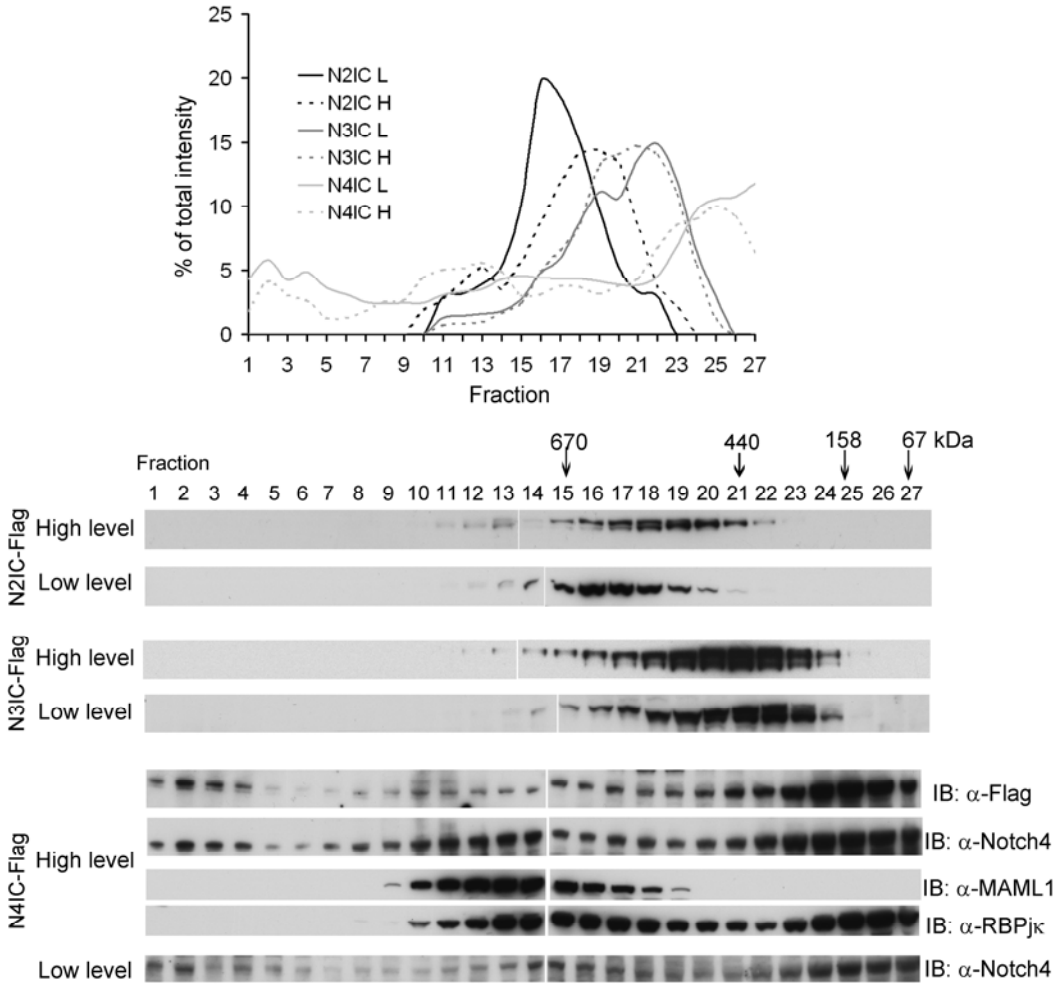

Figure 3-6. N4ICD-Flag shows a distinct elution profile from the other three NICD paralogs. The top panel shows the plotted elution profiles of N2IC-Flag, N3IC-Flag, and N4IC-Flag proteins from MCF-7 cells, and the bottom panels show the original immunoblotting data. The relative protein concentrations between the high level sample and low level sample differed 3-fold for N2ICD-Flag, and 10-fold for N3ICD-Flag and N4ICD-Flag. Differences in the elution profiles indicate the presence of paralog-specific protein complexes.

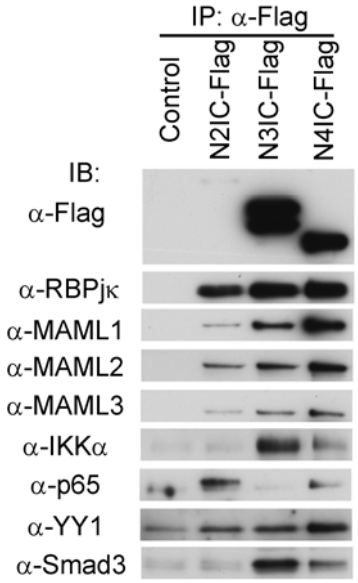

Figure 3-7. The intracellular domains of Notch 2-4 have different affinities to several NICD-interacting proteins. Immunoblotting analysis of the immunoprecipitates of N2/3/4IC-Flag with antibodies against eight known NICD-interacting proteins. The total protein input of four immunoprecipitation experiments are the same.

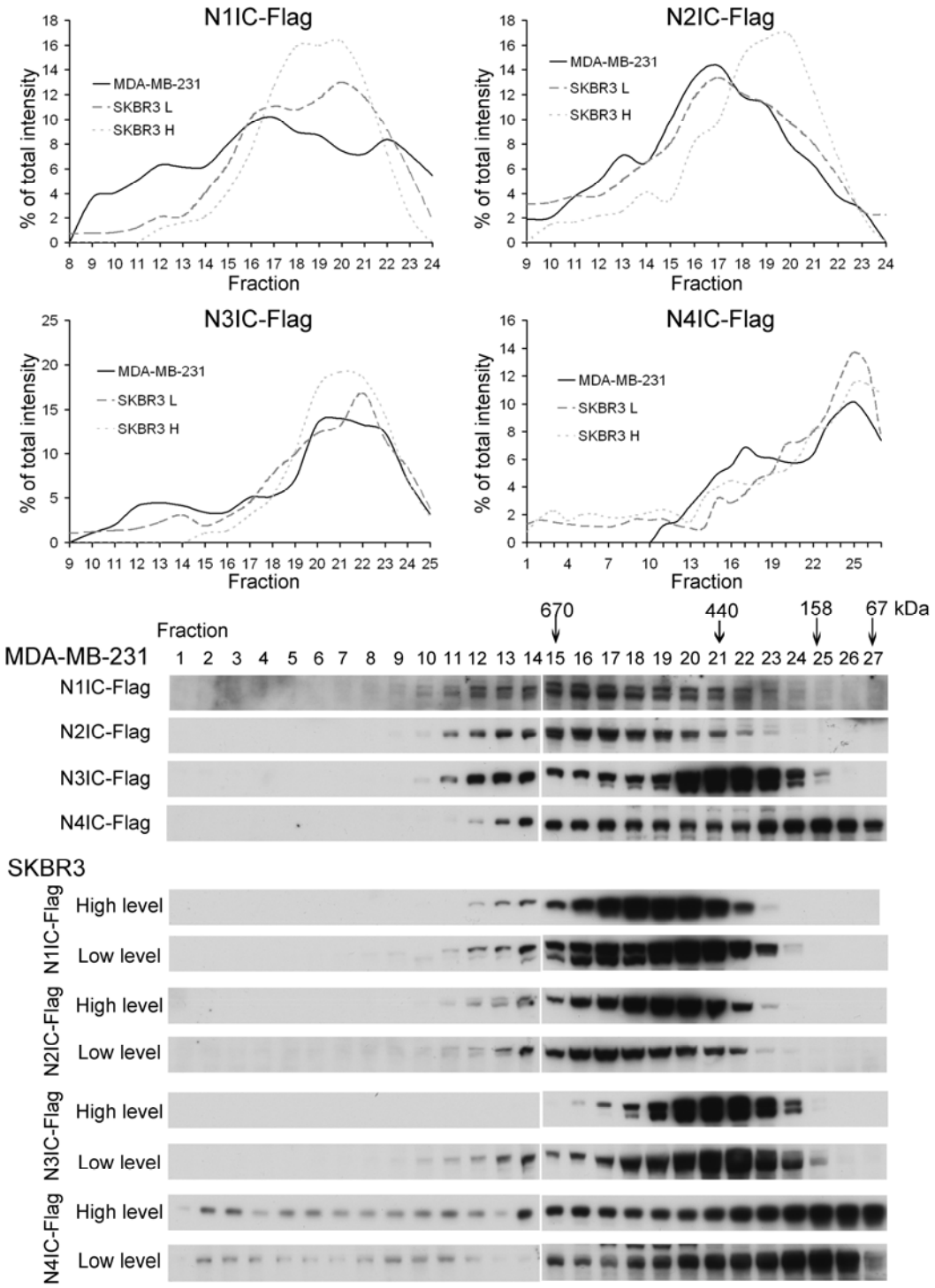

Figure 3-8. The overall elution profiles of individual NICD-Flag paralogs are largely conserved among three breast cancer cell lines. The top panel shows the plotted elution profiles of four NICD-Flag paralogs from MDA-MB-231 and SKBR3 cells, and the middle and bottom panels show the original immunoblotting data. The relative protein concentrations between the high level

SKBR3 sample and low level SKBR3 sample differed by 4-fold for N2ICD-Flag, and by 10-fold for the other three NICD-Flag.

References:

1. Gridley, T. Notch signaling and inherited disease syndromes. Hum Mol Genet, *12 Spec No 1:* R9-13, 2003.
2. Bolos, V., Grego-Bessa, J., and de la Pompa, J. L. Notch signaling in development and cancer. Endocr Rev, *28:* 339-363, 2007.
3. Hansson, E. M., Lendahl, U., and Chapman, G. Notch signaling in development and disease. Semin Cancer Biol, *14:* 320-328, 2004.
4. Kopan, R. and Ilagan, M. X. The canonical Notch signaling pathway: unfolding the activation mechanism. Cell, *137:* 216-233, 2009.
5. Swiatek, P. J., Lindsell, C. E., del Amo, F. F., Weinmaster, G., and Gridley, T. Notch1 is essential for postimplantation development in mice. Genes Dev, *8:* 707-719, 1994.
6. Krebs, L. T., Xue, Y., Norton, C. R., Shutter, J. R., Maguire, M., Sundberg, J. P., Gallahan, D., Closson, V., Kitajewski, J., Callahan, R., Smith, G. H., Stark, K. L., and Gridley, T. Notch signaling is essential for vascular morphogenesis in mice. Genes Dev, *14:* 1343-1352, 2000.
7. Krebs, L. T., Xue, Y., Norton, C. R., Sundberg, J. P., Beatus, P., Lendahl, U., Joutel, A., and Gridley, T. Characterization of Notch3-deficient mice: normal embryonic development and absence of genetic interactions with a Notch1 mutation. Genesis, *37:* 139-143, 2003.
8. Hamada, Y., Kadokawa, Y., Okabe, M., Ikawa, M., Coleman, J. R., and Tsujimoto, Y. Mutation in ankyrin repeats of the mouse Notch2 gene induces early embryonic lethality. Development, *126:* 3415-3424, 1999.
9. Williams, R., Lendahl, U., and Lardelli, M. Complementary and combinatorial patterns of Notch gene family expression during early mouse development. Mech Dev, *53:* 357-368, 1995.
10. Lindsell, C. E., Boulter, J., diSibio, G., Gossler, A., and Weinmaster, G. Expression patterns of Jagged, Delta1, Notch1, Notch2, and Notch3 genes identify ligand-receptor pairs that may function in neural development. Mol Cell Neurosci, *8:* 14-27, 1996.
11. Favier, B., Fliniaux, I., Thelu, J., Viallet, J. P., Demarchez, M., Jahoda, C. A., and Dhouailly, D. Localisation of members of the notch system and the differentiation of vibrissa hair follicles: receptors, ligands, and fringe modulators. Dev Dyn, *218:* 426-437, 2000.
12. Hicks, C., Johnston, S. H., diSibio, G., Collazo, A., Vogt, T. F., and Weinmaster, G. Fringe differentially modulates Jagged1 and Delta1 signalling through Notch1 and Notch2. Nat Cell Biol, *2:* 515-520, 2000.
13. Yang, L. T., Nichols, J. T., Yao, C., Manilay, J. O., Robey, E. A., and Weinmaster, G. Fringe glycosyltransferases differentially modulate Notch1 proteolysis induced by Delta1 and Jagged1. Mol Biol Cell, *16:* 927-942, 2005.
14. Ong, C. T., Cheng, H. T., Chang, L. W., Ohtsuka, T., Kageyama, R., Stormo, G. D., and Kopan, R. Target selectivity of vertebrate notch proteins. Collaboration between discrete domains and CSL-binding site architecture determines activation probability. J Biol Chem, *281:* 5106-5119, 2006.
15. Jeffries, S., Robbins, D. J., and Capobianco, A. J. Characterization of a high-molecular-weight Notch complex in the nucleus of Notch(ic)-transformed RKE cells and in a human T-cell leukemia cell line. Mol Cell Biol, *22:* 3927-3941, 2002.
16. Guan, E., Wang, J., Laborda, J., Norcross, M., Baeuerle, P. A., and Hoffman, T. T cell leukemia-associated human Notch/translocation-associated

Notch homologue has I kappa B-like activity and physically interacts with nuclear factor-kappa B proteins in T cells. J Exp Med, *183:* 2025-2032, 1996.
17. Wang, J., Shelly, L., Miele, L., Boykins, R., Norcross, M. A., and Guan, E. Human Notch-1 inhibits NF-kappa B activity in the nucleus through a direct interaction involving a novel domain. J Immunol, *167:* 289-295, 2001.
18. Shin, H. M., Minter, L. M., Cho, O. H., Gottipati, S., Fauq, A. H., Golde, T. E., Sonenshein, G. E., and Osborne, B. A. Notch1 augments NF-kappaB activity by facilitating its nuclear retention. Embo J, *25:* 129-138, 2006.
19. Vacca, A., Felli, M. P., Palermo, R., Di Mario, G., Calce, A., Di Giovine, M., Frati, L., Gulino, A., and Screpanti, I. Notch3 and pre-TCR interaction unveils distinct NF-kappaB pathways in T-cell development and leukemia. Embo J, *25:* 1000-1008, 2006.
20. Song, L. L., Peng, Y., Yun, J., Rizzo, P., Chaturvedi, V., Weijzen, S., Kast, W. M., Stone, P. J., Santos, L., Loredo, A., Lendahl, U., Sonenshein, G., Osborne, B., Qin, J. Z., Pannuti, A., Nickoloff, B. J., and Miele, L. Notch-1 associates with IKKalpha and regulates IKK activity in cervical cancer cells. Oncogene, *27:* 5833-5844, 2008.
21. Sun, Y., Lowther, W., Kato, K., Bianco, C., Kenney, N., Strizzi, L., Raafat, D., Hirota, M., Khan, N. I., Bargo, S., Jones, B., Salomon, D., and Callahan, R. Notch4 intracellular domain binding to Smad3 and inhibition of the TGF-beta signaling. Oncogene, *24:* 5365-5374, 2005.
22. Asano, N., Watanabe, T., Kitani, A., Fuss, I. J., and Strober, W. Notch1 signaling and regulatory T cell function. J Immunol, *180:* 2796-2804, 2008.
23. Yeh, T. S., Lin, Y. M., Hsieh, R. H., and Tseng, M. J. Association of transcription factor YY1 with the high molecular weight Notch complex suppresses the transactivation activity of Notch. J Biol Chem, *278:* 41963-41969, 2003.
24. Kim, S. B., Chae, G. W., Lee, J., Park, J., Tak, H., Chung, J. H., Park, T. G., Ahn, J. K., and Joe, C. O. Activated Notch1 interacts with p53 to inhibit its phosphorylation and transactivation. Cell Death Differ, *14:* 982-991, 2007.
25. Dignam, J. D., Martin, P. L., Shastry, B. S., and Roeder, R. G. Eukaryotic gene transcription with purified components. Methods Enzymol, *101:* 582-598, 1983.
26. Amersham Biosciences Molecular weight determination and molecular weight distribution analysis. *In:* Gel Filtration: Principles and Methods, AI edition, pp. 79-80. Piscataway, NJ: Amersham Biosciences/GE Healthcare.
27. GE Healthcare Gel Filtration Calibration Kit. Piscataway, NJ: GE Healthcare.
28. Bonifacino, J., Dell'Angelica, E., and TA, S. Immunoprecipitation. *In:* F. Ausubel, R. Brent, R. Kingston, D. Moore, J. Seidman, J. Smith, and K. Struhl (eds.), Current Protocols in Molecular Biology, Vol. 2, pp. 10.16.11-10.16.29. John Wiely & Sons, Inc, 1999.
29. Sakai, T., Furukawa, T., Iwanari, H., Oka, C., Nakano, T., Kawaichi, M., and Honjo, T. Loss of immunostaining of the RBP-J kappa transcription factor upon F9 cell differentiation induced by retinoic acid. J Biochem, *118:* 621-628, 1995.
30. Han, J., Ma, I., Hendzel, M. J., and Allalunis-Turner, J. The cytotoxicity of gamma-secretase inhibitor I to breast cancer cells is mediated by proteasome inhibition, not by gamma-secretase inhibition. Breast Cancer Res, *11:* R57, 2009.
31. Shen, H., McElhinny, A. S., Cao, Y., Gao, P., Liu, J., Bronson, R., Griffin, J. D., and Wu, L. The Notch coactivator, MAML1, functions as a novel coactivator

for MEF2C-mediated transcription and is required for normal myogenesis. Genes Dev, *20:* 675-688, 2006.
32. Alves-Guerra, M. C., Ronchini, C., and Capobianco, A. J. Mastermind-like 1 Is a specific coactivator of beta-catenin transcription activation and is essential for colon carcinoma cell survival. Cancer Res, *67:* 8690-8698, 2007.
33. Jin, B., Shen, H., Lin, S., Li, J. L., Chen, Z., Griffin, J. D., and Wu, L. The maml1 co-activator regulates constitutive NF-{kappa}B signaling and cell survival. J Biol Chem, *285:* 14356-14365, 2010.
34. Zhao, Y., Katzman, R. B., Delmolino, L. M., Bhat, I., Zhang, Y., Gurumurthy, C. B., Germaniuk-Kurowska, A., Reddi, H. V., Solomon, A., Zeng, M. S., Kung, A., Ma, H., Gao, Q., Dimri, G., Stanculescu, A., Miele, L., Wu, L., Griffin, J. D., Wazer, D. E., Band, H., and Band, V. The notch regulator MAML1 interacts with p53 and functions as a coactivator. J Biol Chem, *282:* 11969-11981, 2007.
35. Mazzone, M., Selfors, L. M., Albeck, J., Overholtzer, M., Sale, S., Carroll, D. L., Pandya, D., Lu, Y., Mills, G. B., Aster, J. C., Artavanis-Tsakonas, S., and Brugge, J. S. Dose-dependent induction of distinct phenotypic responses to Notch pathway activation in mammary epithelial cells. Proc Natl Acad Sci U S A, *107:* 5012-5017.
36. Raafat, A., Lawson, S., Bargo, S., Klauzinska, M., Strizzi, L., Goldhar, A. S., Buono, K., Salomon, D., Vonderhaar, B. K., and Callahan, R. Rbpj conditional knockout reveals distinct functions of Notch4/Int3 in mammary gland development and tumorigenesis. Oncogene, *28:* 219-230, 2009.
37. O'Neill, C. F., Urs, S., Cinelli, C., Lincoln, A., Nadeau, R. J., Leon, R., Toher, J., Mouta-Bellum, C., Friesel, R. E., and Liaw, L. Notch2 signaling induces apoptosis and inhibits human MDA-MB-231 xenograft growth. Am J Pathol, *171:* 1023-1036, 2007.
38. Fan, X., Mikolaenko, I., Elhassan, I., Ni, X., Wang, Y., Ball, D., Brat, D. J., Perry, A., and Eberhart, C. G. Notch1 and notch2 have opposite effects on embryonal brain tumor growth. Cancer Res, *64:* 7787-7793, 2004.

Chapter 4
Discussion

Notch signaling pathway has been proposed to be a potential therapeutic target for breast cancer treatment. To investigate how to best exploit Notch inhibition for therapeutic purposes, we performed two independent but related studies. In the first study, we examined the molecular mechanism underlying the cytotoxicity of γ-secretase inhibitor I, Z-LLNle-CHO, in breast cancer. In contrast to previous reports that Z-LLNle-CHO induced cell death and/or growth inhibition by Notch (γ-secretase) inhibition, we found that its cytotoxicity is mediated by proteasome inhibition, not by γ-secretase inhibition. In the second study, we examined the NICD complex formation and found that it is dose-dependent and paralog-specific. In addition, we found that the availability of MAML becomes the limiting factor for continuous formation of NICD/RBPjκ/MAML transactivation complex. This suggests that novel NICD complexes might form when the abundance of NICD is in excess of available MAML, a condition that may occur in cancer cells with aberrant Notch activation, and that blocking the formation of these novel NICD complexes might be a better approach to inhibit oncogenic Notch signaling pathways.

After we published our observation that the cytotoxicity of Z-LLNle-CHO in breast cancer is mediated by proteasome inhibition (1), a similar conclusion was drawn by others who used glioblastoma tumor-initiating cells as a test system (2). Thus, it is evident that Z-LLNle-CHO should not be used as the sole GSI to study the biological outcomes of Notch inhibition, and any data produced in such studies should be interpreted cautiously. Although these findings might undermine the support for using Z-LLNle-CHO or structurally related GSIs as a Notch inhibitors in breast cancer management, they serendipitously reveal another potential therapeutic strategy—proteasome inhibition—for breast cancer treatment.

Proteasome inhibitors, such as Bortezomib, are a new class of anti-tumor drugs whose use has been approved for the treatment of multiple myeloma and mantle cell lymphoma [reviewed in (3)]. Several clinical trials have examined the efficacy

of Bortezomib in breast cancer patients (4-8). When used as a single agent, Bortezomib had no clinical benefit (5, 7), but showed a moderate anti-tumor effect when used in combination with capecitabine, doxorubicin, or docetaxel (4, 6, 8). However, none of the above clinical studies preferentially enrolled ER negative patients only. Given our observation that proteasome inhibitors are more effective against ER negative breast cancer cells, a finding consistent with a previous study (9), the inclusion of ER positive patients in clinical trials of Bortezomib might mask its potential benefit for ER negative patients. Our results suggest that there may be a benefit to refining the inclusion criteria for patient selection in future clinical trials designed to test the efficacy of proteasome inhibitors in breast cancer treatment.

The lack of cytotoxicity of two specific GSIs—DAPT and L-685,458, which we observed in breast cancer cells, might be disappointing. However, similar results have been reported by others (10). Rasul et al. showed that two specific GSIs—DAPT and compound E, had no significant cytotoxicity in MCF-7 and MDA-MB-231 cells at low concentrations, although at higher concentrations (i.e., 50 μM, 10-fold the concentration tested in our study) DAPT inhibited the growth of MCF-7 and MDA-MB-231 cells by up to 50%. However, Compound E at 50 μM showed no effect on the growth of MDA-MB-231 cells. These authors did not test whether inhibition of γ-secretase activity in MDA-MB-231 cells by 50 μM DAPT was greater than that of an equivalent dose of Compound E. However, the *in vitro* efficacy of Compound E (IC_{50} = 0.3 nM) in inhibiting γ-secretase activity has been reported to be greater than that of DAPT (IC_{50} = 20 nM) (11, 12). In addition, a recent publication using HEK293T cells transfected with a N1EXT construct also showed that Compound E (100 nM for maximal inhibition) has a higher efficacy than DAPT (1 μM for maximal inhibition) in inhibiting N1ICD production (13). Therefore, it is reasonable to infer that at doses of 50 μM, Compound E would be no less effective than DAPT in inhibiting γ-secretase activity in MDA-MB-231 cells. Furthermore, since no cytotoxicity was observed when cells were treated with Compound E, it is likely that the cytotoxicity induced by 50 μM DAPT was due to off-target effects. Therefore, γ-secretase inhibition has no detectable cytotoxic effects in breast cancer cell lines *in vitro*.

There are three possible explanations for the lack of cytotoxicity of GSI in breast cancer cells treated *in vitro*. First, as there are more than twenty known γ-secretase substrates, inhibition of the activity of yet-to-be identified γ-secretase substrate(s) might antagonize the cytotoxic effect of Notch inhibition. Second, the breast cancer cell lines used in this study may have lost their sensitivity to Notch activity due to repeated calcium depletion-induced Notch activation as trypsin/EDTA solution is used routinely when passaging cell lines. Third, as there is little active NICD in these cells, further reduction by GSI treatment might not have any effect on cell survival and proliferation.

Results from both Chapter 2 and Chapter 3 provide evidence to support the third possibility. Figure 2-2 shows that endogenous active N1ICD cannot be detected consistently without artificial activation. Results from Chapter 3, Figure 3-2 and Figure 3-3, show that even very low level of exogenous N1ICD-Flag shifted the MAML1 elution profile dramatically, implying that MAML1 in the non-transfected cells is predominantly not associated with NICD/RBPjκ. This, in turn, suggests that there are few endogenous, active NICD molecules. This is in sharp contrast to a previous report of readily detectable N1ICD in eight human breast cancer cell lines, including MCF-7, MDA-MB-231, and SKBR3 used in our studies (14). This discrepancy could be due to genetic drift as a result of the intrinsic genetic instability of these cancer cell lines or the selection of subpopulations during continuous cell culture. Alternatively, the authors of previous study may have unwittingly used trypsin/EDTA, which can introduce artificial Notch activation during sample preparation No other publication has reported readily detectable endogenous N1ICD in these breast cancer cell lines when using an antibody that only recognizes active N1ICD.

While these results highlight the complexities of studying γ-secretase inhibitors *in vitro*, they do not diminish the potential clinical benefit of Notch inhibition in breast cancer treatment. In the first instance, there might be much more active NICD molecules in breast cancer cells *in vivo* if there is enhanced ligand-receptor interaction. IHC staining of human breast cancer tissues using an antibody specifically against active N1ICD detected N1ICD in 75% of breast cancer samples (27/35); in contrast, only 1 normal tissue showed positive staining for

N1ICD (15). In addition, N1ICD protein has been detected in protein extracts from breast cancer tissues using immunoblotting analysis with an antibody specifically against active N1ICD (14). Therefore, GSI treatment, or Notch inhibition in general, might elicit a stronger cytotoxic effect in breast cancer cells *in vivo*. However, it should be noted that interpretation of *in vivo* experimental data will also be complicated because Notch inhibition can inhibit tumour growth by inhibiting angiogenesis even when the tumour cells are not dependent on Notch signalling (16). Second, even though Notch inhibition might not affect the growth and survival of non-tumor-initiating breast cancer cells, Notch inhibition has been shown to affect mammosphere forming efficiency (MFE), indicating its important role in regulating breast cancer stem cells (17). Furthermore, GSI treatment might affect the activity of another γ-secretase substrate that functions to antagonize to active Notch signalling. This could be avoided by using more specific approaches, such as a dominant-negative MAML peptide or paralog-specific neutralizing antibodies. In fact, polyclonal Notch4 neutralizing antibody inhibited the MFE of primary breast cancer cultures more effectively than did DAPT treatment, suggesting either the presence of a γ-secretase substrate as an antagonist to Notch4 signaling or the eliciting of off-target effects. Nonetheless, exploring the therapeutic potential of Notch inhibition in breast cancer treatment is still warranted.

The discrepancy in the Notch1 activation status between the *in vitro* two-dimensionally cultured breast cancer cell lines and the *in viv*o breast cancer tissues might reflect the difference in the interaction between Notch receptors and ligands and, therefore, necessitate the use of three-dimensional (3-D) culture system for further studies. In fact, the response of mammosphere culture—one specialized 3-D culture model that enriches breast cancer stem cell—to DAPT treatment might reflect enhanced Notch activation partially due to enhanced receptor and ligand interaction under 3-D culture system. However, there are several 3-D culture platforms widely used in cancer research, with each having its advantages and disadvantages [reviewed in (18)]. Therefore, we need to investigate which platform can activate Notch signaling pathways in a manner that best mimics the *in vivo* situation. A recently described approach is particularly attractive in its ease to set up and its ability to mimic the hypoxic

condition (19). The reciprocal effects between Notch activity and hypoxia in breast cancer cells demand better understanding as hypoxia is commonly observed in breast cancer tissues and cross-talk between Notch activity and HIF-1 activity has been reported in other physiological settings (20, 21).

In addition, it is worth re-examining the effect of Notch activity on the radiosensitivity of breast cancer cells using the 3-D culture system. Although Phillips et al. reported that fractionated, but not single, doses of γ-radiation increased Jagged1 and N1ICD levels in breast CSC and suggested that active Notch signaling protects CSC from radiation damage (22), there is concern that the Notch activation (increased N1ICD level) might be an artefact because they used EDTA, a treatment that is known to activate Notch by depleting extracellular calcium during sample preparation (23). We did not observe Notch1 activation after irradiation and DAPT treatment did not affect the radiosensitivity of breast cancer cells in monolayer culture (unpublished observation). In the light of recent observation that Notch signaling only protects glioma CSC ($CD133^+$ cells), but not $CD133^-$ glioma cells, from irradiation (24), it is worth re-examining the effect of Notch signaling on the response of breast cancer cells to γ-irradiation using mammosphere culture or other 3-D culture systems.

There are several approaches currently available to inhibit Notch signalling, including, in the order of increasing specificity, GSI treatment, dnMAML peptide, RNA interference, and paralog-specific neutralizing antibodies. However, the most specific approach—treatment with neutralizing antibody, in this case Notch1 antibody, has been reported to cause liver damage and vascular neoplasms *in vivo* due to the essential role of Dll4/Notch1 signaling in maintaining blood vessel integrity (25). Therefore, there remains a need to identify even more precise methods to block Notch signaling pathways that are essential for the survival of cancer cells, but less important for the physiological Notch activities.

One possibility is to block non-canonical RBPjκ-independent Notch signalling pathways. Support for this approach is derived from a recent study by Raafat et al. who reported that active N4ICD could induce mammary gland carcinoma in the absence of RBPjκ via yet-to-be-identified non-canonical RBPjκ-independent

Notch signalling pathways (26). As discussed in Chapter 3, active NICD could exert its functions through three mechanisms: 1) by forming NICD/RBPjκ/MAML-based transcription regulatory complexes, 2) by sequestering MAML proteins from their other interacting proteins to inhibit MAML-dependent signalling pathways other than Notch, and 3) by forming novel NICD-containing regulatory complexes, such as NICD/NFκB or NICD/Smad3 complexes. In the absence of RBPjκ, active NICD does not form a complex with MAML. Therefore, in the study by Raafat et al. (26), N4ICD must be functioning by forming novel NICD-containing complexes. It is reasonable to infer that the induced mammary gland carcinomas depend on these novel NICD complexes to survive and grow. Formation of these novel NICD complexes might not occur under physiological conditions in which NICD levels are tightly controlled and NICD is sequestered in the canonical NICD/RBPjκ/MAML complex. Therefore, blocking their formation should not cause any severe side effects while, at the same time, suppressing tumor growth.

It should be noted that the formation of non-canonical NICD complexes was likely to be underrepresented in the analysis in Chapter 3. We believe significant amounts of non-canonical complexes in the highest expressing cells were lost due to rearrangements that take place during nuclear extract preparation. Readily detectable N1ICD has been observed in breast cancer tissues by both IHC staining and immunoblotting analysis (14, 15). Since the immunoblotting analysis measures the average values of a known-heterogeneous cancer cell population, in which a subset of the cells may have significantly elevated NICD levels, it is reasonable to infer that these non-canonical NICD complexes will form and function in a subset of cancer cells with high levels of NICD.

Although there is currently no direct evidence to justify this hypothesis, indirect support is found in the cytotoxicity of dnMAML1 peptide. It is generally believed that dnMAML1's cytotoxic effects are the consequence of Notch inhibition as dnMAML1 would prevent recruitment of other transcription co-activators, such as the histone acetyltransferase, p300, to NICD transactivation complexes and thus, prevent the activation of Notch target genes. An alternative explanation, in the light of our new working model, is that dnMAML1 also sequesters NICD from

other NICD-interacting proteins, and consequently, blocks the RBPjκ-independent Notch signalling pathways. Understanding the relative contribution of these two mechanisms to the cytotoxicity of dnMAML1 in Notch-dependent cancer cells will have a great impact on developing new approaches to specifically block oncogenic, but not physiological, Notch signaling pathway. To address this question, an intriguing experiment would be to examine the phenotype generated by expressing full-length MAML1 in cancer cells that are sensitive to dnMAML1. This should enhance the canonical Notch signalling pathway but suppress the non-canonical Notch signalling pathway introduced by formation of novel NICD complexes. If my hypothesis is correct, overexpression of functional MAML1 should have a similar effect to the expression of dnMAML1. Although overexpression of wild type MAML1 is unlikely to be suitable as a therapy for cancer patients, any cytotoxicity due to the expression of full-length MAML1 will provide proof-of-principle for developing novel strategies to specifically block oncogenic Notch signalling pathway.

However, even if expression of full-length MAML1 has the potential to kill cancer cells or induce growth arrest, there are still several critical issues that need to be addressed before this strategy can be used to treat Notch-dependent cancers. First, how can we specifically block oncogenic non-canonical signalling pathways without affecting the canonical Notch signalling pathway? If we assume that NICD needs to adopt different conformations for association with different interacting proteins, one choice would be to use a small molecule to prevent NICD from adopting the structural conformation that is required for the targeted interaction. Second, how many and which non-canonical signalling pathways do we need to block? Third, we would also need to investigate whether these non-canonical signalling pathways have any physiological function. Although oncogenic non-canonical Notch signalling pathways are likely to be active only when NICD levels are high, a situation that is unlikely to happen physiologically given the tightly control of Notch activation, this needs to be experimentally validated. Furthermore, if Notch is liberated from these complexes, we also have to consider whether or not additional complexes and activities will arise when the main non-canonical pathways are inhibited. If new interactions occur, what will be their biological consequence? To this end, further investigation of the identities of

the ~500 KDa complex(es) that was preferentially formed with increasing N1ICD-Flag concentration is warranted. In addition, it is expected that canonical Notch signalling pathways will be further enhanced when Notch levels are high, the consequence of which also need to be investigated.

In addition to the potential impact on the development of novel reagents to specifically block oncogenic, but not physiological, Notch signaling, the observation of dose-dependent assembly of NICD complexes is also important for future research on the roles of Notch in many physiological processes. Many studies use gain-of-function approaches to investigate the possible physiological involvement of molecules of interest. However, in the case of Notch, the levels of exogenous NICD molecules relative to the actual or achievable endogenous NICD level under physiological conditions have seldom been quantified, most probably because the endogenous NICD levels are usually below the limits of detection. To complicate things further, it is not only the absolute NICD level that would be relevant, but also its relative abundance compared to MAML proteins and other possible interacting proteins. Determining the relative stoichiometric abundance of these proteins remains a daunting technical challenge. Although the approach we employed has provided valuable information regarding the relative abundance of NICD, RBPjκ, and MAML proteins, it should be noted that the data reflect the averaged values of cell populations that are known to be heterogeneous and thus do not reflect values of individual cells within those populations. Furthermore, biochemical methods cannot be used to study the dynamic changes that occur during development. Therefore, novel techniques that can detect the interaction between NICD and its binding partners are urgently needed if we are to fully understand the significance of the results presented in Chapter 3.

In summary, we have shown that the cytotoxicity of Z-LLNle-CHO in breast cancer cells is mediated by proteasome inhibition, not by γ-secretase inhibition. This correct assignment will avoid waste of limited resources and help to refine the development of proteasome inhibitors for breast cancer treatment. In addition, we have shown that the assembly of NICD complex is dose-dependent and MAML becomes the limiting factor for formation of canonical

NICD/RBPjκ/MAML complex, which provide the molecular basis for the formation of non-canonical NICD complexes and suggest the significance of these non-canonical complexes in the oncogenic Notch signalling pathways. This work will facilitate the development of better therapeutic strategies to specifically block oncogenic Notch signalling pathways without affecting the physiological Notch activities.

References:

1. Han, J., Ma, I., Hendzel, M. J., and Allalunis-Turner, J. The cytotoxicity of gamma-secretase inhibitor I to breast cancer cells is mediated by proteasome inhibition, not by gamma-secretase inhibition. Breast Cancer Res, *11:* R57, 2009.
2. Monticone, M., Biollo, E., Fabiano, A., Fabbi, M., Daga, A., Romeo, F., Maffei, M., Melotti, A., Giaretti, W., Corte, G., and Castagnola, P. z-Leucinyl-leucinyl-norleucinal induces apoptosis of human glioblastoma tumor-initiating cells by proteasome inhibition and mitotic arrest response. Mol Cancer Res, *7:* 1822-1834, 2009.
3. Caravita, T., de Fabritiis, P., Palumbo, A., Amadori, S., and Boccadoro, M. Bortezomib: efficacy comparisons in solid tumors and hematologic malignancies. Nat Clin Pract Oncol, *3:* 374-387, 2006.
4. Awada, A., Albanell, J., Canney, P. A., Dirix, L. Y., Gil, T., Cardoso, F., Gascon, P., Piccart, M. J., and Baselga, J. Bortezomib/docetaxel combination therapy in patients with anthracycline-pretreated advanced/metastatic breast cancer: a phase I/II dose-escalation study. Br J Cancer, *98:* 1500-1507, 2008.
5. Engel, R. H., Brown, J. A., Von Roenn, J. H., O'Regan, R. M., Bergan, R., Badve, S., Rademaker, A., and Gradishar, W. J. A phase II study of single agent bortezomib in patients with metastatic breast cancer: a single institution experience. Cancer Invest, *25:* 733-737, 2007.
6. Schmid, P., Kuhnhardt, D., Kiewe, P., Lehenbauer-Dehm, S., Schippinger, W., Greil, R., Lange, W., Preiss, J., Niederle, N., Brossart, P., Freier, W., Kummel, S., Van de Velde, H., Regierer, A., and Possinger, K. A phase I/II study of bortezomib and capecitabine in patients with metastatic breast cancer previously treated with taxanes and/or anthracyclines. Ann Oncol, *19:* 871-876, 2008.
7. Yang, C. H., Gonzalez-Angulo, A. M., Reuben, J. M., Booser, D. J., Pusztai, L., Krishnamurthy, S., Esseltine, D., Stec, J., Broglio, K. R., Islam, R., Hortobagyi, G. N., and Cristofanilli, M. Bortezomib (VELCADE) in metastatic breast cancer: pharmacodynamics, biological effects, and prediction of clinical benefits. Ann Oncol, *17:* 813-817, 2006.
8. Dees, E. C., O'Neil, B. H., Lindley, C. M., Collichio, F., Carey, L. A., Collins, J., Riordan, W. J., Ivanova, A., Esseltine, D., and Orlowski, R. Z. A phase I and pharmacologic study of the combination of bortezomib and pegylated liposomal doxorubicin in patients with refractory solid tumors. Cancer Chemother Pharmacol, *63:* 99-107, 2008.
9. Codony-Servat, J., Tapia, M. A., Bosch, M., Oliva, C., Domingo-Domenech, J., Mellado, B., Rolfe, M., Ross, J. S., Gascon, P., Rovira, A., and Albanell, J. Differential cellular and molecular effects of bortezomib, a proteasome inhibitor, in human breast cancer cells. Mol Cancer Ther, *5:* 665-675, 2006.
10. Rasul, S., Balasubramanian, R., Filipovic, A., Slade, M. J., Yague, E., and Coombes, R. C. Inhibition of gamma-secretase induces G2/M arrest and triggers apoptosis in breast cancer cells. Br J Cancer, *100:* 1879-1888, 2009.
11. Dovey, H. F., John, V., Anderson, J. P., Chen, L. Z., de Saint Andrieu, P., Fang, L. Y., Freedman, S. B., Folmer, B., Goldbach, E., Holsztynska, E. J., Hu, K. L., Johnson-Wood, K. L., Kennedy, S. L., Kholodenko, D., Knops, J. E., Latimer, L. H., Lee, M., Liao, Z., Lieberburg, I. M., Motter, R. N., Mutter, L. C., Nietz, J., Quinn, K. P., Sacchi, K. L., Seubert, P. A., Shopp, G. M., Thorsett, E. D., Tung, J. S., Wu, J., Yang, S., Yin, C. T., Schenk, D. B., May, P. C., Altstiel, L.

D., Bender, M. H., Boggs, L. N., Britton, T. C., Clemens, J. C., Czilli, D. L., Dieckman-McGinty, D. K., Droste, J. J., Fuson, K. S., Gitter, B. D., Hyslop, P. A., Johnstone, E. M., Li, W. Y., Little, S. P., Mabry, T. E., Miller, F. D., and Audia, J. E. Functional gamma-secretase inhibitors reduce beta-amyloid peptide levels in brain. J Neurochem, *76:* 173-181, 2001.
12. Seiffert, D., Bradley, J. D., Rominger, C. M., Rominger, D. H., Yang, F., Meredith, J. E., Jr., Wang, Q., Roach, A. H., Thompson, L. A., Spitz, S. M., Higaki, J. N., Prakash, S. R., Combs, A. P., Copeland, R. A., Arneric, S. P., Hartig, P. R., Robertson, D. W., Cordell, B., Stern, A. M., Olson, R. E., and Zaczek, R. Presenilin-1 and -2 are molecular targets for gamma-secretase inhibitors. J Biol Chem, *275:* 34086-34091, 2000.
13. Yang, T., Arslanova, D., Gu, Y., Augelli-Szafran, C., and Xia, W. Quantification of gamma-secretase modulation differentiates inhibitor compound selectivity between two substrates Notch and amyloid precursor protein. Mol Brain, *1:* 15, 2008.
14. Stylianou, S., Clarke, R. B., and Brennan, K. Aberrant activation of notch signaling in human breast cancer. Cancer Res, *66:* 1517-1525, 2006.
15. Mittal, S., Subramanyam, D., Dey, D., Kumar, R. V., and Rangarajan, A. Cooperation of Notch and Ras/MAPK signaling pathways in human breast carcinogenesis. Mol Cancer, *8:* 128, 2009.
16. Wu, Y., Cain-Hom, C., Choy, L., Hagenbeek, T. J., de Leon, G. P., Chen, Y., Finkle, D., Venook, R., Wu, X., Ridgway, J., Schahin-Reed, D., Dow, G. J., Shelton, A., Stawicki, S., Watts, R. J., Zhang, J., Choy, R., Howard, P., Kadyk, L., Yan, M., Zha, J., Callahan, C. A., Hymowitz, S. G., and Siebel, C. W. Therapeutic antibody targeting of individual Notch receptors. Nature, *464:* 1052-1057, 2010.
17. Farnie, G., Clarke, R. B., Spence, K., Pinnock, N., Brennan, K., Anderson, N. G., and Bundred, N. J. Novel cell culture technique for primary ductal carcinoma in situ: role of Notch and epidermal growth factor receptor signaling pathways. J Natl Cancer Inst, *99:* 616-627, 2007.
18. Yamada, K. M. and Cukierman, E. Modeling tissue morphogenesis and cancer in 3D. Cell, *130:* 601-610, 2007.
19. Derda, R., Laromaine, A., Mammoto, A., Tang, S. K., Mammoto, T., Ingber, D. E., and Whitesides, G. M. Paper-supported 3D cell culture for tissue-based bioassays. Proc Natl Acad Sci U S A, *106:* 18457-18462, 2009.
20. Gustafsson, M. V., Zheng, X., Pereira, T., Gradin, K., Jin, S., Lundkvist, J., Ruas, J. L., Poellinger, L., Lendahl, U., and Bondesson, M. Hypoxia requires notch signaling to maintain the undifferentiated cell state. Dev Cell, *9:* 617-628, 2005.
21. Zheng, X., Linke, S., Dias, J. M., Zheng, X., Gradin, K., Wallis, T. P., Hamilton, B. R., Gustafsson, M., Ruas, J. L., Wilkins, S., Bilton, R. L., Brismar, K., Whitelaw, M. L., Pereira, T., Gorman, J. J., Ericson, J., Peet, D. J., Lendahl, U., and Poellinger, L. Interaction with factor inhibiting HIF-1 defines an additional mode of cross-coupling between the Notch and hypoxia signaling pathways. Proc Natl Acad Sci U S A, *105:* 3368-3373, 2008.
22. Phillips, T. M., McBride, W. H., and Pajonk, F. The response of CD24(-/low)/CD44+ breast cancer-initiating cells to radiation. J Natl Cancer Inst, *98:* 1777-1785, 2006.
23. Rand, M. D., Grimm, L. M., Artavanis-Tsakonas, S., Patriub, V., Blacklow, S. C., Sklar, J., and Aster, J. C. Calcium depletion dissociates and activates heterodimeric notch receptors. Mol Cell Biol, *20:* 1825-1835, 2000.

24. Wang, J., Wakeman, T. P., Lathia, J. D., Hjelmeland, A. B., Wang, X. F., White, R. R., Rich, J. N., and Sullenger, B. A. Notch promotes radioresistance of glioma stem cells. Stem Cells, *28:* 17-28, 2010.
25. Yan, M., Callahan, C. A., Beyer, J. C., Allamneni, K. P., Zhang, G., Ridgway, J. B., Niessen, K., and Plowman, G. D. Chronic DLL4 blockade induces vascular neoplasms. Nature, *463:* E6-7, 2010.
26. Raafat, A., Lawson, S., Bargo, S., Klauzinska, M., Strizzi, L., Goldhar, A. S., Buono, K., Salomon, D., Vonderhaar, B. K., and Callahan, R. Rbpj conditional knockout reveals distinct functions of Notch4/Int3 in mammary gland development and tumorigenesis. Oncogene, *28:* 219-230, 2009.

Appendix*

Quantitative analysis reveals asynchronous and more than DSB-associated histone H2AX phosphorylation after exposure to ionizing radiation

Overview

DNA double-strand breaks (DSBs) are a common type of DNA damages introduced by radiotherapy and are believed to be the major determinant of treatment response to radiotherapy. The discovery of localized phosphorylation of the histone H2A variant, H2AX, at DSB sites and the visualization of DSBs by immunofluorescent staining of phosphorylated H2AX has revolutionized the study of molecular mechanisms underlying DSB repair because it enables the localization of DSB sites within individual cells, and consequently the detailed dissection of the recruitment of DSB repair proteins to the DSB sites and their dynamics at DSB sites. Early studies reported that H2AX phosphorylation only occurs at DSB sites and that the numbers of phosphorylated H2AX foci, denoted as γ-H2AX foci, are equal to the expected number of DSBs at different time points in the irradiated cells. This implied a one-to-one correlation between γ-H2AX foci and physical presence of DSB sites (1, 2).

In this first software-based objective and quantitative analysis of γ-H2AX foci that I performed when I started my PhD study (3), I observed discordance between γ-H2AX foci kinetics and reported DSB repair kinetics. I also observed H2AX phosphorylation outside of DSB sites, suggesting that the presence of γ-H2AX foci is not a reliable marker for the physical presence of DSBs. Together with several other studies, this has raised concerns about the use of γ-H2AX foci dynamics as a surrogate for DSB repair kinetics [reviewed in (4, 5)].

The significance of non-DSB-associated H2AX phosphorylation remains to be elusive, probably because of the lack of approaches to specifically block this type

* This appendix is my publication in Radiation Res. 2006; 165(3): 283-292

of H2AX phosphorylation without perturbing the DSB-associated H2AX phosphorylation. However, its occurrence is consistent with genome-wide increased chromatin accessibility to micrococcal nuclease and DNaseI after introduction of DSBs with neocarzinostatin treatment reported in a later study (6), although whether the increased non-DSB-associated H2AX phosphorylation is the cause or the result of this nucleus-wide chromatin relaxation remains to be determined. Furthermore, similar non-DSB-associated H2AX phosphorylation was observed in undamaged *Xenopus* sperm chromatin that was added to *Xenopus* egg extract, simultaneously with a DNA double-strand oligonucleotide, $(dA\text{-}dT)_{70}$, which mimics DNA with DSBs (7). It was shown that undamaged *Xenopus* sperm chromatin could enhance the ATM activation and Chk1 phosphorylation in the *Xenopus* egg extract induced by the DNA double-stranded linear oligonucleotide. Most importantly, addition of an antibody that specifically recognizes phosphorylated H2AX at Ser^{139} or addition of a peptide corresponding to the C-terminus of H2AX attenuated the ATM activation. Therefore, the non-DSB-associated H2AX phosphorylation observed after DSBs might enhance the activation of DNA damage response and help to maintain the DNA damage checkpoint activation when only a small fraction of DSBs remain unjoined.

In addition to the observation of non-DSB associated H2AX phosphorylation, we also observed multiple H2AX phosphorylation centers within a subset of γ-H2AX foci, indicating the presence of multiple DSBs within a single γ-H2AX focus that can be identified by naked eyes. The presence of multiple DSBs within the visible volumes of DNA repair foci was later confirmed by computer modelling (8). This observation implies that counting the foci with naked eyes might underestimate the number of DSBs. Furthermore, our observation that S phase cells showed different γ-H2AX foci features was confirmed by a later study (9), suggesting that the cell cycle phase needs to be taken into consideration when using γ-H2AX foci as a surrogate marker for DSB sites.

In summary, our study revealed several novel features of γ-H2AX foci, which helped the research community to realize the caveats, and consequently, to take full advantage, of using foci to indirectly visualize DSBs in cells.

References

1. Rogakou, E. P., Boon, C., Redon, C., and Bonner, W. M. Megabase chromatin domains involved in DNA double-strand breaks in vivo. J Cell Biol, *146:* 905-916, 1999.
2. Rothkamm, K. and Lobrich, M. Evidence for a lack of DNA double-strand break repair in human cells exposed to very low x-ray doses. Proc Natl Acad Sci U S A, *100:* 5057-5062, 2003.
3. Han, J., Hendzel, M. J., and Allalunis-Turner, J. Quantitative analysis reveals asynchronous and more than DSB-associated histone H2AX phosphorylation after exposure to ionizing radiation. Radiat Res, *165:* 283-292, 2006.
4. Kinner, A., Wu, W., Staudt, C., and Iliakis, G. Gamma-H2AX in recognition and signaling of DNA double-strand breaks in the context of chromatin. Nucleic Acids Res, *36:* 5678-5694, 2008.
5. Belyaev, I. Y. Radiation-induced DNA repair foci: Spatio-temporal aspects of formation, application for assessment of radiosensitivity and biological dosimetry. Mutat Res, *704:* 132-141.
6. Ziv, Y., Bielopolski, D., Galanty, Y., Lukas, C., Taya, Y., Schultz, D. C., Lukas, J., Bekker-Jensen, S., Bartek, J., and Shiloh, Y. Chromatin relaxation in response to DNA double-strand breaks is modulated by a novel ATM- and KAP-1 dependent pathway. Nat Cell Biol, *8:* 870-876, 2006.
7. Peng, A., Lewellyn, A. L., and Maller, J. L. Undamaged DNA transmits and enhances DNA damage checkpoint signals in early embryos. Mol Cell Biol, *27:* 6852-6862, 2007.
8. Ponomarev, A. L., Costes, S. V., and Cucinotta, F. A. Stochastic properties of radiation-induced DSB: DSB distributions in large scale chromatin loops, the HPRT gene and within the visible volumes of DNA repair foci. Int J Radiat Biol, *84:* 916-929, 2008.
9. Costes, S. V., Boissiere, A., Ravani, S., Romano, R., Parvin, B., and Barcellos-Hoff, M. H. Imaging features that discriminate between foci induced by high- and low-LET radiation in human fibroblasts. Radiat Res, *165:* 505-515, 2006.

Quantitative Analysis Reveals Asynchronous and More Than DSB-associated Histone H2AX Phosphorylation after Ionizing Irradiation

Jianxun Han, Michael J. Hendzel and Joan Allalunis-Turner
Department of Oncology, University of Alberta, Cross Cancer Institute,
Edmonton, Alberta T6G 1Z2, Canada

Han, J., Hendzel, M. J. and Allalunis-Turner, J. Quantitative Analysis Reveals Asynchronous and more than DSB-associated Histone H2AX Phosphorylation after Ionizing Irradiation. ***Radiat. Res.***

Rapid phosphorylation of histone H2AX after exposing cells to ionizing irradiation occurs at DSB sites and extends to a region including as much as 30 Mbp of chromatin to form visible microscopic structures called γ-H2AX foci. Although the kinetics of total cellular histone H2AX phosphorylation after ionizing irradiation has been characterized, we still know little about the phosphorylation kinetics of individual γ-H2AX foci. In addition, there are hundreds of smaller γ-H2AX foci that are not associated with DNA double-strand breaks. We refer to these sites as DSB-unrelated γ-H2AX foci. By using indirect immunofluorescence microscopy, deconvolution, and three-dimensional image analysis, we established an objective method to quantitatively analyze each γ-H2AX focus as well as to discriminate DSB-related γ-H2AX foci from DSB-unrelated γ-H2AX foci. Using this method, we found that histone H2AX phosphorylation at different DSB sites was asynchronous following exposure to ionizing radiation. This might reflect the heterogeneous characteristic of free DNA ends that are generated under these conditions. In addition, we found that increased histone H2AX phosphorylation also occurred outside of DSB sites after ionizing irradiation. The function of this DSB-unassociated phosphorylation is not known.

INTRODUCTION

DNA double-strand breaks (DSBs) are a common type of DNA damage induced by ionizing radiation and are believed to be the major determinant of treatment response to radiotherapy. One of the earliest biochemical processes after DSB formation is histone H2AX phosphorylation near the double-strand break *(1)*. This phosphorylation can encompass a region that includes as much as 30 Mbp of chromatin *(2)*. Consequently, the phosphoryated domains of histone H2AX can be detected by immunofluorescence as relatively large subnuclear domains, termed γ-H2AX foci. This phosphorylation can be detected as early as 1 min after ionizing irradiation, reaching a maximum at ~30 min after irradiation, at which time about 1% of the total cellular H2AX molecules are phosphorylated *per* Gy of ionizing radiation *(1)*. Although the function of γ-H2AX foci formation is still unclear, their presence is generally regarded as indicator of the existence of DSB(s). This is because γ-H2AX foci have consistently been found at DSB sites, including those induced by drugs or stalled replication forks, and that the number of γ-H2AX foci generally corresponds to the number of DSBs *(3, 4)*.

Although the kinetics of total H2AX phosphorylation are well characterized, we still know little about the kinetics and phosphorylation density of individual γ-H2AX foci after irradiation. This, in large part, is due to the lack of an objective method to analyze each individual γ-H2AX focus. In addition, we have observed that in untreated cells, there are hundreds of small γ-H2AX foci that rarely colocalize with any known DSB repair protein *(5)*. Since the existence of hundreds of DSB in untreated cells is not supported by data from pulsed-field gel-electrophoresis (PFGE) and neutral comet assay analyses *(6-8)*, we assume that these small γ-H2AX foci are not associated with DSB formation and therefore refer to these structures as small DSB-unrelated foci. In the present study, we established an objective method to analyze γ-H2AX foci. Using quantitative criteria for identifying γ-H2AX foci, we find that H2AX phosphorylation at different DSB sites after ionizing irradiation was asynchronous, and that H2AX phosphorylation may be saturated in the highest phosphorylation density site. In addition, we find that DSB-unrelated γ-H2AX foci also increase their degree of H2AX phosphorylation following exposure to ionizing radiation.

MATERIALS AND METHODS

Cell Culture and Treatment

M059K and M059J are two malignant glioma cell lines derived from the same patient tumor sample but have different radiosensitivity and genetic backgrounds. M059J is radiosensitive, lacks DNA-PKcs and has only a low level of ATM; M059K cells are relatively radioresistant and express normal level of DNA-PKcs and ATM *(9, 10)*. GM38 is a normal human diploid fibroblast cell line. All cells were maintained in DMEM/F12 supplemented with 10% FBS and Glutamax (Gibco) and grown in a 37°C humidified atmosphere containing 5% CO_2. 2 Gy of γ-irradiation was given with a ^{137}Cs Mark I-Mode 68A irradiator (J. L. Shepherd & Associates, San Fernando, CA) at a dose rate of 1.08 Gy/min.

Flow Cytometry Analysis

Cells (2 x 10^6) were collected with 0.25% trypsin at indicated times after γ-irradiation and fixed in 1ml of 70% ice-cold ethanol. Fixed cells were maintained at 4°C for up to 1 week before analysis. On the day of analysis, ethanol was removed and cells were incubated with 100µl of a 1:4000 dilution of anti-γ-H2AX mouse monoclonal antibody (JBW301, Upstate Biotechnology) for 1 h at room temperature with gentle shaking. Following this incubation, cells were washed twice with PBS, and the procedure was repeated with 100 µl of a 1:200 dilution of Alexa 488-conjugated anti-mouse secondary antibody (Molecular Probes). Finally, cells were incubated with 1 ml of 100 µg/ml propidium iodide (Sigma) solution containing 100 µg/ml RNase A (Sigma) at 37°C for 30min. Samples were analyzed using a FACSort flow cytometer (Becton Dickson). Cells stained with 1:250 diluted mouse IgG1 (Sigma) followed by Alexa 488-conjugated anti-mouse secondary antibody were used as isotype control. Values of fluorescence signal intensity of cells stained with anti-γ-H2AX mouse monoclonal antibody were obtained after subtraction of the fluorescence signal intensities of the corresponding isotype control. These data were then normalized to the value of the corresponding 30 min sample, arbitrarily set to equal 100%. The Student's t-test was used to analyze relative H2AX phosphorylation levels in irradiated cells from triplicate experiments.

Indirect Immunofluorescent Microscopy

Cells were seeded onto sterilized glass coverslips 24 h before irradiation at a density of 1 X 10^4/cm^2. At various times after irradiation (10 min, 30 min or 4 h), cells

were fixed with 4% paraformaldehyde in PBS at room temperature for 10 min and permeablized with PBS containing 0.5% Triton-X 100 for 5 min. The coverslips were then incubated with anti-γ-H2AX mouse monoclonal antibody (1:4000 in PBS) for 1 h at room temperature, washed three times with PBS, and incubated with Alexa 488-conjugated anti-mouse secondary antibody (1:200 in PBS) for another 1 h at room temperature. Finally, after washing three times with PBS, the coverslips were mounted with 90% glycerol in PBS containing 0.5 μg/ml 4',6-diamidino-2-phenyindole (DAPI[2], Sigma) and 1 mg/mL paraphenylendiamine (Sigma) onto glass slides.

For BrdU and γ-H2AX double staining, cells were first incubated with 100 μg/ml of BrdU (Sigma) for 20 min., then 15 min after irradiation, were fixed and permeablized as before. DNA was denatured by incubating with 4N HCl for 7 min followed by 50 mM Tris base solution for 5 min. Coverslips were then sequentially incubated with anti-BrdU (1:50 in PBS, Roche), Cy3-conjugated anti-mouse (1:200 in PBS, Jackson ImmunoResearch), and FITC-conjugated anti-γ-H2AX (1:50 in PBS, Upstate Biotechnology).

Optical serial (z-) sections were collected at 300 nm intervals from 30 cells of each group. Images were acquired with an Axioplan 2 (Carl Zeiss, Inc.) microscope equipped with a 12-bit Coolsnap HQ cooled CCD camera and a 100X plan apochromatic lens (NA=1.4). Images were then processed by maximum-likelihood-expectation deconvolution in SoftWoRx (Applied Precision).

Quantitative Analysis of γ-H2AX Foci

Deconvolved image sets were analyzed with Imaris v 4.1.2. Because there was significant difference in H2AX phosphorylation among cells in the culture, each cell was analyzed independently. Using a single-cell-based intensity threshold for the FITC channel (1/10 of the maximal fluorescence signal intensity), values of the volume and numbers of all γ-H2AX foci with intensity above this threshold, values of the numbers of DSB-related foci (see the definition below) and numbers of spots (see the definition below) within these foci, as well as values of total signal intensity of both channels within these DSB-related foci and within the whole nucleus were collected <Figure 1>. The nuclear volume was defined by DAPI staining. Data were analyzed with Microsoft Excel. Numbers of γ-H2AX foci/spots were normalized to the average nuclear volume at 30 min after irradiation.

RESULTS

Kinetics of Total Cellular H2AX Phosphorylation and Dephosphorylation

The phosphorylation/dephosphorylation kinetics of H2AX in two repair-proficient cell lines, GM38 and M059K, was similar: the phosphorylation level at 30 min after irradiation was the highest among the three time points analyzed. In contrast, although there was a rapid increase in the H2AX phosphorylation level within the first 10 min after irradiation in repair-deficient M059J cells, it was difficult to identify any increase during the period from 10 min to 30 min after irradiation. In addition, there was no decrease in the phosphorylation level during the period from 30 min to 4 h <Figure 2>. The differences between cell lines and between different time points were not due to different accessibility of antibody to the isotope as identical results were obtained by immunoblotting assay (data not shown).

DSB-related γ-H2AX Foci and DSB-unrelated γ-H2AX Foci Have Different Volumes

Since we have observed hundreds of DSB-unrelated small γ-H2AX foci in untreated cells, and these foci persist after irradiation *(5)*, we tested whether there is an objective way to distinguish these steady-state foci from DSB-induced foci. After plotting the volume of all γ-H2AX foci with intensity above the intensity threshold into a histogram, it was observed that the histogram was not what would be expected of a single population. Rather, there appeared to be a large population of small foci occupying about 60-80% of the total foci and a second population that was evident with a volume of 0.04 μm^3 and greater<Figure 3>.

γ-H2AX foci larger than 0.04 μm^3 are less than initial DSB numbers. The numbers of γ-H2AX foci with a volume larger than or equal to 0.04 μm^3 were then counted to determine whether these foci represented DSB-related foci. As shown in <Table 1>, diploid GM38 cells had an average of 64 large γ-H2AX foci, and the near-tetraploid M059K cells and M059J cells had an average of 103 large γ-H2AX foci at 30 min after irradiation. Considering that the cell population contains cells in S phase or G_2 phase, which have DNA contents greater than that in G_1 phase, these numbers were less than the expected initial DSB numbers (~35 DSBs/Gy in a diploid human G_1 cell as assessed by pulsed-field gel electrophoresis) *(6, 7)*.

The number of γ-H2AX spots within large foci correlated to initial DSB numbers. Although fewer than expected γ-H2AX foci could be explained by some DSBs having

been repaired by 30 min after irradiation *(2)*, we found evidence for another possibility. At high magnification, ~20-30% of DSB-related γ-H2AX foci resolved into more than one intensity center. Therefore, we quantified the number of intensity centers (defined as γ-H2AX spots) within these large foci. The number of spots at 30 min after irradiation was found to correspond very well to the expected average initial DSB numbers <Table 2>. Therefore, these large foci were classified as DSB-related and those foci with a volume smaller than 0.04 μm^3 as DSB-unrelated foci.

H2AX Phosphorylation Occurred Outside of DSB-related γ-H2AX Foci

In addition to the increase in the number of DSB-related γ-H2AX foci during the period from 10 min to 30 min after irradiation, there was also an increase in the number of DSB-unrelated foci with fluorescence signal intensity above the threshold. This increase was significant in all but the M059K cells <Table 3>. This increase could result from two possibilities: more DSB-unrelated γ-H2AX foci with lower intensity were included in the analysis due to a relatively lower intensity threshold used at 30 min compared to that at 10 min, or there was H2AX phosphorylation occurring at sites of small DSB-unrelated γ-H2AX foci during this period and, as a consequence, more small foci had an fluorescent signal intensity above the threshold and were included in the analysis. The former is unlikely since the mean intensity of γ-H2AX staining increased between 10 and 30 min after ionizing radiation. Therefore, the increase in the numbers of small DSB-unrelated foci most likely results from H2AX phosphorylation occurring at sites outside of the DSB sites during this time period.

Different H2AX Phosphorylation Level at Different DSB Sites

The relative phosphorylation density of each DSB-related γ-H2AX focus was measured by calculating the ratio of total γ-H2AX fluorescence signal to the total DAPI (DNA) fluorescence signal within each focus. The values of this ratio from all the DSB-related foci within a cell were then normalized to the largest value within this cell, arbitrarily set to equal 100%. With the assumption that H2AX molecules are evenly distributed throughout the chromatin, this ratio will reflect relative H2AX phosphorylation level within each focus. <Figure 4> shows that the relative phosphorylation level of different DSB-related γ-H2AX foci were different, displaying a wide range with the average relative phosphorylation level close to 50% of the

phosphorylation level of most highly phosphorylated foci in each individual cell in all three cell lines and at most time points.

All H2AX Molecules at a DSB Site Could Be Phosphorylated

By calculating the ratio of the fluorescent signal within DSB-related γ-H2AX foci to the total nuclear fluorescent signal, ~2% of DAPI signal (reflecting the amount of chromatin) and half of total phosphorylated H2AX were found involved in these large foci at 30 min after 2 Gy γ-irradiation in GM38 and M059K cells <Table 4 and Table 5>. Combining this information with the estimate from 2-D gel electrophoresis experiments that ~1% per Gy of total H2AX molecules are phosphorylated at 30 min after ionizing irradiation (*1*), the average phosphorylation level within these DSB-related γ-H2AX foci could be deduced from the following calculation: (1% * 2 * 50%)/2%=50%: where (1% * 2) represents the proportion of total nuclear H2AX molecules phosphorylated after 2 Gy γ-irradiation; 50% represents the percentage of total phosphorylated H2AX molecules within these large DSB-related foci; and /2% represents the phosphorylation density when these phosphorylated H2AX molecules were evenly distributed into the chromatin involved in these foci. Since the results were close to the average relative phosphorylation level in <Figure 4>, it could be inferred that the highest phosphorylated focus at 30 min after ionizing irradiation corresponded to a state where almost all H2AX molecules within the focus were phosphorylated.

Early S-phase Cells Have Distinctive γ-H2AX Foci Pattern but Did Not Affect the Present Analysis

During the process of image analysis, it was noted that there were two different γ-H2AX foci patterns: one with fewer total γ-H2AX foci and a clear boundary between DSB-related and DSB-unrelated foci; and another with more total γ-H2AX foci with poor resolution between DSB-related foci from DSB-unrelated foci. Co-immunofluorescence staining with anti-BrdU antibody (Roche) revealed that the second pattern is early S-phase cell-specific <Figure 5>. Most of the γ-H2AX foci in these early S-phase cells have a volume smaller than 0.04 μm^3 and are counted as DSB-unrelated foci, but they are relatively brighter than DSB-unrelated foci in other cells. The identity of these small but brighter foci is not clear. Since most of them do

not colocalize with BrdU speckles and 2 Gy γ-irradiation is not expected to cause detectable inhibition of ongoing replication fork *(11)* , it is unlikely that they results from stalled replication forks. To test whether including the these cells in the analysis had a significant influence on the present study, all images were reviewed and 2-5 cells with early S-phase cell-specific γ-H2AX foci pattern were identified in each group except 9 in M059J/30 min group. When these cells were excluded from the analysis, it was found that although the absolute values changed a little, the above conclusions remained tenable <Numbers within the parentheses in all 5 tables>.

DISCUSSION

This paper presents the first report of detailed, objective, quantitative analysis of individual γ-H2AX foci from 3-dimensional images. The finding that the average number of γ-H2AX spots within DSB-related foci at 30 min after irradiation was higher than that at 10 min and corresponded well to the number of initial DSBs is a little surprising. It has been reported that 1) the average number of γ-H2AX foci was maximal at 3 min after irradiation and corresponded well to the DSB numbers determined by pulsed-field gel electrophoresis *(6)* and; 2) that the average number of γ-H2AX foci at 30 min after irradiation corresponded well to the residual DSBs *(2)*. However, there are several factors that support our conclusions: 1) the use of deconvolution to process images before analysis improves resolution of the procedure *(12)*, enabling us to identify multiple centers of intensity within single γ-H2AX foci. The numbers of spots obtained using this criterion closely matched the expected number of DSBs for the dose of γ-irradiation applied; 2) the volume threshold we used was determined empirically and corresponded to the most consistent inflection in volume histogram curves (7 out of 9); 3) the DSB-related γ-H2AX foci identified by image analysis corresponded to all of the large and bright foci in the images identified by visual inspection; 4) the kinetics of the foci appearance/disappearance defined by microscopic analysis was consistent with the kinetics of total H2AX phosphorylation determined by flow cytometry; and 5) there are reports that the numbers of γ-H2AX foci or other repair protein foci that colocalize with γ-H2AX foci after DSB formation, such as 53BP1 foci and NFBD1/MDC1 foci, were maximal at 30 min after γ-irradiation (*13-17*). While it would be imprudent to state that all the γ-H2AX foci with a volume above a certain threshold are DSB-

related foci and that all the γ-H2AX foci with a volume below the threshold are steady-state foci, this definition does provide an objective and practical standard for further analysis.

The observation of multi phosphorylation centers, defined as spots in this paper, within ~20-30% of the large DSB-related foci is quite novel. Individual spots cannot be identified by eye, which may partly account for the underestimation of γ-H2AX foci number in previous reports, especially under conditions of high doses of irradiation *(18-20)*. These multi spots per foci may result from clustering of damaged chromatin domains *(21)*, or from generation of close DSBs. The later possibility is not contradictory to the random, but not necessarily even, distribution of DSB generated by low-LET ionizing irradiation. In fact, PFGE data show that the DNA fragments generated from DSBs cover a wide range of length *(7)*. In addition, two points far away in genomic sequence, even when they are located in different chromosomes, can be very close in 3-D space when DNA is compacted into chromatin.

The kinetics of γ-H2AX foci in repair-deficient M059J cells seems contradictory to the total H2AX phosphorylation level determined by the flow cytometry. This paradox can be resolved by the fact that M059J cells have a higher proportion of H2AX phosphorylation outside of DSB-related foci. As a consequence, a small increase in H2AX phosphorylation within large foci during the early time after irradiation may alter the number of large γ-H2AX foci, but cannot be detected by flow cytometry. During the period from 30 min to 4 h after irradiation, relative large foci volume, reflected by the fact that few foci at 4 h compared to that at 30 min occupy more chromatin, may compensate the loss of γ-H2AX signal from some foci. Therefore, the γ-H2AX foci kinetics in M059J cells is not as consistent as those in GM38 cells and M059K cells with the total nuclear H2AX phosphorylation level. The slower decrease in the γ-H2AX foci number in this repair-deficient cell lines was also reported by another group *(22)*, and most likely results from the slow DSB-repair kinetics in this cell line *(23)*.

The dynamic nature and asynchronous formation of γ-H2AX foci are two possible factors contributing to the lack of correspondence between the number of γ-H2AX foci/spots and the presence of physical DSBs. The appearance and disappearance of γ-H2AX foci is a gradual, not an “on/off”, process and H2AX phosphorylation/dephosphorylation at different DSB sites are not synchronous after

ionizing irradiation as implied by the great variation in the relative phosphorylation level of DSB-related foci shown in the present study. As a result, foci may not have formed at some DSB sites at the early time points after DSB formation, while γ-H2AX foci could still persist after the DSB is repaired due to the gradual, not sudden, dephosphorylation or degradation of γ-H2AX. Therefore, as suggested by previous reports, the presence of γ-H2AX foci may not necessarily mark the presence of a physical DSB at the time of analysis *(24-26)*.

The mechanisms underlying the asynchronous kinetics of H2AX phosphorylation after ionizing irradiation are still unclear. Apart from the phosphoinositide 3-kinase related kinase (PIKK[2]) activity, there is no protein that has been reported to be required for H2AX phosphorylation after ionizing irradiation. One possibility is that asynchronous kinetics reflects the complexity of ionizing radiation-produced DSBs *(27)*. For example, DSBs with less additional damage nearby may have an early and rapid H2AX phosphorylation whereas DSBs in multiply damaged sites might need processing before recruiting PIKK kinase activity and H2AX phosphorylation.

H2AX phosphorylation outside of DSB sites after ionizing radiation has not been formally reported but during the course of this study, one group observed inconsistency between the total cellular γ-H2AX level determined by immunoblotting and the fluoresence signal within DSB-related γ-H2AX foci determined by fluorescence microscopy in caffeine, a PIKK kinase inhibitor, and UCN-01, a cell-cycle kinase Chk1 inhibitor, treated Hela cells *(25)*. The authors attributed this inconsistency to the redistribution of γ-H2AX in chromatin at later time after irradiation. However, the “redistribution” cannot satisfactorily explain the inconsistency between unaffected H2AX phosphorylation level determined by immunoblotting and reduced γ-H2AX foci number at early time (1 h) after irradiation in UCN-01 treated HeLa cells. Therefore, it is possible that these treatments can affect H2AX phosphorylation outside of DSB sites. The function of H2AX phosphorylation outside of DSB sites after ionizing radiation is not clear, but may indicate an altered balance between kinase activity and phosphatase activity and/or changed accessibility of PIKK to the ^{Ser}139 of H2AX at these sites.

In a previous review, it was suggested that one tenth of total H2AX molecules at a DSB site are phosphorylated, with the assumption that the phosphorylation levels within different foci are the same *(3)*. Since we observed in our experimental system that the phosphorylation density within different foci was not homogeneous at various

time points after ionizing irradiation, we further estimated the phosphorylation density at DSB sites based on measurements of intensity distributions and find that the H2AX phosphorylation may reach saturation in the most highly phosphorylated γ-H2AX foci. If H2AX phosphorylation alters chromatin structure as proposed *(4)*, the full phosphorylation of all H2AX molecules at DSB sites would be expected to alter chromatin structure on a very large scale.

The detailed and quantitative analyses of individual γ-H2AX foci in the present study provide new insight into the nature of H2AX phosphorylation after ionizing irradiation. However, there are limitations to this method of analysis. The separation of DSB-related foci from DSB-unrelated foci is based on the contrast of their fluorescence intensity and volume. Therefore, when this contrast is not as pronounced as that observed here, such as when analyzing foci resulting from drug treatment or at later times after irradiation, this method may not apply or the thresholds may need to be adjusted. In fact, in mock-irradiated control cells, there are 0-10 large bright foci that can be identified by eye; however, the contrast of these foci with the small dim ones is not always as sharp as observed for irradiation-induced ones. As a result, when the same thresholds used in the present analysis are applied to unirradiated cells, the numbers of the foci with fluorescence intensity and volume above the thresholds are much greater than reasonably be expected. Since the data derived from unirradiated control cells are not essential to address the questions of the kinetics of post-irradiation □H2AX phosphorylation, they are not included in the present study. The intensity threshold used here (1/10 of the maximal) was determined empirically by comparison to 1/3, 1/5, and 1/20 of the maximal signal intensities. The foci volumes generated with the present threshold (1/10) match the boundary of the fluorescence signal best when the images are displayed in such a way that the maximum of the intensity histogram corresponds to the intensity value of the brightest pixel, and the minimum of the intensity histogram correspond to the value of the background. However, it should be kept in mind that there are still many small foci with intensity below this threshold that were not included in the present analysis. Using a fluorphore in the mounting medium could provide an internal standard useful for determining the intensity threshold, but this approach requires further investigation. However, the present method that combines intensity threshold with volume threshold to define foci should apply to a variety of conditions, including analysis of other DSB-repair protein foci.

The present study also raises some important new questions, such as what are the kinetics of phosphorylation generally and within individual sites following the formation of DSBs; and what is the function of H2AX phosphorylation outside of DSB sites. New approaches to studying DSB repair as a dynamic process and with single focus resolution must be developed in order to address these questions.

ACKNOWLEDGMENTS

The authors would like to thank Mr. Trevor Belanger for the help during image analysis, Dr. X. Sun for help with microscopy and image analysis, and Ms. J. Wizniak for technical assistance with flow cytometry. This work was supported by awards from the Alberta Cancer Board Research Initiative Program and by CIHR (MJH). MJH is a scholar of the Alberta Heritage Foundation for Medical Research and a Canadian Institutes of Health Research New Investigator.

REFERENCES

1. E. P. Rogakou, D. R. Pilch, A. H. Orr, V. S. Ivanova and W. M. Bonner, DNA double-stranded breaks induce histone H2AX phosphorylation on serine 139. *J. Biol. Chem.* **273,** 5858-5868 (1998).
2. E. P. Rogakou, C. Boon, C. Redon and W. M. Bonner, Megabase chromatin domains involved in DNA double-strand breaks in vivo. *J. Cell Biol.* **146,** 905-916 (1999).
3. D. R. Pilch, O. A. Sedelnikova, C. Redon, A. Celeste, A, Nussenzweig and W. M. Bonner, Characteristics of γ-H2AX foci at DNA double-strand breaks sites. *Biochem. Cell Biol.* **81,** 123-129 (2003).
4. O. Fernandez-Capetillo, A. Lee, M. Nussenzweig and A. Nussenzweig, H2AX: the histone guardian of the genome. *DNA Repair (Amst).* **3,** 959-967 (2004).
5. K. J. McManus and M. J. Hendzel, ATM-dependent DNA damage-independent mitotic phosphorylation of H2AX in normally growing mammalian cells. *Mol. Biol. Cell.* 2005 Jul 19; [Epub ahead of print]
6. K. Rothkamm and M. Lobrich, Evidence for a lack of DNA double-strand break repair in human cells exposed to very low x-ray doses. *Proc. Natl. Acad. Sci. USA.* **100,** 5057-5062 (2003).
7. M. Pinto, K. M. Prise and B. D. Michael, Quantification of radiation induced DNA double-strand breaks in human fibroblasts by PFGE: testing the applicability of random breakage models. *Int. J. Radiat. Biol.* **78,** 375-388 (2002).
8. M. Wojewodzka, I. Buraczewska and M. Kruszewski, A modified neutral comet assay: elimination of lysis at high temperature and validation of the assay with anti-single-stranded DNA antibody. *Mutat. Res.* **518,** 9-20 (2002).
9. S. P. Lees-Miller, R. Godbout, D. W. Chan, M. Weinfeld, R. S. Day 3rd, G. M. Barron and J. Allalunis-Turner, Absence of p350 subunit of DNA-activated protein kinase from a radiosensitive human cell line. *Science.* **267,** 1183-1185 (1995).
10. D. W. Chan, D. P. Gately, S. Urban, A. M. Galloway, S. P. Lees-Miller, T. Yen and J. Allalunis-Turner, Lack of correlation between ATM protein expression and tumour cell radiosensitivity. *Int. J. Radiat. Biol.* **74,** 217-224 (1998).
11. R. B. Painter, Inhibition of mammalian cell DNA synthesis by ionizing radiation. *Int. J. Radiat. Biol. Relat. Stud. Phys. Chem. Med.* **49,** 771-781 (1986).

12. L. Landmann and P. Marbet, Colocalization analysis yields superior results after image restoration. *Microsc. Res. Tech.* **64,** 103–112 (2004).

13. R. L. Warters, P. J. Adamson, C. D. Pond and S. A. Leachman, Melanoma cells express elevated levels of phosphorylated histone H2AX foci. *J. Invest. Dermatol.* **124,** 807-817 (2005).

14. L. B. Schultz, N. H. Chehab, A. Malikzay and T. D. Halazonetis, p53 binding protein 1 (53BP1) is an early participant in the cellular response to DNA double-strand breaks. *J. Cell Biol.* **151,** 1381-1390 (2000).

15. I. Rappold, K. Iwabuchi, T. Date and J. Chen, Tumor suppressor p53 binding protein 1 (53BP1) is involved in DNA damage-signaling pathways. *J. Cell Biol.* **153,** 613-620 (2001).

16. Y. L. Shang, A. J. Bodero and P. L. Chen, NFBD1, a novel nuclear protein with signature motifs of FHA and BRCT, and an internal 41-amino acid repeat sequence, is an early participant in DNA damage response. *J. Biol. Chem.* **278,** 6323-6329 (2003).

17. X. Xu and D. F. Stern, NFBD1/KIAA0170 is a chromatin-associated protein involved in DNA damage signaling pathways. *J. Biol. Chem.* **278,** 8795-8803 (2003).

18. N. Taneja, M. Davis, J. S. Choy, M. A. Beckett, R. Singh, S. J. Kron and R. R. Weichselbaum, Histone H2AX phosphorylation as a predictor of radiosensitivity and target for radiotherapy. *J. Biol. Chem.* **279,** 2273-2280 (2004).

19. K. H. Karlsson and B. Stenerlow, Focus formation of DNA repair proteins in normal and repair-deficient cells irradiated with high-LET ions. *Radiat Res.* **161,** 517-527 (2004).

20. T. T. Paull, E. P. Rogakou, V. Yamazaki, C. U. Kirchgessner, M. Gellert and W. M. Bonner, A critical role for histone H2AX in recruitment of repair factors to nuclear foci after DNA damage. *Curr. Biol.* **10,** 886-895 (2000).

21. J. A. Aten, J. Stap, P. M. Krawczyk, C. H. van Oven, R. A. Hoebe, J. Essers and R. Kanaar, Dynamics of DNA double-strand breaks revealed by clustering of damaged chromosome domains. *Science.* **303,** 92-95 (2004).

22. T. Stiff, M. O'Driscoll, N. Rief, K. Iwabuchi, M. Lobrich and P. A. Jeggo, ATM and DNA-PK function redundantly to phosphorylate H2AX after exposure to ionizing radiation. *Cancer Res.* **64,** 2390-2396 (2004).

23. M. J. Allalunis-Turner, P. K. Zia, G. M. Barron, R. Mirzayans and R. S. Day 3rd, Radiation-induced DNA damage and repair in cells of a radiosensitive human malignant glioma cell line. *Radiat Res.* **144,** 288-293 (1995).

24. J. P. Banath, S. H. Macphail and P. L. Olive, Radiation sensitivity, H2AX phosphorylation, and kinetics of repair of DNA strand breaks in irradiated cervical cancer cell lines. *Cancer Res.* **64,** 7144-7149 (2004).

25. H. Wang, M. Wang, H. Wang, W. Bocker and G. Iliakis, Complex H2AX phosphorylation patterns by multiple kinases including ATM and DNA-PK in human cells exposed to ionizing radiation and treated with kinase inhibitors. J. Cell. Physiol. **202,** 492-502 (2005).

26. A. Forand, B. Dutrillaux and J. Bernardino-Sgherri, Gamma-H2AX expression pattern in non-irradiated neonatal mouse germ cells and after low-dose gamma-radiation: relationships between chromatid breaks and DNA double-strand breaks. *Biol. Reprod.* **71,** 643-649 (2004).

27. J. F. Ward, Complexity of damage produced by ionizing radiation. *Cold Spring Harbor Symp. Quant. Biol.* **65,** 377–382 (2000).

TABLE 1

Average numbers of DSB-related γ-H2AX foci (Mean ± SD)

Cell line	2 Gy 10 min	2 Gy 30 min	2 Gy 4 h
GM38	49 ± 17 (46 ± 16)	64 ± 32[a,b] (55 ± 22[b])	44 ± 31 (35 ± 18)
M059K	83 ± 41 (85 ± 43)	103 ± 45[b] (102 ± 46[b])	62 ± 38 (55 ± 27)
M059J	67 ± 35 (59 ± 24)	104 ± 56[a] (100 ± 53[a])	80 ± 38 (79 ± 31)

[a] $p<0.05$ (2 Gy 30 min *vs.* 2 Gy 10 min)

[b] $p<0.05$ (2 Gy 30 min *vs.* 2 Gy 4 h)

Values within parentheses are from analysis excluding S-phase cells

TABLE 2

Average numbers of γ-H2AX spots within DSB-related foci (Mean ± SD)

Cell line	2 Gy 10 min	2 Gy 30 min	2 Gy 4 h
GM38	65 ± 22 (62 ± 21)	97 ± 45[a,b] (84 ± 32[a,b])	54 ± 33 (45 ± 21)
M059K	109 ± 51 (112 ± 53)	152 ± 61[a,b] (149 ± 63[a,b])	91 ± 55 (80 ± 36)
M059J	97 ± 50 (89 ± 43)	137 ± 80[a] (134 ± 77[a])	125 ± 63 (111 ± 38)

[a] $p<0.05$ (2 Gy 30 min *vs.* 2 Gy 10 min)

[b] $p<0.05$ (2 Gy 30 min *vs.* 2 Gy 4 h)

Values within parenthesis are from analyses excluding S-phase cells

TABLE 3
Average numbers of DSB-unrelated γ-H2AX foci (Mean ± SD)

Cell line	2 Gy 10 min	2 Gy 30 min	2 Gy 4 h
GM38	63 ± 48 (47 ± 23)	104 ± 91[a] (68 ± 27[a])	125 ± 95 (103 ± 79[b])
M059K	157 ± 97 (140 ± 83)	193 ± 105 (180 ± 93)	213 ± 134 (184 ± 81)
M059J	87 ± 60 (68 ± 31)	210 ± 125[a] (155 ± 86[a])	118 ± 62[b] (114 ± 62)

[a] $p<0.05$ (2 Gy 30 min *vs.* 2 Gy 10 min)

[b] $p<0.05$ (2 Gy 30 min *vs.* 2 Gy 4 h)

Values within parentheses are from analysis excluding S-phase cells

TABLE 4

Average percentages of total nuclear γ-H2AX fluorescence signals within DSB-related foci (Mean ± SD)

Cell line	2 Gy 10 min	2 Gy 30 min	2 Gy 4 h
GM38	53 ± 15 (56 ± 14)	53 ± 9[b] (56 ± 7[b])	29 ± 7 (30 ± 7)
M059K	46 ± 11 (48 ± 8)	51 ± 9 (52 ± 8)	46 ± 13 (47 ± 13)
M059J	32 ± 9 (35 ± 9)	32 ± 13[b] (36 ± 12[b])	40 ± 8 (42 ± 6)

[a] $p<0.05$ (2 Gy 30 min *vs.* 2 Gy 10 min)

[b] $p<0.05$ (2 Gy 30 min *vs.* 2 Gy 4 h)

Values within parentheses are from analysis excluding S-phase cells

TABLE 5
Average percentages of total nuclear DAPI fluorescence signals within DSB-related foci (Mean ± SD)

Cell line	2 Gy 10 min	2 Gy 30 min	2 Gy 4 h
GM38	1.1 ± 0.5 (1.0 ± 0.5)	2.3 ± 1.3[a,b] (2.0 ± 0.8[a,b])	1.4 ± 0.7 (1.2 ± 0.6)
M059K	1.1 ± 0.4 (1.0 ± 0.4)	1.9 ± 0.6[a,b] (1.8 ± 0.6[a,b])	1.3 ± 0.8 (1.3 ± 0.7)
M059J	1.3 ± 0.6 (1.3 ± 0.6)	1.4 ± 0.9 (1.4 ± 0.7)	1.5 ± 0.7 (1.6 ± 0.7)

[a] $p<0.05$ (2 Gy 30 min *vs.* 2 Gy 10 min)

[b] $p<0.05$ (2 Gy 30 min *vs.* 2 Gy 4 h)

Values within parentheses are from analysis excluding S-phase cells

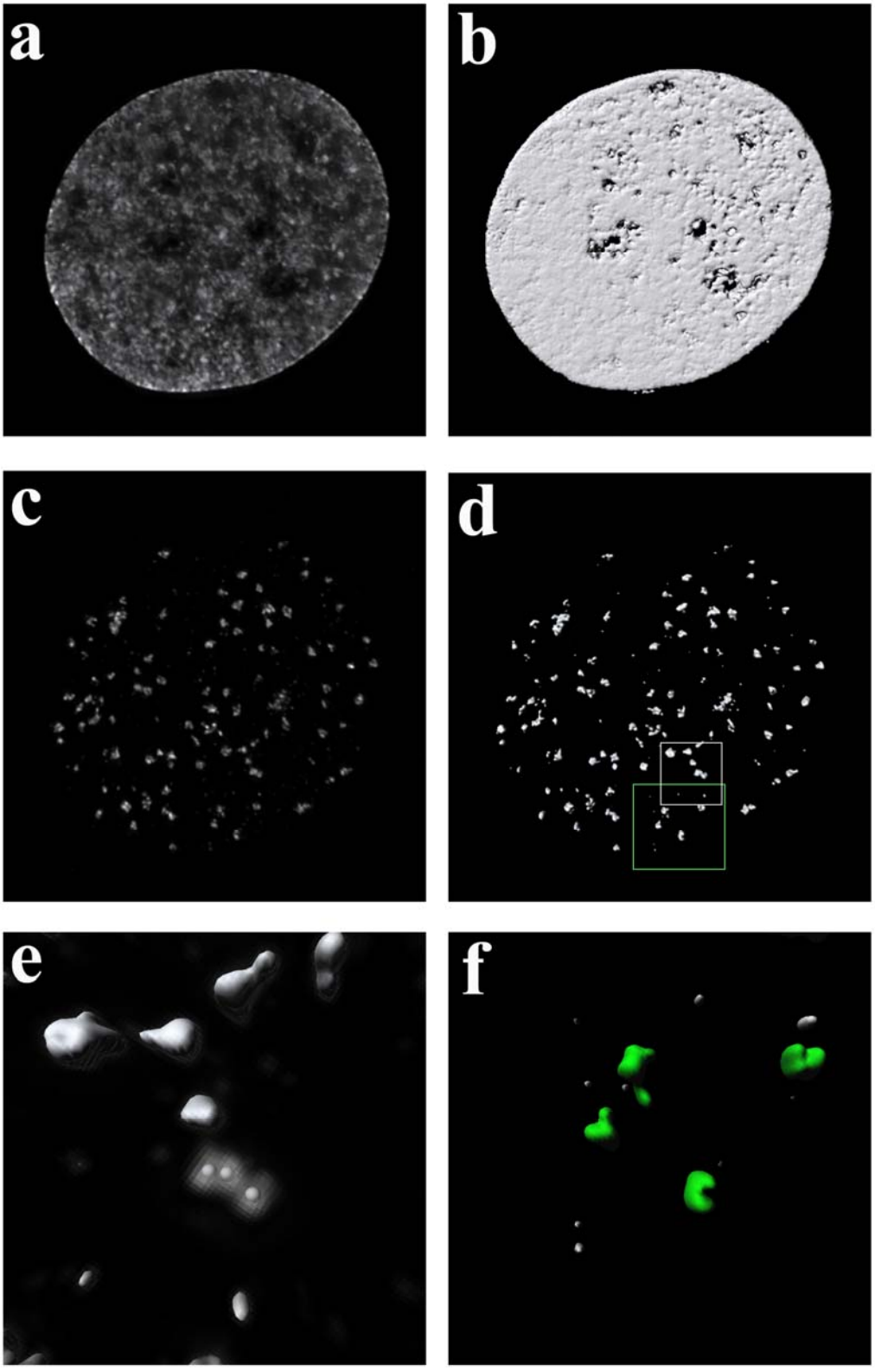

FIG. 1. Representative γ-H2AX and DAPI staining. Panel A: DAPI staining. Panel

B: projection of nuclear volume defined by Imaris. Panel C: γ-H2AX staining. Panel D: projection of all γ-H2AX foci with fluorescent signal intensity above the threshold (1/10 of the maximal fluorescence intensity value). Panel E: Zoomed image of white box region in panel D. Three intensity peaks (spots) can be identified within a γ-H2AX focus. Panel F: zoomed image of the green box region in panel D. Green foci are DSB-related foci and gray foci are DSB-unrelated foci.

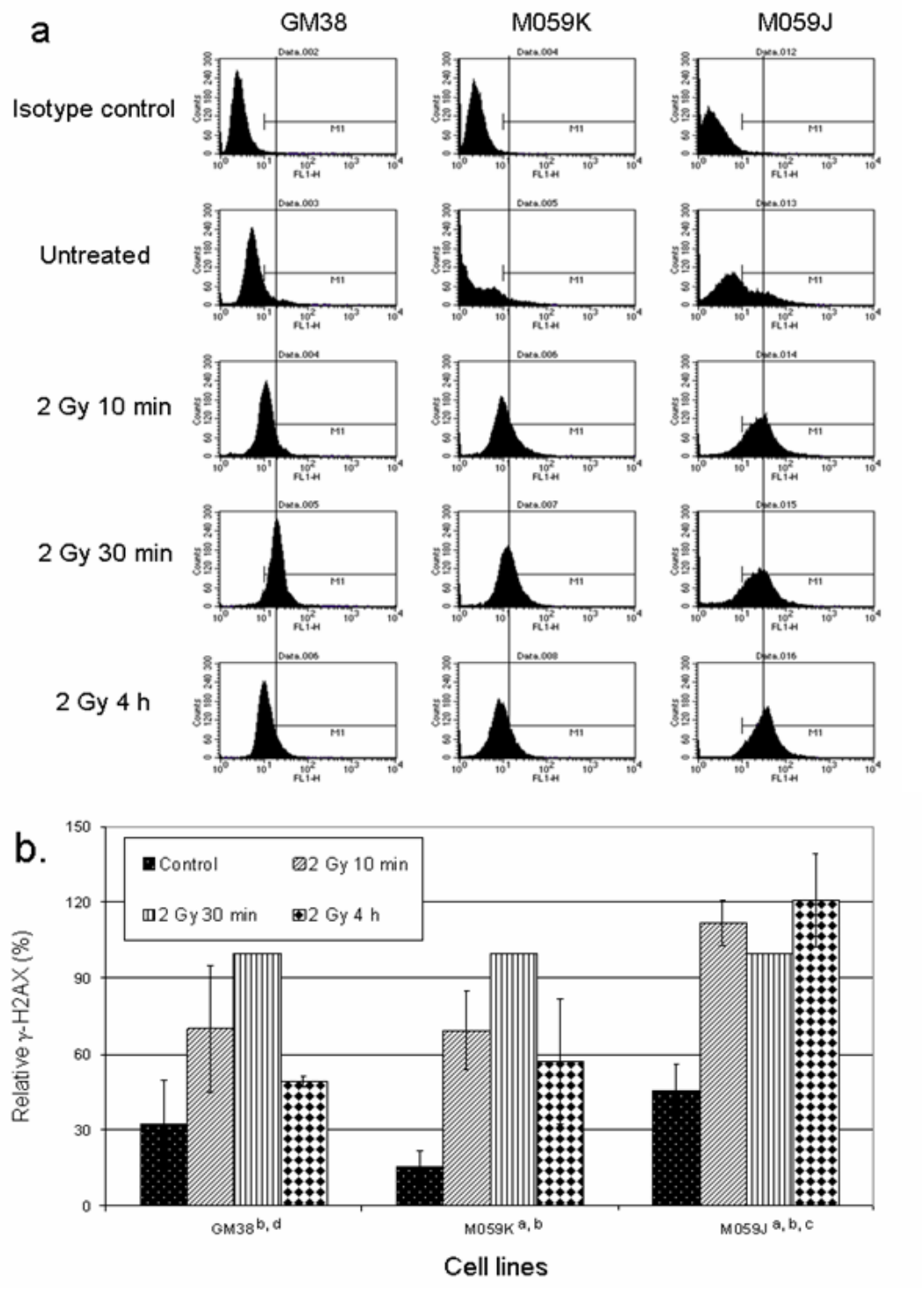

FIG. 2. Total cellular H2AX phosphorylation kinetics determined by flow cytometry. panel A: representative flow cytometry results. Panel B: statistical results calculated from data obtained from three separate experiments. a: $p<0.05$ (Control *vs.* 2 Gy 10 min); b: $p<0.05$ (Control *vs.* 2 Gy 30 min); c: $p<0.05$ (Control *vs.* 2 Gy 4 h); d: $p<0.05$ (2 Gy 30 min *vs.* 2 Gy 4 h).

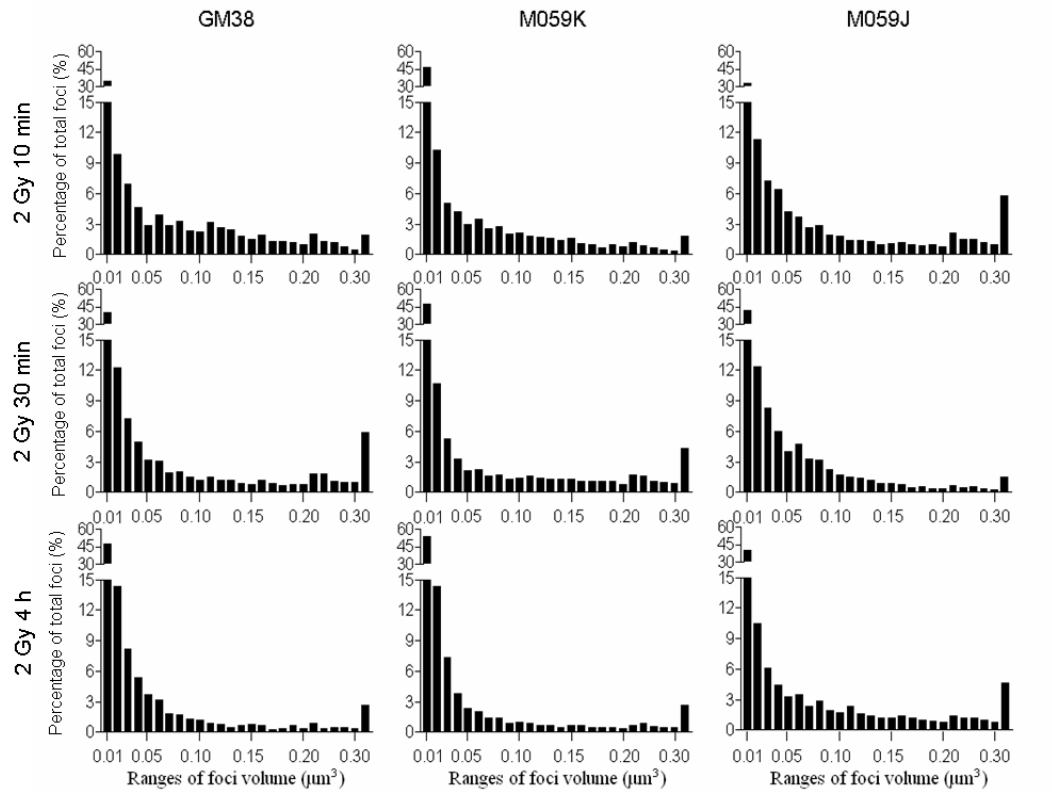

FIG. 3. Histogram of the volume of γ-H2AX foci with fluorescence signal intensity above the threshold. X axis represents the series of ranges of numerical value of foci volume (μm^3) into which data are sorted in histogram analysis and Y axis represents the percentages of total γ-H2AX foci within this range.

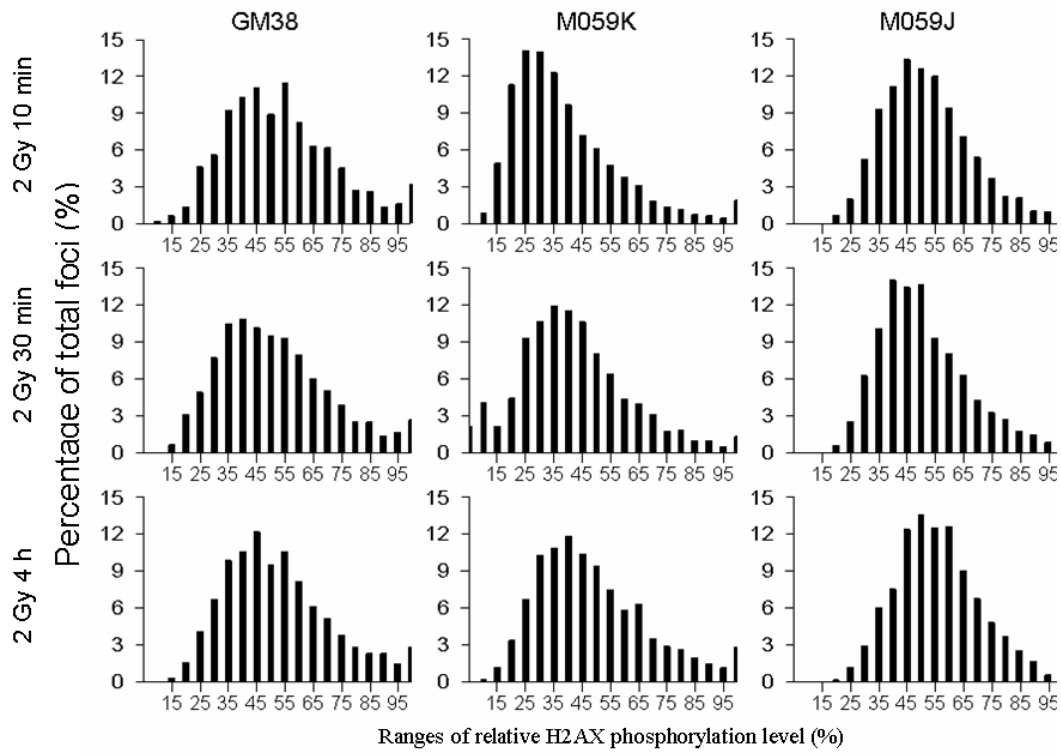

FIG. 4. Histogram of the relative H2AX phosphorylation level within DSB-related γ-H2AX foci. X axis represents the series of ranges of numerical value of relative H2AX phosphorylation level (percentages of the phosphorylation level of the most highly phosphorylated foci in each individual cell) into which data are sorted in histogram analysis and Y axis represents the percentages of total DSB-related γ-H2AX foci within this range.

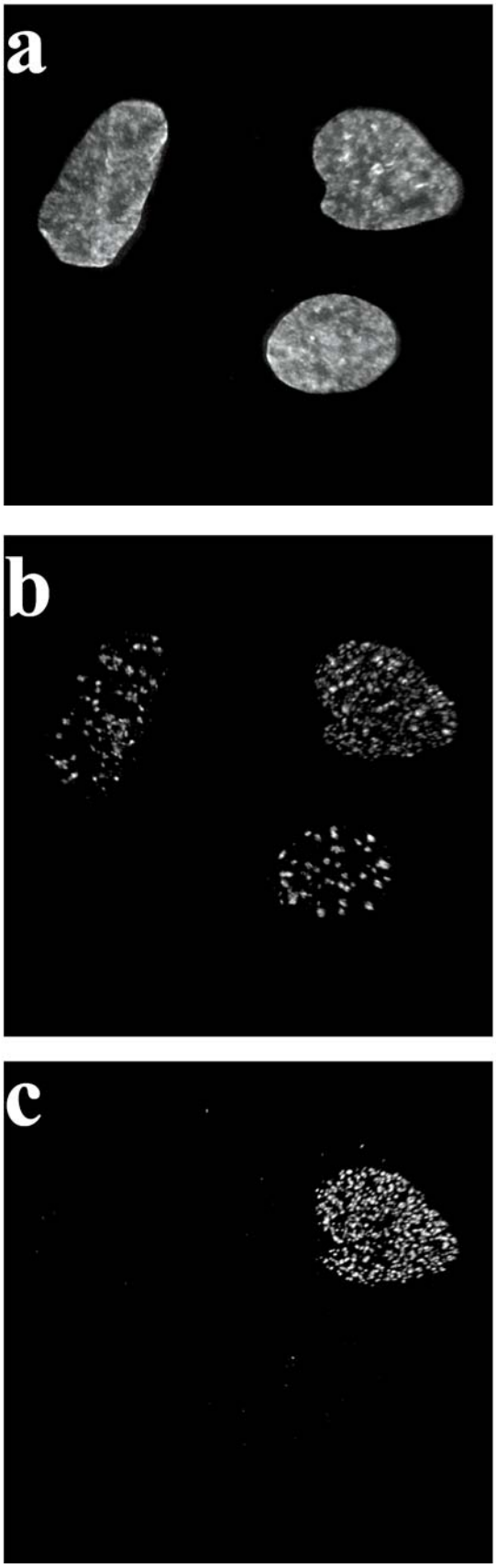

FIG. 5. Early S-phase cell-specific γ-H2AX foci pattern. Panel A: DAPI staining. Panel B: γ-H2AX staining. Panel C: BrdU staining.